Engineering and Economic Impacts of Sea Level Rise

by

Ebru Kirezci

ORCID: https://orcid.org/0000-0002-2319-7235

A thesis submitted in total fulfillment for the
degree of Doctor of Philosophy

in the
Department of Infrastructure Engineering
Melbourne School of Engineering
THE UNIVERSITY OF MELBOURNE

October, 2020

THE UNIVERSITY OF MELBOURNE

Abstract

Department of Infrastructure Engineering
Melbourne School of Engineering

Doctor of Philosophy

by Ebru Kirezci
ORCID: https://orcid.org/0000-0002-2319-7235

Episodic flooding, due to extreme sea levels, can have major impacts on low-lying areas where 10% of the total world's population resides. Combined with climate change induced sea level rise over the next century, the resulting impacts are likely to be exacerbated. One of the most obvious impact is the exposure of such areas to more frequent and increased extreme sea levels resulting in enhanced inundation extent. Global assessment of extreme sea levels together with the sea level rise component and their impacts is critical to assess the resilience and vulnerability of coastal zones. The present dissertation assesses these impacts on a global scale.

The historical values of tide, storm surge, wave setup are reconstructed from recent reanalyses at global coastal locations. Both the sea levels and the extremes are rigorously validated against quasi-global tide gauge records. To determine extreme values, a variety of extreme value analysis methods are applied and compared against each other and the tide gauge records. Future projections of the extreme sea levels are determined in combination with sea level rise scenarios over the upcoming century. The extent of present and future episodic flooding resulting from the corresponding extreme sea levels are presented. The resulting impacts on the global population and assets at risk for present conditions and under various combinations of future socioeconomic scenarios.

Global "hotspots", based on future changes in the flooding and extreme sea levels, are identified in this study to demonstrate coastal areas which potentially will be the most impacted by changes in extreme sea levels. These areas are mostly found to be concentrated in north western Europe and Asia. The results show that for the case of, no present/future coastal protection or adaptation, and a mean RCP8.5 scenario, there will be an increase of 48% of the world's land area, 52% of the global population and 46% of global assets at risk of flooding by 2100.

Regional and national analyses are conducted in order to highlight the values of both Expected Annual Population Affected (EAPA) and Expected Annual Damage (EAD), globally. In order to define a more accurate representation of the global coastal flooding at the aggregated regions, estimated coastal defences are included under various socioeconomic narratives as well as possible adaptation strategies. It is shown that, by 2100 and without future adaptation, global values of EAPA are projected an increase by a factor 3.6 in terms of people impacted. For global values of EAD, the increase relative to present-day values is a factor of 25. It is also demonstrated that the change in the subcontinental regions show significant variations when compared to the present values. In particular, developing areas of Asia will experience significant impacts on both populations and GDP by 2100. These impacts of projected future flooding on the developing world will be far greater than for the developed world.

Declaration of Authorship

I, Ebru Kirezci, declare that this thesis titled, 'Engineering and Economic Impacts of Sea Level Rise' and the work presented in it are my own. I confirm that:

- this thesis comprises only my original work except where indicated,
- due acknowledgement has been made in the text to all other material used, and
- the thesis is fewer than 100,000 word limit in length, exclusive of tables, maps, bibliographies and appendices.

Ebru Kirezci
October, 2020

Preface

This thesis is conducted at the University of Melbourne Department of Infrastructure Engineering. A Melbourne Research Scholarship has been granted in order to complete this research.

This thesis is mainly composed of one published and one unpublished papers. These publications appear in Chapters 4 and 5, respectively.

The first study (Kirezci et al., 2020) is published in Nature Scientific Reports and Chapter 4 of this thesis comprises this work. The research based on this study is conducted in collaboration with Prof. Roshanka Ranasinghe, Prof. Robert Nicholls, Prof. Jochen Hinkel, A/Prof. Sanne Muis and Dr. Daniel Lincke. This study was funded by Australian Research Council through grants DP130100215 and DP160100738, AXA Research Fund and the Deltares Strategic Research Programme, "Coastal and Offshore Engineering". The GOW2 data was generously supplied by Melisa Menendez.

The second study, is in preparation for submission and Chapter 5 of this thesis comprises of this work. The research based on this study is conducted in collaboration with Prof. Roshanka Ranasinghe. This study was funded by Australian Research Council through grants DP130100215 and DP160100738, AXA Research Fund and the Deltares Strategic Research Programme, "Coastal and Offshore Engineering".

Acknowledgements

I would like to thank my principal supervisor of my PhD, Kernot Professor Ian Young who always supported me, enlightened me and led me in the right way in my graduate studies. His wisdom and extensive knowledge always inspired me and expanded my horizon. My academic achievements could not have been possible without his expertise.

My deepest gratitude goes to my thesis committee Prof. Alexander Babanin and A/Prof. Alessandro Toffoli. Their helpful approach throughout my research helped me complete my studies.

My special thanks go to Prof. Roshanka Ranasinghe for his continuous support during my PhD. His views and knowledge on climate change is at the level I wish someday I may reach. Our valuable discussions on my research path gave me a true inspiration.

I would like to express my deepest gratitude to Çağıl Kirezci, the love of my life, my source of inspiration, my better half, my family, my colleague, my best friend and many other things that words can not express. We have grown up together through the time we have spent together. I know that, in the future, he is the hand I will always be holding. I would not be where I am today, without his presence in my life.

I want to express that I am so lucky to be the daughter of my mother, Seval Demirci. She was always there for me, and I know she will be, wherever I am and whatever I am doing in my life. I owe her most of the things that I have. I wish our endless phone talks would last for the many many long years ahead.

I also would like to thank my colleagues at the Ocean Engineering Group as well as in our department. Our lunchtime motivational discussions were always at another level. I am very thankful for knowing them and for providing such a supportive environment.

My special thanks go to my friends at home who have always been there to share moments in my life (despite the time differences).

I also want to acknowledge the University of Melbourne for providing support at every stage of my research.

Contents

List of Figures

List of Tables

Abbreviations

ACE CRC	The **A**ntarctic **C**limate and **E**cosystems **C**ooperative **R**esearch **C**entre
AM	**A**nnual **M**axima
AOGCM	**A**tmosphere–**O**cean **G**eneral **C**irculation **M**odel
AR5	5^{th} **A**ssessment **R**eport
ARIO	**A**daptive **R**egional **I**nput **O**utput Model
CFSR	**C**limate **F**orecast **S**ystem **R**eanalysis
CIESIN	**C**enter for **I**nternational **E**arth**S**cience **I**nformation **N**etwork
CL	**C**onfidence **L**imits
CMIP5	5^{th} **C**limate **M**odel **I**ntercomparison **P**roject
CMIP6	6^{th} **C**limate **M**odel **I**ntercomparison **P**roject
COWCLIP	The **C**oordinated **O**cean **W**ave **Cli**mate **P**roject
DEM	**D**igital **E**levation **M**odel
DCESL	**D**INAS-**C**OAST **E**xtreme **S**ea **L**evels
DINAS-COAST	**D**ynamic and **IN**teractive **AS**sessment of National, Regional and Global Vulnerability of **COAST**tal Zones to Climate Change and Sea Level Rise
DIVA	**D**ynamic **I**nteractive **V**ulnerability **A**ssessment
EAPA	**E**xpected **A**nnual **P**eople **A**ffected
EAD	**E**xpected **A**nnual **D**amage
ECMWF	**E**uropean **C**entre for **M**edium-Range **W**eather **F**orecast
EGM96	**E**arth **G**ravitational **M**odel (1996)
ERA-I	**E**CMWF **Re**A**nalysis **I**nterim
ESL	**E**xtreme **S**ea **L**evel
EVA	**E**xtreme **V**alue **A**nalysis
EVT	**E**xtreme **V**alue **T**heory
EXP	**EX**ponential **D**istribution
FES	**F**inite **E**lement **S**olution
GCM	**G**lobal **C**limate **M**odel
GDP	**G**ross **D**omestic **P**roduct
GESLA	**G**lobal **E**xtreme **S**ea **L**evel **A**nalysis

GEV	**G**eneralized **E**xtreme **V**alue Distribution
GIA	**G**lacial **I**sostatic **A**djustment
GLOBE	**G**lobal **L**and **O**ne-kilometre **B**ase **E**levation
GOW2	**G**lobal **O**cean **W**aves Dataset by IH-Cantabria
GPD	**G**eneralized **P**areto **D**istribution
GPWv4	**G**lobal **P**opulation Dataset version 4
GRUMP	**G**lobal **R**ural–**U**rban **M**apping **P**roject
GSHHG	**G**lobal **S**elf-consistent **H**ierarchical **H**igh-resolution **G**eography
GTSM	**G**lobal **T**ide and **S**urge **M**odel
GTSR	**G**lobal **T**ide and **S**urge **R**eanalysis
GUM	**GUM**bel Distrbution
(IIASA	**I**nternational **I**nstitute for **A**pplied **S**ystems **A**nalysis
IPCC	**I**nternational **P**anel of **C**limate **C**hange
LECZ	**L**ow **E**levated **C**oastal **Z**one
MDOT	**M**ean **D**ynamic **O**cean **T**opograph
MERIT	**M**ulti-**E**rror-**R**emoved **I**mproved-**T**errain
MSL	**M**ean **S**ea **L**evel
NASA	**N**ational **A**eronautics and **S**pace **A**dministration
POT	**P**eak **O**ver **T**hreshold
PSMSL	The **P**ermanent **S**ervice for **M**ean **S**ea **L**evel
RCP	**R**epresentative **C**oncentration **P**athways
RMSE	**R**oot **M**ean **S**quare **E**rror
RSLR	**R**elative **S**ea **L**evel **R**ise
Q-Q	**Q**uantile - **Q**uantile
S	**Surge** Level
SEDAC	**S**ocio**E**conomic **D**ata and **A**pplications **C**enter
SLR	**S**ea **L**evel **R**ise
SPM	**S**hore **P**rotection **M**anual
SRES	**S**pecial **R**eport on **E**missions **S**cenario
SROCC	**S**pecial **R**eport on the **O**cean and Cryosphere in a **C**hanging **C**limate
SRTM	**S**huttle **R**adar **T**opographic **M**ission
SSP	**S**hared **S**ocioeconomic **P**athways
T	**T**ide Level
TSL	**T**otal **S**ea **L**evel
UHSLC	**U**niversity of **H**awaii **S**ea **L**evel **C**entre
WS	**W**ave **S**etup Level

Chapter 1

Introduction

Coastal areas are one of the world's most high-profile zones forming a vital component of national and global economies. More than 600 million people reside in coastal regions with an elevation less than 10 m above mean sea level (McGranahan et al., 2007) and 200 million people live within coastal floodplains less than 1 m above mean sea level, which annually generate more than US $1 trillion globally (Milne et al., 2009). It is estimated that these numbers will increase rapidly in the upcoming century. As maintaining safety and operability of low-lying coastal areas is one of the top priorities of governments and decision makers, both for the present and in the upcoming centuries, the effects of climate change induced consequences on these regions needs to be investigated in depth. Global mean sea level rise is one of the most obvious impacts of anthropogenic climate change. Considering the impacts of such change is quite challenging due to the necessity of considering long-term issues (Nicholls and Lowe, 2004). At a coastal location, sea level rise may lead to subsidence, coastal recession and may decrease the efficiency of coastal protection structures (Koroglu et al., 2019) rendering coastal areas increasingly vulnerable to impacts of sea level extremes. Collecting data of past recorded impacts and hindcast models, as well as modelling future projections are of great significance in developing adaptation and mitigation strategies.

In recent decades, global mean sea level has been rising at a rate of ∼3–4 mm/year (Vitousek et al., 2017; Watson et al., 2015; Yi et al., 2015) and the mean increase for the last 20 years of the 21^{st} century is estimated to be up to ∼1 m (0.26-0.98 m) compared to the mean value of years 1986-2005 (Church et al., 2013a). Even if the recommendations of the Paris Agreement are followed, the global mean sea level at the end of the 21^{st} century will be higher than present day and will continue to rise for all CO_2 projection scenarios (Nicholls, 2018). The main physical processes responsible for global mean sea level change are thermal expansion of water due to ocean warming and

water mass input from land ice melt and land water reservoirs (Nicholls and Cazenave, 2010). Past observations and studies have shown that thermal expansion was the top contributor to global mean sea level rise (Nicholls and Cazenave, 2010). However, more recent findings indicate that global mean sea level rise is now being dominated by the sum of glacier and ice sheet contributions, with very high confidence (Oppenheimer et al., 2019).

Sea level rise is not uniform at every location. It has been observed from satellite altimetry that regional sea level varies due to non-uniform ocean warming, salinity variations, solid Earth response to the last deglaciation and gravitational effects and changes in ocean circulation due to ongoing land ice melting, freshwater input (Milne et al., 2009; Nicholls and Cazenave, 2010; Solomon et al., 2007; Stammer, 2008; Wunsch et al., 2007) and contemporary ice and water redistribution (Oppenheimer et al., 2019). In addition to regional sea level change, vertical land motion due to tectonics, mantle dynamics or glacial isostatic adjustment (Oppenheimer et al., 2019) cause relative sea level change, i.e., sea level relative to a land benchmark. Relative sea level changes may also result from land subsidence due to anthropogenic activities such as drainage and groundwater fluid withdrawal over the 20^{th} century (Nicholls and Cazenave, 2010). It is estimated that regional sea level change deviates from the global mean by $\pm 30\%$ (Oppenheimer et al., 2019), depending on the factors described above.

Local sea levels can be regarded as the time-averaged coastal water level fluctuations comprising wave set-up, tidal level, wind forcing, sea level pressure, the dominant modes of climate variability, seasonal climatic periodicities, mesoscale eddies, changes in river flow, as well as anthropogenic subsidence (Oppenheimer et al., 2019). Extreme sea levels occur when these local contributions are coincidental. For instance, simultaneous occurrence of high astronomic tide levels with storm surge produced from atmospheric pressure drop may cause extreme sea levels that are likely to result in coastal flooding. Moreover, deep water wave heights tend to increase during storm conditions resulting in higher breaking waves which lead to an increase in wave setup contributions to mean sea level. Consequently, wave setup - the static component of wave run-up – may also contribute to extreme sea level occurrence. This contributor can be estimated with simplistic approaches as explained in detail throughout this thesis. Therefore, tide, surge, wave setup and regional sea level rise can be considered as the main contributors to extreme sea levels at a coastal location. Thus, broad investigations and extensive modelling of these components are required for accurate estimation and future projections.

Regional relative sea level changes will exacerbate existing extreme sea levels which already threaten low-lying coastal areas with significant levels of loss of life and damage to property. Specifically, sea level rise at a coastal location intensifies the impact of

extreme sea levels, which is most likely to exacerbate the episodic flooding extend and associated risk. In addition, the increase in the sea level results in more frequent extreme flooding events. In other words, what is presently seen as a rare extreme event may become more frequent in the future. Recent findings show that even an increase of the order of tens of centimetres of sea level change could impact the frequency of extreme water levels significantly in the future [e.g., Vitousek et al. (2017), Vousdoukas et al. (2018b), and Wahl et al. (2017)].

Rising sea levels, in combination with extreme seas expose low-lying coastal areas through (i) the permanent submergence of land by higher mean sea levels or mean high tides; (ii) more frequent or intense coastal flooding; (iii) enhanced coastal erosion; (iv) loss and change of coastal ecosystems; (v) salinization of soils, ground and surface water; and (vi) obstructed drainage (Oppenheimer et al., 2019). These consequences may have both short-term and long term physical and socio-economic impacts to coastal zones such as coastal infrastructure damage or the requirement for inland migration.

Extreme sea levels are very likely to result in episodic coastal flooding whilst exposing the resident population and threatening assets. In order to comprehend the impacts of these extreme events on the coastal zone, coastal flooding risk can be defined as the vulnerability of the coastal areas to coastal hazards, in this case, extreme sea levels. Changes in vulnerability and hazards directly affect the risk. Here, vulnerability of a coastal community depends on the population exposed and potential damage to flood-exposed assets such as infrastructure or private dwellings. Rising seas result in an increase in the episodic flood risk while changing socio-economic parameters of coastal areas render large uncertainties for future coastal flood risk. Increases in exposure due to coastal flooding may have massive and irreversible consequences in the future unless necessary adaptation and mitigation measures are taken. These impacts can be determined from the population exposed to extreme sea levels and the assets (infrastructure, transportation facilities etc.) affected in the coastal zone and the economic consequences. Every year, it is estimated that a substantial portion of the global population is affected, resulting in serious damage in the order of $US billions (Hinkel et al., 2014). Hurricane Katrina, for example caused around US $110 billion in damages, more than 1,800 deaths, and displaced 1.2 million people (Knabb et al., 2005). Therefore, there is an urgent need to understand global scale sea level extremes to determine the vulnerable “hot-spot” coastal locations and to develop coastal flood mitigation strategies and awareness.

The economic impact of extreme sea levels and future sea level rise on coastal resources greatly depends on the adaptation adopted, which is defined as “planned or unplanned active or anticipatory, successful or unsuccessful response of a system to a change in

its environment" (Tol et al., 2008). Without adaptation, the flooding risk will increase in the coastal zones, irrespective of the location and the level of development (Oppenheimer et al., 2019). Therefore, there is an urgent need both for global and regional scale assessments of coastal flooding and its socio-economic implications over the next century. Global studies provide the first-order information for coastal areas that may highlight potentially affected hot-spot locations and a global risk landscape of coastal flooding impacts. On the other hand, regional studies deliver more detailed estimates and projections for a specific coastal area and make possible an understanding of in-depth behaviour of natural hazards. Therefore, it is necessary to improve our understanding of the contributions to sea level rise and extreme sea levels on both small and large scales. Although there are substantial uncertainties associated with future projections of sea level rise, coastal adaptation is still feasible for the next century (Oppenheimer et al., 2019) according to a number of past studies [e.g. (Hallegatte et al., 2013; Hinkel et al., 2014; Schinko et al., 2020; Tiggeloven et al., 2020; Vousdoukas et al., 2020)].

This thesis aims to conduct global-scale assessments of future extreme sea levels under a range of climate change scenarios. The inundation associated with these extreme sea levels is estimated and the populations impacted and assets potentially at risk quantified. An assessment of the impact of global-scale adaptation measures is also considered.

The main research objectives to be addressed in this thesis are as follows:

- Extreme sea levels for the present day and throughout the 21^{st} century are investigated at the global scale. The resulting coastal flooding extent is translated into impacts on the population and asset exposure.
- Importance of the phasing of the various contributors to extreme sea levels is investigated. These contributors are tidal fluctuations, surge levels and breaking wave setup. The relative contributions show that, tide and surge levels dominate the extreme sea levels with wave setup making a minor contribution.
- Regional and relative sea level variations are introduced, and the relative impacts of future changes in coastal flooding are shown at global coastal hot spots where the largest relative change in the coastal flooding occurs.
- Relative impacts of the regional and relative sea level rise are compared to the impacts caused by socioeconomic changes and presented as annual flood impact parameters.
- National and large-scale regional implications of coastal flooding throughout the 21^{st} Century are presented and relative national and regional changes are shown to vary globally with the major impacts on the developing world.

This thesis is arranged as follows. Chapter 2 provides an extensive literature review of various approaches to sea level rise projection, extreme sea level estimation, contributors and the effect of climate change on these contributors, previous global and large-scale extreme sea levels, coastal flooding impacts and risk assessments. Chapter 3 describes the datasets used in this study. Chapter 4 considers the global scale coastal episodic flooding and exposure analysis over the 21^{st} century and is based on the article (Kirezci et al., 2020). Chapter 5 considers the global and regional analysis of the coastal flood risk at present and future projections over the 21^{st} century. It is based on the paper that is in preparation for submission. Chapter 6 consists of conclusion of the thesis and possible future work to carry forward this research.

Chapter 2

Literature on Sea Level Rise, Extreme Sea Levels and Impact Analysis

Global projections of sea level rise in combination with extensive modelling of extreme sea levels provide a significant basis to understand the present and estimate the future implications of coastal flooding on low-lying coastal areas and communities. Extreme sea levels which occur infrequently at present are expected to be more frequent in the future, which provides a significant challenge for coastal planners and decision-making authorities. Therefore, past recorded data and the modelling efforts of present and future sea level extremes are of great importance for providing estimates of coastal impact due to extreme sea levels.

Total sea level at an arbitrary location and time is the combination of a variety of components. The timing of these individual sea level components, as well as their respective magnitudes will contribute to coastal flooding. Thus, it is a prerequisite to define the individual components of the total sea level and investigate the response with changing climate and to understand the interactions between those contributors to accurately compute future sea levels and coastal flooding extent and impacts.

Growth of populations and assets, changing climate and land subsidence are the main drivers of increasing flood exposure in coastal cities. Even though the flood probability may be stabilized with adaptation, the flood risk can still increase due to socioeconomic changes and land subsidence (Hallegatte et al., 2013). While there is a high uncertainty for future projections of sea level rise, extreme sea levels and socioeconomic parameters, it is necessary to attain a full understanding of the risk associated with climate change driven sea level extremes.

In this chapter, the first section is an extensive literature review of sea level rise trends and projections by process-based and semi-empirical projections. The second section consists of the literature on extreme sea level due to individual components and on future change of these components due to climate change. Previous studies on the non-linear relationship between extreme sea level contributors are considered and their significance discussed. Previous publications on the quasi-global tide gauge database, GESLA-2 (see Sections 2.2.6 and 3.5), which is used in this thesis to validate model results is also provided. The third section is devoted to the previous studies on coastal flooding, impact and risk analyses and potential adaptation strategies.

2.1 Sea Level Trends and Future Projections

Sea level rise is one of the most obvious and concerning impacts of climate change. Sea levels have risen by 20 cm since the late 19th century (Rahmstorf, 2007) and is projected to rise with an increasing rate relative to the past observed period (of 1971-2010). The main drivers of global sea level change are ocean thermal expansion and glacier melting as a response to increasing greenhouse gas emissions (Church et al., 2013a).

Mean sea level change can vary substantially for different locations globally due to oceanic movements, sea floor movements, and changes in gravity due to water mass redistribution (Church et al., 2013a). Sea level can also vary due to rapid land movement and human activities (i.e. groundwater extraction) resulting in variations in relative sea level change.

In this thesis, global sea level changes are implemented using projections of regional relative sea level rise, which was previously defined in (Church et al., 2013a).

A number of attempts have been made to investigate sea level change: making use of previous sea level recordings and existing models. There are mainly two approaches to estimate future sea level rise: (i) process-based models as defined in International Panel on Climate Change Fifth Assessment Report (IPCC AR5), (Church et al., 2013a) (e.g. Atmosphere-Ocean General Circulation Models and Geodynamic surface-loading models) and (ii) semi-empirical (as defined in IPCC AR5) and probabilistic models as defined in IPCC Special Report on the Ocean and Cryosphere in a Changing Climate (SROCC) (Oppenheimer et al., 2019). Process-based models include the interaction of atmospheric and oceanic circulation, systematic hydraulic phenomena among the oceanic waters, and modelling of tectonic movements of both land and the ocean bottom. Semi-empirical approaches consider changes in sea level as part of the entire climate system whilst not considering the analysis by its individual physical components (Church et al., 2013a). Probabilistic approaches consider the mean sea level change components as probabilistic distributions, yielding a full probability distribution of the mean sea level change (Oppenheimer et al., 2019).

In this section, literature on the approaches to the estimation and projection of sea level rise, including both (i) process-based and (ii) semi-empirical and probabilistic models, is described in detail.

2.1.1 Process-based Models

Process-based models, as explained in detailed by (Church et al., 2013a), consider the combination of various global mean sea level change contributors including thermostatic expansion, ice mass loss from different glaciers, ice mass loss from the Greenland Ice Sheet and the Antarctic Ice Sheet - often separated into East and West- and the contribution from land water storage variations (Jevrejeva et al., 2019). Church et al. (2013a), in IPCC AR5, have reported that the past global mean sea level rise has been 0.19 m (0.17 m - 0.21 m) between 1901 and 2010 and is very likely to increase during the 21^{st} century.

Sea level rise differs from the global mean along distinct coastlines due to (Kopp et al., 2014);

i. non-uniform changes in ocean dynamics, heat content, and salinity (Levermann et al., 2005; Yin et al., 2009)

ii. perturbations in the Earth's gravitational field and crustal height (together known as static-equilibrium effects) associated with the redistribution of mass between the cryosphere and the ocean (Kopp et al., 2010; Mitrovica et al., 2011)

iii. glacial isostatic adjustment (GIA) (Farrell and Clark, 1976) and

iv. vertical land motion due to tectonics, local groundwater, and hydrocarbon withdrawal, and natural sediment compaction and transport (Miller et al., 2013).

Knowing the variations between the global sea level change patterns, regional relative sea level change can be defined as the combination of the global sea level contributors that are dependent on the oceanic-atmospheric variations as well as the human-driven and tectonic land movements. To date, many studies have investigated the process-based regional relative sea level rise at regional to global scale.

Regional studies include, Sallenger et al. (2012) who reported accelerated sea level rise along the North American Atlantic coast due to steric and dynamic ocean processes. Palanisamy et al. (2014) and Grinsted et al. (2015) calculated regional projections of 21^{st} century sea level rise in Northern Europe with a probabilistic approach applied to the sea level contributors. Recently, Martínez-Asensio et al. (2019) gave estimates of past and future relative sea–level changes at small islands in the South Western Tropical Pacific region. This study also considered the potential impact of the contribution of local vertical land motion on these trends, indicating that the relative sea level has increased more than the global mean over this region. From tide gauges along the

coastlines around the Bohai Sea, the Yellow Sea, the East China Sea, and the South China Sea (the "China Seas"), Qu et al. (2019) investigated sea level rise including the vertical land movements over the past observation period and provided projections under mid and high-end RCP scenarios of 48–61 cm and 84–99 cm by 2100, respectively.

Globally, Church et al. (2013a) estimated that projections of regional sea level rise substantially deviates from the global mean (Figure 13.20 therein) according to an ensemble of 21 CMIP5 models.They considered Representative Concentration Pathways (RCP) 2.6, 4.5, 6.0 and 8.5 and compared between the mean period 1986-2005 and 2081-2100. DeConto and Pollard (2016) coupled ice sheet and climate dynamics models and found that potentially, Antarctica may contribute more than 1 m to sea level rise in 2100. Kopp et al. (2017) have considered an ensemble of Antarctic ice-sheet simulations incorporating these physical processes, to explore their influence on global and relative mean sea level. They find a 21^{st} century global mean sea level rise 146 cm under RCP 8.5.

Projections of sea level change based on process-based models have large uncertainties due to the uncertainty span of the individual components considered. Nevertheless, to date, estimates from the previous studies are mostly consistent amongst each other.

2.1.2 Semi-Empirical and Probabilistic Models

Semi-empirical models estimate future sea level changes by considering the whole oceanic-atmospheric-cryosphere system. As previously noted, this approach does not include the separate components of the physical contributors (i.e. thermal expansion and glacier-ice sheet ablation) of the sea level change separately. Rather, this is a complementary attempt to estimate sea level variation from observed data and projected future atmospheric changes. The approach can be justified since the uncertainties in the process-based models are quite large. Calibrating a portion of the past historical data and validating against a recent time frame is one of the approaches used to estimate future mean sea level height. Using this approach, Rahmstorf (2007) and Jevrejeva et al. (2012) have calibrated and fitted separate observed datasets in order to determine the model parameters required for sea level estimation, resulting in values of global mean sea level rise by 2100 of 0.5 - 1.4 and 0.6 -∼1.7 m for each dataset. Vermeer and Rahmstorf (2009) presented a substantial extension of the method proposed by Rahmstorf (2007) and report a plausible approximation to future sea level response by testing on synthetic and real data. Bittermann et al. (2013) studied twentieth century sea level tide gauge recordings and proxy data. The authors showed that sea levels are predicted reasonably well comparing against tide gauge sea level data.

Probabilistic models are developed to provide the complete probability distributions of sea level changes and can be advantageous for a quantitative risk management perspective (Oppenheimer et al., 2019). Moreover, probabilistic models bridge the gap between process-based and semi-empirical projections while being computationally affordable. Kopp et al. (2014) and Jackson and Jevrejeva (2016) investigated the reconstruction of the sea level change components with a probabilistic approach incorporating global spatial patterns of sea level change. Mengel et al. (2016) constrainted the earlier semi-empirical sea level rise approach (Grinsted et al., 2010) by calibrating a set of observations of sea level rise contributors. These contributors include: ocean thermal expansion, mountain glacier loss, both Greenland and Antarctic Solid Ice Discharge and Surface Mass Balance reconstructions. The results from this study give sea level rise values overlapping with the IPCC AR5 values while accounting for the discrepancies that might have been caused by the process-based models. Rasmussen et al. (2018) determined probabilistic sea level rise projections for the 21st and 22nd centuries. The authors reported that by 2100, global sea level rise projections are 48, 56 and 58 cm for 1.5°, 2.0°and 2.5°C global mean surface temperature stabilization, respectively.

2.2 Literature on Extreme Sea Levels

Coastal areas are exposed to sea level fluctuations due to astronomical and atmospheric variations with varying time scales, from seconds to multidecadal intervals. Extreme sea levels occur due to unusually high combinations of sea level components with respect to time-averaged mean sea values.

Extremes of sea levels that result in coastal flooding (or inundation) pose societal and economic risks. Therefore, to determine the risks that are linked to these episodic floods, to evaluate the consequences of such devastating events, to highlight vulnerable coastal locations and to develop mitigation strategies (e.g. coastal adaptation), extreme sea levels need to be sufficiently understood and analysed.

In the literature, extreme sea levels are extrapolated to future occurrences either from observed tide gauge recordings [e.g., Tsimplis and Blackman (1997), in the Aegean Sea, and Barbosa (2008), in the Baltic Sea] or from hindcast model simulations of storm surge [e.g. Bernier et al. (2007), used a regional barotropic model in the NW Atlantic]. Whilst most of the studies assume stationary statistical behaviour [e.g., Brown et al. (2013), Hauer et al. (2016), and Hinkel et al. (2010, 2014)] of atmospheric processes, some include time-dependent changes [e.g., Mentaschi et al. (2016) and Vousdoukas et al. (2017, 2018a,b)].

In this section, a detailed literature review is undertaken of the contributing components of extreme sea levels derived from hindcast models and tide gauge records. In addition, future changes of the sea level contributors due to climate change are considered and the impacts of nonlinearity between the contributors. Moreover, the background to the global GESLA-2 tide gauge dataset are discussed and methods for determining extremes from timeseries of the total sea levels and sea level change impacts on extreme sea levels are explained in detail.

2.2.1 Extreme Sea Level Contributors

Understanding coastal flooding due to extreme sea level behaviour requires analysis of sea level timeseries and the components that make up the total sea level (TSL) and their relative timing. For example, episodic flooding may not occur if low tide and storm surge coincide, whereas the simultaneous action of high tide and storm surge may result in significant coastal flooding.

Extreme sea levels are comprised of tide, storm surge, wave setup, contributions from seasonal and climatic cycles (e.g. El Niño/Southern Oscillation and Pacific Decadal

Oscillation) and oceanic eddies (Vitousek et al., 2017). However, as detailed in the literature, the main contributors of an episodic flooding can be assumed as tide, storm surge and wave-related components (Melet et al., 2018; Rueda et al., 2017; Vitousek et al., 2017; Vousdoukas et al., 2018b).

Tides (or astronomical tides) are the deterministic components of sea levels. They occur due to the combined effects of gravitational attraction and the revolution of the Earth-moon system about its common centre of mass. These periodic changes of the world's oceans consist of a large number of constituents and mathematically can be determined using harmonic analysis (*What are tides?*). Tides can be predicted with high reliability thanks to recent modelling techniques and computational advances (Haigh, 2017). Globally, a number of astronomical tide timeseries datasets from model hindcasts with assimilated satellite altimetry and/or tide gauge data have been developed (e.g., FES 2014, TPXO9). In order to accurately estimate tidal levels at a coastal location, tide models should perform adequately in the shallow waters, which is often a challenging task, as tidal constituents depend on the coastal bathymetry and the oceanic shelf details (Andersen, 1999; Piccioni et al., 2018). A recent global tide model - Finite Element Solution 2014 (FES2014), which was implemented to determine global hindcast tides in this study, has shown high accuracy in shallow water zones due to finer bathymetry and its optimized assimilation scheme (Carrere et al., 2015; Seifi et al., 2019).

Storm surges are the sea level increase as a result of atmospheric pressure drop and wind stress. Significant storm surges are often associated with the occurrence of tropical and extratropical cyclones. This component of the extreme sea level may result in devastating consequences of flooding especially if it coincides with high tide. To this end, storm surge hindcasting and forecast modelling efforts [e.g., Bernier and Thompson (2006), Bunya et al. (2010), Hubbert and Mclnnes (1999), Hubbert et al. (1991), Verlaan et al. (2005), Westerink et al. (2004, 2008), and Yin et al. (2016)] are crucial to understand the resulting exposure. Such predictions are important for the design of long-term protection and mitigation measures, such as the construction of storm surge barriers or early warning systems. A recent contribution to global storm surge hindcast models, the Global Tide and Surge Model (GTSM) was introduced by Muis et al. (2016) and is the first-of-its-kind global hydrodynamic approach consisting of the GTSM surge heights and FES2012 tide levels, validated against the University of Hawaii Sea Level Centre (UHSLC) tide gauge network dataset. An improvement of this global storm surge modelling approach was conducted by Dullaart et al. (2020) using a recent successor of the ERA-Interim wind fields (Dee et al., 2011), ERA5 (Hersbach et al., 2019) climate reanalysis dataset. Within this new study, it was found that wind fields and associated storm surges, especially smaller scale tropical cyclones are represented better as a result of increased resolution.

Breaking wave setup and swash are the components that result from wave action, although the latter is typically omitted in global studies (Aucan et al., 2019; Muis et al., 2016; Vousdoukas et al., 2018b). In particular, wave setup is the static rise of the water level with respect to mean sea level due to breaking of the waves. It can be further defined as the time averaged elevation of the water level with respect to mean sea level due to wave breaking and it is dependent on the deep-water significant wave height, wave period and nearshore bed slope at a coastal region (Stockdon et al., 2006). Therefore, this component varies significantly depending on the details of the coastal location and the wave conditions. This results in significant uncertainties both temporally and spatially in the determination of setup.

To date, wave setup has been investigated theoretically (e.g. Longuet-Higgins and Stewart (1962, 1964), Longuet-Higgins and Stewart (1963), and Svendsen (1984)), under laboratory conditions [e.g., Battjes (1973), Bowen et al. (1968), Hedges and Mase (2004), Nielsen (1989), and Stive and Wind (1982)] and field conditions [e.g. Davis and Nielsen (1989), Guza and Thornton (1981), Hansen (1978), Hanslow and Nielsen (1993), Holman and Sallenger Jr (1985), King et al. (1990), Nielsen (1988), Raubenheimer et al. (2001), Ruggiero et al. (2001), Stockdon et al. (2006), and Yanagishima and Katoh (1991)]. Comprehensive numerical models to estimate wave setup are reported in the literature [e.g., Kobayashi and Wurjanto (1992) and Larson and Kraus (1989)]. These studies indicate that wave setup can affect both short-term sea level fluctuations and extreme sea levels and hence can impact long-term estimates of extreme sea levels.

Following the Shore Protection Manual (SPM, 1984), the ratio of wave setup (WS) to offshore significant wave height (H_{s0}), S/H_{s0}, can be evaluated as a function of wave steepness and bed slope. Stockdon et al. (2006) have given an empirical formula for wave setup which is again depending on the foreshore bed slope, deep water wave height and wave length as given in Eq. 2.1.

$$WS = 0.35\beta_f \sqrt{(H_{s0}L_0)} \tag{2.1}$$

Here, WS is wave setup, β_f is bed slope, H_0 is the deep-water significant wave height and L_0 deep water significant wavelength.Bed slope was calculated from an offshore depth equal to $2H_0$ to the shoreline (Dean et al., 2005).

For large-scale spatial analyses, computation of wave setup is challenging as this component is highly dependent on the bed slope which can vary considerably both spatially and temporally. Hence, this quantity is difficult to measure on large spatial scales. From a global perspective, a first attempt to account for wave setup impacts on extreme sea level was given by Vousdoukas et al. (2018b) who considered wave setup as a function

only of the deep-water significant wave height (i.e., $S=0.2H_{s0}$) given by the Coastal Engineering Manual (US Army Corps of Engineers, 2002). This approach overcomes the challenges of defining nearshore bed slope on a global scale but ignoring this functional dependence obviously limits the accuracy of the approach. In a recent attempt to determine global wave setup, Melet et al. (2018) investigated the impact of the wave setup and swash contributions to total sea levels and concluded that these components can strongly dampen or enhance the effects of coastal sea level changes. However, in this study, the global bed slope was assumed to be constant globally and taken as 0.1 which results in quite large wave setup heights when compared to smaller bed slopes and may be misleading when considering the world coastlines (Aucan et al., 2019). A recent publication from Athanasiou et al. (2019) introduced a global bed slope dataset showing that the mean bed slope value of the global distribution is approximately 1/100. It should be noted that the SPM approach (SPM, 1984) is less dependent on bed slope than that of Stockdon et al. (2006).

Swash is the non-stationary component of wave run-up, defined as the location of the intersection between the ocean and the beach (Stockdon et al., 2006), which depends on the beach foreshore topography (Vitousek et al., 2017). As this wave-driven sea level component is highly dependent on spatial and temporal parameters, the scarcity of detailed information on these parameters makes it challenging to compute wave run-up globally. In addition, swash (wave runup) does not result in a static elevation in the mean sea level (unlike setup). Therefore, in this study, only the static rise of wave run-up (i.e. wave setup) is considered.

Accurate estimation of these components is of importance in modelling extreme sea levels. Global models of these components (such as the ones that are used in this thesis) present a broad picture of the historical, present and future estimates. These estimates can then be used to define and highlight the most vulnerable coastal locations, subject to high extreme sea levels. However, in order to conduct such large-scale assessments, there are some trade-offs between spatial and temporal resolution and the computational efficiency which must be made. As explained throughout the present section, all of these parameters depend on localised and regional characteristics of the coastal area, such as particular coastal topography or on the larger scale, continental shelf details. Downscaling from a coarser to a finer resolution at those scales may result in large errors. However, thanks to recent improvements in data analysis techniques and computational efficacy, techniques such as data assimilation using altimeter and measurement data to improve data accuracy are continuously being developed.

2.2.2 Future Changes in Surge Heights due to Climate Change

The field of study of future changes of surge height is still an evolving area. To date, the literature is split between two views; either predicting future change of the surge heights or assuming a negligible change of the storm surge height along the coastlines, especially when mean sea level change is considered. Moreover, there are significant regional differences of the effects of climate change on projected surge heights.

As previously mentioned, storm surge is the rise of the sea level with respect to the mean as a result of the atmospheric pressure drop and wind stress. Also, the sea level increase due to storm surge is dependent on the coastal bathymetry. There is a considerable amount of literature on projections of changes of storm surge levels, storm frequency and changes of storminess during an era of climate change. A range of studies have concluded that there will be an increase either in the storm surge height and/or the surge frequency. Wang et al. (2008) studied the influence of anthropogenic climate change on storm surges over Irish waters, particularly on extreme sea levels. Model results showed an increase in the frequency of storm surge events and extreme storm surge heights. Debernard and Røed (2008) investigated changes in wind speed, significant wave height and storm surge for a region covering the northern North Atlantic seas (covering the Norwegian, Greenland and Iceland Seas, together with its adjacent North and Barents Seas) and found a statistically robust storm surge height increase along the Eastern North Sea coast and Skagerrak by the 2071-2100 period. Lin et al. (2016) predicted both sea level rise and potential climatology changes over the 21^{st} century. They concluded that, with an RCP 4.5 emissions scenario, the storm surge height observed during Hurricane Sandy would occur as frequent as 3 to 17× times greater by 2100 (compared to 2000). Vousdoukas et al. (2016b) shows an increasing tendency in extreme storm surge levels along European coastal locations by 2100 assuming RCP 4.5 and RCP 8.5. Sobel et al. (2016) studied projections and recent historical trends of tropical cyclone activity and concluded that there will be storm intensity increases, despite lower confidence in recent trends. Therefore, tropical cyclone induced storm surge increases would compound mean sea level rise. A recent global study by Mori et al. (2019) investigated long-term projections of storm surges using an ensemble of atmospheric global circulation models and a statistical storm surge model. The authors projected an increase of 10% - 30% in storm surge magnitude in the mid latitudes (15°- 35°N) and a decrease in the Southern Hemisphere.

On the other hand, a range of model studies have shown insignificant projected changes in storm surge heights, especially when comparing to the magnitude of projected mean sea level rise. Sterl et al. (2009) concluded there was no statistically significant change of surge height at Dutch coastlines using a large-member ensemble of climate change

simulations for the period 1950-2100. Menéndez and Woodworth (2010) analysed the historical (from 1970 onwards) quasi-global tide gauge data network and concluded that there was only a slight to negligible increasing trend in storm surges that contribute to extreme sea levels when the sea levels are detrended from the mean sea level. Zhang et al. (2000) found no discernible trend in storm frequency and intensity that would impact storm surge heights obtained from tide gauge records of Atlantic coasts of the United States. In the Northwest Atlantic, Bernier and Thompson (2006) have found a slight negative trend of extreme storm surges over a period of 40 years (1960-1999) concluding that over the next century, the main driver of the increase in the flooding risk will be sea level rise. Colberg and McInnes (2012) showed that projected changes of extreme sea levels between 1981-2000 and 1981-2000, is small (within the range of 10 cm) relative to mean sea level change and mainly negative across the southern Australian coast. Church et al. (2013a) reviewed a number of studies and concluded that sea level extremes are very likely to increase in frequency in some regions by 2100 and with high confidence an increase will occur to mean sea level. They also conclude that the effects of the changes in storminess and the storm surge height variations for the next century are yet to be fully understood. Similarly, Garner et al. (2017) concluded that, for New York City, sea level rise is the dominant component responsible for the projected increase in the flood risk, while variations in storm surge height were projected to be minor from 2010 to 2100, or 2300, downscaled from RCP 8.5 simulations from three CMIP5 models. Palmer et al. (2018) suggest that the best representation of the storm-surge contribution to extreme sea level increase is "no change" over the 21^{st} century under RCP 8.5 from an ensemble of storm surge simulations around the coast of the United Kingdom with similar findings from Howard et al. (2019).

In conclusion, although there is a large amount of literature on potential change of storm surge heights, and its potential to change the extent of future coastal flooding, there is not a clear consensus on whether such increases will be significant.

2.2.3 Future Changes in Waves due to Climate Change

Wave height impacts extreme sea levels through wave setup which may potentially have significant impacts during extreme conditions. Therefore, like storm surge, changes in future wave climate may impact extreme sea levels. There are relatively few studies investigation both historical changes in wave height and potential future changes. Mori et al. (2010) found an increase in the mean wave height in the mid-latitudes and the Antarctic Ocean and a decrease at the equator. An international collaborative project on waves and coastal hazards, "The Coordinated Ocean Wave Climate Project (COWCLIP)" was established to developed a consistent international view on wave climate

changes. Based on this project, Hemer et al. (2013) found a projected decrease in annual mean significant wave height over 25.8% of the global ocean area and a decrease over 7.1% of the global ocean. The increases were largely concentrated in the Southern Ocean. Morim et al. (2019) have investigated projected changes in global wave climate by 2100 under RCP8.5 and showed increases in 99^{th} percentile and 100-year return period significant wave height of up to 15%, again, mainly in the Southern Ocean. In a recent study, Young and Ribal (2019) examined a 30-year historical global satellite altimeter dataset which demonstrates that there have been small increases in mean significant wave heights. However, larger increases in extremes were noted, with the largest increase occurring in the Southern Ocean. Meucci et al. (2020) used an ensemble of climate model runs to show small increases in 100-year return period wave heights by 2100, particularly in the Southern Ocean. However, wave setup is only a small fraction of the significant wave height globally (10-20%), therefore, the actual impact on extreme sea level compared to mean sea level rise will be small. As a result, it is reasonable to assume that future changes in global wave climate will have small impact on global scale extreme coastal flooding, especially when uncertainties related with implemented datasets and computational approaches are considered.

2.2.4 Estimating Extreme Sea Levels from Hindcast Models

Predicting extreme sea levels can be challenging due to the complex and irregular nature of shorelines. To analyse the extreme sea level behaviour, it is essential to understand the sea level timeseries. Therefore, an understanding of the extreme sea level contributors and appropriate assumptions, and the approximations needed to model then at the different scales is important. Numerous studies have assumed a linear relationship between the sea level components in order to determine the total sea level timeseries, especially for continental to global scale estimations [e.g., (Muis et al., 2016; Rueda et al., 2017; Vousdoukas et al., 2017, 2018b)]. In order to determine the total sea level (TSL) at an arbitrary time (t), the relationship can be defined as in Eq. 2.2.

$$TSL(t) = T + S + WS \tag{2.2}$$

Here, (T) is tide level, (S) is surge level and (WS) is wave setup.

Although the linear summation assumption in Eq. 2.2 is commonly used to compute extreme sea levels on a global scale, this assumption may lead to significant errors for specific locations. In such cases a more detailed approach, including the non-linear nature (see Section 2.2.5) of those components may be necessary. Thus, there have

been a number of efforts to calculate sea level contributors which include the interaction of these three components of total sea level. (Olbert et al., 2013) applied the joint probability method described by Pugh and Vassie (1980) and revised by Tawn (1992) to estimate the extreme sea levels due to astronomical tides and surges. Vousdoukas et al. (2018b) have determined extreme sea levels from the joint occurrence of the high tide levels with storm surge and wave setup action. Marcos et al. (2019) recently examined the significance of the dependence between extreme storm surge and wave setup on extreme sea levels globally. These studies show the impact of the combined actions of sea level contributors on extreme sea levels at specific at specific locations. Although the impacts at specific locations can be significant, the previous results indicate that at the global scale the linear assumption of Eq. 2.2 is reasonable [e.g. Howard et al. (2010, 2019), Losada et al. (2013), Lowe and Gregory (2005), Sterl et al. (2009), and Vousdoukas et al. (2016b, 2018b)].

2.2.5 Nonlinearity between sea level components

The contributors to extreme sea levels: tide, surge, wave setup and sea level rise, can interact non-linearly, which may potentially create substantial differences from Eq. 2.2 spatially and temporally from the coastal risk point of view. This nonlinear dependence between the extreme sea level contributors can be modelled either separately or collectively (i.e., tide-surge interaction, tide-surge-wave interaction, sea level rise impacts on extreme sea levels). Such impacts become more important as the water level decreases. For example, as the tidal stage changes, so does the water depth which effects the wave setup and storm surge magnitude. A similar behaviour happens with annual to multidecadal mean sea level variations. Therefore, extreme conditions are expected to be increasingly affected due to changing sea level that can potentially increase nonlinear variations to the resulting coastal impacts. Howard et al. (2010) investigated the influence of mean sea level changes, supporting the linear summation of mean and extreme sea level changes at the southern North Sea and the Thames estuary. Arns et al. (2015) investigated the nonlinear impact of sea level rise on extreme sea levels in the German bight and found a slight increase in return period water levels compared to sea level rise alone. Arns et al. (2017) emphasized the significance of changes of wave characteristics due to sea level variations and to a lesser extent, tides and indicated a 50% increase of the design extreme sea levels relative to design changes caused by sea level rise alone.

On the other hand, a number of studies have not detected a significant variation of the extremes due to the interaction between the contributors. This occurs, as non-linear impacts appear to depend on the scale of the study. That is, the impacts are larger at the regional scale than at national or global scales. Sterl et al. (2009) investigated

nonlinear effects between sea level rise, tide and surge and found no significant increase in surge level due to sea level rise while showing the nonlinear interactions between tide and surge manifested as a damping effect of the tide on the total water level. Hunter (2010) indicated that the most impactful contributor to extreme sea levels is the mean sea level rise.Woodworth et al. (2016) confirmed that the nonlinear effects are mainly region dependent. Based on these studies, we can conclude that, at the global scale, nonlinear interactions can be assumed to be negligible considering the uncertainties of global scale extreme sea levels.

In summary, with the present accuracy with which the components contributing to extreme sea level can be calculated, it is reasonable to assume that, at the global scale, a linear approximation such as Eq. 2.2 is a reasonable representation for extreme sea levels.

2.2.6 Background to the GESLA-2 Tide Gauge Dataset

Historical information on sea level variations from tide gauge recordings is important, particularly for the computation and validation of extreme sea levels and sea level rise projections. High frequency (hourly) sea level data is required for the calculation of extreme sea levels, ocean tides, storm surges, and other coastal processes on a quasi-global basis (Woodworth et al., 2016). Both historical investigations and future projections of sea level rise can be determined from low frequency (monthly, annually) sea level fluctuations. The Permanent Service for Mean Sea Level (PSMSL) collects and distributes low frequency sea level data (Holgate et al., 2013).

Since our concern in this thesis is to determine, validate and implement projections of extreme sea levels on a global scale as a coastal flooding hazard, a higher frequency sea level dataset is required. The Antarctic Climate and Ecosystems Cooperative Research Centre (ACE CRC) and the Proudman Oceanographic Laboratory have collated a quasi-global sea level dataset called the "Global Extreme Sea Level Analysis Version 1 (GESLA-1)" (Menéndez and Woodworth, 2010). GESLA-1 comprises a total of 675 individual tide gauge records with 21,197 station-years of data. This dataset was subsequently extended with a further almost decade of data to develop GESLA Version 2 (GESLA-2), which has 1,355 station recordings and 39,151 station-years of information with a temporal resolution of 1-hour (Woodworth et al., 2016).

A number of regional and global studies have been undertaken based on the GESLA-2 tide gauge dataset for various coastal applications. Previous studies include global extreme sea level uncertainties (Wahl et al., 2017), storm surge construction and extreme sea level estimation in South East Asia (Cid et al., 2018), validation of a coastal database

for the Mediterranean region (Wolff et al., 2018), analysis of tidal variability along North Atlantic coasts (Devlin et al., 2019), validation of the sea level impacts on tidal characteristics around Australia (Harker et al., 2019), and development of a global tidal constants database (Piccioni et al., 2019).

2.2.7 Methods to Estimate Extreme Sea Levels

Extreme sea levels, as with most extreme events, can be expressed in terms of the return periods of the events. Here, an extreme sea level with a return period of, for example, 100 years is the event which could be expected to occur once in 100 years. The reciprocal of this value is the probability of occurrence (0.01 in this case). Although there is not a universally accepted approach to determine extreme sea levels (Arns et al., 2013), the most common approach is to apply Extreme Value Theory (EVT). EVT requires an analysis of the probability of occurrence of maxima of the sea levels, obtained from historical recordings or hindcasts. Two methods are commonly applied to determine maxima: block maxima (e.g. annual maxima) and the peaks over threshold methods (Coles, 2001).

Coles (2001) has shown that block maxima data (i.e. data for which maxima from blocks of time are selected) will follow a General Extreme Value (GEV) probability distribution. The GEV is a three-parameter probability distribution. The distribution function (G) for the GEV can be defined as in Eq. 2.3.

$$G(z) = \exp\left\{-\left[1+\xi\left(\frac{z-\mu}{\sigma}\right)\right]^{\frac{-1}{\xi}}\right\} \tag{2.3}$$

defined on the set $\{z : 1+\xi(z-\mu)/\sigma > 0\}$ where the parameters satisfy $-\infty < \mu < \infty$, $\sigma > 0$ and $-\infty < \xi < \infty$. Here, μ is the location parameter, σ is the scale parameter and ξ is the shape parameter.

A simplification of this approach is to fit the two-parameter (i.e., location μ and scale σ) Gumbel distribution given in Eq.2.4 to annual maxima data. Here, ξ (shape) parameter is set to zero.

$$G(z) = \exp\left[-\exp\left\{-\left(\frac{z-\mu}{\sigma}\right)\right\}\right] \tag{2.4}$$

Estimates of extreme quantiles of the annual maximum distribution are then obtained by the Eq. 2.5

$$z_p = \begin{cases} \mu - \frac{\sigma}{\xi}\left[1 - y_p^{-\xi}\right], & \xi \neq 0 \\ \mu - \sigma \log y_p, & \xi = 0 \end{cases} \tag{2.5}$$

where $y_p = -\log(1-p)$ and $G(z_p) = 1 - p$. Here, z_p is defined as the return level associated with the return period $1/p$ and the level z_p can be approximated to be exceeded on average once every $1/p$ years.

The Gumbel distribution can be fit to annual maxima values from the sea levels comprised of surge and tide components (Wahl et al., 2017). For example, Muis et al. (2016) calculated extreme sea levels from modelled surge and tide heights using a Gumbel distribution with annual maxima data. Wahl et al. (2017) used a Gumbel distribution as well as other forms to be fitted to GESLA-2 tide gauge dataset.

An alternative to annual maxima is to include several maxima levels (r-largest method) from each block. As the GEV has an additional fitting parameter compared to the Gumbel distribution, it will generally fit the data better. The GEV has been applied to both r-largest and block maxima sea levels in the literature ((e.g., Menéndez and Woodworth, 2010; Vitousek et al., 2017; Wahl et al., 2017)).

One of the strengths of block maxima approaches is that it is relatively easy to show that the data are statistically independent (a requirement of EVT). That is, each maximum is clearly associated with a separate meteorological event. However, the use of annual maxima means that there are generally relatively few points in the resulting probability distribution function (e.g. 30 values for a 30-year time series). An alternative which can address this issue is the peaks-over-threshold (POT) method, which considers all independent storm peaks that are above a defined threshold level. There is no globally accepted threshold selection method although there are some rule-of-thumb methods (Coles, 2001) or the use of a higher percentiles of the data. Data selected from a peaks-above-threshold (POT) approach can be shown to follow a Generalized Pareto Distribution (GPD) as the distribution function given in Eq.2.6.

$$H(y) = 1 - \left(1 + \frac{\xi y}{\bar{\sigma}}\right)^{\frac{-1}{\xi}} \tag{2.6}$$

defined on $\{y : y > 0 \text{ and } (1 + \xi y/\sigma) > 0\}$ where $\bar{\sigma} = \sigma + \xi(u - \mu)$.

The GPD family has two variations: 3-parameter Generalized Pareto Distribution (GPD) (location, scale and shape) and the 2 parameter Exponential Distribution (EXP) (location and scale). EXP becomes as in Eq. 2.7 with $\xi = 0$.

$$H(y) = 1 - \exp\left(-\frac{y}{\bar{\sigma}}\right),\ y > 0, \tag{2.7}$$

Recent studies adopting the GPD approach to determine extreme sea levels include: for various regional studies such as for the contiguous coastline of the US (Buchanan et al., 2017; Tebaldi et al., 2012) south coast of Sweden (Fredriksson et al., 2016) and for global analyses (Rasmussen et al., 2018; Wahl et al., 2017). Recently, Rasmussen et al. (2018) also conducted a quasi-global analysis of changes in the frequency of extreme sea levels using the University of Hawaii Sea Level Center tide gauge locations using the GPD. The Exponential Distribution is widely used for many environmental studies, although the method has had only limited application for sea level extremes. A few examples include: the study of (Bardet et al., 2011) for the French coastline and (Proske and Gelder, 2006) for the Dutch North-Sea.

EVT analyses such as those described above have uncertainties associated with how well the chosen probability distribution function fits the data and the extent to which the data must be extrapolated to obtain the desired return period (i.e. obtaining a 100-year return period from 30 years of data). Hence, the uncertainties associated with the chosen extreme value analysis methods can be large. These uncertainties are exacerbated when the uncertainty associated with projected means sea level rise is added. A global analysis of the uncertainty may be necessary to prevent maladaptation of the coastal communities (Hinkel et al., 2015; Jones et al., 2014; Wahl et al., 2017). In a global study of the uncertainties of the extreme sea level methods and models, Wahl et al. (2017) investigated the uncertainties across 20 different extreme value models. These models include the Generalized Extreme Value Distribution with r-largest methods and the Generalized Pareto Distribution fitted to peaks over threshold data and applied to quasi global tide gauge records. They found that the 5%-95% uncertainty spans at many sites along the US west coast, South America, Mediterranean, and parts of Australia extend from less than 10 cm to more than a meter at US east coast, East Asia and northern Europe. This study shows that narrowing the span of uncertainties is a crucial step for conducting global sea level extreme analyses that are impacting adaptation assessments.

2.2.8 Effects of Sea Level Change on Extreme Sea Levels

One of the significant impacts of sea level rise on the extreme sea levels is that the frequency of flooding events will increase. In other words, due to projected sea level rise, the return period of a given extreme sea level could be reduced significantly by 2100. The return periods of extreme sea levels have already changed in recent decades due to

sea level rise and there is good evidence this will continue in the future (Oppenheimer et al., 2019).

To date, there have been regional, national and global studies that indicate that the extreme sea level frequency is increasing due to increasing sea levels. Densely populated cities, e.g. New York City, are particularly vulnerable to such increase of flooding frequency and attract high attention. Cooper et al. (2008) found that the New Jersey area in 2100 with a benchmark values of 4 ft (1.22 m) is predicted to be flooded 20 times more frequently compared to the presence day. Tebaldi et al. (2012) investigated the impact of sea level rise on extreme sea levels and frequencies at the coastlines of the United States, with the majority of locations showing substantially higher frequency of previously rare storm-driven water heights in the upcoming decades. Sweet and Park (2014) documented that nuisance flooding (that is lesser extremes) is increasing and varying spatially due to sea level rise and its distribution along US coasts. Garner et al. (2017) indicate decreasing return periods in a similar pattern: what used to be a 500-year flood height had reduced to 25-years in 2017. It was predicted to decrease further to 5-years by the mid-21st century. Reed et al. (2015) also indicate that what used to be 500-year return period flood has now become as frequent as a 25-year return period flood for New York City. Church et al. (2006) studied extreme sea level frequency along the coast of Cairns, Australia, finding the 100-year return period flood event will decreased to a 40-year event for the 2050s, assuming a modest sea level rise (from past sea level data) and a possible cyclone intensity change. They also predict 0.2 m of SLR and a 10% increase in storm wind speeds. Paprotny and Terefenko (2017) reported that an 0.5 m sea level rise will double the number of inhabitants and assets flooded in Poland while 1 m of sea level rise will triple the impact, in a 100-year flood zone. Buchanan et al. (2017) estimated a median 40-fold increase in the expected annual number of 100-year floods for tide gauge locations along the contiguous US coastline by 2050 and 3467-fold increase by 2100 under RCP 8.5. Recent improvements in computational power have made global assessments of extreme sea level and SLR impacts possible. A recent global study conducted by Vitousek et al. (2017) concluded that by 2050, in the tropics, 10 to 20 cm sea level rise will double the frequency of flooding. According to the IPCC SROCC Chapter 4 (Oppenheimer et al., 2019), sea level rise is clearly affecting the frequency of extreme sea levels. Further, the most affected locations are concentrated in low latitudes where historical sea level variability due to tides and surges is lower. Therefore, sea level variations, and sea level rise needs to be carefully assessed over the next century, as studies indicate that even smaller increases in sea level may result in significant consequences.

2.3 Previous Studies on Coastal Flooding Hazard Assessments, Exposure and Risk Analysis

Increases in exposure due to coastal flooding hazards may have massive and irreversible consequences in the future, unless necessary adaptation and mitigation measures are taken. These impacts can be determined from the population exposed to extreme sea levels and the assets (infrastructure, transportation facilities etc.) affected in the coastal zone and the economic consequences. Therefore, economic impact and risk assessment, which depends on extreme sea levels, climate change driven sea level rise or a combination of both is of significance from a socio-economic point of view. Within the scope of such assessments, the "flood risk" can be defined as the product of the following parameters: "hazard", which is the probability of a flood event, "exposure", which can be defined as the population and value of assets subject to flooding and "vulnerability", which is the capacity of a society to deal with the event (Jongman et al., 2012; Kron, 2005). The coastal impact analyses aim to identify the areas which may experience the highest increases in the flooding risks.

In this section, previous studies on coastal flooding hazard assessments, population and asset exposure analyses, the DIVA model and future adaptation implications are explained in detailed.

2.3.1 Coastal Flooding Hazard Assessments

Coastal flooding occurs due to unusual sea levels [i.e. extreme sea levels and hazards can here be defined as the threat posed by natural processes that cannot be influenced (Kron, 2013)] in this thesis, defined as extreme sea levels. As a result of projected climate change induced sea level rise, the frequency of coastal extremes is estimated to increase, which will result in an increase of the episodic flooding frequency and flooding extent in low-lying coastal areas. Therefore, it is important to understand and accurately estimate the coastal flooding hazards in order to assess coastal flooding risks. Many national and quasi-global to global extreme sea level analyses have been conducted with or without considering the change of storminess and sea level changes. These studies have used either hindcast models or actual recordings. Globally, extreme sea levels have been determined from model results (Muis et al., 2016; Rueda et al., 2017; Vitousek et al., 2017; Vousdoukas et al., 2018b) and from extensive tide gauge records (Menéndez and Woodworth, 2010; Wahl et al., 2017). These studies present global variations and frequencies of extreme sea levels, highlighting the significance of extreme sea levels both for present and future climatic conditions.

2.3.2 Coastal Flooding Exposure Analyses

Sea level extremes, mainly generated by storms and wave action, have significant impacts with respect to coastal vulnerability and to efforts that are taken to increase the resilience of the affected coastlines. McGranahan et al. (2007) emphasize the fact that although the low elevation coastal zone accounts for only about 2 per cent of the world's land area, about 10 per cent of the world's population live in this zone. Therefore, while projected sea level rise will have impacts on future extreme sea levels, depending on the future atmospheric and oceanic climate variations, future socioeconomic scenarios might be as important as the climatic changes in determining the vulnerability to the coastal flooding. Recent studies show that socioeconomic changes alone can have significant impacts on coastal flooding exposure (Hauer et al., 2016; Jongman et al., 2012). By 2050, for instance, projected socio-economic change alone will increase the average global expected annual damage almost ninefold (Hallegatte et al., 2013). To this end, efforts to quantify future socioeconomic development is important in identifying projected risk. Shared Socioeconomic Pathways (SSPs), as extensively described by Riahi et al. (2017), comprise five alternative socioeconomic development scenarios and a set of driving forces that quantifies energy and land-use developments and associated uncertainties for greenhouse gas and air pollutant emissions by 2100. Such socioeconomic development assessment allows further determination of the necessary adaptation and impact dimension. These SSP scenarios have also been used with the new generation of earth system models as part of the 6^{th} climate model intercomparison project (CMIP6) (O'Neill et al., 2016).

Hallegatte et al. (2013) determined the present (2005) and future coastal flood losses for the world's 136 largest coastal cities accounting for present (2005) and future coastal flood defences and considering combinations of future sea level rise scenarios and socioeconomic changes as well as a variety of adaptation approaches. The findings show that the average global flood losses will increase by $ 46 billion US with socioeconomic changes alone by 2050, and that existing coastal protection needs to be upgraded to avoid losses of more than $ 1 trillion US. Hinkel et al. (2014) conducted global scale coastal flood damage and adaptation cost analyses by taking into account SLR scenarios from a variety of climate models, topographic data (Shuttle Radar Topographic Mission, SRTM; and Global Land One-kilometre Base Elevation, GLOBE) and population data (Global Rural–Urban Mapping Project, GRUMP and LandScan) and determined the required adaptation with two different approaches (taking dike height constant and increasing dike height with respect to socioeconomic changes). This study shows that, without adaptation, 0.2-4.6% of the global population is expected to be exposed to coastal flooding annually in 2100 with corresponding expected annual damage reaching as high as

0.3-9.3% of global gross domestic product.

2.3.3 Coastal Flood Risk and Impact Analyses based on DIVA Model

Introduced by Vafeidis et al. (2008), the Dynamic and Interactive Assessment of National, Regional and Global Vulnerability of Coastal Zones to Climate Change and Sea-Level Rise (DINAS-COAST) project developed the Dynamic Interactive Vulnerability Assessment (DIVA) database consisting of physical, ecological, and socioeconomic parameters. The database covers the world's coast with 12,148 segments, excluding Antarctica. The dataset includes, for example, population, land use and surge height data (Vafeidis et al., 2008). The DINAS-COAST project is designed specifically for impact and vulnerability analysis under sea-level rise scenarios. The project produced the DINAS-COAST Extreme Sea Levels (DCESL) dataset, which was the only global dataset that provided global extreme sea levels for over a decade (Muis et al., 2017). A number of coastal flood risk (Brown et al., 2013; Hinkel et al., 2010, 2012, 2014; Nicholls et al., 2010) and impact analysis studies (Hallegatte et al., 2013; Jongman et al., 2012; Muis et al., 2015; Sugiyama et al., 2008; Ward et al., 2011) were conducted based on DCESL via the DIVA model.

Muis et al. (2016) have introduced the Global Tide and Surge Reanalysis (GTSR) dataset consisting of a global surge and tide timeseries for the 1979-2014 period. This dataset was based on DIVA database coastal locations, refining them into 16,611 points. The study analysed the time series for the given period, determined the global extreme sea levels based on the constructed time series and validation against a quasi-global tide gauge network (University of Hawaii Sea Level Centre dataset). The GTSR dataset and the tide gauge sea levels were found to be in good agreement both for the timeseries and the extremes that were derived from them. The dataset was used to determine the 1 in a 100-year coastal flooding which was shown to potentially affect approximately 1.3% of the world population. There have been a number of regional assessments conducted based on the DIVA database. Hinkel et al. (2010) analysed the risks of and adaptation to, sea level rise in the European Union (Hallegatte et al., 2011) as an application of the DIVA model. Wolff et al. (2016) investigated Sea Level Rise (SLR) related coastal flood impacts in Italy using the DIVA dataset. Barnard et al. (2019) estimated the climate driven coastal flood hazard exposure for California, USA, impacting more than 6% of the state's Gross Domestic Product (GDP) and 600,000 people by dynamic flooding (i.e. integrating the effects of SLR, tides, waves, storms, and coastal change) by 2100. Recently, Fang et al. (2020) have studied the potential damage and adaptation costs for China using the DIVA framework.

2.3.4 Previous Studies on Coastal Flood Risk Assessment

Flood risk, in general, can be defined as the combination of the hazard, exposure and vulnerability of an area of interest (Kron, 2013). Here, flood risk, or expected annual damage, can be defined as the cumulative area under the exceedance probability and damage curve (Muis et al., 2015). This can be applied both to the exposed population and exposed assets underlying a flood area. Assessing only one return period would not be enough to analyse the consequences of the flooding of an area. Instead, expected annual damage takes into account the mean annual loss across all possible extreme sea levels, and depends on the protection levels (Hallegatte et al., 2011).

Regional, national and global levels of coastal flood risk have been investigated. Hallegatte et al. (2011) investigated the average annual loss values for Copenhagen, introducing a new economic input-output model (ARIO) and concluded that the protection heights decrease the annual average losses for Copenhagen from several billion Euros to 100,000 Euros per year for 180 cm protection, and to zero for protection levels higher than 200 cm. Muis et al. (2015) have investigated the future flood risk for Indonesia, applying a method enabling the probabilistic analysis of future trends (Wolff et al., 2016) in national-level flood risk. They showed that the exposure will increase the coastal flood risk by 120% while sea level rise would increase flood risk trend by 19% - 37%. Nicholls (2004) has analysed the range of global mean sea level rise and socioeconomic scenarios for changes in flooding by storm surges through the 21^{st} century. Depending on the future coastal defence applications and GDP trends, the annual population affected by coastal flooding would be lower than 1 million people per year. However, for the A2 scenario (Special Report on Emissions Scenarios-SRES), which is comparable to RCP 8.5 scenario from IPCC Assessment Report 5, the affected population would increase by up to 18-30 million per year adding an additional 29-50 million people per year for the worst-case scenario. Hanson et al. (2011) determined the population and asset exposure for the world's large port cities under a 1 in a 100-year event. The authors showed that, (in 2005), 0.6% of the global population and assets valued at around 5% of the global GDP were exposed to coastal flood events. It is shown that the combined effects of sea-level rise, subsidence, population growth and urbanisation could exacerbate future population exposure as much as three-fold. In addition, asset exposure would increase ten times compared to the situation at the time of the study. Hallegatte et al. (2013) have determined the average annual loss for 136 coastal cities determining the annual loss changes with varying scenarios of future adaptation. They reported that without adaptation, there would be an increase from $6 billion US to more than $1 trillion US in average global annual loss due to socioeconomic change, climate change and subsidence.

This result highlights the significance of adaptation and the strategies to develop for vulnerable coastal cities.

2.3.5 Coastal Adaptation

Among the extreme sea level and sea level rise impact studies, a substantial number conclude that there is a need for coastal adaptation for the upcoming century to respond both to climatic and socio-economic changes (e.g., Hallegatte et al., 2013; Hinkel et al., 2014). In the literature, the methods for the application of future coastal adaptation includes (i) keeping extreme probabilities constant by enhancing the coastal protection corresponding to sea level rise and (ii) keeping flooding risk constant by enhancing coastal protection measures both to account for sea level rise and socio-economic changes. For example, Hallegatte et al. (2013) applied adaptation strategies to maintain the flood probability by increasing dike heights and maintaining the flood risk by reducing the flood probability with respect to the socioeconomic and sea level rise scenarios for the future. Hinkel et al. (2014) equated the cost and benefit functions in order to determine the needed increase in height of coastal defences and the economic costs of adaptation. Tamura et al. (2019) assumed an increase to the presently built coastal defence structures as 1 m to identify the changes in the flooding extents and found a 40% reduction in the inundated area compared to no-adaptation baseline under the same RCP (2.6, 4.5 and 8.5). Nicholls et al. (2019) have reported the global adaptation costs for the 21^{st} century to be as much as US $18.3 trillion. The studies show significant impacts of future adaptation measures for the potential increase of the extreme sea levels in the next century.

Chapter 3

Detailed Descriptions of Datasets Used in this Study

A number of datasets are implemented in this thesis in order to determine historical timeseries, extreme sea levels, coastal inundation and present and future population and asset exposure. To construct the historical time series as described previously, as in Eq. 2.2, surge, tide and wave hindcast datasets (to compute the wave setup) were required at DIVA coastal locations. Both historical timeseries and computed extreme sea levels are validated against the sea level recordings of at the tide gauges. Coastal flooding heights are datum-corrected and translated to the global topographic elevations. The coastlines are represented by a global coastline dataset to be consistent with all the other datasets used. Present exposed population and assets are obtained from global gridded datasets of population and Gross Domestic Product, respectively. To account for the future population and asset exposure and damage, projected gridded population and GDP data are required. The following sections describe the datasets used to obtain each of the requirements outlined above.

3.1 GTSR – Global Tide and Surge Reanalysis (Surge)

The time series of coastal storm surge values were obtained from the GTSR dataset introduced by Muis et al. (2016) over the period (1979–2014). This dataset was generated with the Global Tide and Surge Model (GTSM), which uses the Delft3D Flexible Mesh software developed by Deltares (Kernkamp et al., 2011), with a locally refined computational grid having unstructured grid cell sizes of ∼50 km in deep ocean reducing to ∼5 km in the shallow areas. The model was forced with wind fields from ERA-Interim developed by The European Centre for Medium-Range Weather Forecasts (ECMWF) (Dee et al., 2011). The wind fields originally have 6 hr temporal and 0.75° x 0.75° spatial resolution commencing from year 1979. The wind fields were downscaled using linear interpolation to a temporal resolution of 10 minutes which ensures a smooth variation in values on the required time-scale. The updated version of this dataset is also available (Muis et al., 2020).

3.2 FES2014 - Finite Element Solution (Tide)

Global tide data were obtained from the latest series of the FES atlas series, namely, Finite Element Solutions 2014 version (FES2014) which is a finite element hydrodynamic model solving the tidal barotropic equations and assimilating in-situ tide gauge and altimeter data (Carrere, Lyard, Cancet, Guillot, Picot, FES 2014, a new tidal model - Validation results and perspectives for improvements, 2016). The global model has a total of 2.9M nodes and a spatial resolution of 1/16°, having an increased mesh resolution and refined tidal height specifically in coastal areas (Piccioni et al., 2018). Nonlinearity in the dynamic equations and resonant and near-resonant responses enhance the challenges of tidal analysis in coastal regions (Andersen, 1999; Seifi et al., 2019). In particular, it is challenging to model tides in shallow water since the tidal range is larger and the tidal waves show complex behaviour in such regions. Bathymetry, the shape of the shelf and the regional tidal regime have significant impact on the shallow water constituents (Andersen, 1999).

3.3 ERA-Interim and GOW2 (Wave Setup)

In order to determine the wave setup, (WS), the nearshore (deep-water) wave conditions (significant wave height, and wavelength) are required. As there is no widely validated and accepted global nearshore wave model dataset, both ERA-Interim (Dee et al., 2011)

and GOW2 (Perez et al., 2017) were tested for this purpose. In the present analysis, the spectral wave parameters, that are H_S and T_p, have been used from both datasets.

ERA-Interim and GOW2 are global surface wave model reanalyses. These have been used to provide deep water wave condition to estimate wave setup. ERA-Interim (ERA-I) is a global atmospheric reanalysis from 1979 (Dee et al., 2011). ERA-I uses the ECMWF Cy31r2 atmospheric model coupled with the WAM spectral wave model (Janssen, 2008). Both the atmospheric model and the wave model used in ERA-I incorporate satellite data assimilation. Output from the model is available at 0.70 global resolution. The temporal resolution of ERA-I is 6 hours. GOW2 (Perez et al., 2017) is a global wave model hindcast. It uses the Wavewatch III (Tolman et al., 2009) model Version 4.18, forced with Climate Forecast System Reanalysis (CFSR) winds (Saha et al., 2010). The hindcast is designed to provide higher resolution coastal wave data and hence uses a system of nested grids of resolution 0.5° in deep water, with finer scale ∼25km resolution in areas with water depths less than 200m. The temporal resolution of the dataset is 1 hour. In contrast to ERA-I which has satellite assimilation in both the wind and wave models, GOW2 has only assimilation in the forcing wind field. GOW2 hindcast data are available over the period 1979-2015.

3.4 IPCC AR5 Regional Relative Sea Level Rise (Mean Sea Level Change)

The change of $ESLs$ in the future, i.e., ESL^F, are calculated by adding the regional relative sea level rise ($RSLR$) values taken from Church et al. (2013a) (Fig. 13.20—`https://icdc.cen.uni-hamburg.de/1/daten/ocean/ar5-slr.html`) for IPCC Representative Concentration Pathways (RCP) 4.5 and 8.5. The contributions of the regional sea level change consist of 10 different geophysical sources: Greenland dynamic ice and surface mass balance, Antarctic dynamic ice and surface mass balance, and glaciers; dynamic sea surface height, global thermosteric sea surface height anomaly, and the inverse barometer effect from the atmosphere; land water storage (terrestrial water); and glacial isostatic adjustment (GIA) which was given as a change in sea level relative to land (Church et al., 2013b). The thermosteric/dynamic sea surface heights are determined from an ensemble of 21 Atmosphere–Ocean General Circulation Models (AOGCMs).

3.5 GESLA-2 – Global Extreme Sea Level Analysis Version 2 (Tide Gauge data)

The validity of constructed historical timeseries and computed extreme sea levels is required to be tested against recordings of tide gauge dataset that is also sufficiently scattered among global coastlines to account for the datasets used in this thesis. GESLA-2 (Woodworth et al., 2016) is such a dataset comprised global tide gauge observations. Although some of the tide gauges go back more than 100 years, the vast majority of the data are from 1950 onwards. Data are generally archived at a temporal resolution of 1 hour or less and are available at a total of 1,355 stations. As the dataset has varying vertical datums depending on the location, and to eliminate the multidecadal variations of sea levels, annual mean values were subtracted from the timeseries for each calendar year, following a similar approach as Muis et al. (2016) and Wahl et al. (2017). In the present analysis a total of 681 unique locations with total water level data over the required period were used to validate the various model results.

3.6 DIVA - Dynamic Interactive Vulnerability Assessment (Output locations Coastal Protection)

A detailed description of and existing literature on DIVA dataset is given in Section 2.3.3. As mentioned previously, DIVA (Hinkel and Klein, 2009; Vafeidis et al., 2008) is a database for assessing coastal vulnerability from sub-national to global levels. Here, 9,866 DIVA locations have been used as the reference output locations for model results. In addition, coastal protection data in the form of design return periods were taken from the DIVA database. These return period values were assumed to follow a given extreme value probability distribution function. To estimate the corresponding coastal protection levels at each DIVA location, the coastal protection return periods given in this dataset are converted to the elevation values.

3.7 MERIT DEM- Multi-Error-Removed Improved-Terrain DEM (Topography)

Land topography and digital elevation model (DEM) accuracy plays a vital role for coastal inundation computations. The Shuttle Radar Topographic Mission (SRTM) (Jarvis et al., 2008) is a quasi-global and satellite-based DEM implemented widely in global calculations of coastal flooding (Hinkel et al., 2014; Muis et al., 2016). However,

SRTM does not include the bare terrain information rather it provides information on the elevations (Kulp and Strauss, 2016) which can be imaged from space. Therefore, it is known to have large vertical errors in densely populated urban or densely vegetated areas. These errors may result in misleading coastal flood exposure outcomes (Kulp and Strauss, 2016).

MERIT DEM (Yamazaki et al., 2017) is a high accuracy global digital topographic dataset at 3 arc sec resolution (∼90m at equator) developed from existing spaceborne DEMs [SRTM3 v2.1 and AW3D-30m v1 (Farr et al., 2007; Tadono et al., 2015)] by eliminating major error components from the existing DEMs. The MERIT DEM data covers lands between 90°N-60°S, vertically referenced to the EGM96 geoid. In this thesis, MERIT DEM data is implemented to determine inundation extents due to extreme sea levels and sea level rise.

3.8 MDOT – Mean Dynamic Ocean Topography (MERIT DEM datum)

Hindcast historical time series constructed in this study, are used to determine extreme sea levels. These values are referenced to mean sea level, whilst the DEM data (MERIT) datum is the EGM 96 geoid (Yamazaki, et al., 2017). In coastal flooding calculations, it is essential to bring the extreme sea level and land topography to the same datum. Therefore, in this study, Mean Dynamic Ocean Topography (MDOT) (Rio et al., 2014) is used to account for the vertical datum difference between the extreme sea levels and the MERIT DEM data, where the MDOT is the difference between the time-averaged sea surface and the geoid.

3.9 GSHHG - Global Self-consistent Hierarchical High-resolution Geography (Coastline)

In this thesis, a number of datasets are brought together to determine the coastal flooding exposure analyses. These datasets (such as land topography, gridded population GDP etc.) have various original resolutions and data extent. To ensure consistency, a global high-resolution shoreline mask is implemented: GSHHG (Wessel and Smith, 1996) which is a coastline dataset at multiple resolutions. Here, the "high resolution" (∼0.2 km) coastline dataset was used to define the global coastline for calculations of flooding extent.

3.10 GPWv4 Rev.11 – Global Population (Population and Asset Exposure & Flood Risk)

Global coastal flooding can be translated into population exposure using a gridded global population dataset with sufficient resolution to account for the coastal population affected. In this thesis, the GPWv4 Rev.11 database is adopted, which is the NASA Socioeconomic Data and Applications Center (SEDAC) (Center for International Earth Science Information Network (CIESIN), 2018) represent the population count from 2010 census with 30 arc sec. (∼1 km at equator) spatial resolution. The data has been extrapolated to a range of years. This dataset was implemented to determine population and assets potentially exposed to flooding using 2015 population estimates.

3.11 GDP – Gross Domestic Product (Asset Exposure & Flood Risk)

Gross Domestic Product (GDP) "measures the monetary value of final goods and services—that is, those that are bought by the final user—produced in a country in a given period of time" (Callen, 2020). Gridded GDP data provides a necessary parameter in determining the value of assets exposed to flooding. The dataset is based on best available areal averages and is a combination of sub-national and national data. The present analysis implements the gridded 2015 GDP data (Kummu et al., 2018) that consists of national and sub-national GDP data on a 30-arc sec (∼1 km at equator) grid.

3.12 SSPs – Shared Socioeconomic Pathways (Future Population and Asset Exposure & Flood Risk)

To account for future socioeconomic impacts, Shared Socioeconomic Pathways (SSPs) (O'Neill et al., 2014) were developed to combine the future radiative forcing and their associated climate changes with plausible and alternative pathways of 5 different socioeconomic storylines (SSP1-5). As noted by Vuuren and Carter (2014), the RCPs and SSPs may be coupled with each other. As such, RCP 4.5 is consistent with SSP1 and RCP 8.5 is consistent with SSP3 and SSP5. In the present analysis, the future projections of the impacted populations were calculated at 2050 and 2100 for SSP1, SSP3 and SSP5 narratives from the gridded data of Gao (2017), which is an enhanced version of the data proposed by Jones and O'Neill (2016). The global projections of the GDP data are obtained from IIASA (Riahi et al., 2017) (`https://tntcat.iiasa.ac.at/SspDb/`).

The population and GDP data are translated into future population and asset exposure as well as future coastal flood risk in 2050 and 2100.

Chapter 4

Projections of global-scale extreme sea levels and resulting episodic coastal flooding over the 21st Century

This chapter is based on the article of Kirezci et al. (2020) published in the Nature Scientific Reports. This study can be summarised as follows.

Global models of tide, storm surge, and wave setup are used to obtain projections of episodic coastal flooding over the coming century. The models are extensively validated against tide gauge data and the impact of uncertainties and assumptions on projections estimated in detail. Global "hotspots" where there is projected to be a significant change in episodic flooding by the end of the century are identified and found to be mostly concentrated in north western Europe and Asia. Results show that for the case of, no coastal protection or adaptation, and a mean RCP8.5 scenario, there will be an increase of 48% of the world's land area, 52% of the global population and 46% of global assets at risk of flooding by 2100. A total of 68% of the global coastal area flooded will be caused by tide and storm events with 32% due to projected regional sea level rise.

4.1 Background

Sea level rise is a well-accepted consequence of climate change (Church et al., 2013a; Milne et al., 2009; Nicholls and Cazenave, 2010). Although the focus of the general public often tends to be on the rate and magnitude of increase in mean sea level, the major threats of coastal flooding and erosion are significantly impacted by episodic storm surge and wave setup (the temporary increase in mean water level due to the presence of breaking waves) as well as their time of occurrence in relation to astronomical tide (Marcos et al., 2019). As approximately 600 million people live in low elevation coastal zones [i.e. LECZs – coastal regions less than 10 m above mean sea level (MSL)] which generate approximately US$1 trillion of global wealth (Hallegatte et al., 2013; McGranahan et al., 2007; Milne et al., 2009; Vitousek et al., 2017), both the environmental and socio-economic impacts associated with episodic coastal flooding can be massive.

Both national and global assessments of projected coastal flooding due to the combination of extreme events and sea level rise are critical in informing policy directions, as detailed in a number of IPCC reports. Such large-scale assessments can also identify regional "hot-spots" where more detailed modelling is required. The time and space scales involved in such large-scale assessment are challenging. The time scales vary from the duration of individual storms (of order hours) to projections over the coming century (of order decades). The physical scales are also demanding, varying from the bathymetry of individual beaches (10s of metres) to basin-scale storms to global comparisons of potential impacts (1000s of kilometres). As a result, to form tractable solutions and guide such policy development, a variety of simplifying assumptions must be made. This study aims to undertake such an analysis. It assembles extensive model and measured datasets at coastlines around the world and combines these to provide projections of global extreme sea level and coastal flooding by 2100. The required simplifications may result in local errors but comparisons with recorded tide gauge data indicates that, to first-order, the simplified model adopted reproduces extreme sea levels to reasonable accuracy at national and global-scale. The Sections 4.13 and 4.14 provide a summary of the simplifications necessarily adopted to undertake this analysis and their potential implications.

In order to determine the frequency and magnitude of episodic coastal flooding, it is first necessary to determine sea levels during extreme storm events. The resulting extreme sea levels are generally made up of four components: tide (T), storm surge (S), wave setup (WS) and regional relative sea-level rise ($RSLR$). Projections of future coastal flooding require not only knowledge of the magnitude of each of these physical processes, but also their relative timing (i.e. does the storm occur at high tide) and an understanding of the probability of occurrence of extreme events. A number of recent studies have considered

some of these elements, with and without validation against recorded data (Melet et al., 2018; Muis et al., 2016; Rueda et al., 2017; Vitousek et al., 2017; Vousdoukas et al., 2018b).

Consistent with previous global-scale studies (Melet et al., 2018; Muis et al., 2016; Rueda et al., 2017; Vitousek et al., 2017; Vousdoukas et al., 2018b), it is assumed the total sea level (TSL) can be approximated by the linear summation given in Eq. 2.2.

The historical TSL estimates are rigorously validated against extensive global tide gauge data both for the historical record and for statistical extreme values. The term extreme sea level (ESL^{H100}_{T+S+WS}) is used here to represent the value of the TSL which occurs, for example, once in 100 years (a return period of 100 years). The superscript "H" signifies the extreme value is determined from the historical record, as opposed to a future projection and the subscript ($T + S + WS$) designates the physical processes considered in the determination of the extreme. For brevity, if the subscript is excluded, it signifies the use of all three processes ($ESL^{H100} \equiv ESL^{H100}_{T+S+WS}$). To obtain future projections, the extreme value estimates of TSL are coupled with global projections of RSLR for IPCC Representative Concentration Pathways (RCPs) 4.5 and 8.5. The resulting projected future extreme sea levels (ESL^{F100}) are then used in conjunction with global topographic data to assess the potential extent of episodic coastal flooding at global scale in 2050 and 2100. As the projected flooding is sensitive to both how well the model dataset represents the physical processes and the appropriateness of the extreme value probability modelling, both of these elements are validated in detail (see Sections 4.7 and 4.10).

The global distribution of episodic coastal flooding is then used to determine global coastal flooding "hotspot" regions, where a significant increase in flooding is projected over the coming century. The relative contributions of each of the individual processes to coastal flooding are also assessed (i.e. surge, tide, wave setup and relative sea level rise), as are the projected changes in probability of occurrence of episodic flooding events in the future. Finally, we estimate the total population and value of exposed assets at risk both at present and in the future (2050 and 2100).

As noted above, as our focus is on an assessment at the global-scale, a number of local processes must be represented using approximations to render the problem tractable. We consider the limitations of these approximations and, where possible, estimate the sensitivity of the results to the inherent assumptions (see Section 4.13). Statistical uncertainties associated with the projections are also estimated (see Section 4.13).

This study builds on previous studies of global-scale sea level rise. Importantly, the present study considers all three major processes, T, S and WS. It quantifies the relative importance of each of S, WS and $RSLR$ processes to episodic coastal flooding by 2100. The modelling approach is extensively validated against tide gauge data for both ambient and extreme conditions. Extreme value estimates require statistical extrapolation of the data which can result in large confidence limits on estimates. The extreme value estimates are considered in detail, comparisons with recorded data undertaken and confidence limits estimated. Finally, the sea level rise estimates are determined to understand episodic coastal flooding extent, the populations impacted and the assets potentially at risk. Within the assumptions required to make such a global-scale study possible, it provides a "first-order" analysis forming a basis for future policy development.

4.2 Analysis Process

In this section, the methods and processes used to estimate future flooding extent, populations impacted and assets exposed are discussed.

Consistent with the linear assumption Eq. 2.2, the time series of T [Fig. 4.1(a)], S [Fig. 4.1(b)] and WS [Fig. 4.1(c)] obtained from the respective datasets were interpolated to a consistent 10-minute temporal resolution and assigned to the closest DIVA point (Section 4.3)(see Fig. 4.2 for DIVA points). This generated an historical time series of $TSL(t)$ at each point. The WS was estimated using both the SPM approach (SPM, 1984) and Stockdon et al. (2006), both GOW2 and ERA-I wave models were tested with a range of different bed slopes. The Stockdon et al. (2006) approach is more sensitive to bed slope but for plausible bed slopes (i.e. $< 1/30$) consistent with SPM (1984) (e.g. see Fig. 4.18). Based on subsequent global comparisons with tide gauge data, a bed slope of 1/30 was adopted with the SPM approach (Sections 4.4 and 4.5). The root mean square error ($RMSE$) was used to test the consistency of these model-derived time series at each location against tide gauge data [Fig. 4.1(f)] for ambient conditions (Section 4.5). The performance of the model results for extreme conditions was also tested by comparing upper percentile values with the tide gauges [Fig. 4.1(f)].

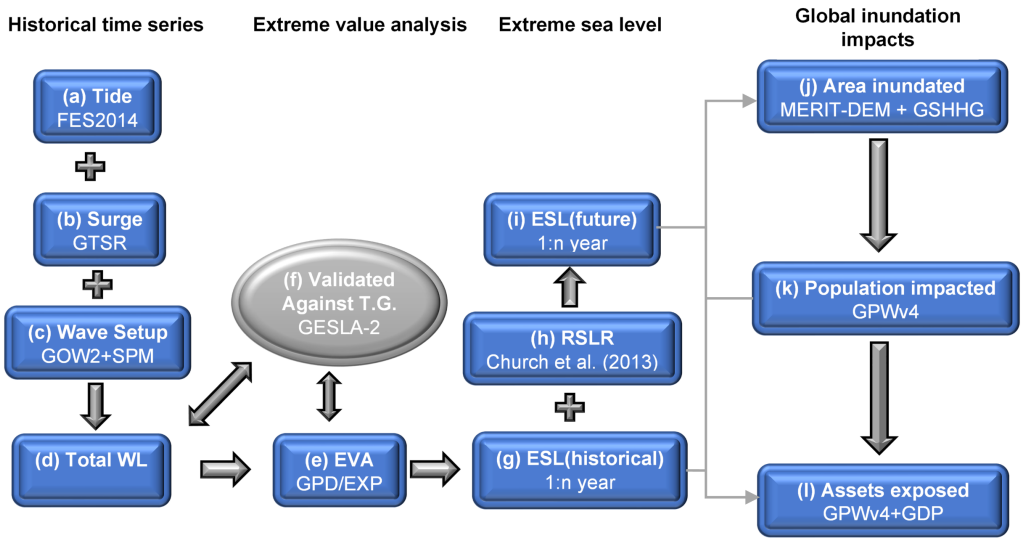

FIGURE 4.1: Diagrammatic representation of the processes used in the analysis of the various dataset in the full analysis.

The 1 in 100-year return period extreme value sea levels (ESL^{H100}) were determined from these model time series at each DIVA point (Section 4.6) [Fig. 4.1(e)]. A wide

range of different extreme value analyses (EVA) were tested. These include the peaks-over-threshold method with both Generalized Pareto Distribution (GPD) and the Exponential Distribution (EXP) and a variety of different threshold levels. The Annual Maximum approach was also tested using the Generalized Extreme Value Distribution (GEV) and Gumbel distribution (GUM) (Sections 4.6 and 4.7) [Fig. 4.1(e)]. These approaches were validated against corresponding EVA analysis of tide gauge data. These comparisons were undertaken for 1 in 20-year return periods, which require no extrapolation of the time series to this probability level and 1 in 100-year return periods (see Section 4.7). Based on this analysis it was found that a GPD distribution with a 98^{th} percentile threshold gave the best agreement between model and tide gauges and inclusion of WS slightly reduced bias between model and tide gauge extreme value estimates (see Section 4.7).

The projected future extreme sea level (ESL^{F100}) [Fig. 4.1(i)] was determined by adding the relative sea level rise ($RSLR$) to ESL^{H100} (Section 4.9) [Fig. 4.1(h)]. Again, this was done at each DIVA point. Using a bathtub flooding assumption, the episodic coastal flooding was determined at each DIVA point with the ESL values assigned to areal regions using Thiessen polygons (Section 4.10). The coastal topography was determined using the MERIT digital elevation model with the coastlines defined using the GSHHG dataset (Section 4.10) [Fig. 4.1(j)].

The population impacted by these flooded regions was determined from the gridded population data of the GPWv4 dataset [Fig. 4.1(k)] (Sections 4.10 and 4.11). The value of assets impacted by the flooding was evaluated from the population impacted and the GDP using the relationships proposed by Hallegatte et al. (2013) and Hinkel et al. (2014) [Fig. 4.1(l)].

4.3 Datasets and Processing

A detailed description of all the datasets used in this study is provided in Chapter 3. As the focus here is at the global-scale, $TSL(t)$ over the 36-year period (1979 - 2014) was determined along global coastlines at a total of 9,866 points which approximate the coastal segments previously defined in the Dynamic Interactive Vulnerability Assessment database (DIVA) (Hinkel and Klein, 2009) (Fig. 4.2), referred to here as "DIVA points".

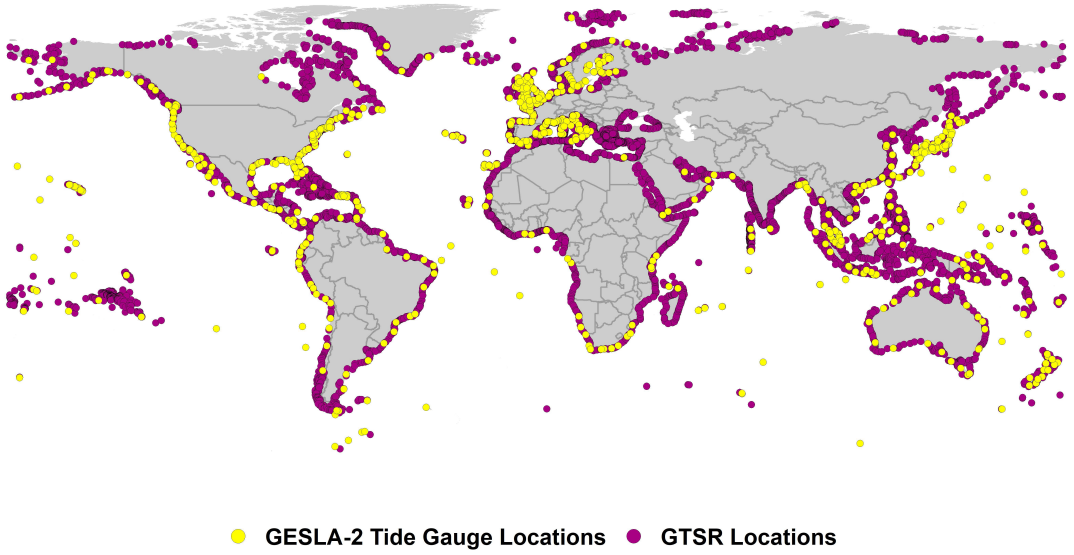

FIGURE 4.2: Global plot of DIVA output locations (purple points) and GESLA-2 tide gauge locations (yellow points).

Historical values of surge (S) were determined over this period from the Global Tide and Surge Reanalysis (GTSR) dataset (Muis et al., 2016). The tide levels (T) were determined from the numerical tide model dataset FES2014 (Finite Element Solution) (Carrere et al., 2016). In order to determine the wave setup, (WS), the nearshore (deep-water) wave conditions (significant wave height, H_{s0} and wavelength, L_0) are required. As there is no widely validated and accepted global nearshore wave model dataset, two different reanalysis wave model datasets were tested for this purpose: ERA-Interim (Dee et al., 2011) and GOW2 (Perez et al., 2017), with the latter ultimately being adopted (see Sections 4.5 and 4.7, Table 4.3). Wave setup was determined as a function of deep-water wave steepness (H_{s0}/L_0) and bed slope using the Shore Protection Manual (SPM) approach (Dean et al., 2005; SPM, 1984). An alternative wave setup formulation proposed by Stockdon et al. (2006) was also tested and found to yield similar results (see Sections 4.5, 4.7 and 4.13). After testing a series of representative bed slopes, a value of 1/30 was finally adopted (see Sections 4.5 and 4.7). As each of the model datasets are on different global grids and at different temporal resolution, every DIVA

point was assigned the value of the closest grid point for each model and the respective quantities of T, S and WS were interpolated in time to a 10-minute resolution. The above approach does not include any contribution of wave run-up, consistent with the majority of published studies (Rueda et al., 2017; Vitousek et al., 2017; Vousdoukas et al., 2018b), as run-up does not result in a sustained (order of hours) elevation of the TSL. This is in contrast to the recent study of Melet et al. (2018).

The historical time series of TSL over the period (1979-2014) was calculated using Eq. 2.2. This approach ignores non-linear interactions among these processes (Muis et al., 2016). For instance, both surge and wave setup will be influenced by the phase of the tide. Comparison with measured tide gauge data suggests such interactions, at least at this global scale, do not appear to have a significant impact on the results (see Sections 4.5 and 4.7). Validation data over the historical period were obtained from the GESLA-2 (Woodworth et al., 2016) tide gauge dataset, which comprises sea level data at 681 locations around the world (see Fig. 4.2).

In order to determine coastal flooding extent, coastal topography data were obtained from the Multi-Error-Removed Improved-Terrain DEM (MERIT DEM) dataset (Yamazaki et al., 2017) as described in detail in Section 3.7. Although the native resolution of the MERIT DEM is ∼90 m at the Equator, a coarser ∼1 km resolution version, consistent with previous studies (Hinkel et al., 2014; Muis et al., 2016, 2017) was used for the present application to reduce computational expense and ensure a resolution comparable to the other datasets used. MERIT is based on the SRTM v4.1 DEM dataset (Jarvis et al., 2008), but with enhanced vertical accuracy.

In order to determine assets exposed due to flooding both gridded population and Gross Domestic Product (GDP) databases are required. Population data were obtained from the Gridded Population of the World, version 4 (GPWv4 Rev. 11) (International Earth Science Information Network (CIESIN), 2017) database (see Section 3.10) and GDP data from Kummu et al. (2018) (see Section 3.11).

4.4 Historical Global Total Sea Level

Validation over the hindcast period is imperative for confidence in future projections. The model TSL time series was compared with the GESLA-2 tide gauge data over the period 1979-2014. Model performance over the hindcast period was evaluated at each of 681 GESLA-2 locations by determining both the root mean square error ($RMSE$) and the upper percentile bias ($bias^p$), difference of higher percentile values (95^{th} to 99^{th}) between the model TSL and the tide gauge data. Overall global model performance was then assessed in terms of the average $RMSE$ ($ARMSE$) and average $bias^p$ ($abias^p$) over all GESLA-2 locations (Muis et al., 2016). The GESLA-2 tide gauge data were compared with both model $T + S + WS$ and $T + S$. In addition, both GOW2 and ERA-Interim wave models, a variety of bed slopes and two different empirical formulations (Dean et al., 2005; SPM, 1984; Stockdon et al., 2006), were used to calculate WS. The complete results are given in Tables 4.1 and 4.2 and also discussed in Section 4.5.

As the differences between the various values of $ARMSE$ and $abias^p$ are not large for the different combinations and because, as subsequently shown, WS is a relatively small component of the total episodic flooding, discussion here is confined to the cases where WS is calculated with the GOW2 model, the SPM (1984) (Dean et al., 2005) formulation and the mid-range bed slope of 1/30 (See also: Section 4.13). As noted above, the global-scale of the analysis meant that a relatively simplistic approach was necessarily used to determine WS (Dean et al., 2005; SPM, 1984). As the results ultimately showed that WS was not a significant component of episodic flooding (5%, see Section 4.10), errors caused by this approach are unlikely to significantly bias the final results.

For $T + S$, the globally averaged $ARMSE$ is 0.197 m (Table 4.1), which is comparable to the value of 0.170 m obtained by Muis et al. (2016), where an older tide model (FES 2012) was used together with a significantly smaller set of tide gauge locations (472). Inclusion of WS makes no appreciable change to $ARMSE$, in fact increasing it slightly to 0.204 m (see Table 4.1). This lack of impact on WS is not surprising, as WS is expected only to represent an appreciable contribution during storm events, which is poorly captured by $ARMSE$. The global distribution of values of $RMSE$ for $T + S + WS$ is shown at each GESLA-2 location in Fig. 4.3. Although there is an occasional outlier in the data, $RMSE$ is less than 0.2 m at 75% of locations and less than 0.5 m at the vast majority (93%) of locations. The contribution of WS during storm periods (e.g., see Figs. 4.7 and 4.8) can be assessed from values of $abias^p$.

Table 4.2, shows that for $T+S$, $abias^p$ increases in magnitude with increasing percentile level. With the addition of WS, $abias^p$ decreases, becoming approximately constant across all percentiles. The reduction in $abias^p$ is 60% at the 99^{th} percentile, indicating

	$ARMSE$ **and** $abias^P$ **between Model and Tide Gauge** TSL **(m)**						
	No WS	ERAI-15	ERAI-30	ERAI-100	GOW2-15	GOW2-30	GOW2-100
$ARMSE$	0.197	0.205	0.204	0.203	0.205	0.204	0.203
$abias^P$	-0.044	-0.010	-0.014	-0.017	-0.013	-0.017	-0.019

TABLE 4.1: Average root mean squared error ($ARMSE$) and average bias of 99^{th} percentile values ($abias^P$) for TSL between model and GESLA-2 tide gauge data. Model values are shown with and without WS calculated using either GOW2 or ERA-I wave models and a variety of bed slopes. [e.g. GOW2-30 indicates GOW2 wave model and bed slope of 1/30 – other combinations similarly named).

	$abias^P$ **between the percentiles of the Model and Tide Gauge** TSL **(m)**				
	95^{th}	96^{th}	97^{th}	98^{th}	99^{th}
$T+S$	-0.031	-0.033	-0.035	-0.039	-0.044
$T+S+WS$	-0.019	-0.019	-0.019	-0.019	-0.017

TABLE 4.2: Average bias ($abias^P$) of percentile values for TSL between model and GESLA-2 tide gauge data. Values for each percentile are shown for model values consisting of $T+S$ (i.e. no WS) and $T+S+WS$. Negative values indicate that model is less than tide gauge. Note that to calculate WS, the GOW2 model was used, and a bed slope of 1/30.

the inclusion of WS results in better agreement between model and tide gauges during storm events. The improvement in $|bias^p|$, at individual tide gauge locations is shown in Fig. 4.4.

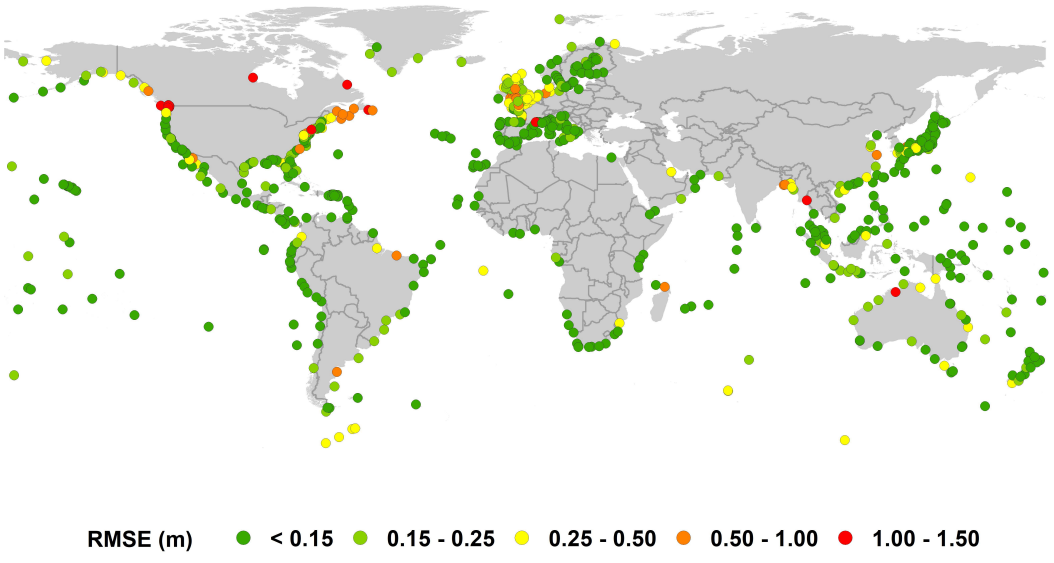

FIGURE 4.3: Values of root mean squared error ($RMSE$) between model total sea level ($TSL = T+S+WS$) and GESLA-2 tide gauge data

The validation outlined above indicates that the model derived TSL estimates are generally in good agreement with tide gauge data and that the inclusion of WS makes an

improvement in performance, particularly during extreme storm events. As noted in Section 4.5, it is unclear how many of the validation tide gauges respond to WS due to their locations. What is clear, however, is that without the inclusion of WS, there is a global underprediction of TSL during storms.

As shown in Fig. 4.4, the improvement in $|bias^p|$ can be seen at the vast majority of tide gauge locations. Whether this is actually due to WS or a systematic under prediction of S is not known. What is clear is that the inclusion of WS, modelled using the relatively simple approach adopted, results in a model which performs well compared to tide gauges at most locations.

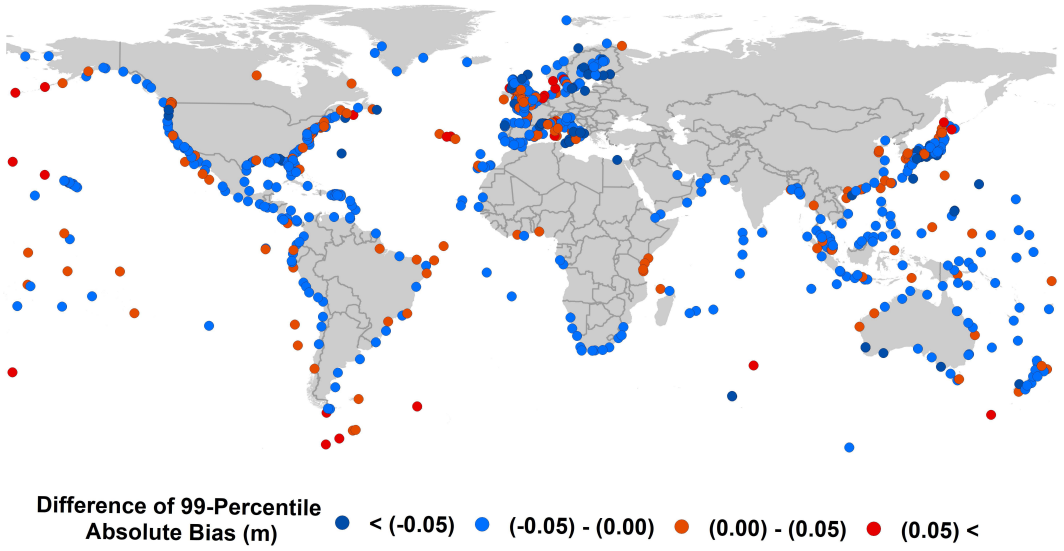

FIGURE 4.4: Change in $|bias^P|$ at the 99^{th} percentile between model and tide gauge as a result of wave setup (WS). i.e.,$|bias^P_{T+S+WS}| - |bias^P_{T+S}|$ evaluated at GESLA-2 tide gauge locations. Negative (blue) values indicate an improvement in agreement between model and tide gauge for extreme values as a result of the inclusion of WS.

4.5 Contributions of processes to Total Sea Level

As noted previously, model estimates of $T+S+WS$ were validated against the GESLA-2 tide gauge data. This was achieved by determining both the $RMSE$ and the difference of higher percentile values (95^{th} to 99^{th}) between the model TSL and the tide gauge data at each of the 681 GESLA-2 tide gauge locations. GESLA-2 data points (Woodworth et al., 2016) used in this study are shown in Fig. 4.2. GESLA-2 provides a more extensive validation dataset than the University of Hawaii Sea Level Center (UHSLC) dataset used by Muis et al. (2016). Both the T and S models use Mean Sea Level as their datum, when these quantities are summed, there can be a small mean offset due to the S. To obtain consistent datum levels, the annual means were subtracted from both the tide gauge and $T + S$ model data at each of the GESLA-2 data points (Muis et al., 2016). As values of WS are always positive, adding WS to the model $T + S$ dataset results in a positive offset. This was again removed by subtracting the annual mean from the $T + S + WS$ model dataset. This validation implicitly assumes that the tide gauges respond to WS. Whether individual gauges do respond to wave setup will depend on their individual locations and the spatial extent of enhanced sea surface elevation resulting from the WS. Note that, when we subsequently use model values to determine extreme sea levels and flooding, the annual mean is not subtracted from the time series. Rather, in those cases a common absolute datum is obtained from the MDOT (Rio et al., 2014) (see Section 4.9).

As shown in Fig. 4.3, the $RMSE$ at individual GESLA-2 data locations is generally less than 0.5m. Such absolute values of $RMSE$ can mask the relative errors for locations where the tidal amplitude is small. In such cases, a small absolute $RMSE$ may still be important. Fig. 4.5 shows the $RMSE$ at each tide gauge location, presented as a percentage of the mean tidal amplitude. The mean tidal amplitude was determined by firstly performing a harmonic analysis on the tidal gauge data, so as to extract the astronomical tide. A zero up-crossing analysis was then performed to determine the mean amplitude of the tidal signal. This figure confirms what is shown in Fig. 4.3 and shows that at the majority of locations (68%) the relative $RMSE$ is less than 20%. The locations where the relative $RMSE$ is larger are enclosed basins (e.g. Mediterranean Sea, Baltic Sea, Sea of Japan) where the tidal amplitude is small and the spatial scales challenge our global-scale analysis, probably due to the performance of the tidal model.

Fig. 4.4 shows that there is generally an improvement in the 99^{th} percentile $bias^P$ (reduction in value) when WS is added to the model time series. Table 4.1 shows values of $ARMSE$ (average $RMSE$ over all tide gauges) and $abias^P$ (average bias of the 99^{th} percentile over all tide gauges). In this table, results are given for $T + S$ (i.e. no WS) as well as $T + S + WS$, with WS calculated from both the ERA-I and GOW2 wave

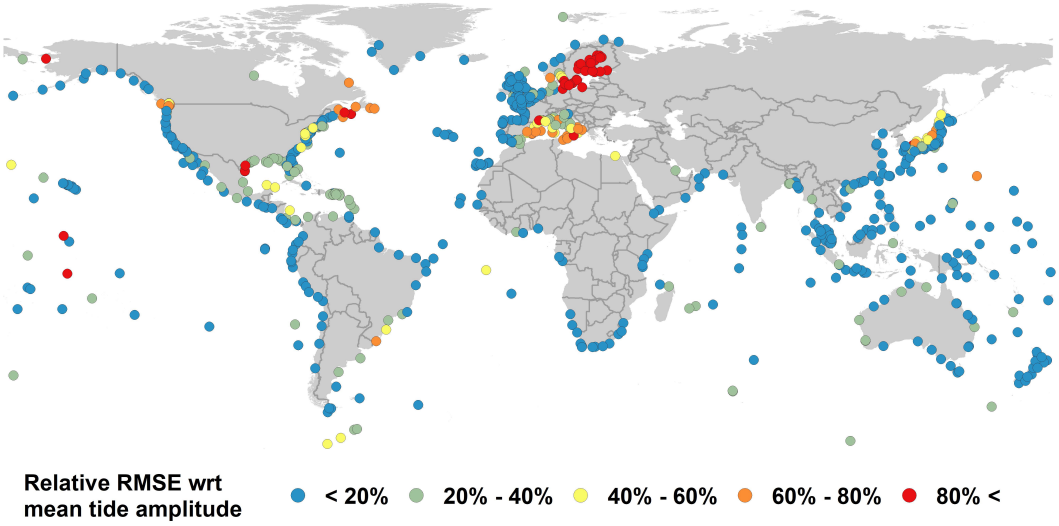

FIGURE 4.5: Values of root mean squared error (RMSE) between model total sea level ($TSL = T + S + WS$) and GESLA-2 tide gauge data (as in Fig. 4.3) as a percentage of the tidal amplitude at that location

models and for a number of different bed slopes (1/15, 1/30 and 1/100). As WS is only significant during episodic storm events, $ARMSE$ is hardly impacted by the inclusion of WS. The values of $ARMSE$ change by only approximately 4% with the inclusion of WS. In fact, the agreement between model and tide gauge data is slightly worse with the inclusion of WS. The impact of WS is, however, larger for $abias^P$, which examines the average 99^{th} percentile differences between model and tide gauges. The inclusion of WS reduces the magnitude of $abias^P$ by approximately 60%. This indicates that the inclusion of WS allows the model to more accurately reproduce the tide gauge data during storm conditions. As shown in Fig. 4.4, this reduction in bias is not limited to specific geographic locations. Rather, there is a consistent reduction in the magnitude of the bias at the 99^{th} percentile across 73% of tide gauge locations. The improvement in bias across all locations is further seen in Fig. 4.6 (*lower panel*), which shows histograms of $bias^P$ both with and without WS included. The inclusion of WS results in a more peaked histogram centred on a value of zero. When WS is excluded, the histogram is skewed to negative values, indicating an underestimation of extremes. As can be seen in Fig. 4.4, this improvement occurs in most global regions, not only tropical cyclone areas, where the GTSM is known to underestimate surge levels.

Table 4.2 shows values of $abias^P$ both with and without WS for a number of percentile levels (95^{th} to 99^{th} percentiles). For the case of $T+S$ (no WS), the magnitude of $abias^P$ increases with percentile level. The inclusion of WS to TSL (i.e., $T+S+WS$) reduces the magnitude of $abias^P$ and also results in an almost constant value, as a function of

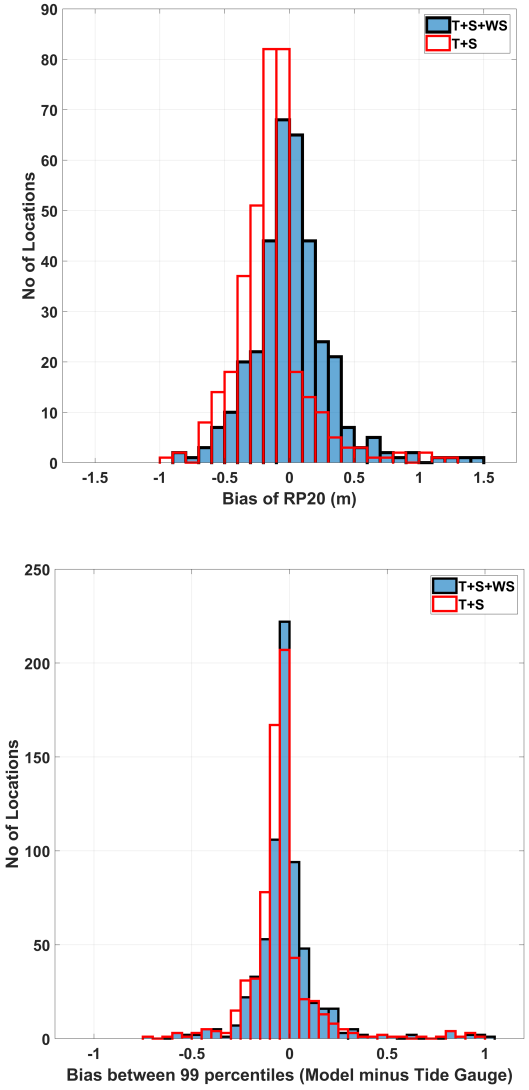

FIGURE 4.6: (upper) Histogram of bias for ESL^{H20} between GESLA-2 tide gauge data and model ($ESL^{H20}_{T+S+WS} - ESL^{H20}_{Gauge}$) (blue bars) and ($ESL^{H20}_{T+S} - ESL^{H20}_{Gauge}$) (unfilled bars). (lower) The bias of the 99^{th} percentile values of TSL between model and GESLA-2 tide gauge data, $bias^P$. $T+S+WS$ shown by blue bars, $T+S$ shown by unfilled bars. The inclusion of WS reduces the absolute magnitude of both the ESL^{H20} average bias and the average 99^{th} percentile $bias^P$ (i.e. more centred around a value of zero)

percentile level. This indicates that the inclusion of WS in the model results in a better approximation of the low probability tail of the pdf.

WS is sensitive to local bed slope and bathymetry which cannot be resolved by the present wave models, not even with the finer resolution GOW2 model. As our focus is at a global scale, these effects can only be modelled in the mean. As seen in Table 4.1, there is very little difference in $ARMSE$ or $abias^P$ between the ERAI and GOW2 models and for different bed slopes. Noting this, we have adopted the GOW2 model and

a medium-range bed slope of 1/30 for subsequent calculations (also see Section 4.13). The sensitivity of this choice for extreme value analysis is discussed in Section 4.7.

The storm-related impact on TSL is highlighted in Figs. 4.7 and 4.8 for two specific locations (Boston, east coast USA) and Fremantle (south-west coast Australia). In each case the T component has been removed from the measured GESLA-2 sea level via a harmonic analysis. The resulting residual sea level is then compared with model S and $S + WS$. Each figure shows both residual sea levels and GOW2 significant wave height (H_{s0}) over a 12-month period. A specific storm event for each location is also expanded for a more detailed analysis. These figures clearly show the episodic storm-related nature of S and WS. They also show that during these storm events, better agreement occurs between measured and model results when WS is included. Surge alone underestimates the residual sea level. In both of these cases, the tide gauges appear to respond to WS, which is well modelled by using the present approach (Dean et al., 2005; SPM, 1984), the GOW2 model wave height and a bed slope of 1/30.

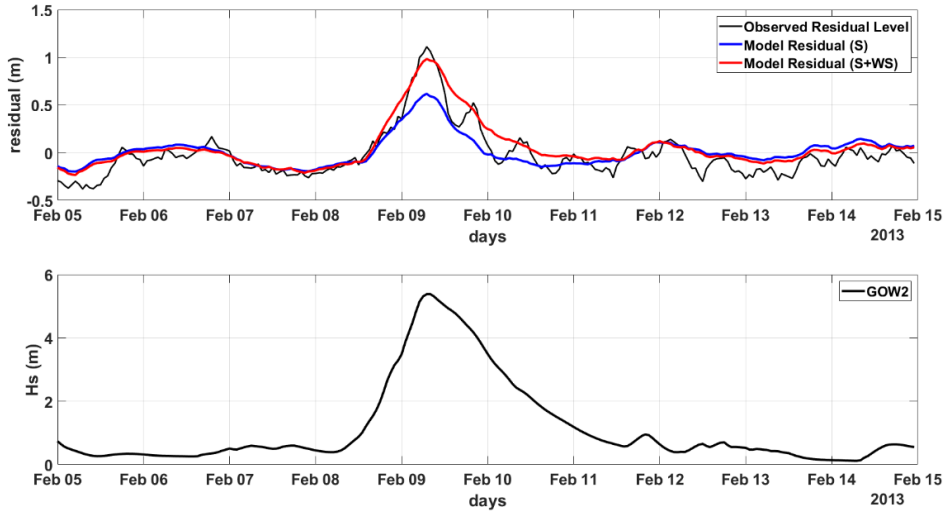

FIGURE 4.7: Residual sea level and significant wave height as a function of time at Boston, USA. (a) Values over the year 2013. (b) Details of the storm event during February 2013. (top) Model storm surge (S) (blue line) and model surge + wave setup (S+WS) (red line). (bottom) GOW2 significant wave height during the same storm event.

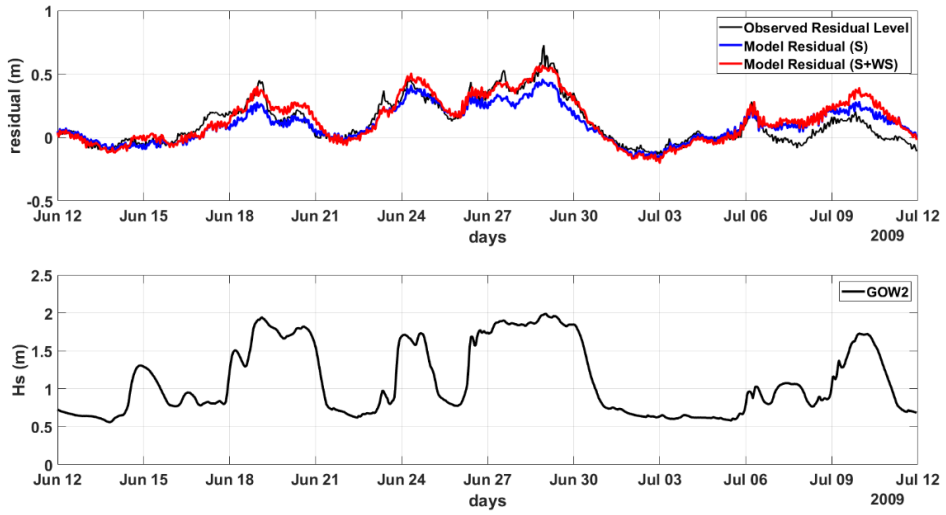

FIGURE 4.8: Residual sea level and significant wave height as a function of time at Fremantle, Australia. (a) Values over the year 2009. (b) Details of the storm event during June 2009. (top) Model storm surge (S) (blue line) and model surge + wave setup (S+WS) (red line). (bottom) GOW2 significant wave height during the same storm event.

4.6 Extreme Value Estimates of Total Sea Level

As noted previously, both S and WS are episodic. For episodic coastal flooding, it is these storm-related contributions to extreme sea levels that are often critical (Barnard et al., 2015; Benavente et al., 2006; Muis et al., 2016; Vitousek et al., 2017). The stochastic prediction of such extremes involves the fitting of an appropriate probability distribution function (pdf) to an historical time series and then extrapolating to the desired probability of occurrence (e.g. 0.01 in any year or the 100-year event). In the case of TSL, the most common approach has been to consider Annual Maxima (AM) and to fit either a two-parameter Gumbel distribution (GUM) (Hunter et al., 2017; Muis et al., 2016) or a three parameter GEV (Hunter et al., 2017; Vitousek et al., 2017; Wahl et al., 2017). A significant limitation of AM approaches is that the resulting extreme value time series have few values (1 per year). This leads to relatively large confidence intervals when fitting and extrapolating the pdf. An alternative is to use all storm peaks above a specified threshold – i.e. the Peaks over Threshold approach, POT (Coles, 2001; Wahl et al., 2017). In this latter case, the data can be shown to follow a Generalized Pareto Distribution (GPD) (Coles, 2001) or its two-parameter variant, the Exponential Distribution (EXP). An alternative to the approach used above of reconstructing the long-term historical time series, is to use an ensemble Monte-Carlo approach (Vousdoukas et al., 2018b). This is discussed in Section 4.12.

The Extreme Value Analysis (EVA) adopted can have a major impact on the resulting statistical estimates of extremes (in this case, extreme sea levels) (Wahl et al., 2017) (see Fig. 4.12). Therefore, it is important to ensure that the chosen EVA optimally approximates both the model and tide gauge data. Hence, a range of EVA approaches were tested to determine which optimally represents both model and tide gauge data (see Section 4.7). Results indicate that the POT approach fitted with a GPD and a 98th percentile threshold (GPD98) fits both the tide gauge and model data with least error. This combination yields the best fit to the tide gauge data in 33% of locations and the best fit to the model data (at DIVA points) in 34% of tide gauge locations (see Fig. 4.11). This result is consistent with the findings of Wahl et al. (2017). The complete EVA analysis is described in Section 4.7.

A further analysis of the impact of the selected EVA approach on projected extreme sea level, as well as the sensitivity of the method used to determine WS is shown in Table 4.3. This table considers the mean bias between tide gauge and model results for a 20-year Return Period ($ESL^{H20} - ESL^{H20}_{Gauge}$) across the 355 (of a total of 681) tide gauge locations which have a duration of at least 20 years within the storm surge model time span (1979-2014). These results indicate a mean bias of 17 mm with the inclusion of WS determined from the GOW2 model, a 1/30 bed slope and a GPD98

	GUM	GEV	GPD98	GPD98.5	GPD99	GPD99.5	EXP98	EXP98.5	EXP99	EXP99.5
No WS	-0.141	-0.153	-0.136	-0.138	-0.139	-0.144	-0.081	-0.077	-0.080	-0.097
ERAI-15	0.046	0.037	0.036	0.043	0.051	0.061	0.040	0.033	0.023	0.023
ERAI-30	0.024	0.017	0.015	0.021	0.029	0.040	0.025	0.018	0.006	0.004
ERAI-100	0.011	0.004	0.002	0.007	0.015	0.026	0.016	0.008	-0.004	-0.008
GOW2-15	0.036	0.031	0.028	0.034	0.043	0.050	0.026	0.017	0.007	0.008
GOW2-30	0.016	0.011	0.017	0.013	0.021	0.030	0.013	0.004	-0.008	-0.009
GOW2-100	0.004	-0.002	-0.004	0.001	0.009	0.018	0.006	-0.004	-0.016	-0.019

TABLE 4.3: The global mean bias between model and tide gauges for extreme sea levels ($ESL^{H20} - ESL^{h20}_{Gauge}$) using all 10 EVA approaches. Results are shown for no WS and with WS calculated either with GOW2 or ERA-I wave models and a variety of bed slopes (e.g., GOW2-30 indicates GOW2 wave model and bed slope of 1/30; GPD98 indicates a Generalized Pareto Distribution with a 98th percentile threshold)

EVA (see Fig. 4.6 (*upper panel*). However, a number of other combinations of EVA and WS calculation yield similar results. All the cases which include WS, have relatively small mean bias, indicating that the results are robust, irrespective of the choice of wave model, bed slope and EVA. What is clear, however, is that if WS is not included, there is a consistent negative bias (model underestimates the extreme sea level). For GPD98 with a 1/30 bed slope, the mean absolute bias is reduced by 88% indicating a significant improvement. Therefore, the inclusion of wave setup appears to produce model extreme sea levels (ESL^{H20}) that are in better agreement with recorded data.

With this validation of modelled ESL^{H20}, the results were extended to a return period of 1 in 100 years (ESL^{H100}) and evaluated at all DIVA points. The global distribution of ESL^{H100} is shown in Fig. 4.9(a). This figure shows that values in excess of 5 m occur along northern parts of both the Atlantic and Pacific coasts of North America, the Atlantic and North Sea coasts of Europe and China. The results show regional consistency with ESL^{H100} varying gradually along coastlines. Note that these ESL^{H100} estimates underestimate values in tropical cyclone regions due to model resolution (Muis et al., 2016) and the limited sample size (Haigh et al., 2014; Lin et al., 2012).

Fig. 4.10 also shows the impact of WS alone, calculated as $ESL^{H100}_{T+S+WS} - ESL^{H100}_{T+S}$. This figure shows extreme WS values up to 0.5 m, with the distribution largely following areas of large extreme significant wave height (Takbash et al., 2019). In particular, the northern parts of both the Atlantic and Pacific coasts of North America, Atlantic coast of Europe, southern tip of the Pacific coast of South America, southern coast of Australia and much of Asia show 100-year return period contributions of WS greater than 0.4 m. Hence, although WS has only a very small impact on the overall values of $ARMSE$ TSL between model and tide gauge data, it becomes a larger component where extreme value sea levels are concerned (on average a 17% increase in ESL^{H100} due to WS over all DIVA points).

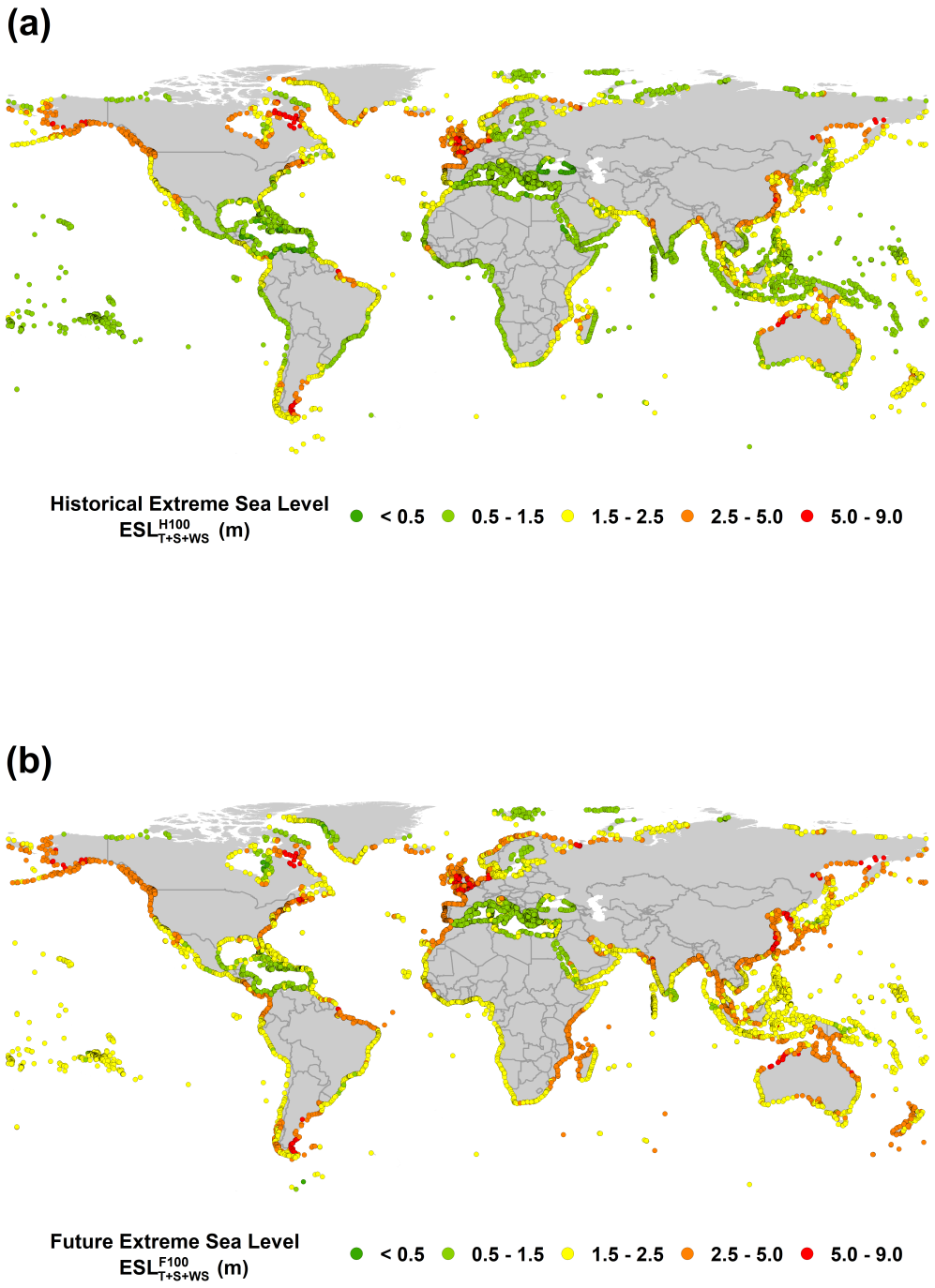

FIGURE 4.9: Global distribution of the (a) historical 100-year return period extreme sea level(ESL^{H100}_{T+S+WS}) based on model data for the period 1979-2014 and (b) projected 100-year return period extreme sea level (ESL^{F100}_{T+S+WS}) for RCP8.5 in 2100 at DIVA locations.

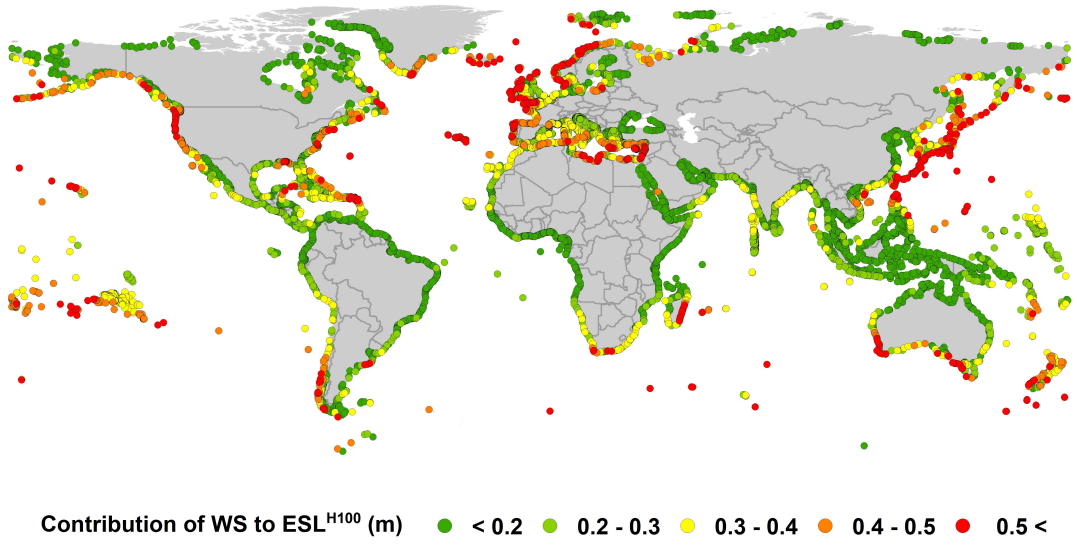

FIGURE 4.10: Global distribution of the contribution of wave setup to the 100-year return period extreme sea level (i.e. $ESL^{H100}_{T+S+WS} - ESL^{H100}_{T+S}$) at DIVA locations. Based on model data for the period 1979-2014.

4.7 Extreme Value Validation

Although the ability of the modelling approach to reproduce long term TSL variations at tide gauge locations is desirable, it is the ability to reproduce extreme sea levels which is most important for the determination of episodic coastal flooding. To this end, a number of different extreme value approaches were investigated to determine which best modelled the tail of the probability distribution functions of both the model and tide gauge data. Ten different Extreme Value Analysis (EVA) approaches were tested. These include two Peaks over Threshold (POT) fits to the data [Generalized Pareto Distribution (GPD) and Exponential (EXP)] and two Annual Maxima (AM) fits [Gumbel (GUM) and Generalized Extreme Value (GEV)]. Each of the POT approaches was evaluated with 4 different threshold values, each determined as a percentile value ($98^{th}, 98.5^{th}, 99^{th}$ and 99.5^{th}) (i.e. 2x4 POT approaches plus 2 AM approaches).

These theoretical extreme value distributions were fitted to the GESLA-2 tide gauge data at a total of 355 stations for which there is at least 20 years of data. The goodness of fit of the chosen distribution was determined by examination of Q-Q relationships between tide gauge data and each theoretical distribution. The $RMSE$ between tide gauge and theoretical distributions were evaluated for data above the 80^{th} percentile. A small $RMSE$ indicates that the tail of the observed pdf is approximated well by the assumed distribution. The lower bound of 80% was adopted as it is high enough to ensure the tail of the pdf is being considered but not so high that comparisons become unacceptably noisy due to limited data. A range of other values (up to the 95^{th} percentile) were tested and produced the same conclusions. This approach allows a ranking of the various approaches over all tide gauge locations. Fig. 4.11 shows a global plot of tide gauge locations and which EVA approach best fits the data. A histogram of the number of locations where each EVA approach produces the best fit to the tide gauge data is also shown. This figure shows that a GPD98 POT pdf best approximates the tide gauge data, consistent with the findings of Wahl et al. (2017). The same analysis was also undertaken for the model ($T + S + WS$) data (at DIVA points), yielding a similar result and confirming that the model data are also best approximated by the GPD98 approach.

It is clear in Fig. 4.11 that the GPD performs better than the EXP distribution. This is not surprising, as the GPD approaches are all 3-parameter pdfs, whereas the EXP distributions are 2-parameter pdfs. The additional parameter in the GPD providing greater flexibility in modelling the data. The same influence can be seen in the AM distributions, where the 3-parameter GEV pdf performs better than the 2-parameter GUM pdf.

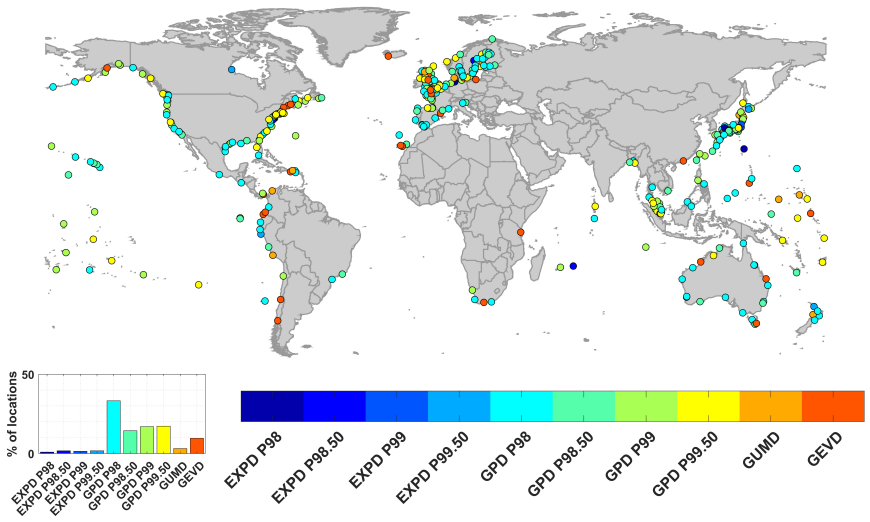

FIGURE 4.11: Best fitting EVA approach at GESLA-2 tide gauge locations. The color of the marker at each location indicates the EVA approach which best fits the tide gauge pdf at that location. The colour bar legend defines each of the EVA approaches (e.g. GPD P98 is the Generalized Pareto Distribution with a 98th percentile). The histogram (top left) shows the relative number of points where each EVA approach gives the best fit to the tide gauge pdf. Only locations with more than 20-years of data shown.

The $RMSE$ analysis of the Q-Q plots provides a quantitative method to rank how well the various EVA approaches approximate the tails of the pdfs. An alternative approach is to evaluate the bias between the tide gauge and model at a specified return period. As the tide gauge stations considered all have measurement durations greater than 20 years, a return period of 20 years was chosen to avoid errors due to extrapolation (ESL^{H20}). Table 4.3 shows the average bias between tide gauge and model ($ESL^{H20} - ESL^{H20}_{Gauge}$) across all 355 locations. The first point to note is that all EVA approaches yield a negative bias when the model TSL is approximated by $T + S$ (i.e. no WS). This negative bias is largely eliminated when WS is included. With the inclusion of WS, all of the EVA approaches yield average bias values less than approximately 50 mm. This result is irrespective of the EVA approach and wave model used to calculate the WS or assumed bed slope. As noted in the Q-Q RMSE analysis (Fig. 4.11), the GPD98 with GOW2 wave model and a bed slope of 1/30 performs well with a mean bias of approximately 17 mm. The impact of WS on the ESL^{H20} values is clearly shown in Fig. 4.6 (*upper panel*), which shows a histogram of bias between model and tide gauge, both with and without WS. Note that this figure was evaluated with a GPD98 EVA, the GOW2 wave model and a bed slope of 1/30 to determine WS. Without the inclusion of WS, the model results underestimate the extreme values compared to the tide gauge data.

Although the combination of a GPD98 EVA, the GOW2 wave model and a bed slope of

1/30 to determine WS produced good agreement with the tide gauge derived predictions of extreme sea levels, a number of the other approaches yield similar or even better results in Table 4.3 (e.g. GPD98.5/GOW2-100). The fact that the average bias is relatively insensitive to the EVA approach and method for determining WS provides confidence in the robustness of the model values. However, the fact that there is not a single bed slope which clearly minimizes errors makes the selection of this value challenging. Athanasiou et al. (2019) compiled data globally and found a mean value of approximately 1/100. Ardhuin and Roland (2012), however, in a study of wave reflection from shorelines found much steeper slopes and adopted values as steep as 1/5. Based on this study, Melet et al. (2016) adopted a global value of 1/10. Noting these discrepancies, we have pragmatically adopted a value of 1/30. This value lies between the estimates of Athanasiou et al. (2019) and Ardhuin and Roland (2012) and is consistent with the results in Table 4.3. The WS increases with increasing bed slope (Dean et al., 2005; SPM, 1984; Stockdon et al., 2006). Therefore, adopting a value of 1/30 over a value of 1/100 will produce larger ESL^{100} values. The ultimate contribution of WS to total ESL^{H100} is approximately 17% on average but makes an even smaller contribution to global area flooded (approximately 5%)(see Sections 4.9 and 4.10). Therefore, we conclude that assuming a bed slope of 1/30 has negligible impact on the final results. Considering the results of both the $RMSE$ and average bias tests and the discussion above, the GPD98/GOW2-30 combination was selected as the reference for subsequent analysis.

Although the results indicate that all EVA approaches provide comparable results at the 20-year return period, as shown by Wahl et al. (2017), they can yield quite different values when extrapolated to larger return periods. This is demonstrated in Fig. 4.12 for the location of Boston. This figure shows the ESL^H calculated using GPD98/GOW2-30 and EXP98/GOW2-30 as a function of return period. Both model and tide gauge ESL^H are shown for a number of return periods and for the model cases, results both with and without the inclusion of WS are considered. As expected from the above analysis, the GPD results (model – tide gauge) are in better agreement than with the EXP distribution. Also, model ESL^H is underestimated when WS is not included. The Boston location is qualitatively representative of other sites.

As shown by Wahl et al. (2017) most of the locations (85%) considered have a negative shape parameter for the GPD99. This means that the distribution is bounded and, as shown in Fig. 4.12 is quite flat as a function of return period. Therefore, as return period increases, there is only a relatively small increase in ESL^H. In contrast, the 2-parameter EXP distribution is unbounded and has a much faster increase in ESL^H as a function of return period. For the GPD case, this means that a small change in ESL^H results in significant changes in equivalent return period.

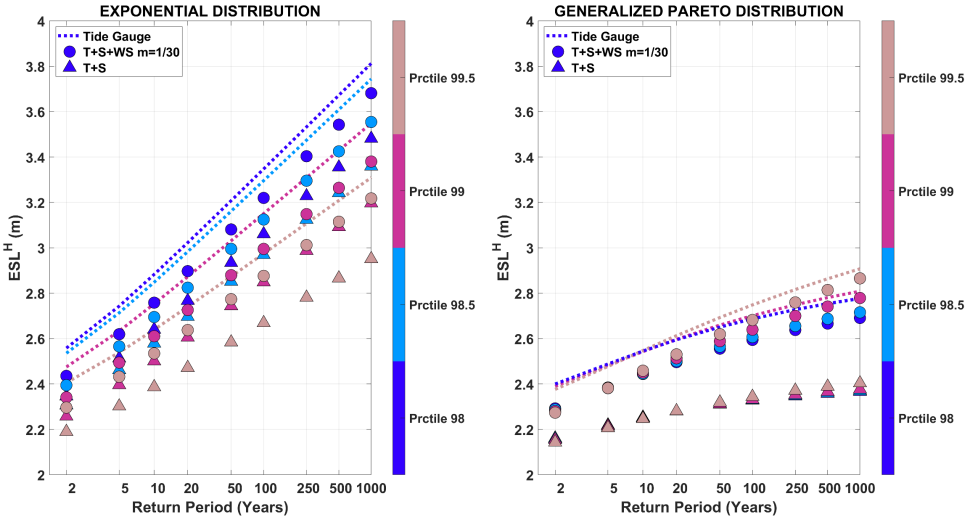

FIGURE 4.12: Extreme value total sea level at Boston, USA as a function of return period. Exponential distribution (EXP) shown on the left and Generalized Pareto Distribution (GPD) on the right. Tide gauge data are shown with the dashed lines. Model results with no wave setup shown with triangles and with wave setup included as filled circles. Different threshold percentile levels for EVA shown with colours defined in the colour bar.

Note that for the GPD98 EVA, there was typically between 800 and 1000 points (extremes) in the fit to the tail of the pdf.

4.8 Confidence Limits

The estimates of extreme value sea levels are statistical quantities and to obtain estimates of the potential uncertainty in the projected ESL^{F100}, the 90^{th} percentile confidence limits on each of the ESL^{H100} values were determined using a bootstrap approach. Bootstrapping is a common approach to determine confidence limits for extreme value estimates (Efron, 1979; Meucci et al., 2018). Using this approach, we computed a sample of 1000 bootstrapped ESL^{F100} estimates taken randomly from the original data sample at each DIVA point. For each sample an estimate of ESL^{F100} was determined and 5.0 percentile and 95.0 percentile values calculated from the 1000 realizations to give the lower and upper 90^{th} percentile confidence limits. The resulting 90^{th} percentile confidence intervals are shown globally in Fig. 4.13. The results indicate that for 99% of the 9866 locations, the span of the 90^{th} percentile confidence interval (i.e. upper CL – lower CL, CL is the value of ESL^{H100} at the confidence limit) is less than 1 m (i.e., ±0.5 m). As ESL^{F100} values are commonly of order 4 m (see Fig. 4.14), the 90^{th} percentile confidence limits are thus less than ±10% (see Section 4.13). The confidence limits for ESL^{H100} and ESL^{F100} were used to determine the confidence limit span for area inundated, population exposed to flooding and assets exposed to damage. These values are shown in Table 4.4.

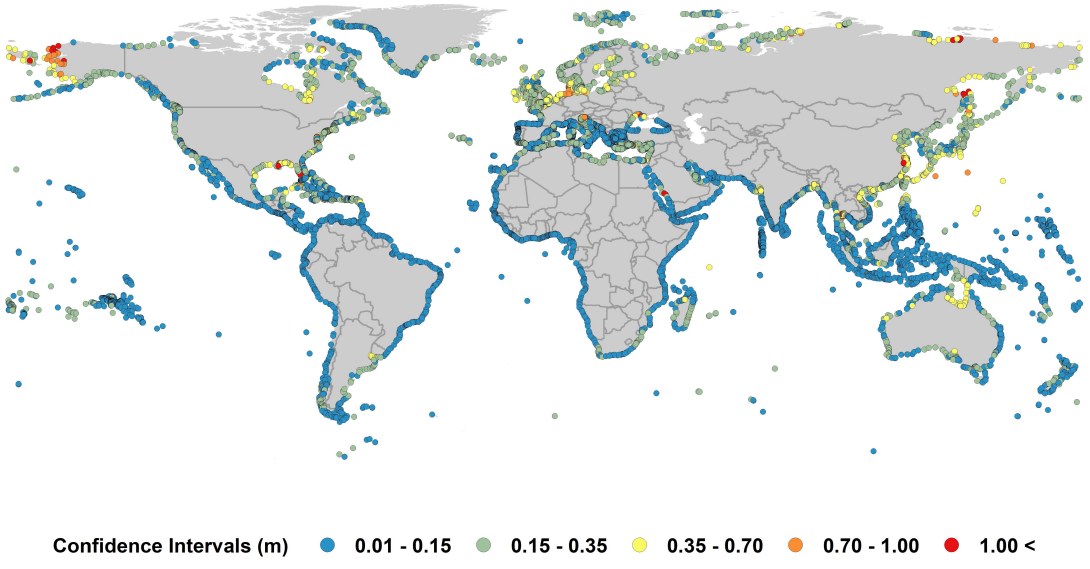

FIGURE 4.13: The 90^{th} percentile confidence interval for present-day extreme sea level estimates (ESL^{H100}_{T+S+WS}) (i.e. upper confidence limit – lower confidence limit).

4.9 Future Projections of Extreme Sea Levels and Coastal Flooding

The ESL^{H100} values provide the basis to determine episodic flooding for the present day and for the future. The values of ESL^{H100} at each DIVA point were associated with a surrounding region (see Section 4.10) and flooding calculated using the following planar bathtub approach (Muis et al., 2016). The topography was defined by the MERIT DEM dataset, which has a vertical datum of the EGM96 geoid (Earth Gravitational Model, 1996). To bring values of ESL^{H100} to this same datum, Mean Dynamic Ocean Topography (MDOT) (Jarvis et al., 2008; Rio et al., 2014) values were added to the extreme value estimates ($ESL^{H100} + MDOT$) (Muis et al., 2017). The coastline was defined using the Global Self-consistent Hierarchical High-resolution Geography (GSHHG) database (Wessel and Smith, 1996). A GIS-based approach was subsequently used whereby any MERIT grid point is considered inundated if it has an elevation less than ESL^{H100} and is connected to the shoreline by water.

To calculate future Extreme Sea Level (ESL^{F100}), projected regional relative sea level rise ($RSLR$) was added to the present-day extreme sea level, $ESL^{F100} = ESL^{H100} + RSLR$. Values of $RSLR$ vary by region around the world and were taken from Church et al. (2013a) (Fig 13.20 in IPCC AR5 – http://icdc.cen.uni-hamburg.de/1/daten/ocean/ar5-slr.html) for IPCC Representative Concentration Pathways (RCP) 4.5 and 8.5 (Note: average global $RSLR$ across all the DIVA points is 0.21-0.71 m for RCP4.5 and 0.34-0.99 m for RCP8.5 by 2100). A range of other projected values of $RSLR$ have been proposed, however, due to the overwhelming precedence of the IPCC projections, they have been adopted here. The values of $RSLR$ include the effects of atmospheric loading, land ice, glacial isostatic adjustment (GIA) and terrestrial water sources. Fig. 4.9 (b) shows global values of ESL^{F100} for 2100 under RCP8.5 (also see Fig. 4.14 (a) for 2050 values). A comparison of Figs. 4.9 (a) and 4.9 (b) shows that by 2100, $T + S + WS$ will still be a significantly larger contribution to extreme sea levels than relative sea level rise. Additionally, Fig. 4.15 demonstrates ESL^{F100} values under RCP 4.5.

The extent of coastal flooding is a function both of ESL^{F100} and the coastal topography. Fig. 4.16 shows a global map of flooding "hotspot" regions in 2100 for RCP8.5. To arrive at this result, the flooding area per unit length of coastline was determined for each of the DIVA points (normalized inundation km^2/km). This analysis assumes there are no coastal defences (dykes, sea walls etc). Therefore, rather than showing absolute values of inundation in 2100, Fig. 4.16 shows the change in inundation from the present to 2100.

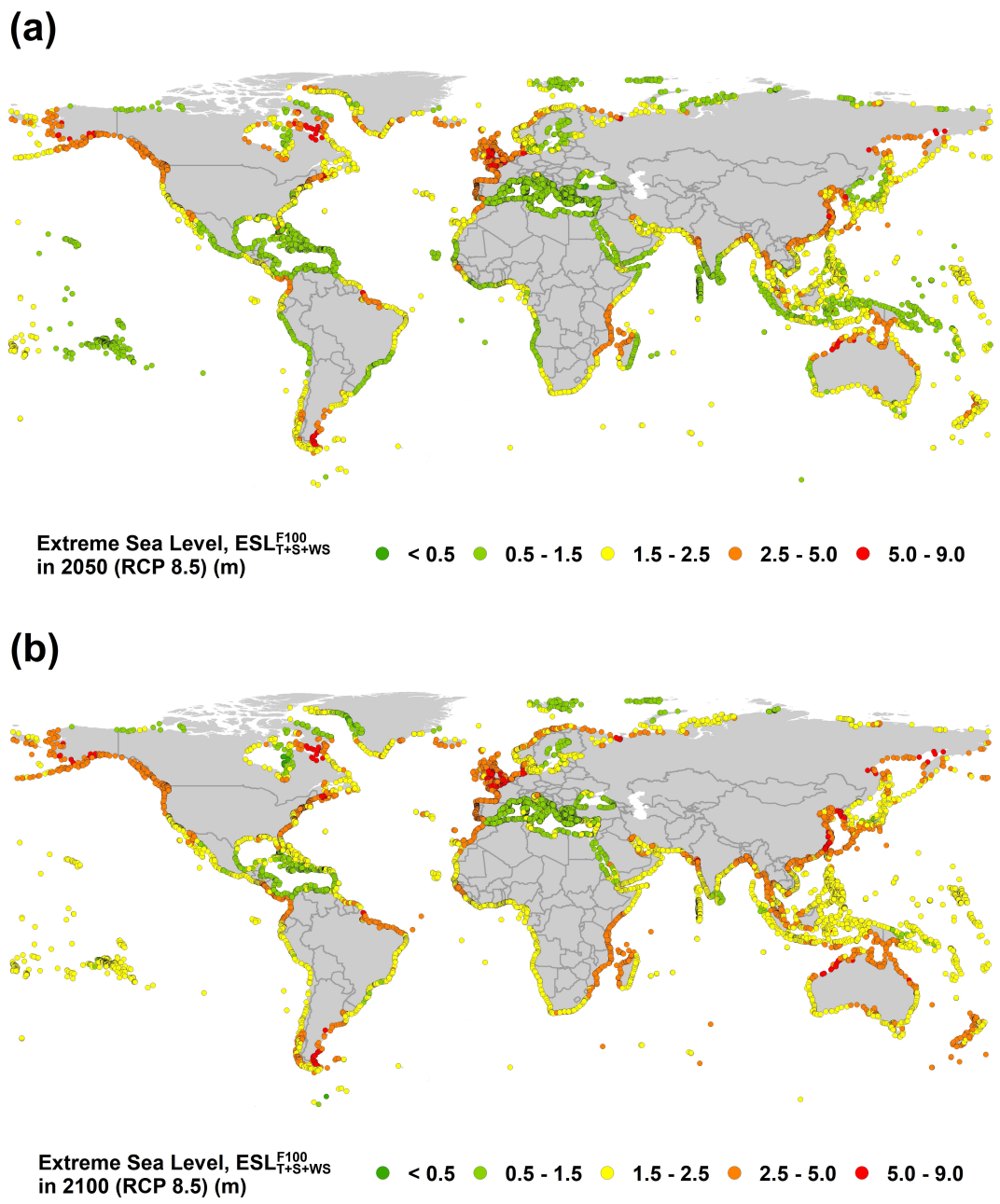

FIGURE 4.14: Global distribution of projected extreme sea level (ESL^{F100}_{T+S+WS}) for RCP8.5 in (a) 2050 and (b) 2100

Areas with significant increases in flooding are seen in north-west Europe, India/Bay of Bengal, south-east and east Asia.

Fig. 4.17 shows both the ESL^{F100} and the resulting flooding area for a number of the "hotspot" regions shown in Fig. 4.16. Although the flooding extent does not appear large in such plots, the global flooding extent for RCP8.5 is 661,000 - 1,009,000 km^2 (approx. 0.5 - 0.7% of the global land area, larger than the land area of France). Note that the range of values represents the 90^{th} percentile confidence interval. Table 4.4

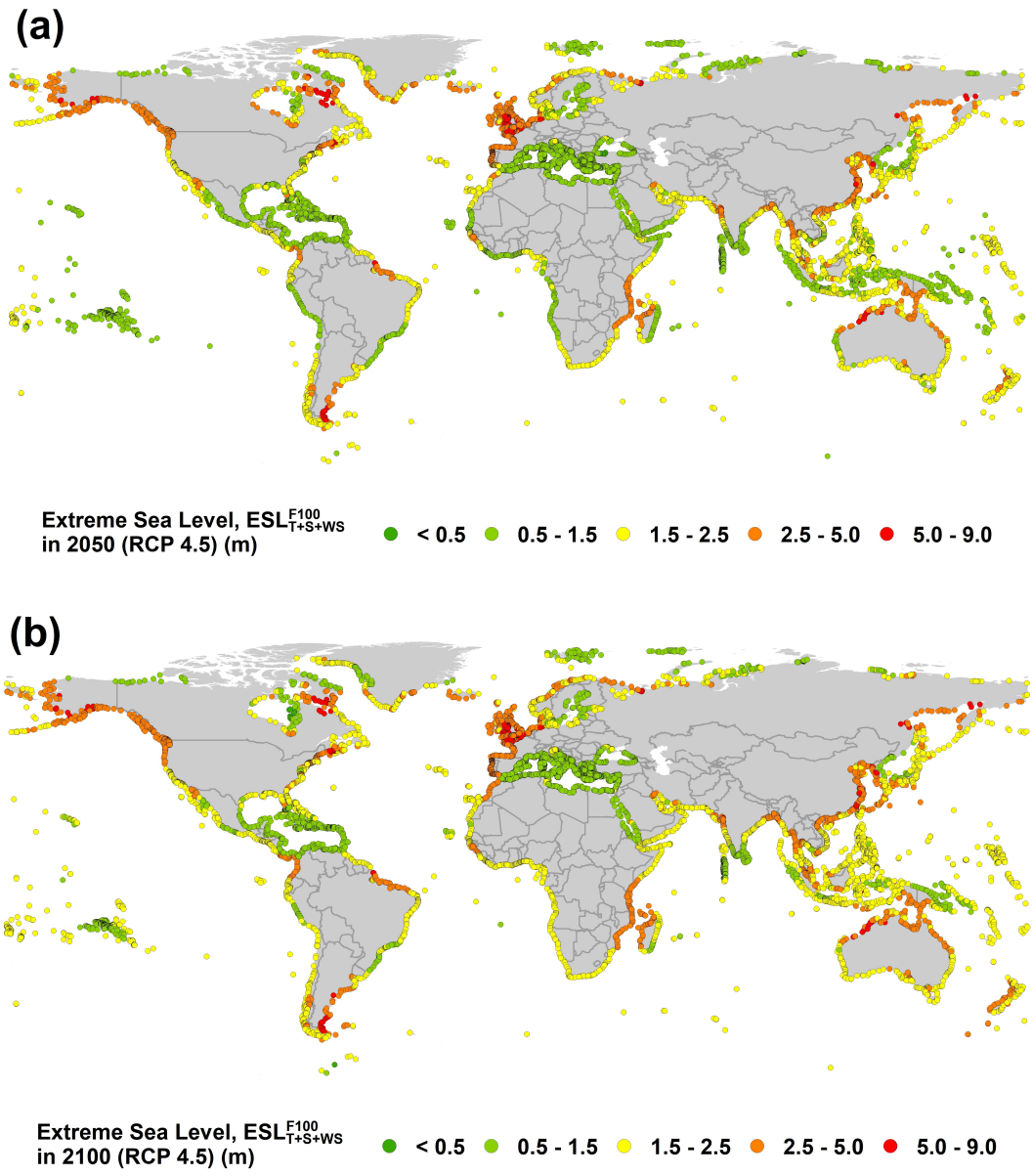

FIGURE 4.15: Global distribution of projected extreme sea level (ESL^{F100}_{T+S+WS}) for RCP4.5 in (a) 2050 and (b) 2100

shows the global flooding extent for each RCP for both 2050 and 2100. The Auxiliary Supplementary Data Google Earth file (Kirezci et al. (2020), Supplementary Material-2 therein) allows examination of values of ESL^{H100} and ESL^{F100} at any output location, interactively.

Further analysis of the relative contributions of the different physical processes to projected episodic coastal flooding (shown in Table 4.4) by the end of the 21^{st} century (see Section 4.10) indicates the following contributions for RCP8.5: $T+S$ (63%), $RSLR$ (32%), WS (5%). This result demonstrates that over the next century, $T+S$ will remain

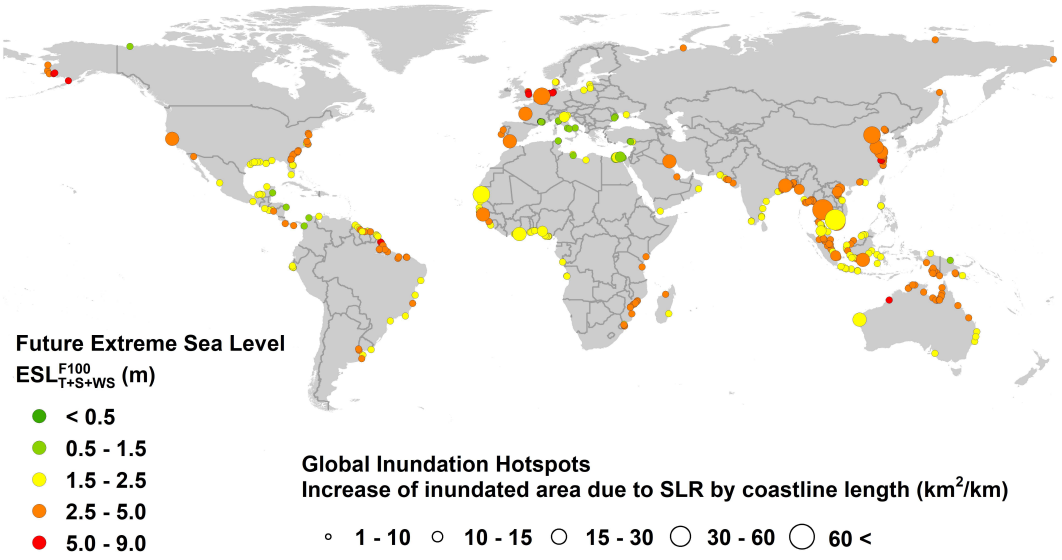

FIGURE 4.16: Global "hotspot" regions of changes in episodic coastal flooding in 2100 for RCP8.5. That is, the difference between projected episodic flooding in 2100 minus present day episodic flooding. Filled circles show locations where the change in normalized inundation (i.e. change in inundated area divided by length of coast) is greater than 1 km^2/km. Size of circle is related to the change in magnitude of the normalized inundation. Colour of the circle is related to the projected extreme sea level in 2100 (ESL^{F100}_{T+S+WS}). Note: to add clarity, where points overlap, not every point is shown on the figure.

		Inundated Area (mean) without WS (10^3 km^2)	Inundated Area with WS $CL^0.5$–*mean*–$CL^0.95$ (10^3 km^2)	Population Exposed $CL^0.5$–*mean*–$CL^0.95$ (million people)	Asset Exposed $CL^0.5$–*mean*–$CL^0.95$ (10^9 US$2011)
Present Day		521	512 – 553 - 603	128 – 148 – 171	6,466 - 7,761 – 9,135
2050	RCP 4.5	593 (14%)	549 – 631 – 721 (14%)	140 – 171 – 204 (16%)	7,094 - 8,848 – 10,672 (14%)
	RCP 8.5	601 (15%)	560 – 640 – 732 (16%)	142 – 173 – 207 (17%)	7,188 - 8,961 – 10,799 (16%)
2100	RCP 4.5	702 (35%)	604 – 737 – 894 (33%)	158 – 202 – 253 (36%)	7,919 - 10,222 – 12,739 (32%)
	RCP 8.5	779 (50%)	661 – 819 – 1,009 (48%)	176 – 225 – 287 (52%)	8,813 - 11,301 – 14,178 (46%)

TABLE 4.4: Values of area of global episodic coastal flooding (with and without the wave setup contribution), population and assets exposed for different RCPs in 2050 and 2100. Present day values shown for comparison purposes. For each case the mean and lower and upper 90^{th} percentile values are shown. Values in brackets represent the percentage change of mean values [i.e., $(future–present)/present$]

the dominant process in determining the extent of global flooding. However, $RSLR$ does significantly increase the frequency of coastal flooding. For RCP8.5, flooding associated with present day 100-year return period events will, on average, occur at least once every 10 years south of the $50°N$ latitude. It should be noted that the exact change in frequency of these extreme flooding events is sensitive to the EVA analysis used (see Section 4.7).

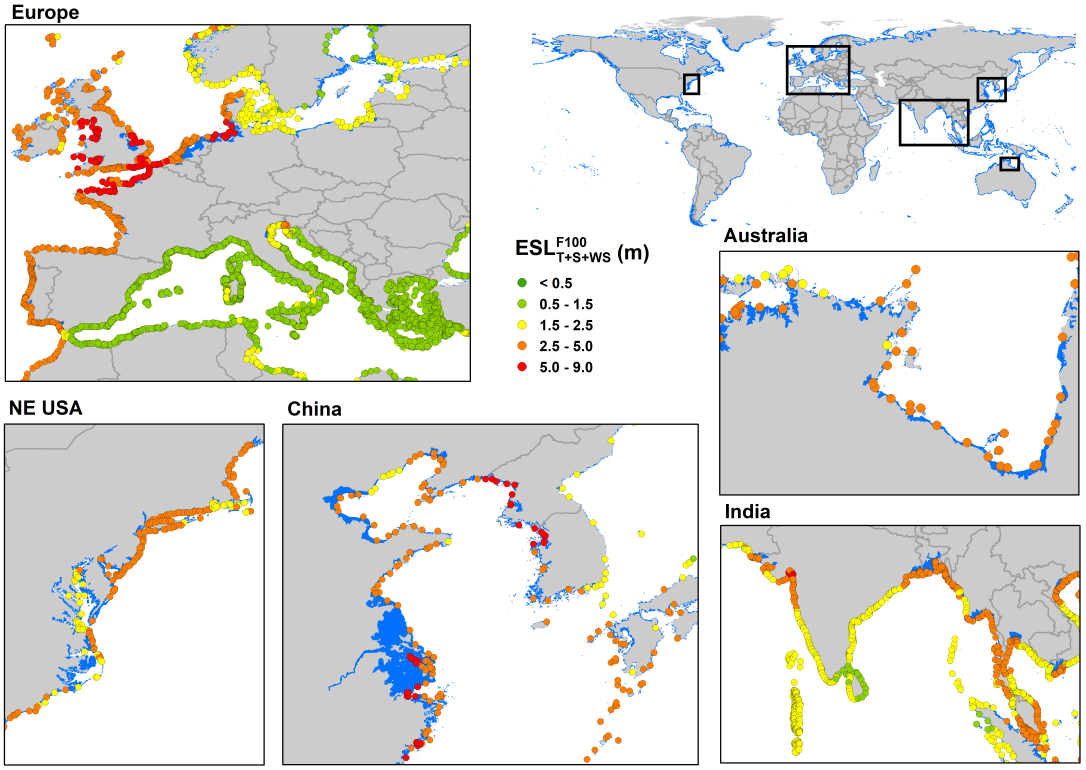

FIGURE 4.17: Regional areas showing the projected flooding associated with a 100-year return period extreme sea level event for 2100 ($T + S + WS + RSLR$). An RCP8.5 scenario is assumed. Coloured dots show the magnitude of the projected extreme sea level (ESL^{F100}_{T+S+WS}) at the coast. Flooding extent shown by blue shading.

4.10 Determination of flooding and contributions of various processes

Values of ESL^{H100} and ESL^{F100} have been estimated at each of the DIVA output points. In order to determine resulting episodic coastal flooding, these values need to be associated with a surrounding area. The association of areal significance to point measurements occurs in a number of disciplines, most notably hydrology. Following these precedents, we assigned Thiessen polygons to each DIVA point. The boundaries of such polygons are defined by lines whose perpendicular bisectors are equidistant between surrounding points. With the regions associated with each DIVA point determined, and the topography within the polygon defined by the MERIT elevations, locations which were shore-connected and where ESL^{H100} or ESL^{F100} were greater than the land elevation were considered to be inundated.

The flooding extent in Table 4.4 provide the basis to determine the relative contributions to episodic coastal flooding of each of the physical process of T, S, WS and $RSLR$. Table 4.4 indicates that for the present day, the total area inundated is $553 \times 10^3 km^2$, which reduces to $521 \times 10^3 km^2$ if WS is excluded. Hence, $T + S$ contributes 94.2% (521/553) and WS the remaining 5.8%. For 2100 and RCP8.5, the total area inundated increases to $819 \times 10^3 km^2$ ($T + S + WS + RSLR$) and if WS is excluded this area decreases to $779 \times 10^3 km^2$. Therefore, WS contributes 4.9% [(819 − 779)/819)], RSLR 32.5% [(819 − 553)/819] and $T + S$ the remaining 62.6%. Therefore, the present analysis shows that by the end of the 21st century, the largest contribution to extreme sea level and flooding will be the combined impacts of $T + S$. This will be responsible for approximately 63% of flooding, $RSLR$ for RCP8.5, 32% and WS 5%. As noted previously, these coastal flooding calculations assume no coastal defences such as dykes or sea walls.

4.11 Population and asset exposure

The global estimates of flooding described above, provide the basis for estimating both the population and the assets at risk from episodic coastal flooding. Asset exposure was estimated using the relationship (Hallegatte et al., 2013; Hinkel et al., 2014), $A = 2.8 \times P \times G$ where A is the asset value exposed to flooding (US$), P is the population and G is the Gross Domestic Product per head of population (US$/head). As noted above, the population was estimated from the GPWv4 database (International Earth Science Information Network (CIESIN), 2017) and the GDP per capita from Kummu et al. (2018). Table 4.4 shows the area inundated together with the population and assets exposed for the present day, 2050 and 2100 under both RCP4.5 and 8.5. All values are in 2011 US$ and assume 2015 population and GDP, consistent with the databases used. To make a direct comparison between present day and future periods, no attempt to project changes in GDP or population in future years has been included here.

The results project that the population potentially exposed to episodic coastal flooding will increase from 128 - 171 million to 176 - 287 million in 2100 under RCP8.5, where the span represents the 90^{th} percentile confidence interval (see Sections 4.8, 4.10 and 4.13) (an increase from approximately 1.8 – 2.4% of the world's population to 2.5 – 4.1%). The total assets exposed are projected to increase from US$6,466 – US$9,135 billion to US$8,813 – US$14,178 billion representing an increase from 9 - 13% to 12 - 20% of global GDP. As noted above, these values assume no flood defenses are in place and hence will overestimate the true values. However, the results indicate that for RCP8.5, by 2100 it is projected that the mean values of area inundated, population affected and assets threatened will increase by 48%, 52% and 46%, respectively.

4.12 Comparison with Previous Studies

The model results in this study were rigorously validated against a comprehensive tide gauge dataset (Woodworth et al., 2016) for both ambient and extreme conditions, so as to be able to obtain reliable projections of extreme sea levels over the 21st century. Importantly, state of the art model data representing tide, surge, wave setup and relative sea level rise is utilized here, demonstrating the contributions of each of these processes to extreme sea level and resulting episodic coastal flooding. This study builds on several previous model studies which have included some, but not all, of these elements.

Muis et al. (2016) adopted an approach similar to the present work but did not include WS. The resulting TSL was validated against a less extensive tide gauge dataset than the present study and used only a single EVA approach (AM with GUM). Based on the present results, ignoring WS means that ESL_{T+S}^{H100} will be underestimated by between 0.3 m and 0.7 m, depending on the region under consideration (Fig. 4.10). Overall, however, it is concluded that WS contributes on average 17% to ESL^{H100} and only approximately 5% to total area flooded. The choice of EVA, however, has a significant impact on these quantities.

Vitousek et al. (2017) include WS and applied a single EVA approach (AM with GEV). The resulting TSL values were not validated either for ambient or extreme conditions and resulting coastal flooding was not investigated therein. Rather, the study concentrated on investigations of the changes in frequency of occurrence of future ESL.

Rueda et al. (2017) considered present day ESL including WS using a GEV distribution applied to an r-largest dataset. However, the study did not validate the data, nor did it consider projections of future ESL.

Vousdoukas et al. (2018b) used a 6-member ensemble of models forced with Global Circulation Models to account for changes in storm frequency and magnitude in the future. These elements were combined in a Monte Carlo analysis to determine extremes. Their analysis assumed that wave setup could be represented by $WS = 0.2 \times H_{s0}$ and that storms always occur at high tide. No validation was undertaken to assess the performance of the model.

Melet et al. (2018) considered the contributions of tide, surge and wave setup to historical TSL data. No EVA was undertaken and the focus of the paper was on the importance of WS. As indicated by Aucan et al. (2019), this analysis assumes that global bed slope is 1/10, uses a relationship to determine WS which is quite sensitive to bed slope (Stockdon et al., 2006) and also includes swash (runup). Hence, the resulting contribution to WS is

larger than may otherwise be expected. This point is discussed in more detail in Section 4.13.

It should be noted that the approach used in the present analysis is to attempt to reconstruct a long duration time series of TSL and then perform EVA on this time series. As T is deterministic and $S + WS$ is stochastic, this approach implicitly assumes that the time series is sufficiently long (36-years) to capture the random phasing of these components. That is, that extremes occur at all phases of the tide. The alternative is to consider the pdf of each process separately and combine these in a Monte-Carlo analysis (Vousdoukas et al., 2018b).

4.13 Limitations and Uncertainty Estimates

Due to the global-scale focus of this work, it has been necessary to make a number of assumptions in order to render the problem computationally tractable. Obviously, these assumptions will have some impact on the accuracy of the final projections. This section outlines these assumptions and makes order-of-magnitude estimates of potential errors:

- TSL is considered to be the linear summation of $T + S + WS$, with each of the components evaluated independently. Therefore, the analysis ignores the influence tidal stage will have on S and WS (Arns et al., 2017; Marcos et al., 2019). It is believed these non-linear effects will be small compared to the accuracy of the EVA analysis (Howard et al., 2010; Sterl et al., 2009; Vousdoukas et al., 2017, 2018b). Also, the extensive validation indicates that at global-scale, the present approach agrees well with tide gauge data both for ambient and extreme conditions.

- The model of T+S+WS is validated against tide gauges. Tide gauges which are offshore or in sheltered locations are likely to underestimate WS (Hoeke et al., 2013; Lambert et al., 2020; Melet et al., 2016; Melet et al., 2018). This may account for some of the scatter in the comparisons between model and tide gauge data, although the agreement is generally good.

- The validation of $T + S + WS$ is conducted with the quasi-global GESLA-2 tide gauge dataset which is the most extensive network of global sea level measurements available. However, such measurements may not demonstrate spatial consistency at the global scale. Such shortcomings are reported in the literature [e.g. (Marcos and Woodworth, 2017)]. However, in the present study, the model results agree well with the GESLA-2 measurements for a first-pass global analysis.

- Model data for the period 1979-2014 is used to determine ESL^{H100}. It is then assumed that these same extreme sea levels apply in 2100. This assumes that the meteorological and ocean wave conditions do not change significantly over this period. Although there is some evidence that changes may occur (Debernard and Røed, 2008; Hemer et al., 2013; Lowe and Gregory, 2005; Wang et al., 2008; Young and Ribal, 2019; Young et al., 2011), determining comprehensive projections of changes in extreme values of global surge and wave height (Mentaschi et al., 2017) is still an evolving research area.

  Mori et al. (2019) have estimated changes in ESL^{F100} for RCP8.5 using a large ensemble of Global Climate Models (GCMs). This ensemble had a spatial resolution of 60 km, subsequently downscaled to 20 km. Storm surge values were calculated in an approximate manner using an empirical relationship relating storm surge to

wind speed and atmospheric pressure drop. The approach could not estimate actual values of ESL^{F100} but provided estimates of percentage changes in ESL^{H100} (i.e., changes from the present day). For mid latitudes ($\pm 30°$), they indicated a decrease in storm surge values of approximately 10% in the Southern Hemisphere and an increase between 10% and 30% in the Northern Hemisphere. These changes were attributed to changes in the frequency and intensity of tropical cyclones. For higher latitudes (both hemispheres) they estimated smaller increases in storm surge (approximately 10%). It should be noted that the Mori et al. (2019) analysis did not include tide (T) and hence cannot be directly related to the present analysis. It should also be pointed out that there is still considerable debate about potential changes in tropical cyclone frequency, intensity and track due to climate change (Patricola and Wehner, 2018). Nevertheless, this analysis suggests possible impacts of up to 20% (noting the impacts of tide) on values of ESL^{F100} .

Morim et al. (2019) and Meucci et al. (2020) have investigated changes in global wave climate from an ensemble of GCMs which were used to force spectral wave models. They show increases in 99th percentile and 100-year return period significant wave height of up to 15%, mainly in the Southern Ocean. The present analysis shows that WS contributes only approximately 5% to total flooding. Therefore, an increase in future extreme wave heights is unlikely to have an appreciable contribution to global flooding.

- It is assumed that $ESL^{F100} = ESL^{H100} + RSLR$. In a similar fashion to the TSL, this assumes that changes in water depth caused by the $RSLR$ do not have a significant impact on extreme values of T, S or WS (Pickering et al., 2017). Noting the accuracy with which the EVA can be conducted, such interactions are likely to have a secondary effect on the results for most locations (Lowe et al., 2001; McInnes et al., 2013; Sterl et al., 2009).

- The estimates of WS are considered to be order of magnitude. As noted, even the GOW2 model cannot resolve bed slope or nearshore refraction and shoaling. In addition, there are a wide range of possible relationships which can be used to determine WS. A common engineering approach [Shore Protection Manual – Dean et al. (2005) and SPM (1984)] has been used here. An alternative approach which has been used in other studies (Melet et al., 2018; Vitousek et al., 2017) is that of Stockdon et al. (2006). In order to test the sensitivity of projected values of WS to the choice of this relationship, the full global analysis for the determination of ESL^{H100} was repeated using Stockdon et al. (2006) and a range of different values of bed slope. Bed slopes of 1/100, 1/30, 1/15 and 1/10 were tested, the value of 1/10 allowing a comparison with the study of Melet et al. (2018). Fig. 4.18(a) shows a comparison between ESL^{H100} at DIVA points using the SPM approach

(Dean et al., 2005; SPM, 1984) and Stockdon et al. (2006), both with a bed slope of 1/30. There is very little difference in the values of WS between the approaches and hence the values all agree well. Fig. 4.18(b) shows the comparison between the SPM approach with a bed slope of 1/30 and Stockdon et al. (2006) with a bed slope of 1/10, as used by Melet et al. (2018). The Stockdon et al. (2006) approach is sensitive to bed slope, increasing significantly as bed slope increases. Fig. 4.18(b) shows that with a bed slope of 1/10, the Stockdon et al. (2006) approach will predict extreme water levels, on average, 58% higher than the SPM approach with a bed slope of 1/30. This explains why Melet et al. (2018) predict a much larger contribution due to wave setup than the present study. Note that Athanasiou et al. (2019) indicate that the mean global bed slope is approximately 1/100 and the present analysis indicates that a value of 1/30 agrees well with tide gauge data, irrespective of which formulation is used for WS (see Section 4.7). Therefore, it is concluded that the present study uses a global mean bed slope consistent with measurements and that the choice of relationship between deep water significant wave height and WS makes no appreciable difference at such representative bed slopes.

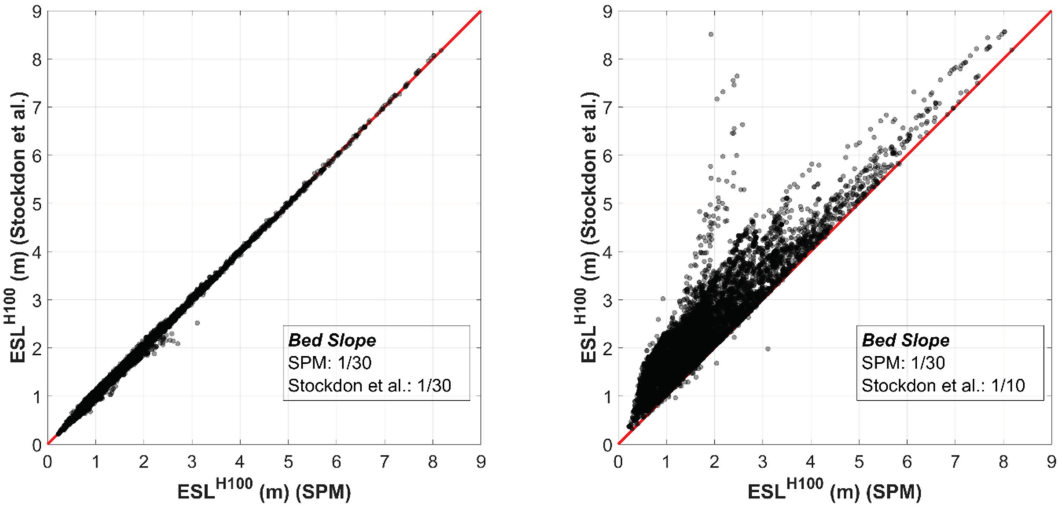

FIGURE 4.18: Comparison between Extreme Sea Levels (ESL^{H100}) determined with different formulations for WS. (*left*) Comparison between SPM (Dean et al., 2005; SPM, 1984) and Stockdon et al. (2006) with a bed slope of 1/30 for both. (*right*) Comparison between SPM (Dean et al., 2005; SPM, 1984) with bed slope of 1/30 and Stockdon et al. (2006) with a bed slope of 1/10 (as used by Melet et al. (2018))

It should also be noted that wave runup is not included in the present analysis. This is because wave runup does not cause an elevation in the mean sea level (Aucan et al., 2019). In localized cases where wave runup causes overtopping it may result in localized flooding. However, such considerations are considered insignificant at global scale.

- It is assumed that no flood protection measures, such as dykes or sea walls, are in place, in this part of the study. It is known that global flood extent is very sensitive to the assumption of current flood protection standards, but to date a comprehensive global database of such measures does not exist (see Chapter 5). Moreover, we apply a simplistic flooding model that ignores flood wave attenuation due to land roughness and an infinite flood duration (bathtub model), which will generally overestimate the flood extent (Ramirez et al., 2016; Vousdoukas et al., 2016a).

- As the MERIT (Yamazaki et al., 2017) topographic model used here to derive projections of episodic coastal flooding has a spatial resolution of 1 km, small-scale features such as estuaries and rivers are not resolved. Hence, estuarine flooding will be ignored, potentially resulting in an under-estimation of the coastal flooding in some regions (Kulp and Strauss, 2016). The vast majority of previous coastal flooding studies (Hallegatte et al., 2013; Hinkel et al., 2014; McGranahan et al., 2007; Muis et al., 2016; Neumann et al., 2015) have used SRTM (Jarvis et al., 2008) topography, which has a vertical resolution of 1 m. In contrast, MERIT provides much enhanced vertical resolution. The lower resolution SRTM was also tested as part of this study. This showed large differences at specific locations, but when averaged over all global locations the differences were at most 10%.

- The population and asset exposure are determined from the global population and GDP datasets as outlined in Sections 3.10 and 3.11. However, global validation of these parameters was not undertaken in this study. Although local exposure and damage observations exist in the literature (Armaroli and Duo, 2018; Jonkman et al., 2009; Kron, 2013; Rappaport, 2014), within the scope and scale of this study, global-to-regional downscaled values may not accurately represent much smaller scale localised observations. As Hinkel et al. (2014) pointed out, validation of global flood costs is a challenging task due to scarcity of the national studies available. Therefore, within the scope of this project, the verification is mainly focused on the statistical factors of the ESLs.

In addition to potential errors due to the assumptions made above, there is statistical uncertainty in the IPCC values of $RSLR$ and in the extreme sea level estimates, ESL^{H100}. Such statistical uncertainty is usually represented in terms of confidence limits for ESL^{H100} (see Section 4.8). These confidence limits provide the basis to set upper and lower bounds on the projected global land area subject to episodic coastal flooding. The global gridded $RSLR$ values include 90^{th} percentile confidence limits, enabling such limits to be determined at each DIVA point. Similar confidence limits can be determined for ESL^{H100} as outlined in Section 4.8. The full analysis process to determine

(a) RCP4.5	$ESL_{lower}(10^3km^2)$	$ESL_{mean}(10^3km^2)$	$ESL_{upper}(10^3km^2)$	Uncertainty span
$RSLR_{lower}(10^3km^2)$	604	647	697	-6.5% to 7.8%
$RSLR_{mean}(10^3km^2)$	699	737	789	-5.2% to 7.0%
$RSLR_{upper}(10^3km^2)$	797	837	894	-4.8% to 6.7%
Uncertainty span	-13.5% to 14.0%	-12.3% to 13.6%	-11.6% to 13.3%	

(b) RCP8.5	$ESL_{lower}(10^3km^2)$	$ESL_{mean}(10^3km^2)$	$ESL_{upper}(10^3km^2)$	Uncertainty span
$RSLR_{lower}(10^3km^2)$	661	700	750	-5.5% to 7.2%
$RSLR_{mean}(10^3km^2)$	779	819	874	-4.9% to 6.8%
$RSLR_{upper}(10^3km^2)$	915	956	1,009	-4.3% to 5.6%
Uncertainty span	-15.1% to 17.5%	-14.5% to 16.8%	-14.2% to 15.4%	

TABLE 4.5: Uncertainty analysis for projected area flooded in 2100 accounting for statistical uncertainty in estimates of Extreme Sea Level (ESL) and Relative Sea Level Rise ($RSLR$). Area flooded in units of $[10^3km^2]$ is shown for the analysis using "upper", "mean" and "lower" bound estimates for both ESL and $RSLR$. The "Uncertainty span" shows the percentage difference for the lower to the upper bound estimates of area flooded relative to the mean [e.g. $(ESL_{upper} - ESL_{mean})/ESL_{mean}$ and $(ESL_{lower} - ESL_{mean})/ESL_{mean}$]. Table (a) shows results for RCP4.5 and Table (b) for RCP8.5.

the global area flooded was repeated for all combinations of upper, mean and lower confidence limits of both quantities. The resulting areas flooded in 2100 for both RCP4.5 and RCP8.5 are shown in Table 4.5. The results in Table 4.5 show that, on average, the uncertainty span (i.e. upper limit – lower limit) on the areas flooded is approximately 31.1% for $RSLR$ and 11.4% for ESL for RCP8.5. Following Wahl et al. (2017), these uncertainties have been combined using the sum of the squares of the individual uncertainties $\Delta_{TOT} = \sqrt{\sum_{i=1}^{N} \Delta_i^2}$, where Δ_{TOT} is the total percentage uncertainty and Δ_i is the percentage uncertainty from process i (in this case either $RSLR$ or ESL). When the above values are combined in this manner the resulting uncertainty span for flooded area is 33.1% or ±16.5%.

4.14 Discussion

Global model outputs of tide, surge and wave setup have been used to develop historical time series of total sea level around the world's coasts. These model results were extensively validated against global tide gauge data, showing good agreement. To estimate the extreme sea levels which occur during storm events, an extreme value analysis was applied to both model and tide gauge data. In order to estimate extreme sea levels over the 21st century, projected relative sea level rise for IPCC RCP4.5 and 8.5 was added to present day extreme sea levels. These projected extreme sea levels were then used to quantify global episodic coastal flooding in 2050 and 2100.

Results show that for RCP8.5, 0.5 - 0.7% of the world's land area will be at risk of episodic coastal flooding by 2100 from a 1 in 100-year return period event (an increase of 48% compared to the present day), impacting 2.5 – 4.1% of the world's population (increase of 52%) and threatening assets worth up to 12 - 20% of global GDP (increase of 46%). Note that these values assume no coastal defences or adaptation measures (see Section 4.13). In many locations, coastal defences are commonly deployed and by 2100, it is expected that adaptation and specifically hard protection will be widespread, hence these estimates need to be seen as illustrations of the scale of adaptation needed to offset risk. Future studies that consider the impact of coastal adaptation and defences could logically build on the present results. As such, we regard the present analysis as a "first-pass" estimate of global impacts of sea level rise.

The analysis shows that tide and storm surge will account for 63% of the global area inundated by 2100, with relative sea level rise accounting for 32% and wave setup accounting for only approximately 5%. Furthermore, projected sea level rise will significantly increase the frequency of coastal flooding by 2100, with results herein showing that for most of the world, flooding associated with a present day 1 in 100-year event could occur as frequently as once in 10 years, primarily as a result of sea level rise. As the episodic events of storm surge and wave setup will, between them, contribute approximately 68% of projected coastal flooding, any climate change driven variations in the frequency and/or severity of storm events could have significant impacts on future episodic coastal flooding.

As noted previously, the present study has a global-scale focus. As such, a number of simplifying assumptions are necessary to render the problem computationally feasible. These simplifications and the resulting implications are discussed in detail in Section 4.13. A summary of these assumptions appears below. The analysis undertaken is linear in nature. It is assumed that the total sea level (TSL) can be represented by the summation of $T + S + WS$. This explicitly ignores interactions between these processes.

Extreme value analysis is undertaken to determine historic extreme sea levels (ESL^{H100}). The linear assumption is again applied to determine future extreme sea levels (ESL^{F100}) by the linear addition of projected relative sea level rise ($RSLR$) by the end of 2100. This assumes that changes in wind speed and wave height over the coming century will be small, which is consistent with a number of recent studies (Meucci et al., 2018; Mori et al., 2019; Morim et al., 2019). Section 4.13 outlines the precedence for such linear superposition approaches for global-scale studies (Marcos et al., 2019; Melet et al., 2018; Muis et al., 2016; Rueda et al., 2017; Vitousek et al., 2017; Vousdoukas et al., 2018b) and concludes that the potential errors are relatively small compared to the uncertainties in the extreme value analysis and $RSLR$ projections.

In order to calculate the magnitude of the wave setup (WS) at global scale, it is necessary to use relatively simple models (SPM, 1984; Stockdon et al., 2006) and to assume a global average bed slope. These assumptions will most likely result in errors at specific locations. However, the analysis ultimately shows that WS is a relatively small component of the ESL, and hence the adopted "first-order" representation of WS appears justified.

To validate the model adopted above, extensive tide gauge data is used (Fig. 4.2), as this is the only global water surface elevation data source available. An extensive comparison is undertaken for both ambient and extreme conditions. It should be noted, however, that it is likely that many tide gauges, due to their locations, will not respond to WS. Hence, this validation dataset has its limitations for this application. Although model and tide gauge data agree well at the global scale, there are clear differences at specific locations. For example, in more than 30% of examined locations, the $RMSE$ related to the mean tidal amplitude is greater than 20%. This is largely associated with semi-enclosed basins or regions with wide shelves (e.g. Mediterranean Sea, Baltic Sea, Sea of Japan) and with regions of small tidal range (see Fig. 4.5, Section 4.5).

The MERIT (Yamazaki et al., 2017) topographic model is used with a "bathtub" flooding model. This assumption is expected to generally overestimate flood extent (Ramirez et al., 2016; Vousdoukas et al., 2016a). Importantly, the analysis also assumes no flood protection is in place, such as dykes or other structures. As a result, the absolute values of flood extent will be over-estimated in many locations. For this reason, we emphasise relative changes in flood extent rather than absolute values. This is also addressed in Chapter 5.

The above assumptions mean that the present analysis may not model projected flooding at specific sites well. However, results show that, when aggregated to the global scale, the approach adopted here is able to produce first-order estimates of global flooding and its implications. In addition to these simplifying assumptions, both the ESL and

RSLR estimates have associated statistical uncertainties. The present study considered these uncertainties in assessing statistical variability associated with estimated flooding extent. The full analysis, given in Section 4.13 and Table 4.5, indicates the uncertainty associated with projected flooding in 2100 (RCP8.5) is approximately ±16.5%.

Chapter 5

Global analysis of the regional impacts of coastal flooding over the 21st Century

This chapter is based on the version of the paper that is in preparation for submission.

Building on a global database of projected extreme coastal flooding over the coming century, an analysis that accounts for both existing levels of coastal defences and two scenarios for future changes in defence levels is undertaken to determine future expected annual people affected ($EAPA$) and expected annual damage (EAD). A range of plausible future climate change scenarios is considered along with narratives for socioeconomic change (population and gross domestic product changes over the 21^{st} century). We find that with *no further adaptation*, global $EAPA$ could change by +92 M people/year and EAD by +US$ 11.7 T/year by 2100. If coastal defences are increased at a rate whereby the probability of coastal flooding does not increase, these changed values are reduced to +30 M people/year and +US$ 4.9 T/year, respectively. The impacts of such flooding will disproportionately affect the developing world. By 2100, Asia, West Africa and Egypt will be the regions most impacted in terms of both $EAPA$ and EAD. Many developing nations will experience EAD greater than 5% of GDP, whilst almost all developed nations will experience EAD less than 2% of GDP.

5.1 Background

Globally, low elevation coastal zones [coastal regions less than 10 m above mean sea level (MSL)] are home to approximately 600 million people and generate approximately US$ 1 trillion of global wealth (Hallegatte et al., 2013; Marcos et al., 2019; McGranahan et al., 2007; Milne et al., 2009; Nicholls and Cazenave, 2010; Vitousek et al., 2017). A number of recent studies have shown that both the populations and infrastructure assets of these regions are at significant risk due to episodic coastal flooding (Kirezci et al., 2020; Melet et al., 2018; Muis et al., 2016; Rueda et al., 2017; Vitousek et al., 2017; Vousdoukas et al., 2018b). Episodic coastal flooding occurs due to extreme sea levels (ESL) resulting from the processes of: storm surge, wave set-up, astronomical tide and climate-induced relative sea level rise (Kirezci et al., 2020) (also see Chapter 4). In order to assess the projected impacts of increases in ESL over the next century, it is necessary to estimate global magnitudes of coastal flooding, the levels of coastal defences which are already in place and may be developed in the future, the probability of damage to assets and projected populations at risk. In addition, such an analysis needs to consider both how populations and gross domestic product (GDP) may change in the future (Shared Socio-economic Pathways, SSPs) (O'Neill et al., 2014) and also projected changes to greenhouse gas levels (Representative Concentration Pathways, RCPs) (Church et al., 2013a). As all these quantities vary regionally, such an analysis needs to be regional by nature, aggregating results to the global scale.

Analyses which assess the impacts of projected coastal flooding at the national and regional level within a coastal flood risk framework have been recognized as important planning tools (Schinko et al., 2020; Tiggeloven et al., 2020; Vousdoukas et al., 2020). This study undertakes such a detailed analysis for countries and regions globally, estimating values of both Expected Annual Population Affected ($EAPA$) and Expected Annual Damage (EAD), building on previous analyses. As such, the outcomes of this study are intended to be a resource for policy developers considering the impacts of projected coastal flooding and the mitigation and adaptation measures which may be required for flood risk reduction in the coastal zone.

The present analysis builds on the study of Kirezci et al. (2020) which estimated coastal flooding extent for a 1 in 100-year event at each of a total of 9,866 points along global coastlines defined by the Dynamic Interactive Vulnerability Assessment database (DIVA) (Hinkel and Klein, 2009). Kirezci et al. (2020) adopted the MERIT (Yamazaki et al., 2017) digital elevation model and assumed no coastal flood protection was in place. Here we consider existing coastal defences at each of these global locations, estimated from national policies for the levels of flood defence, expressed as return period design values. Based on the calculated probability distribution function of coastal flooding at each

	Population		***Annual GDP***	
	Present (2015)		***Present (2015)***	
	7,330M (762M)		$94,022B ($13,248B)	
	2050	***2100***	***2050***	***2100***
SSP1	8,473M (839M)	6,889M (649M)	$286,159B ($29,988B)	$566,417B ($54,936B)
SSP3	9,965M (913M)	12,640M (1,035M)	$178,222B ($17,536B)	$278,785B ($26,173B)
SSP5	8,575M (845M)	7,381M (690M)	$363,007B ($37,735B)	$1,017,654B ($97,083B)

TABLE 5.1: Global and Low Elevation Coastal Zone (shown in parentheses) Population and GDP estimations (Billions of US$ in 2005 currency) for various Shared Socioeconomic Pathway (SSP) narratives. [SSP1, SSP3 and SSP5 population data taken from (Gao, 2017; Jones and O'Neill, 2016) and GDP data is taken from IIASA-OECD available from `https://tntcat.iiasa.ac.at/SspDb/`]. Present day is assumed to be 2015.

location and a depth-damage relationship (Hinkel et al., 2014), the $EAPA$ and EAD (Hinkel et al., 2014; Zhou et al., 2012) are calculated for each region/nation, both for the present day and a range of future scenarios. The inclusion of a depth-damage relationship means that actual damage can be estimated, rather than simply determining the assets exposed to damage by flooding (Kirezci et al., 2020). The calculation of $EAPA$ and EAD requires an extension of the analysis to probabilities other than the 1 in 100-year event presented by Kirezci et al. (2020) and the integration over all such possible extreme events.

The calculation of $EAPA$ and EAD require gridded projections of gross domestic product (GDP) and population, from which exposed assets can be estimated (Hallegatte et al., 2013; Hinkel et al., 2014). In order to guide climate change studies, a set of reference pathways describing plausible alternative trends in the evolution of society and ecosystems over the coming century have been developed [Shared Socioeconomic pathways (SSPs)] (O'Neill et al., 2014). Global gridded values of population are available for these SSPs (Gao, 2017; Jones and O'Neill, 2016; Riahi et al., 2017). The SSPs can be combined with radiative forcing pathways RCP4.5 and RCP8.5 to define plausible futures for the Earth. Three scenario combinations: 'Sustainable world' (RCP4.5 combined with SSP1, SSP1-4.5); 'Fragmented world' (RCP8.5 and SSP3, SSP3-8.5) and 'Fossil-fuel based world' (RCP8.5 and SSP5, SSP5-8.5) (Vousdoukas et al., 2018a) are considered in this study. The gridded values of population and corresponding spatial GDP distributions can be summed to estimate global values for the present, 2050 and 2100, as shown in Table 5.1. For both SSP1 and SSP5 the global population increases by 2050 before declining by 2100. In contrast, the global population continues to grow for SSP3. All three SSPs show a continually increasing global GDP, with SSP5 resulting in the most rapid increase. It should be noted that the various SSPs show rather different trajectories in the developed and developing worlds. Hence, the global trends shown in Table 5.1 are not equally reflected in all regions of the world.

At both 2050 and 2100, values of $EAPA$ and EAD at any location will be impacted by: the ESL, determined here for both RCP4.5 and 8.5; the population and GDP, determined by the SSP and the vertical elevation of coastal defences which is determined by the adaptation scenario adopted. The analysis considers all of these variables. Initially we consider a "baseline case" where population and GDP remain constant at values for the baseline year (here taken as 2015) and only the ESL varies for each of RCP4.5 and 8.5 (*no socio-economic change*). Although this is not a plausible future case, it provides a means of determining how much of the calculated $EAPA$ and EAD is attributable to future changes in ESL and how much is attributable to population and GDP change. In addition, two adaptation scenarios are considered for each RCP/SSP combination. The first adaptation scenario (*constant flood probability*), assumes that the coastal flooding probabilities for future years remain the same as 2015 and that the SSPs define changes in population and GDP. Here, society responds to future sea level rise by greater adaptation, such that the flood probabilities remain constant. In the second adaptation scenario, both flood probabilities and SSP narratives define changes that are projected for the future. That is, the world does not introduce additional adaptation measures to respond to increased flooding. This can be considered a worst-case scenario (*no additional adaptation*).

5.2 Determination of Extreme Sea Levels

The extreme sea levels at each DIVA point were calculated using the approach described by Kirezci et al. (2020) (also in Chapter 4) and shown diagrammatically in Fig. 5.1(a-i). The time series of the historical total sea level $[TSL(t)]$ was defined at each point as the linear summation of tide (T), storm surge (S) and breaking wave set-up (W) [Fig. 5.1 (a-d)]. The TSL values were validated against an extensive database of tide gauge data for both ambient conditions and upper percentiles [Fig. 5.1 (f)].

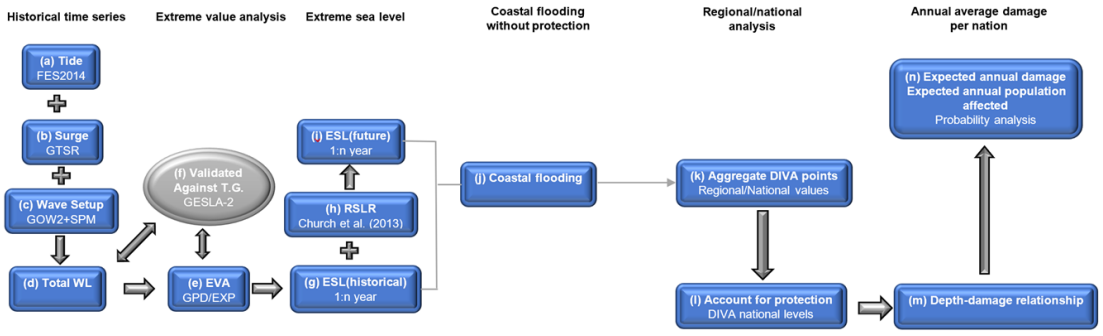

FIGURE 5.1: Diagrammatic representation of the processes used in the analysis of the various datasets in the full analysis.

The 1 in 100-year return period extreme value sea levels for these historical time series (ESL^{H100}) were determined from these model time series at each location using a peaks-over-threshold analysis with a probability distribution defined by the Generalized Pareto Distribution (GPD) [Fig. 5.1 (e)] as also described in Section 4.6. Again, these values of (ESL^{H}) were validated against tide gauge data (see Section 4.7).

The projected future extreme sea level (ESL^{F100}) [Fig. 5.1 (i)] was determined by adding the relative sea level rise due to climate change $(RSLR)$ to ESL^{H100} [Fig. 5.1 (h)]. This was done at each coastal location defined by the DIVA points with $RSLR$ varying regionally and defined on a global grid (Church et al., 2013a).

5.3 Determination of Coastal Flooding Extent

The Kirezci et al. (2020) coastal flooding analysis assumed no coastal defences and assigned values of ESL^{F100} to areal regions using Thiessen polygons. Coastal flooding was then calculated using a "bathtub" approximation [Fig. 5.1 (j)]. The present analysis modifies this approach to approximate the impacts of coastal defences at the global scale. The DIVA database contains data of the recommended return period protection levels specified at sub-national scale. The DIVA points were assigned to national boundaries and the protection level return period determined for each point [Fig. 5.1 (n)]. The GPD probability distributions were then used at each location to determine the ESL^{Hx}, where x is the national protection level return period for that location. The superscript "H" indicates that this is an historical value of extreme sea level (i.e. no relative sea level rise included). It was assumed that this level of coastal protection was in place at each location and the calculated ESL^{Hx} was taken as the new datum. That is, if ESL^{Fn} is below this value, no coastal flooding occurs in that polygon. The probability of exceedance of an extreme sea level for a given return period n, ESL^{Fn}, is related to the probability of exceedance, P by $n = 1/P$, where the probability of the event occurring in any one year is P.

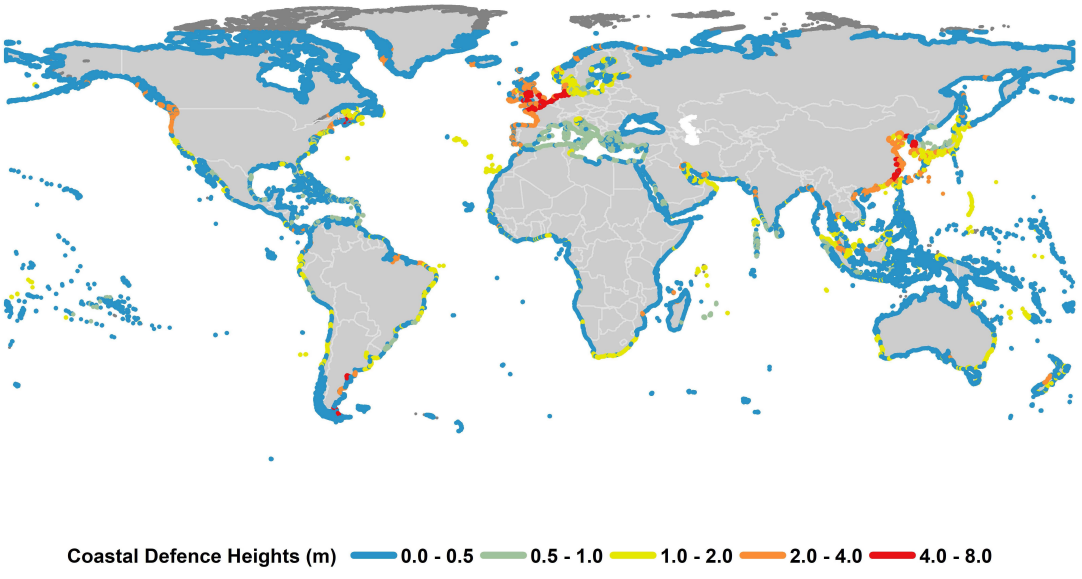

FIGURE 5.2: Global plot of coastal defence heights at DIVA points

5.4 Expected Annual Damage and Expected Annual People Affected

Knowing the value of assets in an area flooded does not provide a direct measure of the resulting damage. Such an understanding can be obtained by defining a depth-damage function (Hinkel et al., 2014; Messner et al., 2014), which defines the percentage of the value of the assets damaged as a function of flood depth. Following Hinkel et al. (2014), such functions generally have a declining slope, indicating that additional damage decreases with flooding depth, with a common form given by Hinkel et al. (2014) and Messner et al. (2014):

$$V = d/d + 1 \tag{5.1}$$

where V is the proportion of the assets damaged and d is the water depth above the defence level, ESL^{Hx} [Fig. 5.1 (o)]. Eq. 5.1 indicates that at a water depth of 1 m, 50% of the value of the assets are lost. The extreme sea level for a given return period, n is related to the probability of exceedance, P, by $ESL^{Fn} = 1/P$ and the probability of the event occurring in any one year is P. As events of all probabilities can occur in any year, to determine the $EAPA$ or EAD it is necessary to sum over all probabilities of occurrence (Hinkel et al., 2014; Zhou et al., 2012).

$$EAPA = \int \xi \times PdP \tag{5.2}$$

$$EAD = \int V \times A \times PdP \tag{5.3}$$

where ξ and A are the population and assets exposed to inundated by flooding above the defence level, respectively. The assets exposed were calculated using the relationship proposed by Hallegatte et al. (2013) and Hinkel et al. (2014) $A = 2.8 \times \xi \times GDP$ [Fig. 5.1 (p)]. The product $V \times A$ in Eq. 5.3 defines the value of the damage to the assets. The populations were calculated at 2050 and 2100 for SSP1, SSP3 and SSP5 narratives from the gridded data of Gao (2017), which is an enhanced version of the data proposed by Jones and O'Neill (2016). The global GDP data is obtained from IIASA (Riahi et al., 2017) (`https://tntcat.iiasa.ac.at/SspDb/`). Here, the projected (future) country level GDP is distributed spatially according to the spatial distribution of the corresponding population [i.e. $GDP_i = (GDP_{country}/\xi_{country})\xi_i$, where the subscript "i" is the value a grid point "i"]. The integrals in Eqs. 5.2 and

5.3 were determined numerically with values of "ESL^{Fn}" at each DIVA point for return periods of $n = 1, 10, 100, 1000, 10000$ and the associated values of flooded area, V, A and ξ. Thus, the present analysis extends the results of Kirezci et al. (2020) by determining extreme flooding at probability levels other than the 1 in 100-year event. For all of these different probability levels the flooding extent was determined and the integrals in Eqs. 5.2 and 5.3 were applied.

5.5 Confidence Limits

The estimated values of ESL^{Fn} are statistical quantities obtained from the GPD fit to the model data and extrapolated to the desired probability level, n. As such, there is statistical uncertainty associated with these values. Confidence limits for the values of ESL^{Hn} at each DIVA point were calculated using a bootstrap approach (Efron, 1979; Meucci et al., 2018) in which 1000 realizations of the ESL were generated at each DIVA point. From this analysis 90^{th} percentile confidence limits were calculated for ESL and subsequent quantities which are calculated from these values (e.g. $EAPA$ and EAD). Therefore, the confidence limits were determined at each probability level considered and the results aggregated through the integrals in Eqs. 5.2 and 5.3. Tables 5.2, 5.3, 5.4, and 5.5 reflect these confidence intervals together with mean values. The uncertainties associated with the $RSLR$ ensemble model are included for the lower and upper estimates of the ESL^{Fn}, as described in detail in Section 4.13.

5.6 Analysis Results

As outlined in Sections 5.2 and 5.3, the global-scale, but regional-resolution, analysis undertaken here requires a number of simplifying assumptions in calculating ESL and flooding extent. These assumptions may result in imperfections at specific coastal locations. However, as shown in the extensive validations of Kirezci et al. (2020), when aggregated to regional and global values, the computed $ESLs$ are in good agreement with historical tide gauge data. As a result, in the present analysis, results are not presented at individual DIVA points. Rather, results are presented as figures and tables showing values aggregated into 51 Climate Reference Regions taken from Iturbide et al. (2020) and as tables at the national level.

Here, the results are presented at both the Global scale and the Regional/national scale. Within each of these sections, we consider the case of *no socio-economic change* and the adaptation scenarios of *constant flood probability* and *no additional adaptation*. Table 5.5 shows all the combinations considered. For the baseline *no socio-economic change case*, changes in $EAPA$ and EAD result only from changes in ESL and hence the results demonstrate only the impacts associated with climate scenarios (here, RCP4.5 and RCP8.5). For the *constant flood probability* scenario all impacts are a result of changes in population and GDP. Therefore, results for each of SSP1, SSP3 and SSP5 are considered. In the worst-case scenario of *no additional adaptation*, $EAPA$ and EAD are impacted by changes in flood probability, population and GDP. Therefore, each of SSP1-4.5, SSP3-8.5 and SSP5-8.5 are considered.

5.6.1 Global Scale Results

The global values of present and projected future population and GDP under various SSP narratives are not necessarily representative of coastal regions. Therefore, to provide a representative foundation for our analysis, we first determine the projections of population and GDP for the Low Elevation Coastal Zone (LECZ), defined as the area below an elevation of 10 m above mean sea level (McGranahan et al., 2007). These values were determined by summing the gridded population and GDP datasets (Gao, 2017; Jones and O'Neill, 2016; Riahi et al., 2017) below an elevation of 10 m (above MSL) for present day and future SSP narratives. As shown in Table 5.1, at present 762M people reside in the LECZ (10.4% of the global population) generating annually US$ 13,248B (14.1% of global GDP). These values are comparable (slightly lower) to the results of Jones and O'Neill (2016), the differences likely being due to differences in the elevation datasets used and the geospatial masking adopted. Consistent with the projected global changes (Table 5.1), the LECZ population and GDP are projected to

increase by 2050 for all three SSP narratives. By 2100, however, the LECZ population decreases under SSP1 and SSP5, but continues to increase under SSP3. The percentage of both the global population in LECZ regions and GDP generated in these regions in both 2050 and 2100 is, however, projected to remain comparable to the present day (decreases for all SSPs by less than 1%). Note that the "present" (baseline) population and GDP are based on 2015 values. Hence, the relative importance of the LECZ in terms of population and GDP generated is not projected to change significantly over the 21^{st} century.

As shown in Table 5.2, the analysis applied here shows that for present day (2015) ESL, mean global Expected Annual People Affected, $EAPA$ (by flooding) is 35M (34M – 37M) people, where the range shown in brackets is the 90% confidence interval. Similarly, the present day mean global Expected Annual Damage, EAD is $ 349B ($ 330B - $ 376B), where all values are in 2005 US dollars. Note that these values are significantly lower than figures reported by Kirezci et al. (2020). There are a number of reasons for this: the present figures are "annual" values, rather than 100-year return period values, the present values account for existing coastal defences and the values reported here are estimates of actual damage to assets rather than the value of assets exposed to flooding.

5.6.1.1 *No socio-economic change case*

As noted above, under the *no socio-economic change* case, it is assumed that there are no changes in population or GPD, but ESL probabilities, and hence the flood risk, change for emission representative concentration pathways, RCP4.5 and RCP8.5. The resulting global increases in values of $EAPA$ and EAD in 2050 and 2100 are shown in Table 5.2. By 2100 for RCP4.5 the $EAPA$ changes by +25M people (+71% change) and for RCP8.5, $EAPA$ changes by +36M people compared to the present day (+103% change). Similarly, by 2100, EAD changes by +$ 324B (+93% change) for RCP4.5 and by +$ 481B (+138% change) for RCP8.5. Note, for clarity, throughout this paper increases (or decreases) are shown with a "+" ("-") sign whereas absolute totals have no sign. Also, all such change values are relative to the baseline year 2015.

5.6.1.2 *Constant flood probability scenario*

The impact due only to the projected population and GDP changes (constant flood probability scenario), as defined by the various SSP narratives, is shown in Table 5.3. This scenario would occur if new adaptation measures introduced were such that the probabilities of coastal flooding remained unchanged from that at present. Under SSP1, both the global and LECZ populations increase by 2050 and then decrease by 2100

(relative to 2015). The mean $EAPA$ shows a similar behaviour, increasing by +7.0M people by 2050 and subsequently decreasing by -3M people by 2100 (both figures relative to the present-day, 2015; confidence limits shown in Table 5.3). With SSP3, the global and LECZ populations increase continually through the 21^{st} century, which are also reflected in the $EAPA$ (Table 5.3), with a change of +17.0M people affected by 2050 and a change of +30M people affected by 2100. The changes in global and LECZ populations for SSP5 (Table 5.1) are similar to SSP1, increasing in 2050 and subsequently decreasing by 2100. There is a resulting change in $EAPA$ of +7M people by 2050 and a subsequent change (relative to 2015) of -3M by 2100 for SSP5. The EAD is a function of both population and GDP and hence, its projected changes under this scenario are more complex than that of the $EAPA$. Unlike population, the global GDP is projected to continually increase over the 21^{st} century for all SSPs. The largest growth is projected for SSP5 and the smallest for SSP3. In response, there is a continual growth in EAD for all three SSPs. The largest changes both at 2050 and 2100 are seen for SSP5 (Table 5.3), +US$ 1,343B by 2050 and +US$ 4,863B by 2100. This reflects the projected high level of growth in GDP which overwhelms the relatively small population decreases (compared to the baseline year 2015) projected in coastal regions.

A comparison of the *no socio-economic change case* and the *constant flood probability scenario* shows the impact that projected changes in population and GDP have compared to projected increases in ESL on values of $EAPA$ and EAD. For $EAPA$, changes in ESL alone have a larger impact than the effects of socioeconomic changes alone. However, for EAD, the impacts of the socioeconomic changes (*constant flood probability* scenario) can be an order of magnitude larger than that of ESL impacts alone (*no socio-economic change* case). This result clearly shows the importance of considering projected changes in all three quantities: extreme sea levels, population and GDP, when assessing the impact of episodic coastal flooding in the future.

5.6.1.3 *No additional adaptation scenario*

Table 5.4 shows the results for the no additional adaptation scenario, where there are changes in population, GDP and flooding extent as a function of time. In this case, for all SSP narratives, the $EAPA$ continually increases with time. This occurs because, even if the population densities decrease, as is the case under SSP1 and SSP5, the area flooded continues to increase. The result is that more people are affected annually. By 2100, most people are impacted under the SSP3-8.5 pathway with a change of +92M people. In terms of EAD, again there is an increase with time across all SSPs. By 2100, the SSP3-8.5 pathway shows the lowest change in EAD at +US$ 3,165B, reflecting the low GDP growth for this narrative. In contrast, the SSP5-8.5 pathway shows the largest

	Expected Annual People Affected (M people)	
	Present	
	(34M) 35M (38M)	
No socio-economic change	*2050*	*2100*
RCP4.5	(+4M) +10M (+16M)	(+14M) +25M (+38M)
RCP8.5	(+5M) +12M (+17M)	(+20M) +36M (+53M)

	Expected Annual Damage (US$ B)	
	Present	
	($335) $353 ($380)	
No socio-economic change	2050	2100
RCP4.5	(+$52) +$127 (+$218)	(+$160) +$324 (+$522)
RCP8.5	(+$63) +$146 (+$239)	(+$257) +$481 (+$849)

TABLE 5.2: Global Expected Annual People Affected ($EAPA$) and Expected Annual Damage (EAD) for the present-day (2015), 2050 and 2100 for RCP4.5 and RCP8.5 emission pathways and the scenario of no socio-economic change. For each quantity the mean value is shown, along with the 5^{th} and 95^{th} percentile confidence limits (in brackets). The values for the present day (2015) are absolute values. The values for 2050 and 2100 are the changes compared to 2015 (represented by the ± sign). All dollar values are expressed in constant 2005 US$. [This scenario assumes there is no change in population or GDP with time]

change in EAD of +US$ 11,734B, again as a result of the large growth in GDP for this narrative.

Table 5.5 shows the values of EAD expressed as percentages of the total produced GDP at the date considered for each RCP/SSP combination (note – total values, not changes). At present, the global EAD is 0.37% of GDP. In the absence of a future increase in adaptation measures (*no additional adaptation scenario*), this value is estimated to increase to approximately 0.65% - 0.67% by 2050 irrespective of the SSP narrative, reflecting that population and GDP values do not diverge greatly under any of the SSP narratives by the mid-century. By 2100, however, the largest percentage increase in EAD occurs under SSP3-8.5 with a value of 1.26% of GDP. This is because, the lowest increase in the global GDP and highest increase in the population considered in this study is for this RCP/SSP combination. Keeping the flood probabilities unchanged throughout the century (*constant flood probability scenario*), that is, enhancing adaptation measures, reduces the highest percentage EAD (under SSP3) to 0.54% of global GDP. Note that this value is still higher than for the present day.

Hence, ensuring that global levels of flood protection keep pace with otherwise projected increases in coastal flooding, can approximately halve the globally averaged mean EAD compared to the case of taking no additional action.

	Expected Annual People Affected (M people)	
	Present	
	(34M) 35M (38M)	
Constant flood probability	*2050*	*2100*
SSP1	(+7M) +7M (+8M)	(-3M) -3M (-3M)
SSP3	(+17M) +17M (+18M)	(+29M) +30M (+31M)
SSP5	(+7M) +7M (+8M)	(-3M) -3M (-3M)

	Expected Annual Damage (US$B)	
	Present	
	($335) $353 ($380)	
Constant flood probability	2050	2100
SSP1	(+$941) +$986 (+$1,061)	(+$2,620) +$2,724 (+$2,908)
SSP3	(+$433) +$454 (+$489)	(+$1,112) +$1,157 (+$1,232)
SSP5	(+$1,282) +$1,343 (+$1,444)	(+$4,669) +$4,863 (+$5,201)

TABLE 5.3: Global Expected Annual People Affected ($EAPA$) and Expected Annual Damage (EAD) for the present-day (2015), 2050 and 2100 for SSP1, SSP3 and SSP5 pathways and the scenario of constant flood probability. For each quantity the mean value is shown, along with the 5^{th} and 95^{th} confidence limits (in brackets). The values for the present day (2015) are absolute values. The values for 2050 and 2100 are the change compared to 2015 (represented by the ± sign). All dollar values are expressed in constant 2005 US$. [This scenario assumes there is no change in flooding extent in the future with all changes due to changed population and GDP with time]

	Expected Annual People Affected (M people)	
	Present	
	(34M) 35M (38M)	
No additional adaptation	*2050*	*2100*
RCP4.5-SSP1	(+12M) +20M (+28M)	(+11M) +21M (+32M)
RCP8.5-SSP3	(+24M) +35M (+43M)	(+66M) +92M (+121M)
RCP8.5-SSP5	(+13M) +22M (+29M)	(+18M) +32M (+49M)

	Expected Annual Damage (US$B)	
	Present	
	($335) $353 ($380)	
No additional adaptation	2050	2100
RCP4.5-SSP1	(+$1,136) +$1,507 (+$1,870)	(+$4,209) +$5,589 (+$7,127)
RCP8.5-SSP3	(+$579) +$808 (+$1,021)	(+$2,279) +$3,165 (+$4,361)
RCP8.5-SSP5	(+$1,583) +$2,091 (+$2,550)	(+$8,690) +$11,734 (+$16,075)

TABLE 5.4: Global Expected Annual People Affected ($EAPA$) and Expected Annual Damage (EAD) for the present-day (2015), 2050 and 2100 for SSP1-4.5, SSP3-8.5 and SSP5-8.5 pathways and the scenario of no additional adaptation. For each quantity the mean value is shown, along with the 5^{th} and 95^{th} percentile confidence limits (in brackets). The values for the present day (2015) are absolute values. The values for 2050 and 2100 are the change compared to 2015 (represented by the ± sign). All dollar values are expressed in constant 2005 US$. [This scenario assumes that the flooding extent increases in the future with no changes in coastal defences and that population and GDP change with time]

	Expected Annual Damage (% of GDP)	
	Present	
	(0.35%) 0.37% (0.40%)	
Scenario 1	*2050*	*2100*
RCP4.5	(0.41%) 0.51% (0.63%)	(0.53%) 0.72% (0.96%)
RCP8.5	(0.42%) 0.53% (0.65%)	(0.63%) 0.88% (1.30%)
Scenario 2	*2050*	*2100*
SSP1	(0.44%) 0.47% (0.50%)	(0.52%) 0.54% (0.58%)
SSP3	(0.43%) 0.45% (0.49%)	(0.52%) 0.54% (0.58%)
SSP5	(0.44%) 0.47% (0.50%)	(0.49%) 0.51% (0.55%)
Scenario 3	*2050*	*2100*
RCP4.5 – SSP1	(0.51%) 0.65% (0.78%)	(0.80%) 1.05% (1.32%)
RCP8.5 – SSP3	(0.51%) 0.65% (0.78%)	(0.94%) 1.26% (1.70%)
RCP8.5 – SSP5	(0.53%) 0.67% (0.81%)	(0.89%) 1.19% (1.62%)

TABLE 5.5: Expected Annual Damage (EAD) for the present (2015), 2050 and 2100 for the scenarios of: no socio-economic change, constant flood probability and no additional adaptation and different RCP/SSP pathways/narratives. All values represent the EAD as a percentage of the GDP at the calculation time frame (present, 2050, 2100) under that scenario. For each quantity the mean value is shown, along with the 5^{th} and 95^{th} percentile confidence limits (in brackets).

5.6.2 Regional and National Scale Analysis

To discretize the above global scale assessment into regional and national scales, the values at each DIVA point were aggregated into the climate reference regions presented by Iturbide et al. (2020). Figure 5.3 shows the mean $EAPA$ and EAD for 2015 across these regions. The regions are ranked in terms of these quantities in Table A.1. As shown in Figure 5.3, S.E. Asia, S. Asia, E. Asia and W. Africa dominate global $EAPA$. This occurs because of relatively low levels of coastal defences ($<$ 0.5m – Figure 5.2), large populations and, in the cases of E. Asia and S. Asia, relatively large flooded areas (Kirezci et al., 2020). In total, S.E. Asia, E. Asia and S. Asia account for a total of 31M people impacted annually. Note that the global total $EAPA$ is 35M people (Table 5.2), demonstrating how these regions dominate the global totals (89% of the total). The EAD shows a similar global distribution, but with a reduced impact on W. Africa as a result of the very low GDP of this region. The three highest ranked regions in terms of EAD (2015), S.E. Asia, E. Asia and S. Asia account for an EAD of US$ 245B (Table A.1) compared to the global total EAD of US$ 349B (Table 5.2) (69%), a lower percentage of the total compared to $EAPA$ (69% compared to 89%). This reflects the lower GDP of these mostly developing Asian regions, relative to developed countries.

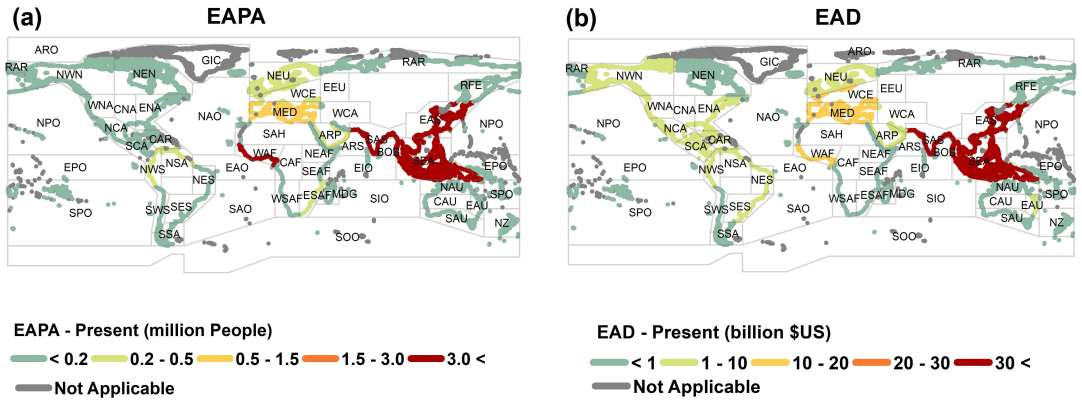

FIGURE 5.3: Present-day values (2015) of (a) Expected Annual People Affected ($EAPA$) and (b) Expected Annual Damage (EAD) in each of the 51 climate reference regions defined by Iturbide et al. (2020).

5.6.2.1 No socio-economic change case

Under the *no socio-economic change case* (no changes in population or GDP), S. Asia, S.E. Asia, the Mediterranean and E. Asia regions have the largest increase in $EAPA$ by 2050. However, by 2100, S.E. Asia dominates (Figures 5.4, 5.5, Tables A.2 and A.3). These results are consistent across both RCPs 4.5 and 8.5. This occurs because of the more rapid increases in the flooded area in S.E. Asia between 2050 and 2100 (Kirezci et al., 2020). A similar result is obtained for the increase in EAD, with the Mediterranean having the largest values in 2050 (Fig. 5.4, and Table A.4) but is overtaken in the ranking by S.E. Asia by 2100 (Fig. 5.5 and Table A.5). The Mediterranean dominates in 2050 because of its higher GDP but the relatively higher growth in the flooded area in S.E. Asia changes the ranking order by 2100. Note that the Mediterranean values are dominated by Egypt (see Section 5.6.2.4).

5.6.2.2 Constant flood probability scenario

Under the constant flood probability scenario (no change in flooding extent but changing population and GDP), in 2050, S. Asia followed by W. Africa show the highest increases in $EAPA$ (Fig. 5.6 and Table A.6) for all SSP narratives. By 2100 (Fig. 5.7 and Table A.7), the changing population shifts result in S. Asia being the most impacted region in terms of $EAPA$ for SSP3. However, W. Africa becomes the region with the highest increase in $EAPA$ for SSP1 and SSP5. In 2100, the largest increase in EAD (Figure 5.7, Table A.9) occurs for S. Asia followed by S.E. Asia for all SSP narratives. All increases mentioned are relative to 2015 values.

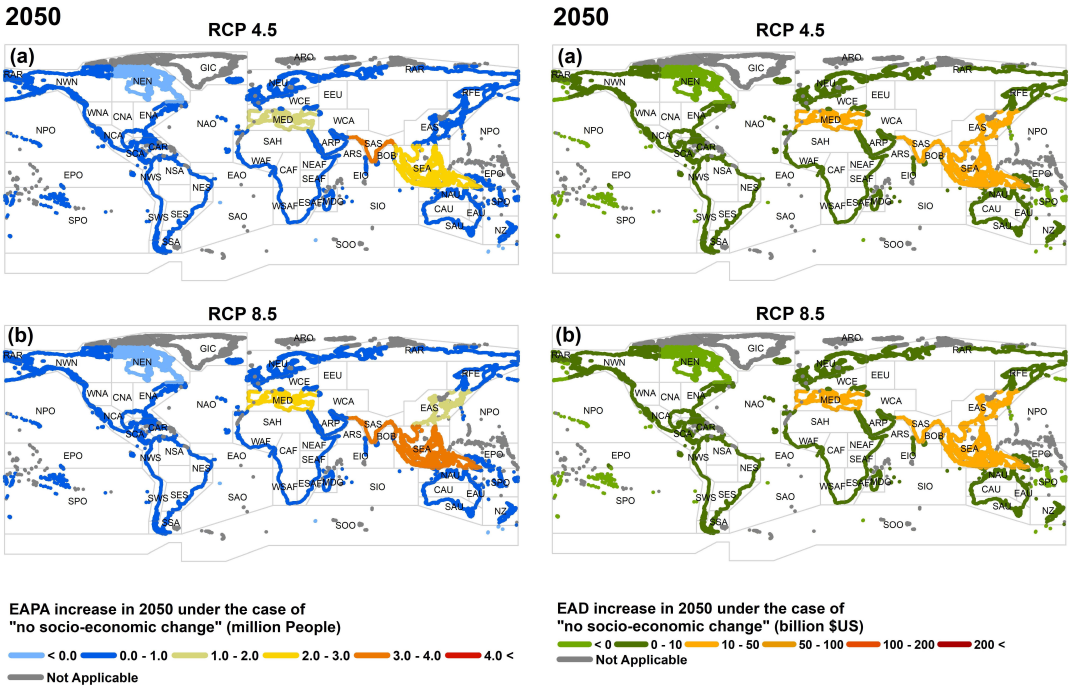

FIGURE 5.4: Change in $EAPA$ (left panels) and EAD (right panels) in 2050 for scenario of no socio-economic change [i.e. no changes in population or GDP as a function of time]. (a) RCP4.5, (b) RCP8.5. Values represent change relative to 2015.

5.6.2.3 No additional adaptation scenario

The *no additional adaptation scenario* assumes that the flooding extent increases in the future with no changes in coastal defences and that population and GDP change with time. Figure 5.8 and Figure 5.9 show the values of $EAPA$ and EAD for 2050 and 2100, respectively. The ranked list of regional impacts is also shown in Table 5.6 (top 5) and Tables A.10, A.11, A.12 and A.13 (full list).

The distribution and magnitudes of $EAPA$ under the three different RCP/SSP combinations shown in Figures 5.8 and 5.9 (Table 5.6) differ markedly. In each case, however, it is the S. Asia region which has the highest $EAPA$ and EAD values. By 2100 (relative to 2015), the projected number of people impacted annually in S. Asia will change by between +6.5M and +30.8M (Table 5.6, Table A.11) depending on the RCP/SSP combination. As clearly seen in Figure 5.9, W. Africa, the Mediterranean (largely Egypt) and S.E. Asia also show a significant change in people impacted annually by 2100 relative to 2015 (between +5.3M and +18.6M – Table 5.6). Table 5.6 also shows that the different SSP narratives have a striking impact on the $EAPA$. The values of $EAPA$ for SSP3-8.5 are typically 3 times larger than those for SSP5-8.5, driven by the higher population growth under the SSP3 narrative. The much lower population growth projected to occur in N. Europe and N. America, together with the higher levels of coastal

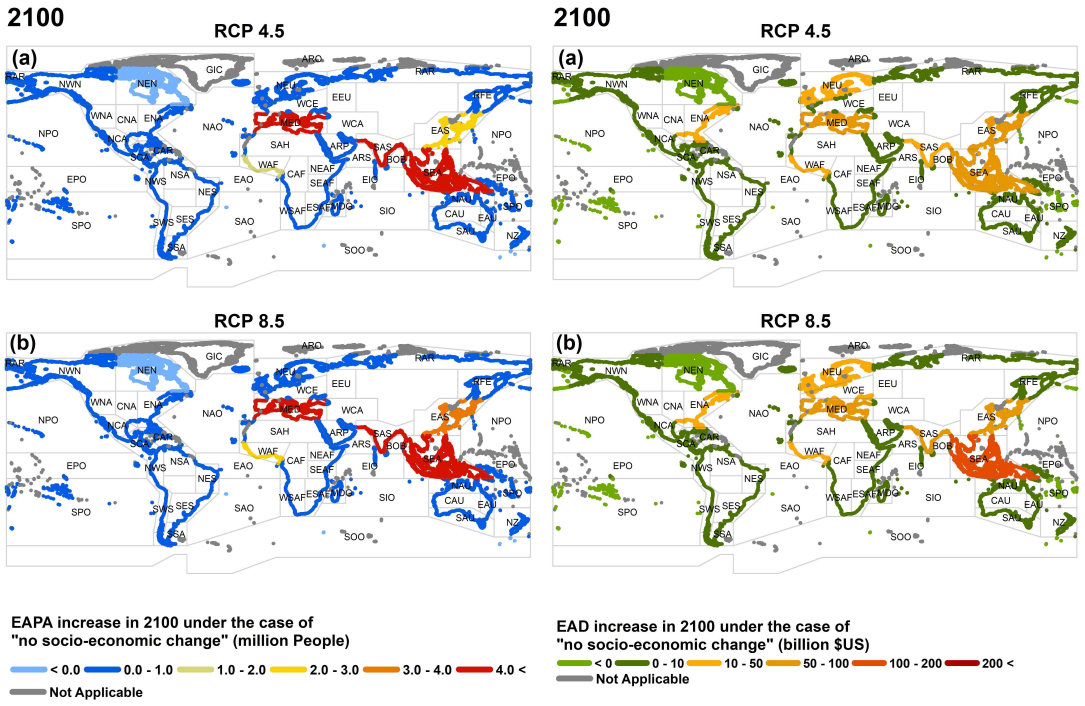

FIGURE 5.5: Change in $EAPA$ (left panels) and EAD (right panels) in 2100 for scenario of no socio-economic change [i.e. no changes in population or GDP as a function of time]. (a) RCP4.5, (b) RCP8.5. Values represent change relative to 2015.

protection in place (Figure 5.2), mean that these regions have a much lower increase in $EAPA$ than the developing regions mentioned above.

The regional distributions of EAD (Figure 5.8, Figure 5.9, Table 5.6 and Table A.12, A.13) are similar to $EAPA$ but the differences between developing and developed regions are less striking (both for 2050 and 2100). Again, by 2100, S. Asia shows the largest change in EAD ranging between (+US$ 765B and +US$ 3,353B), depending on the RCP/SSP combination. For all combinations of RCP/SSP the top five regions impacted are S. Asia, S.E. Asia, W. Africa, E. Asia and the Mediterranean. Across these 5 regions the aggregate changes in EAD are +US$ 2,706B (SSP3-8.5), +US$ 4,808B (SSP1-4.5), +US$ 9,682B (SSP5-8.5). Under the SSP5-8.5 scenario, the developed world is also impacted by 2100 with N. Europe ranking 6^{th} (Table A.13, +US$ 269B), E.N. America ranking 7^{th} (Table A.13, +US$ 232B) and C.N. America ranking 9^{th} (Table A.13, +US$ 220B).

5.6.2.4 *National Analysis*

The regional analysis described above can also be performed at the national level. Tables A.14 to A.26 show the top 10 countries for present-day (2015) coastal flooding impacts as well as increases by 2050 and 2100 (relative to 2015) under both combinations of

No additional adaptation	**Change in Expected Annual People Affected (M people)**							
								2050
SSP1-4.5			**SSP3-8.5**			**SSP5-8.5**		
Rank	**Region**	*EAPA*	**Rank**	**Region**	*EAPA*	**Rank**	**Region**	*EAPA*
1	S Asia	+8.4	1	S Asia	+13.9	1	S Asia	+8.8
2	Med	+2.9	2	SE Asia	+6.8	2	Med	+3.4
3	SE Asia	+2.9	3	W Africa	+4.7	3	SE Asia	+3.0
4	W Africa	+2.6	4	Med.	+4.4	4	W Africa	+2.6
5	E Asia	+0.9	5	E Asia	+1.2	5	E Asia	+1.1
								2100
SSP1-4.5			**SSP3-8.5**			**SSP5-8.5**		
Rank	**Region**	*EAPA*	**Rank**	**Region**	*EAPA*	**Rank**	**Region**	*EAPA*
1	S Asia	+6.5	1	S Asia	+30.8	1	S Asia	+8.3
2	W Africa	+5.3	2	SE Asia	+18.6	2	Med	+6.5
3	Med	+5.1	3	W Africa	+16.5	3	W Africa	+6.2
4	SE Asia	+1.0	4	Med	+13.6	4	SE Asia	+3.0
5	CN Amer	+0.6	5	SE Africa	+1.9	5	CN Amer	+1.1
No additional adaptation	**Change in Expected Annual Damage (US$B)**							
								2050
SSP1-4.5			**SSP3-8.5**			**SSP5-8.5**		
Rank	**Region**	*EAD*	**Rank**	**Region**	*EAD*	**Rank**	**Region**	*EAD*
1	S Asia	+$490B	1	S Asia	+$222B	1	S Asia	+$663B
2	SE Asia	+$339B	2	SE Asia	+$167B	2	SE Asia	+$461B
3	E Asia	+$224B	3	E Asia	+$114B	3	E Asia	+$319B
4	Med	+$145B	4	Med	+$109B	4	Med	+$207B
5	W Africa	+$91B	5	W Africa	+$39B	5	W Africa	+$126B
								2100
SSP1-4.5			**SSP3-8.5**			**SSP5-8.5**		
Rank	**Region**	*EAD*	**Rank**	**Region**	*EAD*	**Rank**	**Region**	*EAD*
1	S Asia	+$1,174B	1	S Asia	+$765B	1	S Asia	+$3,353B
2	SE Asia	+$1,105B	2	SE Asia	+$743B	2	SE Asia	+$2,285B
3	W Africa	+$899B	3	Med	+$564B	3	W Africa	+$1,747B
4	Med	+$686B	4	W Africa	+$414B	4	Med	+$1,377B
5	E Asia	+$374B	5	E Asia	+$222B	5	E Asia	+$921B

TABLE 5.6: Regional ranking of changes in $EAPA$ and EAD relative to 2015 for the scenario of no additional adaptation [assumes that the flooding extent increases in the future with no changes in coastal defences and that population and GDP change with time]. Projected values are shown for both 2050 and 2100 and for three RCP/SSP pathways/narratives. All dollar values are expressed in 2005 US$

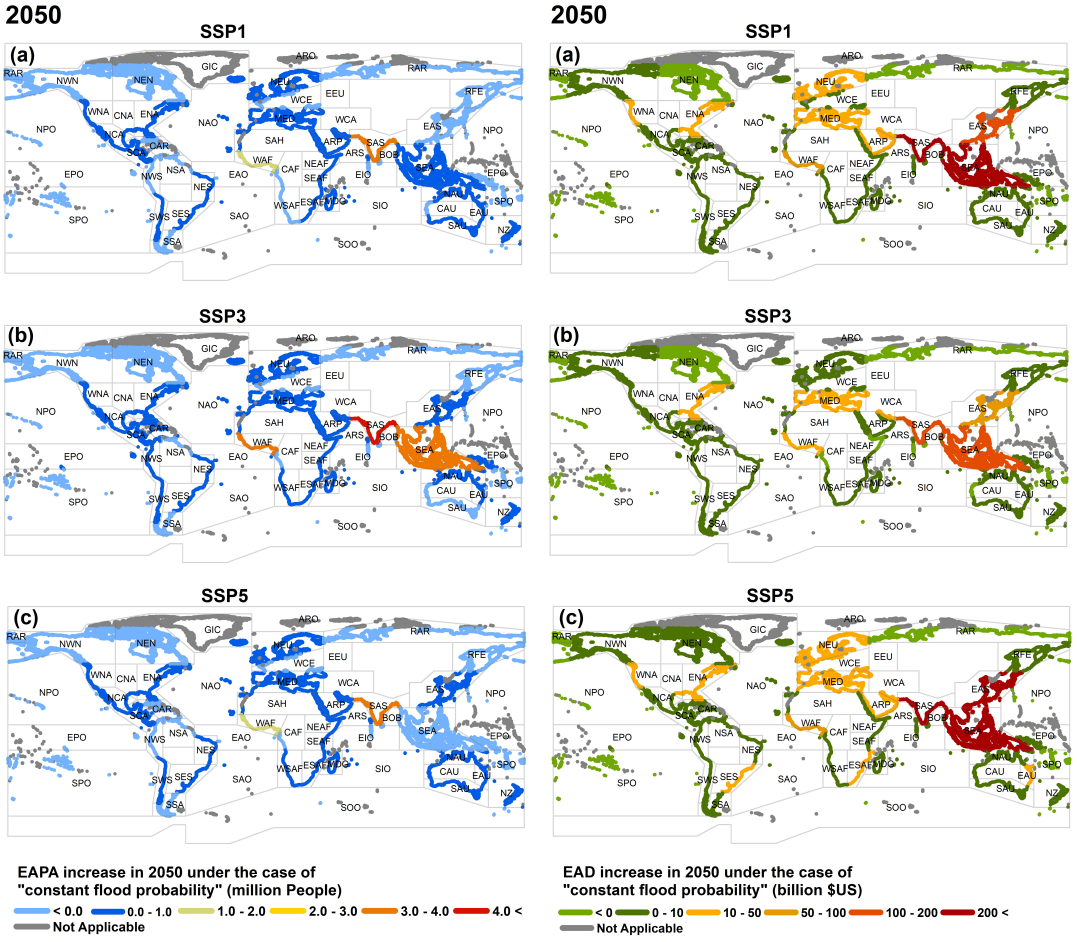

FIGURE 5.6: *EAPA* (left panels) and *EAD* (right panels) in 2050 for the scenario of constant flood probability, where adaptation measures increase over time such that flooding probability remains constant. Values shown represent the change relative to 2015. Panels show different Shared Socio-economic narratives (a) SSP1, (b) SSP3, (c) SSP5.

adaptation scenarios and SSP narratives considered. When ranked by order of *EAPA*, by 2050, India is projected to experience the highest changes under all combinations of scenarios (values between +2.1 M and +8.8 M people/year). These compare to the present-day value for India of 7.5M people/year. By 2100, the rank order of *EAPA* changes is more complicated. India is projected to have the highest changes of *EAPA* in 2100 for, the *constant flood probability scenario* - SSP3 and the *no additional adaptation scenario* – SSP1-4.5, SSP3-8.5 and SSP5-8.5. Nigeria ranks first for the *constant flood probability scenario* - SSP1 and SSP5. The projected changes in *EAD* show a more straightforward situation than the *EAPA*. For all future SSP narratives considered and both adaptation scenarios, India is projected to have the largest changes in *EAD* in both 2050 and 2100.

Tables A.27 and A.28 show the *EAD* as a percentage of national GDP (note: total

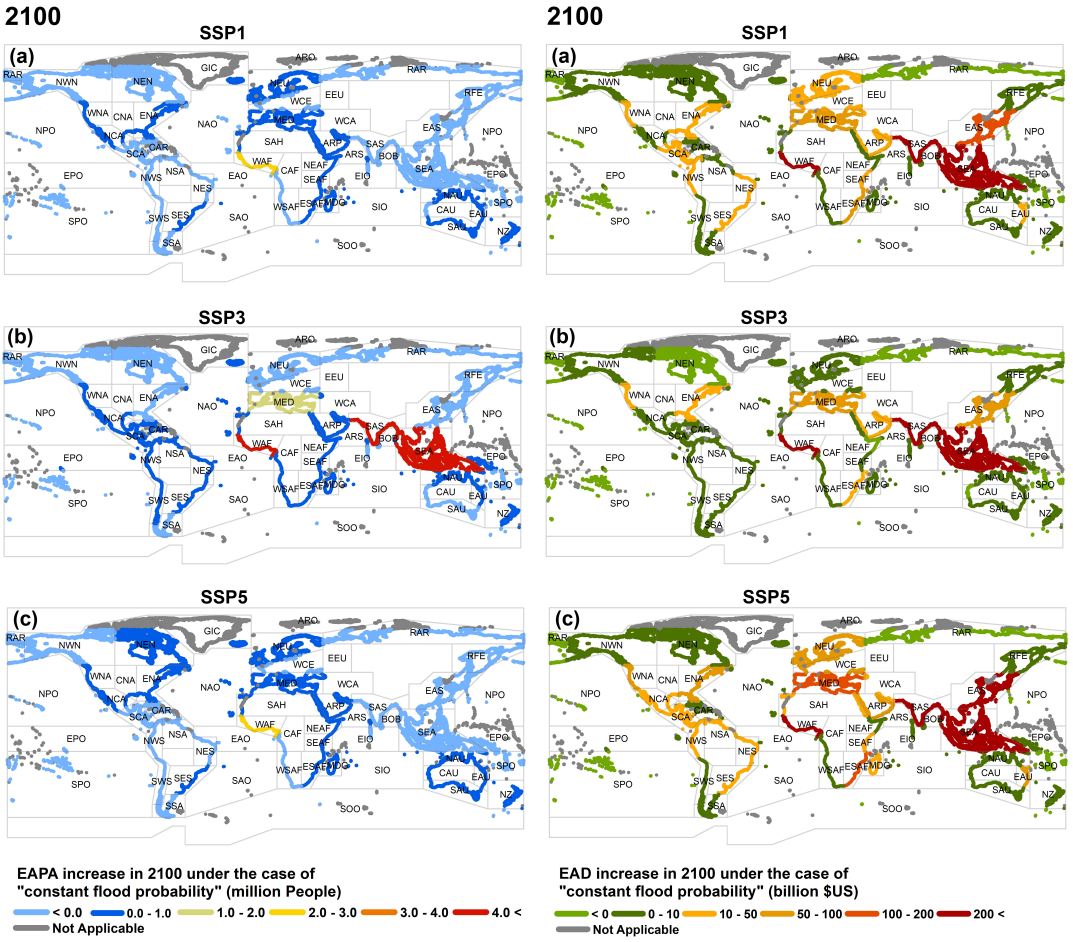

FIGURE 5.7: *EAPA* (left panels) and *EAD* (right panels) in 2100 for the scenario of constant flood probability, where adaptation measures increase over time such that flooding probability remains constant. Values shown represent the change relative to 2015. Panels show different Shared Socio-economic narratives (a) SSP1, (b) SSP3, (c) SSP5.

values, not changes) for 2050 and 2100 under the *no additional adaptation scenario*. Whereas the absolute changes presented above illustrate the comparative impact, the percentage figures better illustrate the impact on individual nations. When expressed in this form, the differences between the various RCP/SSP combinations are much reduced at national level. By 2100, the high growth in global GDP and the relatively high land areas flooded yields the highest values for SSP5-8.5. This is only 1% or 2% higher than for SSP3-8.5 but up to 6% higher than SSP1-4.5. The striking feature of the rankings is that developing nations are clearly the most impacted. Guyana, Vietnam, Mauritania, Myanmar and Egypt make up the top 5 nations in terms of the *EAD*/GDP ratio for all RCP/SSP combinations. These values are generally larger than 6% of GDP for the *EAD* and as high as 17.7% for Guyana. Very few developed nations appear in the top 50 nations for *EAD*/GDP ratio across all RCP/SSP narratives for the no additional adaptation scenario. Those that do appear, are nations which have a relatively large

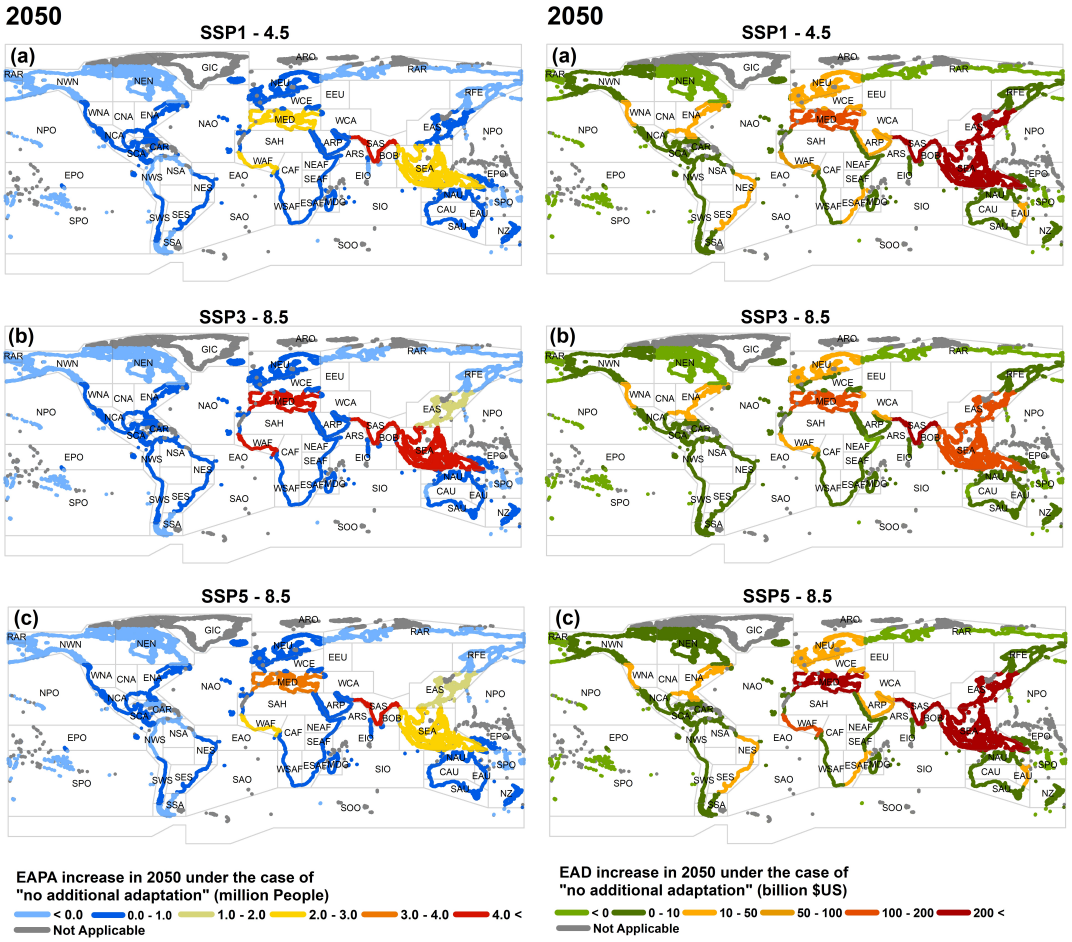

FIGURE 5.8: *EAPA* (left panels) and *EAD* (right panels) in 2050 for the scenario of no additional adaptation, where there are no changes in adaptation measures from present-day and flooding probability increases with time. Values shown represent the change relative to 2015. Panels show different RCP/SSP narratives (a) SSP1-4.5, (b) SSP3-8.5, (c) SSP5-8.5.

percentage of their infrastructure close to the coast. Japan appears in the top 35 with a projected impact of approximately 2% of GDP and Australia ranks between 45 and 50 with an impact of less than 1.5% of GDP (all figures for 2100, Table A.28).

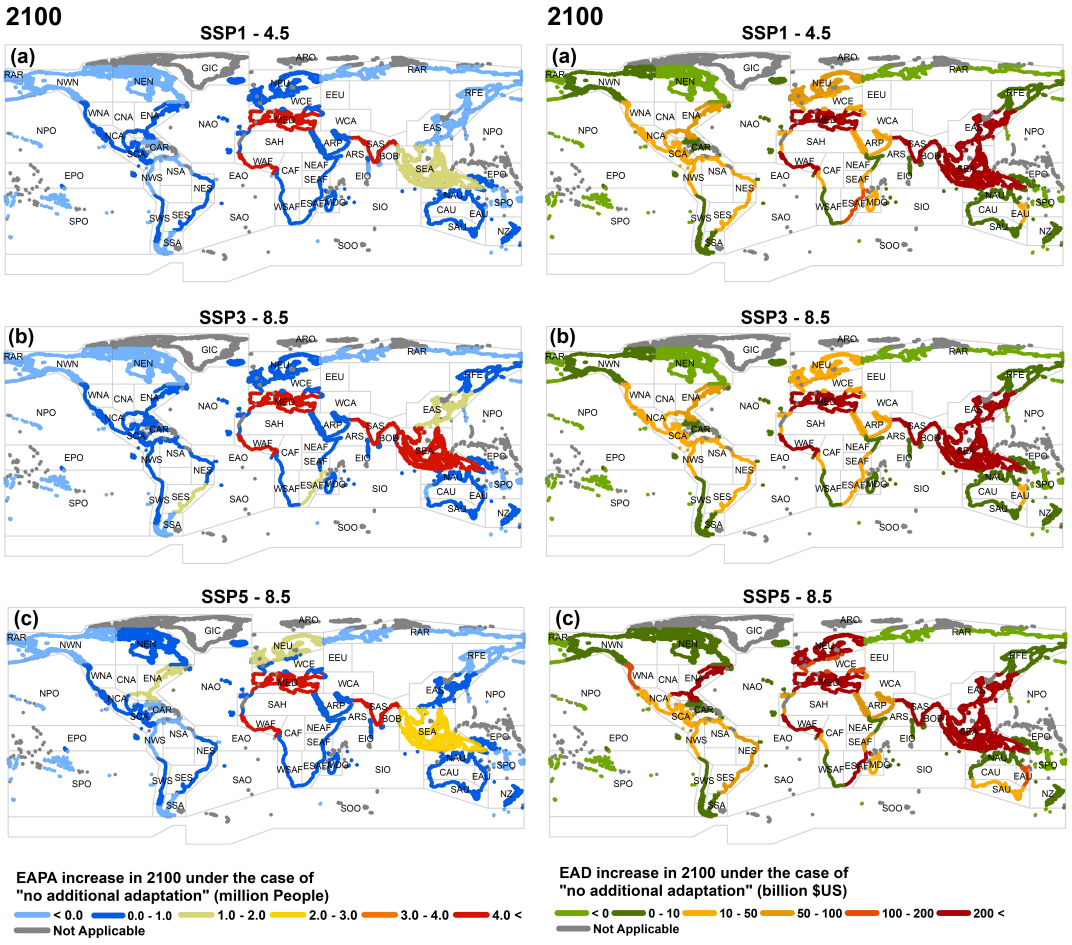

FIGURE 5.9: *EAPA* (left panels) and *EAD* (right panels) in 2100 for the scenario of no additional adaptation, where there are no changes in adaptation measures from present-day and flooding probability increases with time. Values shown represent the change relative to 2015. Panels show different RCP/SSP narratives (a) SSP1-4.5, (b) SSP3-8.5, (c) SSP5-8.5.

5.7 Limitations

A global-scale analysis of the type undertaken here requires a number of simplifying assumptions to make the problem tractable. This analysis extends the approach of Kirezci et al. (2020) to probability levels other than 1 in 100 years and integrates these values to determine $EAPA$ and EAD. Kirezci et al. (2020) validated their extreme value analysis approach against an extensive network of global historical tide gauge data. This same extreme value analysis was adopted here (i.e. Generalized Pareto Distribution). The future projections of ESL do not, however, include possible changes in extreme values of surge, tide levels and wave climate over the coming century, which were assumed small compared to the effect relative sea level rise has on changes in $ESLs$. Extreme value analyses as undertaken here are stochastic projections and hence involve uncertainty. Following Kirezci et al. (2020), the 90^{th} percentile confidence limits on all projections were calculated using a bootstrap approach (See Section 5.5 and are shown in Tables 5.2, 5.3, 5.4 and 5.5.

A "bath tub" flooding approach has been assumed to estimate areas impacted by coastal flooding. Such an approach ignores the attenuation of the overland flooding and potentially overestimates the potential impacts (Vafeidis et al., 2019). However, at global scale a more detailed flooding approach is not practical.

No global dataset of absolute values of coastal protection is available. Rather, the DIVA database (Hinkel and Klein, 2009) contains values of the design return periods at a sub-national basis. These were used here with an assumed probability distribution to estimate the corresponding protection levels. Although such an approach is consistent with design standards in each nation, whether such protection levels are always followed is unknown. This will result in uncertainties in some areas regarding the exact levels of present-day coastal protection.

A commonly used depth-damage relation, Eq. 5.1, (Hinkel et al., 2014) is used to estimate infrastructure damage given the depth of flooding and value of assets exposed. Although this approach has precedence in the literature, it is a global average value and will vary in specific locations giving rise to uncertainty.

The $EAPA$ and EAD were estimated from integration of the probability distribution function of extreme flooding extent (Eqs. 5.2 and 5.3). Based on the results of Kirezci et al. (2020) a Generalized Pareto Distribution (GPD) was assumed (see Section 5.2). If an alternative distribution had been used, there will be variation in these resulting values. However, the GPD has been shown to fit both modelled and measured ESL optimally.

The present analysis does not include land subsidence due to human induced groundwater or gas extraction, which may result in underestimation of the flooding impacts. Although regional relative sea level rise has the greatest impact on the increased coastal flooding extent, groundwater extraction poses a great challenge especially for densely populated coastal delta regions (Ericson et al., 2006; Syvitski et al., 2009; Tiggeloven et al., 2020). However, it is difficult to estimate and model projections of groundwater extraction at the global scale, as these trends are subject to change in time and are highly dependent on the dynamics of local communities (Hinkel et al., 2014).

5.8 Comparison with previous studies

Direct comparisons between the present study and previous global analyses (Diaz, 2016; Hinkel et al., 2014; Schinko et al., 2020; Tamura et al., 2019; Tiggeloven et al., 2020) are difficult due to differences in the methodologies and datasets used, which can result in large variations between the detailed findings. Nevertheless, there is general consensus across most of these studies, particularly in terms of the importance of future adaptation. Different studies assume a variety of different adaptation approaches and levels, making quantitative comparisons impossible. A common approach, however, is to determine the impacts "without future adaptation" (Hinkel et al., 2014) (as in the *no additional adaptation* scenario in this study). Therefore, here we confine comparisons to previous coastal flooding studies that consider present-day defence levels but do not account for any future adaptation by 2100.

- Hinkel et al. (2014), applied a range of datasets and adaptation strategies to account for uncertainties in coastal flood impact projections and adaptation cost estimates. Factors considered include: a range of regional sea level rise scenarios, population and asset exposure as well as socioeconomic scenarios SSP1-5. They found 2100 values of global $EAPA$ of: 0.2% - 2.9% (RCP 2.6) and 0.5% - 4.6% (RCP8.5) of global population. Values of $EAPA$ for the present study as a percentage of global population can be obtained from Table 5.4 and Table 5.5. Including the span of the 90^{th} percentile confidence limits, this yields values between 0.65% and 1.25% across all combinations of RCP/SSP. Hinkel et al. (2014) also found 2100 values of EAD ranging between 0.3 - 5.0% GDP (RCP 2.6) and 1.2% – 9.3% (RCP8.5), compared to 0.8% to 1.7% obtained in this study across all combinations of RCP/SSP (Table 5.5). Hence, the present results are at the lower end of the Hinkel et al. (2014) projections.

- Diaz (2016) developed an optimization model (Coastal Impact and Adaptation Model -CIAM) within the perspective of economic efficiency and found that, in the absence of future adaptation, the global EAD ranged between ($\sim$ US$ 1.5 - US$ 3.2T) by 2100. This compares with the range US$ 2.6T to US$ 16.5T for the present study (Table 5.4) across all combinations of RCP/SSP.

- Tamura et al. (2019) project global $EAPA$ by 2100 between 55.3M (RCP2.6, SSP1) and 106M (RCP8.5, SSP3). This compares with values between 45M and 158M (Table 5.4) across all RCP/SSP combinations in the present study. Tamura et al. (2019) projections of EAD range between US$ 169B (SSP3-2.6) and US$ 482B (SSP1-8.5), compared to the range US$ 2.6T to US$ 16.5T (present-day absolute values plus future change in Table 5.4) for the present study. Hence the present

values of $EAPA$ are comparable to Tamura et al. (2019) but the values of EAD for the present study are much higher than those of Tamura et al. (2019).

- Tiggeloven et al. (2020) determined global adaptation costs by 2080 for SSP5-8.5, obtaining a range of US$ 3T to US$ 6.8T/year. Table 5.4 shows values of EAD for SSP5-8.5 of US$ 1.8T to US$ 2.8T in 2050 and US$ 9.0T to US$ 16.3T by 2100 for the present study. Therefore, the Tiggeloven et al. (2020) 2080 values lie between these limits, indicating the studies yield comparable results.

- Schinko et al. (2020) considered economic impacts addressing the macro-economic implications of coastal flooding together with the direct damage and found that in the absence of the future adaptation, under SSP2-2.6 and SSP2-4.5, by 2050 the global EAD would be 0.17% - 0.55% (SSP2-4.5) and 0.13% - 0.54% (SSP2-2.6) of GDP. This compares to values between 0.51% and 0.81% (Table 5.5) across all combinations of RCP/SSP by 2050 in the present study. By 2100 Schinko et al. (2020) project a global EAD of 1.5% - 4.5% (SSP2-4.5) and 0.6% - 3.5% of GDP (SSP2-2.6). In comparison, the present study projects a global EAD of between 0.8% and 1.7% of GDP by 2100 across all combinations of RCP/SSP. Noting the different methodologies used, the results are comparable.

  As noted above, these previous studies produce a very large range of $EAPA$ and EAD values, and due to differences in methodology and datasets used, direct comparisons with the present study are difficult. Noting this, however, the projections provided by these previous studies span the range of projections obtained in our analysis.

5.9 Discussion

The majority of global-scale analyses of future coastal flooding consider the impacts of episodic events such as 1 in 100-year floods and, where they extend this to socio-economic consideration, the populations potentially impacted and the assets exposed to damage (Kirezci et al., 2020; Muis et al., 2016). Such studies provide a valuable understanding of potential "hot-spots" where episodic coastal flooding is likely to be a significant problem. However, aggregation of the results tends to significantly overestimate potential impacts. To address these issues, the present study, builds on the recent global analysis of Kirezci et al. (2020) and considers: expected annual values rather than 1 in 100-year values over the 21st century using IPCC RCP 4.5 and RCP 8.5 sea level rise scenarios, estimates of the present levels of coastal protection in place, estimates of infrastructure damage rather than assets exposed and considers how population and GDP may change in the future. As noted previously, these are similar to the approaches used by Tiggeloven et al. (2020) and Schinko et al. (2020).

Impacts for the World

Our results demonstrate that both projected changes in episodic coastal flooding and changes in future population and GDP result in substantial differences between the present and future coastal flood impacts in terms of people affected and damage caused to infrastructure. Without any future adaptation (*no additional adaptation scenario*), global $EAPA$ and EAD in 2100 change by +92M people/year (Table 5.4, SSP3-8.5) and +US$ 11,734B/year (Table 5.4, SSP5-8.5), relative to 2015. As noted below, these estimates are sensitive to assumptions made in computing flooding extent, coastal topography databases used and projected changes in population and GDP. Previous studies produce a wide range of values (see Section 5.8), with the results of the present study falling approximately in the middle of such studies (Diaz, 2016; Hallegatte et al., 2011; Hinkel et al., 2014; Schinko et al., 2020; Tamura et al., 2019; Tiggeloven et al., 2020). Our results indicate that under even a simplistic adaptation approach (*constant flood probability scenario*) that responds to changes in regional $RSLR$, the impacts of potential coastal flooding in terms of affected population, changes in $EAPA$, are significantly reduced (to +30M people/year, Table 5.3, SSP3), a factor of 3.1. Similarly, the change in EAD is reduced to +US$ 4,863B/year (Table 5.3, SSP5), a factor of 2.4.

The regional impacts of adaptation can be assessed by comparison of the constant flood probability and no additional adaptation scenarios in 2100 for $EAPA$ (Tables A.7 and A.11) and EAD (Tables A.9 and A.13). Relative changes in projected LECZ population changes tend to be more significant in developed rather than developing countries. Therefore, the inclusion of the adaptation measures in the constant flood probability

scenario (SSP3-8.5) results in a decrease in $EAPA$ for S. Asia by a factor of 2.4; W. Africa by 2.0; S.E. Asia by 4.4 and W.N. America by 8.0. The impact of adaptation on EAD by 2100 shows less regional variability with S. Asia decreasing by a factor of 2.1; W. Africa by 2.0, S.E. Asia by 2.3; W.N. America by 1.7 and E.N. America by 3.0.

A comparison of global present-day values of $EAPA$ with the *no additional adaptation scenario* values in 2100 (no changes to adaptation and SSP3-8.5) projects a factor 3.6 increase in of the number of people impacted (Table 5.4). For EAD the increase relative to present-day values is a factor as large as 25 (SSP5-8.5), (Table 5.4). The regional changes between present-day and the no additional adaptation scenario in 2100 show significant regional variation from these global values. For $EAPA$, we project increases for (compare Table A.1 with SSP3-8.5, Table A.11): S. Asia by a factor of 3.6; W. Africa by 6.2; S.E. Asia by 2.6; W.N. America by 9.0 and E.N. America by 1.5. The corresponding increases in values for EAD by 2100 are (compare Table A.1 with SSP5-8.5, Table A.13): S. Asia by a factor of 53; W. Africa by 89; S.E. Asia by 25 times; W.N. America by 18 and E.N. America by 25.

These results show that adaptation measures will be a critical element of addressing episodic coastal flooding under any plausible RCP/SSP narratives, as they significantly reduce projected $EAPA$ and EAD. However, the impacts of coastal flooding will disproportionately fall on the developing world, both in absolute terms and relative to GDP. As shown by Table 5.6, by 2100 the largest increases in both $EAPA$ and EAD will be borne by S. Asia, S.E. Asia, E. Asia, W. Africa and the Mediterranean (Egypt). This is clearly seen in Table A.28 which shows the EAD as a percentage of GDP by country in 2100 for the no additional adaptation scenario. The top ten places in the world ranking are dominated by developing countries such as: Guyana, Vietnam, Mauritania, Myanmar, Egypt, Bangladesh and Fiji. All of these have an EAD in excess of 6% of GDP. In contrast, almost all of the developed world have an EAD of less than 2% of GDP, with the global mean EAD being 1.2% (Table 5.5, *no additional adaptation* scenario). At these levels, it is likely that developed nations will be able to cope with impacts of this magnitude without major disruption. However, the developing world will face major disruption.

Chapter 6

Discussion and Conclusion

Episodic coastal flooding due to extreme sea levels poses one of the greatest challenges for coastal societies and the global economy, specifically in low lying coastal areas. Future projections of such complex natural occurrences over the upcoming century are even more challenging, due to large uncertainties associated with future climate change. Sea level rise is one of the most obvious impact of climate change and recent estimates highlight its significance for the coastal zones. It is crucial to identify the areas which are likely to be most affected by the impacts of coastal flooding in a changing climate: from small scale regional coastal communities to the global scale. Although there is a large body of literature based on local to continental scale estimates and projections of the coastal flooding over the 21^{st} century, investigation of global scale implications of episodic coastal flooding is still an evolving research area. Future projections of global analyses provide a broad picture of at-risk coastal areas in order to assess their resilience and vulnerabilities. The results of such an investigation provides a baseline for decision and policy makers as detailed in a number IPCC reports.

One of the most obvious impacts of climate change induced sea level rise is increased levels and frequencies of extreme flooding of the LECZs. It follows that it is a fundamental task to determine values of the present impacts as accurate as possible.These present day predicts form the basis for projections of future conditions. Although there are rather large uncertainties inherent in future estimates of coastal flooding, it is still important to estimate the potential risk with associated estimates of error. Such studies then provide the basis for future policy development and considerations of adaptation required.

The main scope of this PhD thesis is to investigate and identify the present and future impacts of sea level rise in coastal areas: both at global and regional scales.

To construct time series of historical sea levels, global models of surge, tide and wave setup are combined at 9,866 coastal points predefined by the Dynamic Interactive Vulnerability Assessment (DIVA) database, and rigorously validated against a quasi-global tide gauge network (GESLA-2). The validation demonstrates good agreement between model data and the observations both for ambient conditions and extremes. Modelling wave setup is a challenging task for large scale application due to limitations of the datasets and is generally ignored or given less importance at the global scale. Here, we show that inclusion of wave setup improves the TSL estimates especially for extreme conditions (e.g., during storms).

Stochastic prediction of extreme sea levels is conducted using Extreme Value Analysis methods with a wide range of approaches explored to determine the best-fit to the data. An extensive validation against tide gauge records is conducted for the historical extreme sea levels to ensure the robustness of the calculated values. To determine extreme sea levels over the 21^{st} century, future values are calculated by adding the projected sea level rise under RCP 4.5 and 8.5 to the present extreme sea levels. The resulting values are then translated into coastal flooding extent using a GIS based approach. The resulting flood inundation levels make it possible to conduct coastal impact analysis from the socioeconomic perspective, i.e., population and asset exposure over the next century. Under RCP 8.5, we project for most of the global coastal areas that what is presently a 1 in a 100-year event, is likely to occur as frequent as 1 in 10 years by 2100, due to projected sea level rise. In the absence of coastal protection, the analysis shows that by 2100 for RCP 8.5, global coastal flooding extent will increase by 48% compared to the present day, impacting 2.5 – 4.1% of the world's population (increase of 52%) and threatening assets worth up to 12 - 20% of global GDP (increase of 46%). Despite the limitations that are necessary to conduct such a global-scale analysis, the results provide a "first-pass" analysis which is essential for further policy development.

Future implications of the coastal flooding for exposed populations and assets are highly dependent on the projected changes in the socioeconomic parameters which vary regionally. Therefore, to identify and highlight the most impacted coastal areas, and inform decision and policy makers, aggregating the coastal flooding parameters available at individual coastal locations to the regional and national level is necessary. In this study, further calculations of the present and future values of Expected Annual People Affected ($EAPA$) and Expected Annual Damage (EAD) are also determined considering estimates of global coastal defences in-place at present. To determine the values of EAPA and EAD, combinations of IPCC RCP 4.5 and 8.5, Shared Socioeconomic Pathways (1, 3 and 5) and three simplistic adaptation scenarios are considered over the 21^{st} century. We show that these future changes in coastal flooding impacts on coastal areas are dominated by the socioeconomic projections. We demonstrate the critical importance of

adaptation in reducing increases in EAPA and EAD. Another important finding is that, future impacts of climate change on episodic coastal flooding will disproportionately affect developing nations. By 2100, the largest increases in both EAPA and EAD will be borne by S. Asia, S.E. Asia, E. Asia, W. Africa and the Mediterranean. Our results show that the EAD as a percentage of national GDP will significantly impact developing countries such as Guyana, Vietnam, Myanmar, Egypt, Bangladesh, and Fiji which will have EAD in excess of 5% of national GDP. In contrast, almost all of the developed world is projected to have an EAD of less than 2% of their respective national GDP. At such levels the developed world is likely to be able to respond to future coastal flooding. However, the developing world is likely to be plunged into greater poverty.

6.1 Future Work

As noted previously, the present study is a first-order analysis and there is much scope for future work. An obvious extension is to investigate future changes in surge and wave climate over next century. The large uncertainty around extreme sea levels and the projections of sea level rise indicate further sensitivity analysis around the impacts of these contributors is warranted. Our analysis uses a simplistic "bath-tub" flooding model. As computing resources develop, more sophisticated overland flooding models could be used to refine projections.

The stochastic extreme value analyses used in this and comparable studies introduce large uncertainties. Although we quantify the confidence limits on our estimates, more advanced approaches using, for example, ensemble of models have great potential. Moreover, future work could be undertaken by conducting multi-parameter sensitivity analysis as well as exploration of the uncertainties within the topographic and socioeconomic datasets used.

Finally, the present study provides the basis for much policy development as to how the world should best mitigate the inevitable impacts of future coastal flooding. Such analysis will be critical for many of the most vulnerable communities of the world.

Bibliography

Andersen, Ole Baltazar (1999). "Shallow water tides in the northwest European shelf region from TOPEX/POSEIDON altimetry". In: *Journal of Geophysical Research: Oceans* 104.C4, pp. 7729–7741.

Ardhuin, Fabrice and Aron Roland (2012). "Coastal wave reflection, directional spread, and seismoacoustic noise sources". In: *Journal of Geophysical Research: Oceans* 117.C11.

Armaroli, Clara and Enrico Duo (2018). "Validation of the coastal storm risk assessment framework along the Emilia-Romagna coast". In: *Coastal Engineering* 134, pp. 159–167.

Arns, A et al. (2013). "Estimating extreme water level probabilities: A comparison of the direct methods and recommendations for best practise". In: *Coastal Engineering* 81, pp. 51–66.

Arns, Arne et al. (2015). "The impact of sea level rise on storm surge water levels in the northern part of the German Bight". In: *Coastal Engineering* 96, pp. 118–131.

Arns, Arne et al. (2017). "Sea-level rise induced amplification of coastal protection design heights". In: *Scientific reports* 7, p. 40171.

Athanasiou, Panagiotis et al. (2019). "Global distribution of nearshore slopes with implications for coastal retreat." In: *Earth system science data* 11.4.

Aucan, Jerome et al. (2019). "On the contribution of waves to total coastal water level changes in the context of sea level rise: a response to Melet, et al.(2018)". In: *Climate Change* 9.2.

Barbosa, Susana M (2008). "Quantile trends in Baltic sea level". In: *Geophysical Research Letters* 35.22.

Bardet, L et al. (2011). "Regional frequency analysis of extreme storm surges along the French coast". In: *Natural Hazards and Earth System Sciences* 11.6, p. 1627.

Barnard, Patrick L et al. (2015). "Coastal vulnerability across the Pacific dominated by El Nino/Southern oscillation". In: *Nature Geoscience* 8.10, pp. 801–807.

Barnard, Patrick L et al. (2019). "Dynamic flood modeling essential to assess the coastal impacts of climate change". In: *Scientific reports* 9.1, pp. 1–13.

Battjes, Jurjen Anno (1973). "Set-up due to irregular waves". In: *Coastal Engineering 1972*, pp. 1993–2004.

Benavente, Javier et al. (2006). "Coastal flooding hazard related to storms and coastal evolution in Valdelagrana spit (Cadiz Bay Natural Park, SW Spain)". In: *Continental Shelf Research* 26.9, pp. 1061–1076.

Bernier, NB and KR Thompson (2006). "Predicting the frequency of storm surges and extreme sea levels in the northwest Atlantic". In: *Journal of Geophysical Research: Oceans* 111.C10.

Bernier, NB et al. (2007). "Mapping the return periods of extreme sea levels: allowing for short sea level records, seasonality, and climate change". In: *Global and Planetary Change* 57.1-2, pp. 139–150.

Bittermann, Klaus et al. (2013). "Predictability of twentieth century sea-level rise from past data". In: *Environmental Research Letters* 8.1, p. 014013.

Bowen, AJ, DL Inman, and VP Simmons (1968). "Wave 'set-down'and set-up". In: *Journal of Geophysical Research* 73.8, pp. 2569–2577.

Brown, Sally et al. (2013). "Sea-level rise impacts and responses: a global perspective". In: *Coastal hazards*. Springer, pp. 117–149.

Buchanan, Maya K, Michael Oppenheimer, and Robert E Kopp (2017). "Amplification of flood frequencies with local sea level rise and emerging flood regimes". In: *Environmental Research Letters* 12.6, p. 064009.

Bunya, S et al. (2010). "A high-resolution coupled riverine flow, tide, wind, wind wave, and storm surge model for southern Louisiana and Mississippi. Part I: Model development and validation". In: *Monthly weather review* 138.2, pp. 345–377.

Carrere, L et al. (2016). "FES 2014, a new tidal model—Validation results and perspectives for improvements". In: *Proceedings of the ESA living planet symposium*, pp. 9–13.

Carrere, Loren et al. (2015). "FES 2014, a new tidal model on the global ocean with enhanced accuracy in shallow seas and in the Arctic region". In: *EGUGA*, p. 5481.

Church, John A et al. (2006). "Sea-level rise around the Australian coastline and the changing frequency of extreme sea-level events". In: *Australian Meteorological Magazine* 55.4, pp. 253–260.

Church, John A et al. (2013a). *Sea level change*. Tech. rep. PM Cambridge University Press.

– (2013b). "Sea Level Change Supplementary Material". In: *Climate Change 2013: The Physical Science Basis: Working Group I Contribution to the Fifth Assessment Report of the Intergovernmental Panel on Climate Change*. Ed. by T.F. Stocker et al. Cambridge University Press, pp. 1137–1216.

Cid, Alba et al. (2018). "Storm surge reconstruction and return water level estimation in Southeast Asia for the 20th century". In: *Journal of Geophysical Research: Oceans* 123.1, pp. 437–451.

Colberg, Frank and Kathleen L McInnes (2012). "The impact of future changes in weather patterns on extreme sea levels over southern Australia". In: *Journal of Geophysical Research: Oceans* 117.C8.

Coles, Stuart (2001). *An introduction to statistical modeling of extreme values*. Vol. 208. Springer.

Cooper, Matthew JP, Michael D Beevers, and Michael Oppenheimer (2008). "The potential impacts of sea level rise on the coastal region of New Jersey, USA". In: *Climatic Change* 90.4, p. 475.

Davis, Gregory A and Peter Nielsen (1989). "Field measurement of wave set-up". In: *Coastal Engineering 1988*, pp. 539–552.

Dean, Bob et al. (2005). "FEMA Coastal Flood Hazard Analysis and Mapping Guidelines Focused Study Report". In:

Debernard, Jens Boldingh and Lars Petter Røed (2008). "Future wind, wave and storm surge climate in the Northern Seas: a revisit". In: *Tellus A: Dynamic Meteorology and Oceanography* 60.3, pp. 427–438.

DeConto, Robert M and David Pollard (2016). "Contribution of Antarctica to past and future sea-level rise". In: *Nature* 531.7596, pp. 591–597.

Dee, Dick P et al. (2011). "The ERA-Interim reanalysis: Configuration and performance of the data assimilation system". In: *Quarterly Journal of the royal meteorological society* 137.656, pp. 553–597.

Devlin, Adam T, Jiayi Pan, and Hui Lin (2019). "Extended spectral analysis of tidal variability in the North Atlantic Ocean". In: *Journal of Geophysical Research: Oceans* 124.1, pp. 506–526.

Diaz, Delavane B (2016). "Estimating global damages from sea level rise with the Coastal Impact and Adaptation Model (CIAM)". In: *Climatic Change* 137.1-2, pp. 143–156.

Dullaart, Job CM et al. (2020). "Advancing global storm surge modelling using the new ERA5 climate reanalysis". In: *Climate Dynamics* 54.1-2, pp. 1007–1021.

Efron, B. (Jan. 1979). "Bootstrap Methods: Another Look at the Jackknife". In: *Ann. Statist.* 7.1, pp. 1–26. DOI: 10.1214/aos/1176344552. URL: https://doi.org/10.1214/aos/1176344552.

Ericson, Jason P et al. (2006). "Effective sea-level rise and deltas: Causes of change and human dimension implications". In: *Global and Planetary Change* 50.1-2, pp. 63–82.

Fang, Jiayi et al. (2020). "Coastal flood risks in China through the 21st century–An application of DIVA". In: *Science of the Total Environment* 704, p. 135311.

Farr, Tom G et al. (2007). "The shuttle radar topography mission". In: *Reviews of geophysics* 45.2.

Farrell, WE and James A Clark (1976). "On postglacial sea level". In: *Geophysical Journal International* 46.3, pp. 647–667.

Fredriksson, Caroline et al. (2016). "Statistical analysis of extreme sea water levels at the falsterbo peninsula, south Sweden". In: *Vatten, J. Water Manage. Res* 72, pp. 129–142.

Gao, Jing (2017). "Downscaling global spatial population projections from 1/8-degree to 1-km grid cells". In: *Technical Notes NCAR, National Center for Atmospheric Researcher, Boulder, CO., USA*.

Garner, Andra J et al. (2017). "Impact of climate change on New York City's coastal flood hazard: Increasing flood heights from the preindustrial to 2300 CE". In: *Proceedings of the National Academy of Sciences* 114.45, pp. 11861–11866.

Grinsted, Aslak, John C Moore, and Svetlana Jevrejeva (2010). "Reconstructing sea level from paleo and projected temperatures 200 to 2100 AD". In: *Climate dynamics* 34.4, pp. 461–472.

Grinsted, Aslak et al. (2015). "Sea level rise projections for northern Europe under RCP8. 5". In: *Climate Research* 64.1, pp. 15–23.

Guza, RT and Edward B Thornton (1981). "Wave set-up on a natural beach". In: *Journal of Geophysical Research: Oceans* 86.C5, pp. 4133–4137.

Haigh, Ivan D (2017). "Tides and water levels". In: *Encyclopedia of Maritime and Offshore Engineering*, pp. 1–13.

Haigh, Ivan D et al. (2014). "Estimating present day extreme water level exceedance probabilities around the coastline of Australia: tides, extra-tropical storm surges and mean sea level". In: *Climate Dynamics* 42.1-2, pp. 121–138.

Hallegatte, Stéphane et al. (2011). "Assessing climate change impacts, sea level rise and storm surge risk in port cities: a case study on Copenhagen". In: *Climatic change* 104.1, pp. 113–137.

Hallegatte, Stephane et al. (2013). "Future flood losses in major coastal cities". In: *Nature climate change* 3.9, pp. 802–806.

Hansen, Uwe A (1978). "Wave set-up in the surf zone". In: *Coastal Engineering 1978*, pp. 1071–1084.

Hanslow, David J and Peter Nielsen (1993). "Wave setup on beaches and in river entrances". In: *Coastal Engineering 1992*, pp. 240–252.

Hanson, Susan et al. (2011). "A global ranking of port cities with high exposure to climate extremes". In: *Climatic change* 104.1, pp. 89–111.

Harker, Alexander et al. (2019). "The impact of sea-level rise on tidal characteristics around Australia." In: *Ocean Science* 15.1.

Hauer, Mathew E, Jason M Evans, and Deepak R Mishra (2016). "Millions projected to be at risk from sea-level rise in the continental United States". In: *Nature Climate Change* 6.7, pp. 691–695.

Hedges, TS and H Mase (2004). "Modified Hunt's equation incorporating wave setup". In: *Journal of waterway, port, coastal, and ocean engineering* 130.3, pp. 109–113.

Hemer, Mark A et al. (2013). "Projected changes in wave climate from a multi-model ensemble". In: *Nature climate change* 3.5, pp. 471–476.

Hersbach, Hans et al. (2019). "Global reanalysis: goodbye ERA-Interim, hello ERA5". In: *ECMWF newsletter* 159, pp. 17–24.

Hinkel, Jochen and Richard JT Klein (2009). "Integrating knowledge to assess coastal vulnerability to sea-level rise: The development of the DIVA tool". In: *Global Environmental Change* 19.3, pp. 384–395.

Hinkel, Jochen et al. (2010). "Assessing risk of and adaptation to sea-level rise in the European Union: an application of DIVA". In: *Mitigation and adaptation strategies for global change* 15.7, pp. 703–719.

Hinkel, Jochen et al. (2012). "Sea-level rise impacts on Africa and the effects of mitigation and adaptation: an application of DIVA". In: *Regional Environmental Change* 12.1, pp. 207–224.

Hinkel, Jochen et al. (2014). "Coastal flood damage and adaptation costs under 21st century sea-level rise". In: *Proceedings of the National Academy of Sciences* 111.9, pp. 3292–3297.

Hinkel, Jochen et al. (2015). "Sea-level rise scenarios and coastal risk management". In: *Nature Climate Change* 5.3, pp. 188–190.

Hoeke, Ron K et al. (2013). "Widespread inundation of Pacific islands triggered by distant-source wind-waves". In: *Global and Planetary Change* 108, pp. 128–138.

Holgate, Simon J et al. (2013). "New data systems and products at the permanent service for mean sea level". In: *Journal of Coastal Research* 29.3, pp. 493–504.

Holman, RA and AH Sallenger Jr (1985). "Setup and swash on a natural beach". In: *Journal of Geophysical Research: Oceans* 90.C1, pp. 945–953.

Howard, Tom, Jason Lowe, and Kevin Horsburgh (2010). "Interpreting century-scale changes in southern North Sea storm surge climate derived from coupled model simulations". In: *Journal of Climate* 23.23, pp. 6234–6247.

Howard, Tom, Matthew D Palmer, and Lucy M Bricheno (2019). "Contributions to 21st century projections of extreme sea-level change around the UK". In: *Environmental Research Communications* 1.9, p. 095002.

Hubbert, Graeme D and Kathleen L Mclnnes (1999). "A storm surge inundation model for coastal planning and impact studies". In: *Journal of Coastal Research*, pp. 168–185.

Hubbert, Graeme D et al. (1991). "A real-time system for forecasting tropical cyclone storm surges". In: *Weather and Forecasting* 6.1, pp. 86–97.

Hunter, John (2010). "Estimating sea-level extremes under conditions of uncertain sea-level rise". In: *Climatic change* 99.3-4, pp. 331–350.

Hunter, JR et al. (2017). "Using global tide gauge data to validate and improve the representation of extreme sea levels in flood impact studies". In: *Global and Planetary Change* 156, pp. 34–45.

International Earth Science Information Network (CIESIN), Center for (2017). "Documentation for the gridded population of the world, Version 4 (GPWv4), Revision 10 Data Sets". In:

Iturbide, Maialen et al. (2020). "An update of IPCC climate reference regions for subcontinental analysis of climate model data: definition and aggregated datasets". In: *Earth System Science Data Discussions*, pp. 1–16.

Jackson, Luke P and Svetlana Jevrejeva (2016). "A probabilistic approach to 21st century regional sea-level projections using RCP and High-end scenarios". In: *Global and Planetary Change* 146, pp. 179–189.

Janssen, Peter AEM (2008). "Progress in ocean wave forecasting". In: *Journal of Computational Physics* 227.7, pp. 3572–3594.

Jarvis, Andy et al. (2008). "Hole-filled SRTM for the globe Version 4". In: *available from the CGIAR-CSI SRTM 90m Database (http://srtm. csi. cgiar. org)* 15, pp. 25–54.

Jevrejeva, S et al. (2019). "Probabilistic sea level projections at the coast by 2100". In: *Surveys in Geophysics* 40.6, pp. 1673–1696.

Jevrejeva, Svetlana, John C Moore, and Aslak Grinsted (2012). "Potential for bias in 21st century semiempirical sea level projections". In: *Journal of Geophysical Research: Atmospheres* 117.D20.

Jones, Bryan and Brian C O'Neill (2016). "Spatially explicit global population scenarios consistent with the Shared Socioeconomic Pathways". In: *Environmental Research Letters* 11.8, p. 084003.

Jones, Roger et al. (2014). "Foundations for decision making". In:

Jongman, Brenden, Philip J Ward, and Jeroen CJH Aerts (2012). "Global exposure to river and coastal flooding: Long term trends and changes". In: *Global Environmental Change* 22.4, pp. 823–835.

Jonkman, Sebastiaan N et al. (2009). "Loss of life caused by the flooding of New Orleans after Hurricane Katrina: analysis of the relationship between flood characteristics and mortality". In: *Risk Analysis: An International Journal* 29.5, pp. 676–698.

Kernkamp, Herman WJ et al. (2011). "Efficient scheme for the shallow water equations on unstructured grids with application to the Continental Shelf". In: *Ocean Dynamics* 61.8, pp. 1175–1188.

King, BA et al. (1990). "Observations of wave-induced set-up on a natural beach". In: *Journal of Geophysical Research: Oceans* 95.C12, pp. 22289–22297.

Kirezci, Ebru et al. (2020). "Projections of global-scale extreme sea levels and resulting episodic coastal flooding over the 21st Century". In: *Scientific Reports* 10.1, pp. 1–12.

Knabb, Richard D, Jamie R Rhome, and Daniel P Brown (2005). *Tropical cyclone report: Hurricane katrina, 23-30 august 2005*. National Hurricane Center.

Kobayashi, Nobuhisa and Andojo Wurjanto (1992). "Irregular wave setup and run-up on beaches". In: *Journal of waterway, port, coastal, and ocean engineering* 118.4, pp. 368–386.

Kopp, Robert E et al. (2010). "The impact of Greenland melt on local sea levels: a partially coupled analysis of dynamic and static equilibrium effects in idealized water-hosing experiments". In: *Climatic Change* 103.3-4, pp. 619–625.

Kopp, Robert E et al. (2014). "Probabilistic 21st and 22nd century sea-level projections at a global network of tide-gauge sites". In: *Earth's future* 2.8, pp. 383–406.

Kopp, Robert E et al. (2017). "Evolving understanding of Antarctic ice-sheet physics and ambiguity in probabilistic sea-level projections". In: *Earth's Future* 5.12, pp. 1217–1233.

Koroglu, Aysun et al. (2019). "Comparison of coastal vulnerability index applications for Barcelona Province". In: *Ocean & coastal management* 178, p. 104799.

Kron, Wolfgang (2005). "Flood risk= hazard• values• vulnerability". In: *Water international* 30.1, pp. 58–68.

– (2013). "Coasts: the high-risk areas of the world". In: *Natural hazards* 66.3, pp. 1363–1382.

Kulp, Scott and Benjamin H Strauss (2016). "Global DEM errors underpredict coastal vulnerability to sea level rise and flooding". In: *Frontiers in Earth Science* 4, p. 36.

Kummu, Matti, Maija Taka, and Joseph HA Guillaume (2018). "Gridded global datasets for gross domestic product and Human Development Index over 1990–2015". In: *Scientific data* 5, p. 180004.

Lambert, Erwin et al. (2020). "Adaptation time to magnified flood hazards underestimated when derived from tide gauge records". In: *Environmental Research Letters* 15.7, p. 074015. DOI: 10.1088/1748-9326/ab8336. URL: https://doi.org/10.1088/1748-9326/ab8336.

Larson, Magnus and Nicholas C Kraus (1989). *SBEACH: numerical model for simulating storm-induced beach change. Report 1. Empirical foundation and model development.* Tech. rep. Coastal Engineering research center Vicksburg Ms.

Levermann, Anders et al. (2005). "Dynamic sea level changes following changes in the thermohaline circulation". In: *Climate Dynamics* 24.4, pp. 347–354.

Lin, Ning et al. (2012). "Physically based assessment of hurricane surge threat under climate change". In: *Nature Climate Change* 2.6, pp. 462–467.

Lin, Ning et al. (2016). "Hurricane Sandy's flood frequency increasing from year 1800 to 2100". In: *Proceedings of the National Academy of Sciences* 113.43, pp. 12071–12075.

Longuet-Higgins, Michael S and RW Stewart (1962). "Radiation stress and mass transport in gravity waves, with application to 'surf beats'". In: *Journal of Fluid Mechanics* 13.4, pp. 481–504.

– (1964). "Radiation stresses in water waves; a physical discussion, with applications". In: *Deep sea research and oceanographic abstracts*. Vol. 11. 4. Elsevier, pp. 529–562.

Longuet-Higgins, MS and RW Stewart (1963). "A note on wave set-up". In: *Journal of Marine Research* 21.1, pp. 4–10.

Losada, IJ et al. (2013). "Long-term changes in sea-level components in Latin America and the Caribbean". In: *Global and Planetary Change* 104, pp. 34–50.

Lowe, JA and JM Gregory (2005). "The effects of climate change on storm surges around the United Kingdom". In: *Philosophical Transactions of the Royal Society A: Mathematical, Physical and Engineering Sciences* 363.1831, pp. 1313–1328.

Lowe, JA, Jonathan M Gregory, and RA Flather (2001). "Changes in the occurrence of storm surges around the United Kingdom under a future climate scenario using a dynamic storm surge model driven by the Hadley Centre climate models". In: *Climate dynamics* 18.3-4, pp. 179–188.

Marcos, Marta and Philip L Woodworth (2017). "Spatiotemporal changes in extreme sea levels along the coasts of the N orth A tlantic and the G ulf of M exico". In: *Journal of Geophysical Research: Oceans* 122.9, pp. 7031–7048.

Marcos, Marta et al. (2019). "Increased extreme coastal water levels due to the combined action of storm surges and wind waves". In: *Geophysical Research Letters* 46.8, pp. 4356–4364.

Martínez-Asensio, Adrian et al. (2019). "Relative sea-level rise and the influence of vertical land motion at Tropical Pacific Islands". In: *Global and Planetary Change* 176, pp. 132–143.

McGranahan, Gordon, Deborah Balk, and Bridget Anderson (2007). "The rising tide: assessing the risks of climate change and human settlements in low elevation coastal zones". In: *Environment and urbanization* 19.1, pp. 17–37.

McInnes, Kathleen L et al. (2013). "An assessment of current and future vulnerability to coastal inundation due to sea-level extremes in Victoria, southeast Australia". In: *International Journal of Climatology* 33.1, pp. 33–47.

Melet, Angelique, Rafael Almar, and Benoit Meyssignac (2016). "What dominates sea level at the coast: a case study for the Gulf of Guinea". In: *Ocean Dynamics* 66.5, pp. 623–636.

Melet, Angélique et al. (2018). "Under-estimated wave contribution to coastal sea-level rise". In: *Nature Climate Change* 8.3, pp. 234–239.

Menéndez, Melisa and Philip L Woodworth (2010). "Changes in extreme high water levels based on a quasi-global tide-gauge data set". In: *Journal of Geophysical Research: Oceans* 115.C10.

Mengel, Matthias et al. (2016). "Future sea level rise constrained by observations and long-term commitment". In: *Proceedings of the National Academy of Sciences* 113.10, pp. 2597–2602.

Mentaschi, Lorenzo et al. (2016). "Non-stationary extreme value analysis: a simplified approach for Earth science applications". In: *Hydrol. Earth Syst. Sci. Discuss* 2016, pp. 1–38.

Mentaschi, Lorenzo et al. (2017). "Global changes of extreme coastal wave energy fluxes triggered by intensified teleconnection patterns". In: *Geophysical Research Letters* 44.5, pp. 2416–2426.

Messner, F et al. (2014). "Evaluating flood damages: guidance and recommendations on principles and methods, FLOODsite Project Deliverable D9. 1". In: *Contract No: GOCE-CT-2004-505420, available at: http://www. floodsite. net/html/partner area/project docs* 9, p. 06.

Meucci, Alberto, Ian R Young, and Øyvind Breivik (2018). "Wind and wave extremes from atmosphere and wave model ensembles". In: *Journal of Climate* 31.21, pp. 8819–8842.

Meucci, Alberto et al. (2020). "Projected 21st century changes in extreme wind-wave events". In: *Science Advances* 6.24, eaaz7295.

Miller, Kenneth G et al. (2013). "A geological perspective on sea-level rise and its impacts along the US mid-Atlantic coast". In: *Earth's Future* 1.1, pp. 3–18.

Milne, Glenn A et al. (2009). "Identifying the causes of sea-level change". In: *Nature Geoscience* 2.7, pp. 471–478.

Mitrovica, Jerry X et al. (2011). "On the robustness of predictions of sea level fingerprints". In: *Geophysical Journal International* 187.2, pp. 729–742.

Mori, Nobuhito et al. (2010). "Projection of extreme wave climate change under global warming". In: *Hydrological Research Letters* 4, pp. 15–19.

Mori, Nobuhito et al. (2019). "Future changes in extreme storm surges based on mega-ensemble projection using 60-km resolution atmospheric global circulation model". In: *Coastal Engineering Journal* 61.3, pp. 295–307.

Morim, Joao et al. (2019). "Robustness and uncertainties in global multivariate wind-wave climate projections". In: *Nature Climate Change* 9.9, pp. 711–718.

Muis, Sanne et al. (2015). "Flood risk and adaptation strategies under climate change and urban expansion: A probabilistic analysis using global data". In: *Science of the Total Environment* 538, pp. 445–457.

Muis, Sanne et al. (2016). "A global reanalysis of storm surges and extreme sea levels". In: *Nature communications* 7.1, pp. 1–12.

Muis, Sanne et al. (2017). "A comparison of two global datasets of extreme sea levels and resulting flood exposure". In: *Earth's Future* 5.4, pp. 379–392.

Muis, Sanne et al. (2020). "A High-Resolution Global Dataset of Extreme Sea Levels, Tides, and Storm Surges, Including Future Projections". In: *Frontiers in Marine Science* 7, p. 263.

National Tidal and Sea Level Facility. *What are tides?* `https://www.ntslf.org/about-tides`. Accessed: 2021-01-22.

Neumann, Barbara et al. (2015). "Future coastal population growth and exposure to sea-level rise and coastal flooding-a global assessment". In: *PloS one* 10.3, e0118571.

Nicholls, RJ et al. (2010). "Economics of coastal zone adaptation to climate change". In:

Nicholls, Robert J (2004). "Coastal flooding and wetland loss in the 21st century: changes under the SRES climate and socio-economic scenarios". In: *Global Environmental Change* 14.1, pp. 69–86.

– (2018). "Adapting to sea-level rise". In: *Resilience*. Elsevier, pp. 13–29.

Nicholls, Robert J and Anny Cazenave (2010). "Sea-level rise and its impact on coastal zones". In: *science* 328.5985, pp. 1517–1520.

Nicholls, Robert J and Jason A Lowe (2004). "Benefits of mitigation of climate change for coastal areas". In: *Global environmental change* 14.3, pp. 229–244.

Nicholls, Robert John et al. (2019). *Global investment costs for coastal defense through the 21st century*. The World Bank.

Nielsen, Peter (1988). "Wave setup: A field study". In: *Journal of Geophysical Research: Oceans* 93.C12, pp. 15643–15652.

– (1989). "Wave setup and runup: An integrated approach". In: *Coastal Engineering* 13.1, pp. 1–9.

Olbert, Agnieszka Indiana et al. (2013). "Tide–surge interactions and their effects on total sea levels in Irish coastal waters". In: *Ocean Dynamics* 63.6, pp. 599–614.

O'Neill, Brian C et al. (2016). "The scenario model intercomparison project (ScenarioMIP) for CMIP6". In:

Oppenheimer, Michael et al. (2019). "Sea level rise and implications for low lying islands, coasts and communities". In:

O'Neill, Brian C et al. (2014). "A new scenario framework for climate change research: the concept of shared socioeconomic pathways". In: *Climatic change* 122.3, pp. 387–400.

Palanisamy, H et al. (2014). "Regional sea level variability, total relative sea level rise and its impacts on islands and coastal zones of Indian Ocean over the last sixty years". In: *Global and Planetary Change* 116, pp. 54–67.

Palmer, Matthew et al. (2018). "UKCP18 Marine report". In:

Paprotny, Dominik and Paweł Terefenko (2017). "New estimates of potential impacts of sea level rise and coastal floods in Poland". In: *Natural Hazards* 85.2, pp. 1249–1277.

Patricola, Christina M and Michael F Wehner (2018). "Anthropogenic influences on major tropical cyclone events". In: *Nature* 563.7731, pp. 339–346.

Perez, Jorge, Melisa Menendez, and Inigo J Losada (2017). "GOW2: A global wave hindcast for coastal applications". In: *Coastal Engineering* 124, pp. 1–11.

Piccioni, Gaia et al. (2018). "Coastal improvements for tide models: the impact of ALES retracker". In: *Remote Sensing* 10.5, p. 700.

Piccioni, Gaia et al. (2019). "TICON: TIdal CONstants based on GESLA sea-level records from globally located tide gauges". In: *Geoscience Data Journal* 6.2, pp. 97–104.

Pickering, MD et al. (2017). "The impact of future sea-level rise on the global tides". In: *Continental Shelf Research* 142, pp. 50–68.

Proske, D and PHAJM van Gelder (2006). "Analysis about extreme water levels along the Dutch north-sea using Grey models: Preliminary analysis". In: *ESREL 2006 Conference, September*. Citeseer.

Pugh, DT and JM Vassie (1980). "Applications of the joint probability method for extreme sea level computations." In: *Proceedings of the Institution of Civil Engineers* 69.4, pp. 959–975.

Qu, Ying et al. (2019). "Coastal Sea level rise around the China Seas". In: *Global and Planetary Change* 172, pp. 454–463.

Rahmstorf, Stefan (2007). "A semi-empirical approach to projecting future sea-level rise". In: *Science* 315.5810, pp. 368–370.

Ramirez, Jorge A et al. (2016). "Hyper-resolution mapping of regional storm surge and tide flooding: comparison of static and dynamic models". In: *Natural Hazards* 82.1, pp. 571–590.

Rappaport, Edward N (2014). "Fatalities in the United States from Atlantic tropical cyclones: New data and interpretation". In: *Bulletin of the American Meteorological Society* 95.3, pp. 341–346.

Rasmussen, DJ et al. (2018). "Extreme sea level implications of 1.5 C, 2.0 C, and 2.5 C temperature stabilization targets in the 21st and 22nd centuries". In: *Environmental Research Letters* 13.3, p. 034040.

Raubenheimer, B, RT Guza, and Steve Elgar (2001). "Field observations of wave-driven setdown and setup". In: *Journal of Geophysical Research: Oceans* 106.C3, pp. 4629–4638.

Reed, Andra J et al. (2015). "Increased threat of tropical cyclones and coastal flooding to New York City during the anthropogenic era". In: *Proceedings of the National Academy of Sciences* 112.41, pp. 12610–12615.

Riahi, Keywan et al. (2017). "The shared socioeconomic pathways and their energy, land use, and greenhouse gas emissions implications: an overview". In: *Global Environmental Change* 42, pp. 153–168.

Rio, M-H, S Mulet, and N Picot (2014). "Beyond GOCE for the ocean circulation estimate: Synergetic use of altimetry, gravimetry, and in situ data provides new insight into geostrophic and Ekman currents". In: *Geophysical Research Letters* 41.24, pp. 8918–8925.

Rueda, Ana et al. (2017). "A global classification of coastal flood hazard climates associated with large-scale oceanographic forcing". In: *Scientific reports* 7.1, pp. 1–8.

Ruggiero, Peter et al. (2001). "Wave runup, extreme water levels and the erosion of properties backing beaches". In: *Journal of coastal research*, pp. 407–419.

Saha, Suranjana et al. (2010). "The NCEP climate forecast system reanalysis". In: *Bulletin of the American Meteorological Society* 91.8, pp. 1015–1058.

Sallenger, Asbury H, Kara S Doran, and Peter A Howd (2012). "Hotspot of accelerated sea-level rise on the Atlantic coast of North America". In: *Nature Climate Change* 2.12, pp. 884–888.

Schinko, Thomas et al. (2020). "Economy-wide effects of coastal flooding due to sea level rise: A multi-model simultaneous treatment of mitigation, adaptation, and residual impacts". In: *Environmental Research Communications* 2.1, p. 015002.

Seifi, Fardin, Xiaoli Deng, and Ole Baltazar Andersen (2019). "Assessment of the accuracy of recent empirical and assimilated tidal models for the Great Barrier Reef, Australia, using satellite and coastal data". In: *Remote Sensing* 11.10, p. 1211.

Sobel, Adam H et al. (2016). "Human influence on tropical cyclone intensity". In: *Science* 353.6296, pp. 242–246.

Solomon, Susan et al. (2007). *IPCC fourth assessment report: climate change 2007 (AR4)*. Tech. rep. Technical report, Intergovernmental panel on climate change.

SPM, US Army Engineer Waterways Experiment Station. Coastal Engineering Research Center (1984). *SHORE PROTECTION MANUAL*. US Government Printing Office.

Stammer, D (2008). "Response of the global ocean to Greenland and Antarctic ice melting". In: *Journal of Geophysical Research: Oceans* 113.C6.

Sterl, Andreas et al. (2009). "An ensemble study of extreme storm surge related water levels in the North Sea in a changing climate". In: *Ocean Science* 5.3, pp. 369–378.

Stive, Marcel JF and Herman G Wind (1982). "A study of radiation stress and set-up in the nearshore region". In: *Coastal engineering 6 (1), 1-25.(1982)*.

Stockdon, Hilary F et al. (2006). "Empirical parameterization of setup, swash, and runup". In: *Coastal engineering* 53.7, pp. 573–588.

Sugiyama, Masahiro, Robert J Nicholls, and Athanasios Vafeidis (2008). *Estimating the economic cost of sea-level rise*. Tech. rep. MIT Joint Program on the Science and Policy of Global Change.

Svendsen, Ib A (1984). "Wave heights and set-up in a surf zone". In: *Coastal engineering* 8.4, pp. 303–329.

Sweet, William V and Joseph Park (2014). "From the extreme to the mean: Acceleration and tipping points of coastal inundation from sea level rise". In: *Earth's Future* 2.12, pp. 579–600.

Syvitski, James PM et al. (2009). "Sinking deltas due to human activities". In: *Nature Geoscience* 2.10, pp. 681–686.

Tadono, Takeo et al. (2015). "Status of "ALOS World 3D (AW3D)" global DSM generation". In: *2015 IEEE International Geoscience and Remote Sensing Symposium (IGARSS)*. IEEE, pp. 3822–3825.

Takbash, Alicia, Ian R Young, and Øyvind Breivik (2019). "Global wind speed and wave height extremes derived from long-duration satellite records". In: *Journal of Climate* 32.1, pp. 109–126.

Tamura, Makoto et al. (2019). "Global assessment of the effectiveness of adaptation in coastal areas based on RCP/SSP scenarios". In: *Climatic Change* 152.3-4, pp. 363–377.

Tawn, Jonathan A (1992). "Estimating probabilities of extreme sea-levels". In: *Journal of the Royal Statistical Society: Series C (Applied Statistics)* 41.1, pp. 77–93.

Tebaldi, Claudia, Benjamin H Strauss, and Chris E Zervas (2012). "Modelling sea level rise impacts on storm surges along US coasts". In: *Environmental Research Letters* 7.1, p. 014032.

Tiggeloven, Timothy et al. (2020). "Global-scale benefit–cost analysis of coastal flood adaptation to different flood risk drivers using structural measures". In: *Natural Hazards and Earth System Sciences* 20.4, pp. 1025–1044.

Tol, Richard SJ, Richard JT Klein, and Robert J Nicholls (2008). "Towards successful adaptation to sea-level rise along Europe's coasts". In: *Journal of Coastal Research* 24.2 (242), pp. 432–442.

Tolman, Hendrik L et al. (2009). "User manual and system documentation of WAVEWATCH III TM version 3.14". In: *Technical note, MMAB Contribution* 276, p. 220.

Tsimplis, MN and D Blackman (1997). "Extreme sea-level distribution and return periods in the Aegean and Ionian Seas". In: *Estuarine, coastal and shelf science* 44.1, pp. 79–89.

US Army Corps of Engineers (2002). *Coastal engineering manual*.

Vafeidis, Athanasios T et al. (2008). "A new global coastal database for impact and vulnerability analysis to sea-level rise". In: *Journal of coastal research* 24.4 (244), pp. 917–924.

Vafeidis, Athanasios T et al. (2019). "Water-level attenuation in global-scale assessments of exposure to coastal flooding: a sensitivity analysis". In: *Natural Hazards and Earth System Sciences* 19.5, pp. 973–984.

Verlaan, Martin et al. (2005). "Operational storm surge forecasting in the Netherlands: developments in the last decade". In: *Philosophical Transactions of the Royal Society A: Mathematical, Physical and Engineering Sciences* 363.1831, pp. 1441–1453.

Vermeer, Martin and Stefan Rahmstorf (2009). "Global sea level linked to global temperature". In: *Proceedings of the national academy of sciences* 106.51, pp. 21527–21532.

Vitousek, Sean et al. (2017). "Doubling of coastal flooding frequency within decades due to sea-level rise". In: *Scientific reports* 7.1, pp. 1–9.

Vousdoukas, Michalis I et al. (2016a). "Developments in large-scale coastal flood hazard mapping". In: *Natural Hazards and Earth System Sciences* 16.8, pp. 1841–1853.

Vousdoukas, Michalis I et al. (2016b). "Projections of extreme storm surge levels along Europe". In: *Climate Dynamics* 47.9-10, pp. 3171–3190.

Vousdoukas, Michalis I et al. (2017). "Extreme sea levels on the rise along Europe's coasts". In: *Earth's Future* 5.3, pp. 304–323.

Vousdoukas, Michalis I et al. (2018a). "Climatic and socioeconomic controls of future coastal flood risk in Europe". In: *Nature Climate Change* 8.9, pp. 776–780.

Vousdoukas, Michalis I et al. (2018b). "Global probabilistic projections of extreme sea levels show intensification of coastal flood hazard". In: *Nature communications* 9.1, pp. 1–12.

Vousdoukas, Michalis I et al. (2020). "Economic motivation for raising coastal flood defenses in Europe". In: *Nature Communications* 11.1, pp. 1–11.

Vuuren, Detlef P van and Timothy R Carter (2014). "Climate and socio-economic scenarios for climate change research and assessment: reconciling the new with the old". In: *Climatic Change* 122.3, pp. 415–429.

Wahl, Thomas et al. (2017). "Understanding extreme sea levels for broad-scale coastal impact and adaptation analysis". In: *Nature communications* 8.1, pp. 1–12.

Wang, Shiyu et al. (2008). "The impact of climate change on storm surges over Irish waters". In: *Ocean Modelling* 25.1-2, pp. 83–94.

Ward, PJ et al. (2011). "Coastal inundation and damage exposure estimation: a case study for Jakarta". In: *Natural Hazards* 56.3, pp. 899–916.

Watson, Christopher S et al. (2015). "Unabated global mean sea-level rise over the satellite altimeter era". In: *Nature Climate Change* 5.6, pp. 565–568.

Wessel, Pål and Walter HF Smith (1996). "A global, self-consistent, hierarchical, high-resolution shoreline database". In: *Journal of Geophysical Research: Solid Earth* 101.B4, pp. 8741–8743.

Westerink, Joannes J et al. (2004). "A new generation hurricane storm surge model for southern Louisiana". In: *Bulletin of the American Meteorological Society, in review.*

Westerink, Joannes J et al. (2008). "A basin-to channel-scale unstructured grid hurricane storm surge model applied to southern Louisiana". In: *Monthly weather review* 136.3, pp. 833–864.

Wolff, Claudia et al. (2016). "Effects of scale and input data on assessing the future impacts of coastal flooding: An application of DIVA for the Emilia-Romagna coast". In: *Frontiers in Marine Science* 3, p. 41.

Wolff, Claudia et al. (2018). "A Mediterranean coastal database for assessing the impacts of sea-level rise and associated hazards". In: *Scientific data* 5, p. 180044.

Woodworth, Philip L et al. (2016). "Towards a global higher-frequency sea level dataset". In: *Geoscience Data Journal* 3.2, pp. 50–59.

Wunsch, Carl, Rui M Ponte, and Patrick Heimbach (2007). "Decadal trends in sea level patterns: 1993–2004". In: *Journal of Climate* 20.24, pp. 5889–5911.

Yamazaki, Dai et al. (2017). "A high-accuracy map of global terrain elevations". In: *Geophysical Research Letters* 44.11, pp. 5844–5853.

Yanagishima, Shin-ichi and Kazumasa Katoh (1991). "Field observation on wave set-up near the shoreline". In: *Coastal Engineering 1990*, pp. 95–108.

Yi, Shuang et al. (2015). "An increase in the rate of global mean sea level rise since 2010". In: *Geophysical Research Letters* 42.10, pp. 3998–4006.

Yin, Jianjun, Michael E Schlesinger, and Ronald J Stouffer (2009). "Model projections of rapid sea-level rise on the northeast coast of the United States". In: *Nature Geoscience* 2.4, pp. 262–266.

Yin, Jie, Ning Lin, and Dapeng Yu (2016). "Coupled modeling of storm surge and coastal inundation: A case study in N ew Y ork C ity during H urricane S andy". In: *Water Resources Research* 52.11, pp. 8685–8699.

Young, Ian R and Agustinus Ribal (2019). "Multiplatform evaluation of global trends in wind speed and wave height". In: *Science* 364.6440, pp. 548–552.

Young, IR, S Zieger, and Alexander V Babanin (2011). "Global trends in wind speed and wave height". In: *Science* 332.6028, pp. 451–455.

Zhang, Keqi, Bruce C Douglas, and Stephen P Leatherman (2000). "Twentieth-century storm activity along the US east coast". In: *Journal of Climate* 13.10, pp. 1748–1761.

Zhou, Qianqian et al. (2012). "Framework for economic pluvial flood risk assessment considering climate change effects and adaptation benefits". In: *Journal of Hydrology* 414, pp. 539–549.

Appendix A

Additional Tables

Rank #	*Region*	Million People
1	*S.E.Asia*	11.88
2	*S.Asia*	11.76
3	*E.Asia*	4.19
4	*Western-Africa*	3.17
5	*Mediterranean*	0.82
6	*E.Southern-Africa*	0.44
7	*West&Central-Europe*	0.29
8	*N.W.South-America*	0.29
9	*N.South-America*	0.24
10	*Arabian-Peninsula*	0.21
11	*N.Europe*	0.20
12	*E.North-America*	0.20
13	*S.Eastern-Africa*	0.19
14	*N.E.South-America*	0.19
15	*S.E.South-America*	0.16
16	*S.Central-America*	0.14
17	*W.C.Asia*	0.12
18	*W.North-America*	0.11
19	*Caribbean*	0.10
20	*E.Australia*	0.10
21	*Central-Africa*	0.08
22	*Madagascar*	0.08
23	*Sahara*	0.07
24	*N.Central-America*	0.06
25	*C.North-America*	0.05
26	*S.Pacific-Ocean*	0.04
27	*Equatorial.Pacific-Ocean*	0.04
28	*Bay-of-Bengal*	0.04
29	*S.Australia*	0.02
30	*E.Europe*	0.02
31	*Equatorial.Indic-Ocean*	0.02
32	*N.W.North-America*	0.02
33	*N.Australia*	0.01
34	*N.Pacific-Ocean*	0.01
35	*N.Eastern-Africa*	0.01
36	*S.W.South-America*	0.01
37	*New-Zealand*	0.01
38	*Russian-Far-East*	0.00
39	*N.E.North-America*	0.00
40	*Russian-Arctic*	0.00
41	*S.Indic-Ocean*	0.00
42	*S.South-America*	0.00
43	*W.Southern-Africa*	0.00
44	*Equatorial.Atlantic-Ocean*	0.00
45	*N.Atlantic-Ocean*	0.00
46	*C.Australia*	0.00
47	*Greenland/Iceland*	0.00
48	*Arabian-Sea*	0.00
49	*Arctic-Ocean*	0.00
50	*S.Atlantic-Ocean*	0.00
51	*Southern-Ocean*	0.00

Rank #	*Region*	Billion $US-2005
1	*S.E.Asia*	$92.77B
2	*E.Asia*	$89.20B
3	*S.Asia*	$63.07B
4	*Western-Africa*	$19.48B
5	*West&Central-Europe*	$11.08B
6	*Mediterranean*	$10.39B
7	*N.Europe*	$9.51B
8	*E.North-America*	$9.47B
9	*W.North-America*	$6.12B
10	*Arabian-Peninsula*	$5.70B
11	*E.Australia*	$4.14B
12	*N.South-America*	$3.97B
13	*W.C.Asia*	$3.51B
14	*N.W.South-America*	$3.32B
15	*S.E.South-America*	$2.65B
16	*C.North-America*	$2.17B
17	*Caribbean*	$1.62B
18	*N.Central-America*	$1.30B
19	*N.W.North-America*	$1.19B
20	*S.Central-America*	$1.19B
21	*N.E.South-America*	$1.02B
22	*Central-Africa*	$0.97B
23	*S.Australia*	$0.94B
24	*S.Eastern-Africa*	$0.75B
25	*E.Southern-Africa*	$0.42B
26	*Bay-of-Bengal*	$0.41B
27	*Sahara*	$0.34B
28	*E.Europe*	$0.26B
29	*N.Australia*	$0.26B
30	*Equatorial.Indic-Ocean*	$0.23B
31	*N.E.North-America*	$0.22B
32	*Russian-Arctic*	$0.20B
33	*New-Zealand*	$0.20B
34	*Russian-Far-East*	$0.19B
35	*Madagascar*	$0.11B
36	*S.W.South-America*	$0.10B
37	*Equatorial.Pacific-Ocean*	$0.08B
38	*C.Australia*	$0.06B
39	*S.South-America*	$0.06B
40	*S.Indic-Ocean*	$0.05B
41	*Greenland/Iceland*	$0.02B
42	*N.Atlantic-Ocean*	$0.02B
43	*N.Eastern-Africa*	$0.02B
44	*W.Southern-Africa*	$0.02B
45	*Equatorial.Atlantic-Ocean*	$0.01B
46	*Arabian-Sea*	$0.00B
47	*Arctic-Ocean*	$0.00B
48	*N.Pacific-Ocean*	$0.00B
49	*S.Pacific-Ocean*	$0.00B
50	*S.Atlantic-Ocean*	$0.00B
51	*Southern-Ocean*	$0.00B

TABLE A.1: (a) Present-day (2015) values of EAPA and (b) Present-day (2015) values of EAD (absolute values).

Rank #	Region	RCP 4.5
1	S.Asia	+3.23
2	S.E.Asia	+2.75
3	Mediterranean	+1.76
4	E.Asia	+0.88
5	Western-Africa	+0.76
6	West&Central-Europe	+0.16
7	C.North-America	+0.10
8	E.North-America	+0.10
9	N.South-America	+0.10
10	E.Southern-Africa	+0.08
11	N.Europe	+0.08
12	S.Central-America	+0.07
13	S.E.South-America	+0.06
14	N.E.South-America	+0.04
15	Central-Africa	+0.04
16	N.W.South-America	+0.03
17	W.C.Asia	+0.03
18	Madagascar	+0.03
19	S.Pacific-Ocean	+0.03
20	Caribbean	+0.02
21	Sahara	+0.02
22	W.North-America	+0.02
23	Arabian-Peninsula	+0.02
24	E.Australia	+0.02
25	S.Eastern-Africa	+0.01
26	Equatorial.Indic-Ocean	+0.01
27	N.Central-America	+0.01
28	Bay-of-Bengal	+0.01
29	S.Australia	+0.01
30	Equatorial.Pacific-Ocean	+0.00
31	E.Europe	+0.00
32	N.Pacific-Ocean	+0.00
33	Russian-Arctic	+0.00
34	N.Australia	+0.00
35	W.Southern-Africa	+0.00
36	N.W.North-America	+0.00
37	New-Zealand	+0.00
38	Russian-Far-East	+0.00
39	S.W.South-America	+0.00
40	N.Atlantic-Ocean	+0.00
41	N.Eastern-Africa	+0.00
42	S.South-America	+0.00
43	Equatorial.Atlantic-Ocean	+0.00
44	C.Australia	+0.00
45	Greenland/Iceland	+0.00
46	S.Indic-Ocean	+0.00
47	Arabian-Sea	+0.00
48	Arctic-Ocean	+0.00
49	S.Atlantic-Ocean	+0.00
50	Southern-Ocean	+0.00
51	N.E.North-America	-0.00

Rank #	Region	RCP 8.5
1	S.Asia	+3.74
2	S.E.Asia	+3.03
3	Mediterranean	+2.06
4	E.Asia	+1.04
5	Western-Africa	+0.85
6	West&Central-Europe	+0.17
7	N.South-America	+0.11
8	E.North-America	+0.11
9	C.North-America	+0.10
10	E.Southern-Africa	+0.09
11	N.Europe	+0.09
12	S.Central-America	+0.07
13	S.E.South-America	+0.06
14	N.E.South-America	+0.05
15	N.W.South-America	+0.04
16	W.C.Asia	+0.04
17	Central-Africa	+0.04
18	Madagascar	+0.03
19	S.Pacific-Ocean	+0.03
20	Caribbean	+0.03
21	Sahara	+0.03
22	W.North-America	+0.02
23	Arabian-Peninsula	+0.02
24	E.Australia	+0.02
25	S.Eastern-Africa	+0.01
26	Equatorial.Indic-Ocean	+0.01
27	N.Central-America	+0.01
28	Bay-of-Bengal	+0.01
29	S.Australia	+0.01
30	E.Europe	+0.00
31	Equatorial.Pacific-Ocean	+0.00
32	N.Pacific-Ocean	+0.00
33	Russian-Arctic	+0.00
34	N.Australia	+0.00
35	N.W.North-America	+0.00
36	New-Zealand	+0.00
37	W.Southern-Africa	+0.00
38	Russian-Far-East	+0.00
39	S.W.South-America	+0.00
40	N.Atlantic-Ocean	+0.00
41	N.Eastern-Africa	+0.00
42	S.South-America	+0.00
43	C.Australia	+0.00
44	Equatorial.Atlantic-Ocean	+0.00
45	Greenland/Iceland	+0.00
46	S.Indic-Ocean	+0.00
47	Arabian-Sea	+0.00
48	Arctic-Ocean	+0.00
49	S.Atlantic-Ocean	+0.00
50	Southern-Ocean	+0.00
51	N.E.North-America	-0.00

TABLE A.2: Scenario of no socio-economic change - EAPA 2050 – full rankings by region (values show change relative to 2015 in millions of people/year impacted).

Rank #	Region	RCP 4.5	Rank #	*Region*	RCP 8.5
1	S.E.Asia	+7.87	1	*S.E.Asia*	+11.83
2	S.Asia	+6.80	2	*S.Asia*	+9.16
3	Mediterranean	+4.01	3	*Mediterranean*	+5.18
4	E.Asia	+2.16	4	*E.Asia*	+3.17
5	Western-Africa	+1.77	5	*Western-Africa*	+2.51
6	N.Europe	+0.26	6	*N.Europe*	+0.53
7	West&Central-Europe	+0.24	7	*West&Central-Europe*	+0.43
8	C.North-America	+0.24	8	*N.South-America*	+0.36
9	E.North-America	+0.24	9	*E.North-America*	+0.32
10	N.South-America	+0.23	10	*C.North-America*	+0.31
11	E.Southern-Africa	+0.17	11	*Central-Africa*	+0.28
12	S.Central-America	+0.16	12	*E.Southern-Africa*	+0.22
13	Central-Africa	+0.15	13	*S.Central-America*	+0.22
14	S.E.South-America	+0.12	14	*S.E.South-America*	+0.20
15	N.E.South-America	+0.12	15	*N.E.South-America*	+0.16
16	N.W.South-America	+0.10	16	*N.W.South-America*	+0.16
17	W.C.Asia	+0.08	17	*W.C.Asia*	+0.13
18	Madagascar	+0.07	18	*Sahara*	+0.10
19	Caribbean	+0.07	19	*Madagascar*	+0.10
20	Arabian-Peninsula	+0.06	20	*Caribbean*	+0.10
21	Sahara	+0.05	21	*Arabian-Peninsula*	+0.10
22	S.Pacific-Ocean	+0.05	22	*W.North-America*	+0.07
23	W.North-America	+0.05	23	*S.Eastern-Africa*	+0.07
24	S.Eastern-Africa	+0.03	24	*S.Pacific-Ocean*	+0.07
25	E.Australia	+0.03	25	*E.Australia*	+0.05
26	N.Central-America	+0.02	26	*N.Central-America*	+0.03
27	Equatorial.Indic-Ocean	+0.02	27	*Equatorial.Indic-Ocean*	+0.03
28	Equatorial.Pacific-Ocean	+0.01	28	*Bay-of-Bengal*	+0.02
29	Bay-of-Bengal	+0.01	29	*E.Europe*	+0.02
30	S.Australia	+0.01	30	*Equatorial.Pacific-Ocean*	+0.01
31	E.Europe	+0.01	31	*S.Australia*	+0.01
32	N.Australia	+0.00	32	*New-Zealand*	+0.01
33	New-Zealand	+0.00	33	*N.Australia*	+0.01
34	N.W.North-America	+0.00	34	*S.W.South-America*	+0.00
35	N.Pacific-Ocean	+0.00	35	*Russian-Arctic*	+0.00
36	Russian-Arctic	+0.00	36	*N.W.North-America*	+0.00
37	W.Southern-Africa	+0.00	37	*N.Pacific-Ocean*	+0.00
38	Russian-Far-East	+0.00	38	*Russian-Far-East*	+0.00
39	S.W.South-America	+0.00	39	*W.Southern-Africa*	+0.00
40	N.Atlantic-Ocean	+0.00	40	*N.Atlantic-Ocean*	+0.00
41	N.Eastern-Africa	+0.00	41	*N.Eastern-Africa*	+0.00
42	S.South-America	+0.00	42	*S.South-America*	+0.00
43	C.Australia	+0.00	43	*C.Australia*	+0.00
44	Equatorial.Atlantic-Ocean	+0.00	44	*Equatorial.Atlantic-Ocean*	+0.00
45	Arabian-Sea	+0.00	45	*S.Indic-Ocean*	+0.00
46	S.Indic-Ocean	+0.00	46	*Arabian-Sea*	+0.00
47	Greenland/Iceland	+0.00	47	*Greenland/Iceland*	+0.00
48	Arctic-Ocean	+0.00	48	*Arctic-Ocean*	+0.00
49	S.Atlantic-Ocean	+0.00	49	*S.Atlantic-Ocean*	+0.00
50	Southern-Ocean	+0.00	50	*Southern-Ocean*	+0.00
51	N.E.North-America	-0.00	51	*N.E.North-America*	-0.00

TABLE A.3: Scenario of no socio-economic change - EAPA 2100 – full rankings by region (values show change relative to 2015 in millions of people/year impacted).

Rank #	*Region*	RCP 4.5
1	*Mediterranean*	+$27.74B
2	*S.E.Asia*	+$25.05B
3	*E.Asia*	+$21.60B
4	*S.Asia*	+$19.79B
5	*Western-Africa*	+$4.99B
6	*E.North-America*	+$4.99B
7	*West&Central-Europe*	+$4.14B
8	*C.North-America*	+$4.07B
9	*N.Europe*	+$3.87B
10	*W.North-America*	+$1.27B
11	*E.Australia*	+$1.11B
12	*Arabian-Peninsula*	+$1.03B
13	*S.E.South-America*	+$1.03B
14	*S.Central-America*	+$0.99B
15	*N.South-America*	+$0.97B
16	*W.C.Asia*	+$0.90B
17	*N.W.South-America*	+$0.56B
18	*Central-Africa*	+$0.53B
19	*Caribbean*	+$0.52B
20	*N.Central-America*	+$0.39B
21	*N.E.South-America*	+$0.37B
22	*S.Australia*	+$0.37B
23	*E.Southern-Africa*	+$0.13B
24	*S.Eastern-Africa*	+$0.12B
25	*N.W.North-America*	+$0.11B
26	*Russian-Arctic*	+$0.11B
27	*Sahara*	+$0.09B
28	*Equatorial.Indic-Ocean*	+$0.09B
29	*Bay-of-Bengal*	+$0.08B
30	*E.Europe*	+$0.07B
31	*New-Zealand*	+$0.05B
32	*Madagascar*	+$0.05B
33	*N.Australia*	+$0.04B
34	*Russian-Far-East*	+$0.04B
35	*Equatorial.Pacific-Ocean*	+$0.02B
36	*C.Australia*	+$0.01B
37	*S.W.South-America*	+$0.01B
38	*N.Atlantic-Ocean*	+$0.01B
39	*W.Southern-Africa*	+$0.01B
40	*S.South-America*	+$0.01B
41	*S.Indic-Ocean*	+$0.00B
42	*N.Eastern-Africa*	+$0.00B
43	*Equatorial.Atlantic-Ocean*	+$0.00B
44	*Greenland/Iceland*	+$0.00B
45	*Arabian-Sea*	+$0.00B
46	*Arctic-Ocean*	+$0.00B
47	*N.Pacific-Ocean*	+$0.00B
48	*S.Pacific-Ocean*	+$0.00B
49	*S.Atlantic-Ocean*	+$0.00B
50	*Southern-Ocean*	+$0.00B
51	*N.E.North-America*	-$0.03B

Rank #	*Region*	RCP 8.5
1	*Mediterranean*	+$33.32B
2	*S.E.Asia*	+$27.70B
3	*E.Asia*	+$25.23B
4	*S.Asia*	+$22.84B
5	*Western-Africa*	+$5.64B
6	*E.North-America*	+$5.40B
7	*N.Europe*	+$4.37B
8	*West&Central-Europe*	+$4.35B
9	*C.North-America*	+$4.22B
10	*W.North-America*	+$1.35B
11	*Arabian-Peninsula*	+$1.27B
12	*E.Australia*	+$1.19B
13	*W.C.Asia*	+$1.16B
14	*S.E.South-America*	+$1.16B
15	*S.Central-America*	+$1.14B
16	*N.South-America*	+$1.09B
17	*N.W.South-America*	+$0.69B
18	*Central-Africa*	+$0.58B
19	*Caribbean*	+$0.57B
20	*N.Central-America*	+$0.42B
21	*N.E.South-America*	+$0.41B
22	*S.Australia*	+$0.37B
23	*E.Southern-Africa*	+$0.14B
24	*S.Eastern-Africa*	+$0.14B
25	*Russian-Arctic*	+$0.13B
26	*N.W.North-America*	+$0.13B
27	*Sahara*	+$0.11B
28	*E.Europe*	+$0.11B
29	*Equatorial.Indic-Ocean*	+$0.10B
30	*Bay-of-Bengal*	+$0.08B
31	*New-Zealand*	+$0.06B
32	*Madagascar*	+$0.05B
33	*N.Australia*	+$0.04B
34	*Russian-Far-East*	+$0.04B
35	*Equatorial.Pacific-Ocean*	+$0.02B
36	*S.W.South-America*	+$0.01B
37	*C.Australia*	+$0.01B
38	*W.Southern-Africa*	+$0.01B
39	*N.Atlantic-Ocean*	+$0.01B
40	*S.South-America*	+$0.01B
41	*S.Indic-Ocean*	+$0.01B
42	*N.Eastern-Africa*	+$0.00B
43	*Equatorial.Atlantic-Ocean*	+$0.00B
44	*Greenland/Iceland*	+$0.00B
45	*Arabian-Sea*	+$0.00B
46	*Arctic-Ocean*	+$0.00B
47	*N.Pacific-Ocean*	+$0.00B
48	*S.Pacific-Ocean*	+$0.00B
49	*S.Atlantic-Ocean*	+$0.00B
50	*Southern-Ocean*	+$0.00B
51	*N.E.North-America*	-$0.02B

TABLE A.4: Scenario of no socio-economic change - EAD 2050 – full rankings by region (values show change relative to 2015 in billion US$/year)

Rank #	*Region*	RCP 4.5
1	*S.E.Asia*	+$73.96B
2	*Mediterranean*	+$67.81B
3	*E.Asia*	+$54.53B
4	*S.Asia*	+$43.78B
5	*E.North-America*	+$12.72B
6	*Western-Africa*	+$12.32B
7	*N.Europe*	+$11.75B
8	*C.North-America*	+$10.54B
9	*West&Central-Europe*	+$7.01B
10	*W.North-America*	+$3.39B
11	*S.Central-America*	+$3.14B
12	*S.E.South-America*	+$2.80B
13	*Arabian-Peninsula*	+$2.80B
14	*W.C.Asia*	+$2.67B
15	*N.South-America*	+$2.60B
16	*E.Australia*	+$2.37B
17	*Central-Africa*	+$1.83B
18	*N.W.South-America*	+$1.58B
19	*Caribbean*	+$1.42B
20	*N.E.South-America*	+$0.94B
21	*N.Central-America*	+$0.88B
22	*S.Australia*	+$0.81B
23	*E.Southern-Africa*	+$0.29B
24	*N.W.North-America*	+$0.28B
25	*S.Eastern-Africa*	+$0.27B
26	*Sahara*	+$0.25B
27	*Equatorial.Indic-Ocean*	+$0.23B
28	*Russian-Arctic*	+$0.21B
29	*Bay-of-Bengal*	+$0.17B
30	*New-Zealand*	+$0.13B
31	*E.Europe*	+$0.12B
32	*Madagascar*	+$0.11B
33	*N.Australia*	+$0.10B
34	*Russian-Far-East*	+$0.09B
35	*Equatorial.Pacific-Ocean*	+$0.05B
36	*S.W.South-America*	+$0.03B
37	*C.Australia*	+$0.02B
38	*W.Southern-Africa*	+$0.02B
39	*N.Atlantic-Ocean*	+$0.02B
40	*S.South-America*	+$0.02B
41	*S.Indic-Ocean*	+$0.01B
42	*N.Eastern-Africa*	+$0.01B
43	*Equatorial.Atlantic-Ocean*	+$0.00B
44	*Greenland/Iceland*	+$0.00B
45	*Arabian-Sea*	+$0.00B
46	*Arctic-Ocean*	+$0.00B
47	*N.Pacific-Ocean*	+$0.00B
48	*S.Pacific-Ocean*	+$0.00B
49	*S.Atlantic-Ocean*	+$0.00B
50	*Southern-Ocean*	+$0.00B
51	*N.E.North-America*	-$0.04B

Rank #	*Region*	RCP 8.5
1	*S.E.Asia*	+$114.86B
2	*Mediterranean*	+$83.72B
3	*E.Asia*	+$82.22B
4	*S.Asia*	+$61.75B
5	*N.Europe*	+$26.87B
6	*E.North-America*	+$18.12B
7	*Western-Africa*	+$18.00B
8	*West&Central-Europe*	+$15.19B
9	*C.North-America*	+$14.40B
10	*W.North-America*	+$4.81B
11	*S.Central-America*	+$4.65B
12	*Arabian-Peninsula*	+$4.61B
13	*S.E.South-America*	+$4.47B
14	*W.C.Asia*	+$4.33B
15	*N.South-America*	+$4.24B
16	*E.Australia*	+$3.32B
17	*Central-Africa*	+$3.26B
18	*N.W.South-America*	+$2.36B
19	*Caribbean*	+$2.13B
20	*N.E.South-America*	+$1.33B
21	*N.Central-America*	+$1.22B
22	*S.Australia*	+$1.07B
23	*Sahara*	+$0.40B
24	*S.Eastern-Africa*	+$0.39B
25	*E.Southern-Africa*	+$0.39B
26	*N.W.North-America*	+$0.37B
27	*E.Europe*	+$0.37B
28	*Russian-Arctic*	+$0.35B
29	*Equatorial.Indic-Ocean*	+$0.32B
30	*Bay-of-Bengal*	+$0.26B
31	*New-Zealand*	+$0.23B
32	*Madagascar*	+$0.16B
33	*N.Australia*	+$0.15B
34	*Russian-Far-East*	+$0.13B
35	*S.W.South-America*	+$0.09B
36	*Equatorial.Pacific-Ocean*	+$0.06B
37	*C.Australia*	+$0.03B
38	*W.Southern-Africa*	+$0.03B
39	*S.South-America*	+$0.03B
40	*N.Atlantic-Ocean*	+$0.02B
41	*S.Indic-Ocean*	+$0.01B
42	*N.Eastern-Africa*	+$0.01B
43	*Equatorial.Atlantic-Ocean*	+$0.00B
44	*Greenland/Iceland*	+$0.00B
45	*Arabian-Sea*	+$0.00B
46	*Arctic-Ocean*	+$0.00B
47	*N.Pacific-Ocean*	+$0.00B
48	*S.Pacific-Ocean*	+$0.00B
49	*S.Atlantic-Ocean*	+$0.00B
50	*Southern-Ocean*	+$0.00B
51	*N.E.North-America*	-$0.02B

TABLE A.5: Scenario of no socio-economic change - EAD 2100 – full rankings by region (values show change relative to 2015 in billion US$/year).

Rank #	*Region*	SSP1
1	*S.Asia*	+3.73
2	*Western-Africa*	+1.59
3	*Mediterranean*	+0.41
4	*E.Southern-Africa*	+0.27
5	*Arabian-Peninsula*	+0.20
6	*S.E.South-America*	+0.19
7	*W.C.Asia*	+0.18
8	*S.Eastern-Africa*	+0.11
9	*S.E.Asia*	+0.11
10	*W.North-America*	+0.09
11	*E.North-America*	+0.08
12	*E.Australia*	+0.08
13	*C.North-America*	+0.07
14	*N.Central-America*	+0.05
15	*N.E.South-America*	+0.05
16	*Madagascar*	+0.05
17	*N.Europe*	+0.05
18	*S.Central-America*	+0.02
19	*Sahara*	+0.01
20	*N.Australia*	+0.01
21	*New-Zealand*	+0.01
22	*N.Eastern-Africa*	+0.00
23	*S.Indic-Ocean*	+0.00
24	*S.Australia*	+0.00
25	*S.W.South-America*	+0.00
26	*Greenland/Iceland*	+0.00
27	*S.Atlantic-Ocean*	+0.00
28	*N.Atlantic-Ocean*	+0.00
29	*Arabian-Sea*	+0.00
30	*Arctic-Ocean*	+0.00
31	*N.Pacific-Ocean*	+0.00
32	*S.Pacific-Ocean*	+0.00
33	*Southern-Ocean*	+0.00
34	*W.Southern-Africa*	-0.00
35	*Equatorial.Pacific-Ocean*	-0.00
36	*C.Australia*	-0.00
37	*Equatorial.Atlantic-Ocean*	-0.00
38	*S.South-America*	-0.00
39	*N.E.North-America*	-0.00
40	*Russian-Far-East*	-0.00
41	*Russian-Arctic*	-0.00
42	*N.W.North-America*	-0.00
43	*Equatorial.Indic-Ocean*	-0.01
44	*Bay-of-Bengal*	-0.01
45	*Caribbean*	-0.02
46	*E.Europe*	-0.02
47	*Central-Africa*	-0.02
48	*West&Central-Europe*	-0.05
49	*N.W.South-America*	-0.05
50	*E.Asia*	-0.08
51	*N.South-America*	-0.08

Rank #	*Region*	SSP3
1	*S.Asia*	+7.98
2	*Western-Africa*	+3.19
3	*S.E.Asia*	+3.05
4	*Mediterranean*	+0.90
5	*E.Southern-Africa*	+0.40
6	*W.C.Asia*	+0.27
7	*S.E.South-America*	+0.25
8	*S.Eastern-Africa*	+0.23
9	*Arabian-Peninsula*	+0.22
10	*Madagascar*	+0.11
11	*S.Central-America*	+0.10
12	*N.Central-America*	+0.09
13	*N.E.South-America*	+0.09
14	*E.Asia*	+0.08
15	*W.North-America*	+0.05
16	*C.North-America*	+0.05
17	*N.W.South-America*	+0.05
18	*E.Australia*	+0.04
19	*E.North-America*	+0.03
20	*Sahara*	+0.03
21	*Equatorial.Pacific-Ocean*	+0.01
22	*N.Europe*	+0.01
23	*Caribbean*	+0.01
24	*N.Australia*	+0.01
25	*N.Eastern-Africa*	+0.00
26	*New-Zealand*	+0.00
27	*S.Indic-Ocean*	+0.00
28	*S.W.South-America*	+0.00
29	*N.Atlantic-Ocean*	+0.00
30	*S.Atlantic-Ocean*	+0.00
31	*Greenland/Iceland*	+0.00
32	*W.Southern-Africa*	+0.00
33	*Arabian-Sea*	+0.00
34	*Equatorial.Atlantic-Ocean*	+0.00
35	*Arctic-Ocean*	+0.00
36	*N.Pacific-Ocean*	+0.00
37	*S.Pacific-Ocean*	+0.00
38	*Southern-Ocean*	+0.00
39	*C.Australia*	-0.00
40	*S.South-America*	-0.00
41	*Russian-Far-East*	-0.00
42	*N.E.North-America*	-0.00
43	*Russian-Arctic*	-0.00
44	*Bay-of-Bengal*	-0.00
45	*S.Australia*	-0.00
46	*Equatorial.Indic-Ocean*	-0.01
47	*N.W.North-America*	-0.01
48	*Central-Africa*	-0.01
49	*E.Europe*	-0.02
50	*N.South-America*	-0.04
51	*West&Central-Europe*	-0.07

Rank #	*Region*	SSP5
1	*S.Asia*	+3.48
2	*Western-Africa*	+1.52
3	*Mediterranean*	+0.40
4	*E.Southern-Africa*	+0.26
5	*Arabian-Peninsula*	+0.21
6	*W.C.Asia*	+0.20
7	*S.E.South-America*	+0.19
8	*E.North-America*	+0.12
9	*W.North-America*	+0.12
10	*E.Australia*	+0.11
11	*S.Eastern-Africa*	+0.10
12	*C.North-America*	+0.09
13	*N.Europe*	+0.08
14	*Madagascar*	+0.05
15	*N.E.South-America*	+0.05
16	*N.Central-America*	+0.05
17	*E.Asia*	+0.02
18	*Sahara*	+0.01
19	*S.Central-America*	+0.01
20	*N.Australia*	+0.01
21	*New-Zealand*	+0.01
22	*S.Australia*	+0.01
23	*N.Eastern-Africa*	+0.00
24	*S.Indic-Ocean*	+0.00
25	*S.W.South-America*	+0.00
26	*Greenland/Iceland*	+0.00
27	*S.Atlantic-Ocean*	+0.00
28	*N.Atlantic-Ocean*	+0.00
29	*C.Australia*	+0.00
30	*W.Southern-Africa*	+0.00
31	*Arabian-Sea*	+0.00
32	*Arctic-Ocean*	+0.00
33	*N.Pacific-Ocean*	+0.00
34	*S.Pacific-Ocean*	+0.00
35	*Southern-Ocean*	+0.00
36	*Equatorial.Pacific-Ocean*	-0.00
37	*Equatorial.Atlantic-Ocean*	-0.00
38	*N.E.North-America*	-0.00
39	*S.South-America*	-0.00
40	*Russian-Far-East*	-0.00
41	*N.W.North-America*	-0.00
42	*Russian-Arctic*	-0.00
43	*Equatorial.Indic-Ocean*	-0.01
44	*Bay-of-Bengal*	-0.01
45	*E.Europe*	-0.02
46	*Central-Africa*	-0.02
47	*Caribbean*	-0.03
48	*West&Central-Europe*	-0.03
49	*N.W.South-America*	-0.06
50	*S.E.Asia*	-0.07
51	*N.South-America*	-0.08

TABLE A.6: Scenario of constant flood probability - EAPA 2050 – full rankings by region (values show change relative to 2015 in millions of people/year impacted).

Rank #	*Region*	SSP1
1	*Western-Africa*	+2.47
2	*E.Southern-Africa*	+0.26
3	*Arabian-Peninsula*	+0.21
4	*W.C.Asia*	+0.14
5	*S.Eastern-Africa*	+0.13
6	*Mediterranean*	+0.11
7	*W.North-America*	+0.11
8	*E.North-America*	+0.10
9	*E.Australia*	+0.10
10	*C.North-America*	+0.08
11	*S.E.South-America*	+0.07
12	*N.Europe*	+0.06
13	*Madagascar*	+0.05
14	*N.Central-America*	+0.03
15	*Sahara*	+0.01
16	*N.Australia*	+0.01
17	*New-Zealand*	+0.01
18	*S.Australia*	+0.00
19	*N.Eastern-Africa*	+0.00
20	*S.Indic-Ocean*	+0.00
21	*Greenland/Iceland*	+0.00
22	*S.Atlantic-Ocean*	+0.00
23	*Arabian-Sea*	+0.00
24	*Arctic-Ocean*	+0.00
25	*N.Pacific-Ocean*	+0.00
26	*S.Pacific-Ocean*	+0.00
27	*Southern-Ocean*	+0.00
28	*N.Atlantic-Ocean*	-0.00
29	*C.Australia*	-0.00
30	*W.Southern-Africa*	-0.00
31	*Equatorial.Atlantic-Ocean*	-0.00
32	*S.South-America*	-0.00
33	*N.E.North-America*	-0.00
34	*S.W.South-America*	-0.00
35	*Russian-Far-East*	-0.00
36	*Russian-Arctic*	-0.00
37	*Equatorial.Pacific-Ocean*	-0.01
38	*N.W.North-America*	-0.01
39	*Equatorial.Indic-Ocean*	-0.01
40	*E.Europe*	-0.02
41	*Bay-of-Bengal*	-0.02
42	*S.Central-America*	-0.02
43	*Central-Africa*	-0.03
44	*N.E.South-America*	-0.03
45	*Caribbean*	-0.06
46	*West&Central-Europe*	-0.08
47	*N.W.South-America*	-0.12
48	*N.South-America*	-0.12
49	*S.Asia*	-0.80
50	*E.Asia*	-1.72
51	*S.E.Asia*	-4.09

Rank #	*Region*	SSP3
1	*S.Asia*	+12.87
2	*Western-Africa*	+8.39
3	*S.E.Asia*	+4.23
4	*Mediterranean*	+1.49
5	*E.Southern-Africa*	+0.75
6	*S.Eastern-Africa*	+0.52
7	*W.C.Asia*	+0.50
8	*Arabian-Peninsula*	+0.46
9	*S.E.South-America*	+0.29
10	*Madagascar*	+0.24
11	*S.Central-America*	+0.18
12	*N.W.South-America*	+0.15
13	*N.Central-America*	+0.12
14	*N.E.South-America*	+0.11
15	*Sahara*	+0.09
16	*Equatorial.Pacific-Ocean*	+0.03
17	*C.North-America*	+0.03
18	*W.North-America*	+0.02
19	*E.Australia*	+0.01
20	*N.South-America*	+0.01
21	*Central-Africa*	+0.01
22	*Caribbean*	+0.01
23	*N.Eastern-Africa*	+0.01
24	*N.Australia*	+0.01
25	*Bay-of-Bengal*	+0.01
26	*S.W.South-America*	+0.00
27	*S.Indic-Ocean*	+0.00
28	*New-Zealand*	+0.00
29	*N.Atlantic-Ocean*	+0.00
30	*W.Southern-Africa*	+0.00
31	*S.Atlantic-Ocean*	+0.00
32	*Arabian-Sea*	+0.00
33	*Equatorial.Atlantic-Ocean*	+0.00
34	*Greenland/Iceland*	+0.00
35	*Arctic-Ocean*	+0.00
36	*N.Pacific-Ocean*	+0.00
37	*S.Pacific-Ocean*	+0.00
38	*Southern-Ocean*	+0.00
39	*C.Australia*	-0.00
40	*S.South-America*	-0.00
41	*Russian-Far-East*	-0.00
42	*N.E.North-America*	-0.00
43	*Russian-Arctic*	-0.00
44	*Equatorial.Indic-Ocean*	-0.00
45	*S.Australia*	-0.01
46	*N.W.North-America*	-0.01
47	*E.Europe*	-0.02
48	*E.North-America*	-0.02
49	*N.Europe*	-0.05
50	*West&Central-Europe*	-0.13
51	*E.Asia*	-0.79

Rank #	*Region*	SSP5
1	*Western-Africa*	+2.33
2	*E.North-America*	+0.25
3	*E.Southern-Africa*	+0.24
4	*Arabian-Peninsula*	+0.23
5	*W.North-America*	+0.22
6	*E.Australia*	+0.20
7	*N.Europe*	+0.19
8	*W.C.Asia*	+0.15
9	*C.North-America*	+0.15
10	*Mediterranean*	+0.13
11	*S.Eastern-Africa*	+0.11
12	*S.E.South-America*	+0.07
13	*Madagascar*	+0.04
14	*N.Central-America*	+0.03
15	*S.Australia*	+0.02
16	*N.Australia*	+0.01
17	*New-Zealand*	+0.01
18	*Sahara*	+0.01
19	*Greenland/Iceland*	+0.00
20	*S.Indic-Ocean*	+0.00
21	*N.Eastern-Africa*	+0.00
22	*C.Australia*	+0.00
23	*N.E.North-America*	+0.00
24	*S.Atlantic-Ocean*	+0.00
25	*Arabian-Sea*	+0.00
26	*N.Atlantic-Ocean*	+0.00
27	*Arctic-Ocean*	+0.00
28	*N.Pacific-Ocean*	+0.00
29	*S.Pacific-Ocean*	+0.00
30	*Southern-Ocean*	+0.00
31	*W.Southern-Africa*	-0.00
32	*Equatorial.Atlantic-Ocean*	-0.00
33	*S.South-America*	-0.00
34	*S.W.South-America*	-0.00
35	*Russian-Far-East*	-0.00
36	*N.W.North-America*	-0.00
37	*Russian-Arctic*	-0.00
38	*Equatorial.Pacific-Ocean*	-0.01
39	*West&Central-Europe*	-0.01
40	*Equatorial.Indic-Ocean*	-0.01
41	*E.Europe*	-0.02
42	*Bay-of-Bengal*	-0.02
43	*Central-Africa*	-0.03
44	*N.E.South-America*	-0.03
45	*S.Central-America*	-0.04
46	*Caribbean*	-0.07
47	*N.W.South-America*	-0.13
48	*N.South-America*	-0.13
49	*S.Asia*	-1.10
50	*E.Asia*	-1.36
51	*S.E.Asia*	-4.32

TABLE A.7: Scenario of constant flood probability - EAPA 2100 – full rankings by region (values show change relative to 2015 in millions of people/year impacted).

Rank #	*Region*	SSP1
1	*S.Asia*	+$343.62B
2	*S.E.Asia*	+$247.74B
3	*E.Asia*	+$158.88B
4	*Western-Africa*	+$69.01B
5	*Mediterranean*	+$29.90B
6	*E.North-America*	+$13.89B
7	*W.C.Asia*	+$12.99B
8	*Arabian-Peninsula*	+$12.37B
9	*W.North-America*	+$11.04B
10	*N.Europe*	+$10.97B
11	*E.Australia*	+$9.69B
12	*S.E.South-America*	+$8.49B
13	*E.Southern-Africa*	+$8.09B
14	*C.North-America*	+$7.95B
15	*N.E.South-America*	+$7.40B
16	*West&Central-Europe*	+$6.69B
17	*S.Central-America*	+$5.86B
18	*N.W.South-America*	+$4.79B
19	*S.Eastern-Africa*	+$3.54B
20	*N.Central-America*	+$3.54B
21	*N.South-America*	+$2.26B
22	*Caribbean*	+$1.26B
23	*Sahara*	+$1.23B
24	*Madagascar*	+$0.98B
25	*N.Australia*	+$0.90B
26	*Equatorial.Pacific-Ocean*	+$0.68B
27	*S.Australia*	+$0.48B
28	*S.W.South-America*	+$0.43B
29	*Bay-of-Bengal*	+$0.38B
30	*New-Zealand*	+$0.32B
31	*Central-Africa*	+$0.24B
32	*S.Indic-Ocean*	+$0.23B
33	*N.W.North-America*	+$0.19B
34	*N.Eastern-Africa*	+$0.12B
35	*Greenland/Iceland*	+$0.10B
36	*Equatorial.Indic-Ocean*	+$0.08B
37	*Russian-Far-East*	+$0.05B
38	*W.Southern-Africa*	+$0.05B
39	*N.Atlantic-Ocean*	+$0.03B
40	*Equatorial.Atlantic-Ocean*	+$0.03B
41	*S.South-America*	+$0.03B
42	*S.Atlantic-Ocean*	+$0.01B
43	*C.Australia*	+$0.00B
44	*Arabian-Sea*	+$0.00B
45	*Arctic-Ocean*	+$0.00B
46	*N.Pacific-Ocean*	+$0.00B
47	*S.Pacific-Ocean*	+$0.00B
48	*Southern-Ocean*	+$0.00B
49	*N.E.North-America*	-$0.06B
50	*Russian-Arctic*	-$0.20B
51	*E.Europe*	-$0.26B

Rank #	*Region*	SSP3
1	*S.Asia*	+$146.40B
2	*S.E.Asia*	+$107.64B
3	*E.Asia*	+$68.18B
4	*Western-Africa*	+$25.78B
5	*Mediterranean*	+$16.94B
6	*E.North-America*	+$13.18B
7	*W.C.Asia*	+$12.32B
8	*W.North-America*	+$9.00B
9	*C.North-America*	+$6.38B
10	*Arabian-Peninsula*	+$6.23B
11	*E.Australia*	+$6.22B
12	*N.Europe*	+$5.40B
13	*S.E.South-America*	+$4.94B
14	*S.Central-America*	+$4.25B
15	*N.Central-America*	+$4.22B
16	*N.E.South-America*	+$3.70B
17	*E.Southern-Africa*	+$3.08B
18	*N.W.South-America*	+$2.23B
19	*West&Central-Europe*	+$2.10B
20	*N.South-America*	+$1.68B
21	*S.Eastern-Africa*	+$1.27B
22	*N.W.North-America*	+$0.80B
23	*N.Australia*	+$0.47B
24	*Caribbean*	+$0.45B
25	*Madagascar*	+$0.35B
26	*Equatorial.Pacific-Ocean*	+$0.31B
27	*S.W.South-America*	+$0.28B
28	*Sahara*	+$0.26B
29	*S.Australia*	+$0.25B
30	*New-Zealand*	+$0.18B
31	*Bay-of-Bengal*	+$0.08B
32	*S.Indic-Ocean*	+$0.08B
33	*Greenland/Iceland*	+$0.05B
34	*Russian-Far-East*	+$0.04B
35	*W.Southern-Africa*	+$0.02B
36	*N.Atlantic-Ocean*	+$0.02B
37	*Equatorial.Atlantic-Ocean*	+$0.02B
38	*S.South-America*	+$0.00B
39	*S.Atlantic-Ocean*	+$0.00B
40	*Arabian-Sea*	+$0.00B
41	*Arctic-Ocean*	+$0.00B
42	*N.Pacific-Ocean*	+$0.00B
43	*S.Pacific-Ocean*	+$0.00B
44	*Southern-Ocean*	+$0.00B
45	*N.Eastern-Africa*	-$0.01B
46	*C.Australia*	-$0.03B
47	*Central-Africa*	-$0.05B
48	*Equatorial.Indic-Ocean*	-$0.05B
49	*N.E.North-America*	-$0.07B
50	*Russian-Arctic*	-$0.20B
51	*E.Europe*	-$0.26B

Rank #	*Region*	SSP5
1	*S.Asia*	+$450.44B
2	*S.E.Asia*	+$334.83B
3	*E.Asia*	+$223.03B
4	*Western-Africa*	+$93.68B
5	*Mediterranean*	+$38.53B
6	*E.North-America*	+$21.24B
7	*W.C.Asia*	+$20.99B
8	*Arabian-Peninsula*	+$19.66B
9	*W.North-America*	+$17.14B
10	*N.Europe*	+$17.05B
11	*E.Australia*	+$14.77B
12	*West&Central-Europe*	+$11.27B
13	*E.Southern-Africa*	+$10.99B
14	*S.E.South-America*	+$10.93B
15	*C.North-America*	+$10.90B
16	*N.E.South-America*	+$9.33B
17	*S.Central-America*	+$7.06B
18	*N.W.South-America*	+$6.43B
19	*S.Eastern-Africa*	+$4.78B
20	*N.South-America*	+$4.58B
21	*N.Central-America*	+$4.41B
22	*Sahara*	+$1.63B
23	*Caribbean*	+$1.55B
24	*Madagascar*	+$1.39B
25	*N.Australia*	+$1.39B
26	*S.Australia*	+$1.04B
27	*Equatorial.Pacific-Ocean*	+$0.91B
28	*Bay-of-Bengal*	+$0.57B
29	*N.W.North-America*	+$0.56B
30	*S.W.South-America*	+$0.54B
31	*Central-Africa*	+$0.53B
32	*New-Zealand*	+$0.48B
33	*S.Indic-Ocean*	+$0.30B
34	*N.Eastern-Africa*	+$0.15B
35	*Equatorial.Indic-Ocean*	+$0.15B
36	*Greenland/Iceland*	+$0.14B
37	*Russian-Far-East*	+$0.14B
38	*W.Southern-Africa*	+$0.07B
39	*N.E.North-America*	+$0.06B
40	*S.South-America*	+$0.05B
41	*N.Atlantic-Ocean*	+$0.05B
42	*Equatorial.Atlantic-Ocean*	+$0.04B
43	*C.Australia*	+$0.04B
44	*S.Atlantic-Ocean*	+$0.01B
45	*Arabian-Sea*	+$0.00B
46	*Arctic-Ocean*	+$0.00B
47	*N.Pacific-Ocean*	+$0.00B
48	*S.Pacific-Ocean*	+$0.00B
49	*Southern-Ocean*	+$0.00B
50	*Russian-Arctic*	-$0.20B
51	*E.Europe*	-$0.26B

TABLE A.8: Scenario of constant flood probability - EAD 2050 – full rankings by region (values show change relative to 2015 in billion US$/year).

Rank #	*Region*	SSP1
1	*S.Asia*	+$951.55B
2	*S.E.Asia*	+$582.55B
3	*Western-Africa*	+$546.36B
4	*E.Asia*	+$192.79B
5	*Mediterranean*	+$68.70B
6	*E.Southern-Africa*	+$67.66B
7	*N.Europe*	+$28.64B
8	*E.North-America*	+$28.15B
9	*Arabian-Peninsula*	+$27.34B
10	*S.Eastern-Africa*	+$25.64B
11	*W.North-America*	+$23.97B
12	*E.Australia*	+$23.22B
13	*W.C.Asia*	+$22.39B
14	*West&Central-Europe*	+$17.55B
15	*S.E.South-America*	+$15.39B
16	*C.North-America*	+$13.94B
17	*N.W.South-America*	+$13.78B
18	*S.Central-America*	+$13.03B
19	*N.E.South-America*	+$12.66B
20	*Sahara*	+$8.58B
21	*Madagascar*	+$8.54B
22	*N.South-America*	+$7.91B
23	*N.Central-America*	+$7.28B
24	*Equatorial.Pacific-Ocean*	+$2.97B
25	*Central-Africa*	+$2.39B
26	*Caribbean*	+$2.25B
27	*N.Australia*	+$2.17B
28	*S.Australia*	+$1.80B
29	*Bay-of-Bengal*	+$1.21B
30	*New-Zealand*	+$0.98B
31	*S.W.South-America*	+$0.61B
32	*N.Eastern-Africa*	+$0.48B
33	*S.Indic-Ocean*	+$0.43B
34	*Equatorial.Indic-Ocean*	+$0.42B
35	*N.W.North-America*	+$0.35B
36	*Greenland/Iceland*	+$0.24B
37	*W.Southern-Africa*	+$0.11B
38	*Russian-Far-East*	+$0.09B
39	*N.Atlantic-Ocean*	+$0.07B
40	*Equatorial.Atlantic-Ocean*	+$0.06B
41	*S.South-America*	+$0.06B
42	*C.Australia*	+$0.05B
43	*N.E.North-America*	+$0.02B
44	*S.Atlantic-Ocean*	+$0.01B
45	*Arabian-Sea*	+$0.01B
46	*Arctic-Ocean*	+$0.00B
47	*N.Pacific-Ocean*	+$0.00B
48	*S.Pacific-Ocean*	+$0.00B
49	*Southern-Ocean*	+$0.00B
50	*Russian-Arctic*	-$0.20B
51	*E.Europe*	-$0.26B

Rank #	*Region*	SSP3
1	*S.Asia*	+$373.28B
2	*S.E.Asia*	+$295.95B
3	*Western-Africa*	+$208.92B
4	*E.Asia*	+$74.68B
5	*Mediterranean*	+$50.26B
6	*W.C.Asia*	+$18.59B
7	*Arabian-Peninsula*	+$14.94B
8	*E.Southern-Africa*	+$11.93B
9	*E.North-America*	+$11.82B
10	*W.North-America*	+$10.13B
11	*S.Central-America*	+$9.77B
12	*N.W.South-America*	+$9.75B
13	*S.Eastern-Africa*	+$9.00B
14	*N.South-America*	+$7.28B
15	*E.Australia*	+$7.17B
16	*N.Central-America*	+$6.58B
17	*S.E.South-America*	+$6.38B
18	*N.Europe*	+$5.92B
19	*C.North-America*	+$5.67B
20	*N.E.South-America*	+$4.25B
21	*West&Central-Europe*	+$2.98B
22	*Madagascar*	+$2.83B
23	*Sahara*	+$1.93B
24	*Caribbean*	+$1.77B
25	*Equatorial.Pacific-Ocean*	+$1.35B
26	*Central-Africa*	+$1.00B
27	*N.Australia*	+$0.67B
28	*S.W.South-America*	+$0.53B
29	*Bay-of-Bengal*	+$0.51B
30	*N.W.North-America*	+$0.38B
31	*New-Zealand*	+$0.34B
32	*S.Australia*	+$0.31B
33	*S.Indic-Ocean*	+$0.15B
34	*Russian-Far-East*	+$0.14B
35	*Equatorial.Indic-Ocean*	+$0.09B
36	*Greenland/Iceland*	+$0.06B
37	*W.Southern-Africa*	+$0.05B
38	*S.South-America*	+$0.04B
39	*N.Atlantic-Ocean*	+$0.03B
40	*Equatorial.Atlantic-Ocean*	+$0.03B
41	*Arabian-Sea*	+$0.00B
42	*S.Atlantic-Ocean*	+$0.00B
43	*Arctic-Ocean*	+$0.00B
44	*N.Pacific-Ocean*	+$0.00B
45	*S.Pacific-Ocean*	+$0.00B
46	*Southern-Ocean*	+$0.00B
47	*N.Eastern-Africa*	-$0.00B
48	*C.Australia*	-$0.03B
49	*N.E.North-America*	-$0.09B
50	*Russian-Arctic*	-$0.20B
51	*E.Europe*	-$0.26B

Rank #	*Region*	SSP5
1	*S.Asia*	+$1,592.62B
2	*S.E.Asia*	+$1,002.51B
3	*Western-Africa*	+$905.42B
4	*E.Asia*	+$427.97B
5	*Mediterranean*	+$123.31B
6	*E.Southern-Africa*	+$114.07B
7	*N.Europe*	+$78.67B
8	*E.North-America*	+$78.19B
9	*W.North-America*	+$64.73B
10	*E.Australia*	+$61.58B
11	*Arabian-Peninsula*	+$54.48B
12	*West&Central-Europe*	+$50.22B
13	*W.C.Asia*	+$45.48B
14	*S.Eastern-Africa*	+$41.24B
15	*C.North-America*	+$34.96B
16	*S.E.South-America*	+$26.64B
17	*N.W.South-America*	+$23.37B
18	*N.E.South-America*	+$21.45B
19	*S.Central-America*	+$19.63B
20	*N.South-America*	+$17.90B
21	*Madagascar*	+$14.82B
22	*Sahara*	+$13.82B
23	*N.Central-America*	+$12.76B
24	*S.Australia*	+$5.88B
25	*N.Australia*	+$5.68B
26	*Equatorial.Pacific-Ocean*	+$5.07B
27	*Central-Africa*	+$4.67B
28	*Caribbean*	+$3.40B
29	*New-Zealand*	+$2.54B
30	*N.W.North-America*	+$2.31B
31	*Bay-of-Bengal*	+$2.20B
32	*S.W.South-America*	+$1.07B
33	*Equatorial.Indic-Ocean*	+$0.78B
34	*N.Eastern-Africa*	+$0.78B
35	*S.Indic-Ocean*	+$0.74B
36	*Greenland/Iceland*	+$0.61B
37	*N.E.North-America*	+$0.57B
38	*Russian-Far-East*	+$0.34B
39	*C.Australia*	+$0.26B
40	*W.Southern-Africa*	+$0.21B
41	*N.Atlantic-Ocean*	+$0.15B
42	*S.South-America*	+$0.13B
43	*Equatorial.Atlantic-Ocean*	+$0.10B
44	*S.Atlantic-Ocean*	+$0.01B
45	*Arabian-Sea*	+$0.01B
46	*Arctic-Ocean*	+$0.00B
47	*N.Pacific-Ocean*	+$0.00B
48	*S.Pacific-Ocean*	+$0.00B
49	*Southern-Ocean*	+$0.00B
50	*Russian-Arctic*	-$0.20B
51	*E.Europe*	-$0.26B

TABLE A.9: Scenario of constant flood probability - EAD 2100 – full rankings by region (values show change relative to 2015 in billion US$/year).

Rank #	*Region*	SSP1-4.5
1	*S.Asia*	+8.37
2	*Mediterranean*	+2.94
3	*S.E.Asia*	+2.93
4	*Western-Africa*	+2.57
5	*E.Asia*	+0.87
6	*E.Southern-Africa*	+0.40
7	*S.E.South-America*	+0.34
8	*C.North-America*	+0.27
9	*W.C.Asia*	+0.23
10	*Arabian-Peninsula*	+0.23
11	*E.North-America*	+0.23
12	*Sahara*	+0.18
13	*N.Europe*	+0.15
14	*S.Eastern-Africa*	+0.14
15	*W.North-America*	+0.11
16	*Madagascar*	+0.10
17	*E.Australia*	+0.10
18	*N.E.South-America*	+0.10
19	*N.Central-America*	+0.08
20	*West&Central-Europe*	+0.07
21	*S.Central-America*	+0.07
22	*Central-Africa*	+0.04
23	*N.Australia*	+0.01
24	*S.Australia*	+0.01
25	*New-Zealand*	+0.01
26	*Equatorial.Pacific-Ocean*	+0.00
27	*Caribbean*	+0.00
28	*N.Eastern-Africa*	+0.00
29	*S.W.South-America*	+0.00
30	*S.Indic-Ocean*	+0.00
31	*N.Atlantic-Ocean*	+0.00
32	*Greenland/Iceland*	+0.00
33	*W.Southern-Africa*	+0.00
34	*S.Atlantic-Ocean*	+0.00
35	*C.Australia*	+0.00
36	*Arabian-Sea*	+0.00
37	*Equatorial.Atlantic-Ocean*	+0.00
38	*Arctic-Ocean*	+0.00
39	*N.Pacific-Ocean*	+0.00
40	*S.Pacific-Ocean*	+0.00
41	*Southern-Ocean*	+0.00
42	*S.South-America*	-0.00
43	*Equatorial.Indic-Ocean*	-0.00
44	*Russian-Far-East*	-0.00
45	*N.E.North-America*	-0.00
46	*Russian-Arctic*	-0.00
47	*N.W.North-America*	-0.00
48	*Bay-of-Bengal*	-0.01
49	*E.Europe*	-0.02
50	*N.South-America*	-0.02
51	*N.W.South-America*	-0.03

Rank #	*Region*	SSP3-8.5
1	*S.Asia*	+13.94
2	*S.E.Asia*	+6.84
3	*Western-Africa*	+4.70
4	*Mediterranean*	+4.37
5	*E.Asia*	+1.18
6	*E.Southern-Africa*	+0.58
7	*S.E.South-America*	+0.43
8	*Sahara*	+0.39
9	*W.C.Asia*	+0.35
10	*S.Eastern-Africa*	+0.26
11	*Arabian-Peninsula*	+0.25
12	*C.North-America*	+0.22
13	*Madagascar*	+0.19
14	*S.Central-America*	+0.18
15	*E.North-America*	+0.16
16	*N.E.South-America*	+0.15
17	*N.Central-America*	+0.13
18	*N.Europe*	+0.10
19	*N.W.South-America*	+0.09
20	*W.North-America*	+0.07
21	*Central-Africa*	+0.06
22	*E.Australia*	+0.06
23	*West&Central-Europe*	+0.06
24	*N.South-America*	+0.05
25	*Caribbean*	+0.04
26	*Equatorial.Pacific-Ocean*	+0.02
27	*N.Australia*	+0.01
28	*N.Eastern-Africa*	+0.01
29	*New-Zealand*	+0.00
30	*S.W.South-America*	+0.00
31	*Equatorial.Indic-Ocean*	+0.00
32	*S.Indic-Ocean*	+0.00
33	*N.Atlantic-Ocean*	+0.00
34	*W.Southern-Africa*	+0.00
35	*S.Australia*	+0.00
36	*S.Atlantic-Ocean*	+0.00
37	*Greenland/Iceland*	+0.00
38	*Equatorial.Atlantic-Ocean*	+0.00
39	*Arabian-Sea*	+0.00
40	*Bay-of-Bengal*	+0.00
41	*Arctic-Ocean*	+0.00
42	*N.Pacific-Ocean*	+0.00
43	*S.Pacific-Ocean*	+0.00
44	*Southern-Ocean*	+0.00
45	*C.Australia*	-0.00
46	*Russian-Far-East*	-0.00
47	*S.South-America*	-0.00
48	*N.E.North-America*	-0.00
49	*Russian-Arctic*	-0.00
50	*N.W.North-America*	-0.01
51	*E.Europe*	-0.02

Rank #	*Region*	SSP5-8.5
1	*S.Asia*	+8.83
2	*Mediterranean*	+3.41
3	*S.E.Asia*	+2.98
4	*Western-Africa*	+2.62
5	*E.Asia*	+1.12
6	*E.Southern-Africa*	+0.41
7	*S.E.South-America*	+0.34
8	*C.North-America*	+0.32
9	*E.North-America*	+0.30
10	*Sahara*	+0.28
11	*W.C.Asia*	+0.26
12	*Arabian-Peninsula*	+0.25
13	*N.Europe*	+0.21
14	*W.North-America*	+0.15
15	*E.Australia*	+0.14
16	*S.Eastern-Africa*	+0.13
17	*West&Central-Europe*	+0.11
18	*Madagascar*	+0.11
19	*N.E.South-America*	+0.10
20	*N.Central-America*	+0.08
21	*S.Central-America*	+0.05
22	*Central-Africa*	+0.04
23	*S.Australia*	+0.01
24	*N.Australia*	+0.01
25	*New-Zealand*	+0.01
26	*Equatorial.Pacific-Ocean*	+0.00
27	*N.Eastern-Africa*	+0.00
28	*S.W.South-America*	+0.00
29	*S.Indic-Ocean*	+0.00
30	*N.Atlantic-Ocean*	+0.00
31	*Greenland/Iceland*	+0.00
32	*W.Southern-Africa*	+0.00
33	*C.Australia*	+0.00
34	*S.Atlantic-Ocean*	+0.00
35	*Equatorial.Indic-Ocean*	+0.00
36	*Arabian-Sea*	+0.00
37	*Equatorial.Atlantic-Ocean*	+0.00
38	*Arctic-Ocean*	+0.00
39	*N.Pacific-Ocean*	+0.00
40	*S.Pacific-Ocean*	+0.00
41	*Southern-Ocean*	+0.00
42	*N.E.North-America*	-0.00
43	*Russian-Far-East*	-0.00
44	*S.South-America*	-0.00
45	*N.W.North-America*	-0.00
46	*Russian-Arctic*	-0.00
47	*Caribbean*	-0.01
48	*Bay-of-Bengal*	-0.01
49	*E.Europe*	-0.02
50	*N.South-America*	-0.03
51	*N.W.South-America*	-0.03

TABLE A.10: Scenario of no additional adaptation - EAPA 2050 – full rankings by region (values show change relative to 2015 in millions of people/year impacted).

Rank #	*Region*	SSP1-4.5
1	*S.Asia*	+6.46
2	*Western-Africa*	+5.26
3	*Mediterranean*	+5.06
4	*S.E.Asia*	+1.00
5	*C.North-America*	+0.59
6	*E.Southern-Africa*	+0.51
7	*E.North-America*	+0.48
8	*N.Europe*	+0.35
9	*Sahara*	+0.32
10	*S.E.South-America*	+0.32
11	*Arabian-Peninsula*	+0.29
12	*W.C.Asia*	+0.24
13	*S.Eastern-Africa*	+0.20
14	*W.North-America*	+0.18
15	*E.Australia*	+0.16
16	*Madagascar*	+0.15
17	*Central-Africa*	+0.12
18	*N.Central-America*	+0.07
19	*West&Central-Europe*	+0.07
20	*N.E.South-America*	+0.06
21	*S.Central-America*	+0.05
22	*S.Australia*	+0.02
23	*N.Australia*	+0.01
24	*New-Zealand*	+0.01
25	*Equatorial.Pacific-Ocean*	+0.00
26	*N.Eastern-Africa*	+0.00
27	*N.Atlantic-Ocean*	+0.00
28	*S.Indic-Ocean*	+0.00
29	*Greenland/Iceland*	+0.00
30	*C.Australia*	+0.00
31	*W.Southern-Africa*	+0.00
32	*S.W.South-America*	+0.00
33	*S.Atlantic-Ocean*	+0.00
34	*Arabian-Sea*	+0.00
35	*Arctic-Ocean*	+0.00
36	*N.Pacific-Ocean*	+0.00
37	*S.Pacific-Ocean*	+0.00
38	*Southern-Ocean*	+0.00
39	*Equatorial.Indic-Ocean*	-0.00
40	*Equatorial.Atlantic-Ocean*	-0.00
41	*S.South-America*	-0.00
42	*N.E.North-America*	-0.00
43	*Russian-Far-East*	-0.00
44	*Russian-Arctic*	-0.00
45	*N.W.North-America*	-0.01
46	*Bay-of-Bengal*	-0.02
47	*E.Europe*	-0.02
48	*Caribbean*	-0.02
49	*N.South-America*	-0.02
50	*N.W.South-America*	-0.05
51	*E.Asia*	-0.40

Rank #	*Region*	SSP3-8.5
1	*S.Asia*	+30.77
2	*S.E.Asia*	+18.63
3	*Western-Africa*	+16.51
4	*Mediterranean*	+13.59
5	*E.Asia*	+1.92
6	*E.Southern-Africa*	+1.38
7	*S.E.South-America*	+1.00
8	*Sahara*	+0.90
9	*W.C.Asia*	+0.87
10	*S.Eastern-Africa*	+0.76
11	*Arabian-Peninsula*	+0.69
12	*Madagascar*	+0.62
13	*Central-Africa*	+0.58
14	*S.Central-America*	+0.51
15	*C.North-America*	+0.42
16	*N.W.South-America*	+0.42
17	*N.E.South-America*	+0.37
18	*N.South-America*	+0.34
19	*N.Europe*	+0.32
20	*E.North-America*	+0.28
21	*N.Central-America*	+0.27
22	*West&Central-Europe*	+0.17
23	*Caribbean*	+0.12
24	*W.North-America*	+0.08
25	*E.Australia*	+0.06
26	*Equatorial.Pacific-Ocean*	+0.06
27	*Equatorial.Indic-Ocean*	+0.02
28	*Bay-of-Bengal*	+0.02
29	*N.Australia*	+0.02
30	*N.Eastern-Africa*	+0.01
31	*New-Zealand*	+0.01
32	*S.W.South-America*	+0.01
33	*S.Australia*	+0.00
34	*W.Southern-Africa*	+0.00
35	*N.Atlantic-Ocean*	+0.00
36	*S.Indic-Ocean*	+0.00
37	*Russian-Far-East*	+0.00
38	*Equatorial.Atlantic-Ocean*	+0.00
39	*Arabian-Sea*	+0.00
40	*S.Atlantic-Ocean*	+0.00
41	*Greenland/Iceland*	+0.00
42	*Arctic-Ocean*	+0.00
43	*N.Pacific-Ocean*	+0.00
44	*S.Pacific-Ocean*	+0.00
45	*Southern-Ocean*	+0.00
46	*C.Australia*	-0.00
47	*S.South-America*	-0.00
48	*N.E.North-America*	-0.00
49	*Russian-Arctic*	-0.00
50	*N.W.North-America*	-0.01
51	*E.Europe*	-0.02

Rank #	*Region*	SSP5-8.5
1	*S.Asia*	+8.33
2	*Mediterranean*	+6.48
3	*Western-Africa*	+6.19
4	*S.E.Asia*	+2.97
5	*C.North-America*	+1.13
6	*N.Europe*	+1.07
7	*E.North-America*	+1.01
8	*E.Asia*	+0.86
9	*E.Southern-Africa*	+0.59
10	*West&Central-Europe*	+0.49
11	*S.E.South-America*	+0.44
12	*Sahara*	+0.40
13	*Arabian-Peninsula*	+0.38
14	*W.North-America*	+0.37
15	*E.Australia*	+0.33
16	*W.C.Asia*	+0.31
17	*Central-Africa*	+0.28
18	*S.Eastern-Africa*	+0.20
19	*Madagascar*	+0.19
20	*N.E.South-America*	+0.10
21	*N.Central-America*	+0.09
22	*S.Australia*	+0.05
23	*S.Central-America*	+0.04
24	*New-Zealand*	+0.03
25	*N.Australia*	+0.03
26	*Equatorial.Pacific-Ocean*	+0.00
27	*Equatorial.Indic-Ocean*	+0.00
28	*C.Australia*	+0.00
29	*Greenland/Iceland*	+0.00
30	*N.Eastern-Africa*	+0.00
31	*S.W.South-America*	+0.00
32	*N.Atlantic-Ocean*	+0.00
33	*W.Southern-Africa*	+0.00
34	*S.Indic-Ocean*	+0.00
35	*N.E.North-America*	+0.00
36	*S.Atlantic-Ocean*	+0.00
37	*Arabian-Sea*	+0.00
38	*Arctic-Ocean*	+0.00
39	*N.Pacific-Ocean*	+0.00
40	*S.Pacific-Ocean*	+0.00
41	*Southern-Ocean*	+0.00
42	*Equatorial.Atlantic-Ocean*	-0.00
43	*S.South-America*	-0.00
44	*Russian-Far-East*	-0.00
45	*N.W.North-America*	-0.00
46	*Russian-Arctic*	-0.00
47	*N.W.South-America*	-0.01
48	*Bay-of-Bengal*	-0.01
49	*E.Europe*	-0.02
50	*N.South-America*	-0.02
51	*Caribbean*	-0.03

TABLE A.11: Scenario of no additional adaptation - EAPA 2100 – full rankings by region (values show change relative to 2015 in millions of people/year impacted).

Rank #	*Region*	SSP1-4.5
1	*S.Asia*	+$490.29B
2	*S.E.Asia*	+$338.91B
3	*E.Asia*	+$224.46B
4	*Mediterranean*	+$144.90B
5	*Western-Africa*	+$91.49B
6	*E.North-America*	+$25.97B
7	*C.North-America*	+$22.81B
8	*N.Europe*	+$18.40B
9	*W.C.Asia*	+$15.88B
10	*Arabian-Peninsula*	+$15.07B
11	*West&Central-Europe*	+$14.35B
12	*W.North-America*	+$13.84B
13	*S.E.South-America*	+$13.07B
14	*E.Australia*	+$12.96B
15	*E.Southern-Africa*	+$10.62B
16	*N.E.South-America*	+$10.04B
17	*S.Central-America*	+$7.49B
18	*N.W.South-America*	+$6.50B
19	*N.Central-America*	+$5.11B
20	*Sahara*	+$4.56B
21	*S.Eastern-Africa*	+$4.23B
22	*N.South-America*	+$3.66B
23	*Caribbean*	+$2.09B
24	*Central-Africa*	+$1.96B
25	*Madagascar*	+$1.41B
26	*S.Australia*	+$1.11B
27	*N.Australia*	+$1.08B
28	*Equatorial.Pacific-Ocean*	+$0.82B
29	*Bay-of-Bengal*	+$0.51B
30	*New-Zealand*	+$0.48B
31	*S.W.South-America*	+$0.47B
32	*N.W.North-America*	+$0.29B
33	*S.Indic-Ocean*	+$0.26B
34	*Equatorial.Indic-Ocean*	+$0.22B
35	*N.Eastern-Africa*	+$0.15B
36	*Greenland/Iceland*	+$0.10B
37	*Russian-Far-East*	+$0.09B
38	*W.Southern-Africa*	+$0.07B
39	*N.Atlantic-Ocean*	+$0.06B
40	*Equatorial.Atlantic-Ocean*	+$0.04B
41	*S.South-America*	+$0.03B
42	*C.Australia*	+$0.02B
43	*S.Atlantic-Ocean*	+$0.01B
44	*Arabian-Sea*	+$0.00B
45	*Arctic-Ocean*	+$0.00B
46	*N.Pacific-Ocean*	+$0.00B
47	*S.Pacific-Ocean*	+$0.00B
48	*Southern-Ocean*	+$0.00B
49	*N.E.North-America*	-$0.08B
50	*Russian-Arctic*	-$0.20B
51	*E.Europe*	-$0.26B

Rank #	*Region*	SSP3-8.5
1	*S.Asia*	+$221.65B
2	*S.E.Asia*	+$167.35B
3	*E.Asia*	+$114.12B
4	*Mediterranean*	+$109.00B
5	*Western-Africa*	+$38.93B
6	*E.North-America*	+$25.02B
7	*C.North-America*	+$19.38B
8	*W.C.Asia*	+$15.85B
9	*W.North-America*	+$11.81B
10	*N.Europe*	+$11.54B
11	*E.Australia*	+$8.82B
12	*Arabian-Peninsula*	+$8.73B
13	*West&Central-Europe*	+$8.29B
14	*S.E.South-America*	+$8.06B
15	*N.Central-America*	+$6.23B
16	*S.Central-America*	+$5.66B
17	*N.E.South-America*	+$5.15B
18	*E.Southern-Africa*	+$4.05B
19	*Sahara*	+$3.64B
20	*N.W.South-America*	+$3.52B
21	*N.South-America*	+$3.01B
22	*S.Eastern-Africa*	+$1.62B
23	*Central-Africa*	+$1.31B
24	*Caribbean*	+$1.09B
25	*S.Australia*	+$0.96B
26	*N.W.North-America*	+$0.95B
27	*N.Australia*	+$0.61B
28	*Madagascar*	+$0.57B
29	*Equatorial.Pacific-Ocean*	+$0.39B
30	*S.W.South-America*	+$0.32B
31	*New-Zealand*	+$0.31B
32	*Bay-of-Bengal*	+$0.16B
33	*S.Indic-Ocean*	+$0.09B
34	*Russian-Far-East*	+$0.09B
35	*Greenland/Iceland*	+$0.05B
36	*Equatorial.Indic-Ocean*	+$0.04B
37	*N.Atlantic-Ocean*	+$0.03B
38	*W.Southern-Africa*	+$0.03B
39	*Equatorial.Atlantic-Ocean*	+$0.02B
40	*S.South-America*	+$0.01B
41	*S.Atlantic-Ocean*	+$0.01B
42	*Arabian-Sea*	+$0.00B
43	*Arctic-Ocean*	+$0.00B
44	*N.Pacific-Ocean*	+$0.00B
45	*S.Pacific-Ocean*	+$0.00B
46	*Southern-Ocean*	+$0.00B
47	*N.Eastern-Africa*	-$0.01B
48	*C.Australia*	-$0.02B
49	*N.E.North-America*	-$0.08B
50	*Russian-Arctic*	-$0.20B
51	*E.Europe*	-$0.26B

Rank #	*Region*	SSP5-8.5
1	*S.Asia*	+$662.51B
2	*S.E.Asia*	+$460.58B
3	*E.Asia*	+$318.55B
4	*Mediterranean*	+$207.48B
5	*Western-Africa*	+$126.01B
6	*E.North-America*	+$38.05B
7	*C.North-America*	+$30.56B
8	*N.Europe*	+$27.91B
9	*W.C.Asia*	+$26.39B
10	*Arabian-Peninsula*	+$24.54B
11	*West&Central-Europe*	+$21.55B
12	*W.North-America*	+$21.13B
13	*E.Australia*	+$19.56B
14	*S.E.South-America*	+$17.21B
15	*E.Southern-Africa*	+$14.67B
16	*N.E.South-America*	+$12.95B
17	*S.Central-America*	+$9.11B
18	*N.W.South-America*	+$8.85B
19	*Sahara*	+$8.68B
20	*N.South-America*	+$6.57B
21	*N.Central-America*	+$6.44B
22	*S.Eastern-Africa*	+$5.74B
23	*Central-Africa*	+$2.81B
24	*Caribbean*	+$2.55B
25	*Madagascar*	+$2.03B
26	*S.Australia*	+$1.93B
27	*N.Australia*	+$1.67B
28	*Equatorial.Pacific-Ocean*	+$1.11B
29	*Bay-of-Bengal*	+$0.75B
30	*New-Zealand*	+$0.71B
31	*N.W.North-America*	+$0.70B
32	*S.W.South-America*	+$0.60B
33	*S.Indic-Ocean*	+$0.33B
34	*Equatorial.Indic-Ocean*	+$0.33B
35	*Russian-Far-East*	+$0.19B
36	*N.Eastern-Africa*	+$0.19B
37	*Greenland/Iceland*	+$0.14B
38	*W.Southern-Africa*	+$0.09B
39	*N.Atlantic-Ocean*	+$0.08B
40	*C.Australia*	+$0.06B
41	*S.South-America*	+$0.06B
42	*Equatorial.Atlantic-Ocean*	+$0.05B
43	*N.E.North-America*	+$0.03B
44	*S.Atlantic-Ocean*	+$0.01B
45	*Arabian-Sea*	+$0.00B
46	*Arctic-Ocean*	+$0.00B
47	*N.Pacific-Ocean*	+$0.00B
48	*S.Pacific-Ocean*	+$0.00B
49	*Southern-Ocean*	+$0.00B
50	*Russian-Arctic*	-$0.20B
51	*E.Europe*	-$0.26B

TABLE A.12: Scenario of no additional adaptation - EAD 2050 – full rankings by region (values show change relative to 2015 in billion US$/year).

Rank #	*Region*	SSP1-4.5
1	*S.Asia*	+$1,744.08B
2	*S.E.Asia*	+$1,104.83B
3	*Western-Africa*	+$899.14B
4	*Mediterranean*	+$686.00B
5	*E.Asia*	+$373.85B
6	*E.Southern-Africa*	+$113.15B
7	*E.North-America*	+$75.42B
8	*C.North-America*	+$73.51B
9	*N.Europe*	+$65.16B
10	*S.E.South-America*	+$41.26B
11	*Arabian-Peninsula*	+$38.39B
12	*West&Central-Europe*	+$37.26B
13	*E.Australia*	+$37.19B
14	*W.North-America*	+$36.96B
15	*Sahara*	+$35.88B
16	*S.Eastern-Africa*	+$34.94B
17	*W.C.Asia*	+$34.82B
18	*N.E.South-America*	+$24.66B
19	*N.W.South-America*	+$24.12B
20	*S.Central-America*	+$21.13B
21	*Madagascar*	+$16.67B
22	*N.South-America*	+$15.76B
23	*Central-Africa*	+$15.58B
24	*N.Central-America*	+$13.74B
25	*Caribbean*	+$5.27B
26	*S.Australia*	+$4.52B
27	*Equatorial.Pacific-Ocean*	+$4.41B
28	*N.Australia*	+$3.21B
29	*Bay-of-Bengal*	+$1.88B
30	*New-Zealand*	+$1.86B
31	*Equatorial.Indic-Ocean*	+$1.21B
32	*S.W.South-America*	+$0.83B
33	*N.Eastern-Africa*	+$0.65B
34	*N.W.North-America*	+$0.58B
35	*S.Indic-Ocean*	+$0.52B
36	*Greenland/Iceland*	+$0.25B
37	*W.Southern-Africa*	+$0.20B
38	*Russian-Far-East*	+$0.19B
39	*N.Atlantic-Ocean*	+$0.18B
40	*C.Australia*	+$0.17B
41	*Equatorial.Atlantic-Ocean*	+$0.08B
42	*S.South-America*	+$0.08B
43	*S.Atlantic-Ocean*	+$0.02B
44	*Arabian-Sea*	+$0.01B
45	*Arctic-Ocean*	+$0.00B
46	*N.Pacific-Ocean*	+$0.00B
47	*S.Pacific-Ocean*	+$0.00B
48	*Southern-Ocean*	+$0.00B
49	*N.E.North-America*	-$0.02B
50	*Russian-Arctic*	-$0.20B
51	*E.Europe*	-$0.26B

Rank #	*Region*	SSP3-8.5
1	*S.Asia*	+$764.52B
2	*S.E.Asia*	+$742.52B
3	*Mediterranean*	+$563.76B
4	*Western-Africa*	+$413.51B
5	*E.Asia*	+$221.98B
6	*E.North-America*	+$50.12B
7	*C.North-America*	+$44.51B
8	*N.Europe*	+$40.51B
9	*W.C.Asia*	+$34.59B
10	*Arabian-Peninsula*	+$27.45B
11	*West&Central-Europe*	+$27.33B
12	*S.E.South-America*	+$23.10B
13	*E.Southern-Africa*	+$22.61B
14	*N.W.South-America*	+$20.89B
15	*S.Central-America*	+$19.97B
16	*Sahara*	+$19.27B
17	*W.North-America*	+$19.19B
18	*N.South-America*	+$17.35B
19	*E.Australia*	+$15.14B
20	*N.Central-America*	+$14.94B
21	*S.Eastern-Africa*	+$14.12B
22	*Central-Africa*	+$11.96B
23	*N.E.South-America*	+$11.24B
24	*Madagascar*	+$7.74B
25	*Caribbean*	+$5.79B
26	*S.Australia*	+$2.41B
27	*Equatorial.Pacific-Ocean*	+$2.21B
28	*N.Australia*	+$1.25B
29	*Bay-of-Bengal*	+$1.04B
30	*New-Zealand*	+$1.02B
31	*S.W.South-America*	+$0.86B
32	*N.W.North-America*	+$0.68B
33	*Equatorial.Indic-Ocean*	+$0.62B
34	*Russian-Far-East*	+$0.37B
35	*S.Indic-Ocean*	+$0.20B
36	*W.Southern-Africa*	+$0.10B
37	*N.Atlantic-Ocean*	+$0.09B
38	*S.South-America*	+$0.07B
39	*Greenland/Iceland*	+$0.06B
40	*Equatorial.Atlantic-Ocean*	+$0.04B
41	*C.Australia*	+$0.01B
42	*S.Atlantic-Ocean*	+$0.01B
43	*N.Eastern-Africa*	+$0.01B
44	*Arabian-Sea*	+$0.01B
45	*Arctic-Ocean*	+$0.00B
46	*N.Pacific-Ocean*	+$0.00B
47	*S.Pacific-Ocean*	+$0.00B
48	*Southern-Ocean*	+$0.00B
49	*N.E.North-America*	-$0.08B
50	*E.Europe*	-$0.18B
51	*Russian-Arctic*	-$0.20B

Rank #	*Region*	SSP5-8.5
1	*S.Asia*	+$3,353.44B
2	*S.E.Asia*	+$2,284.79B
3	*Western-Africa*	+$1,746.95B
4	*Mediterranean*	+$1,376.66B
5	*E.Asia*	+$920.56B
6	*N.Europe*	+$268.71B
7	*E.North-America*	+$232.00B
8	*E.Southern-Africa*	+$220.65B
9	*C.North-America*	+$220.26B
10	*West&Central-Europe*	+$154.78B
11	*E.Australia*	+$108.97B
12	*W.North-America*	+$107.46B
13	*S.E.South-America*	+$91.79B
14	*Arabian-Peninsula*	+$86.84B
15	*W.C.Asia*	+$80.41B
16	*Sahara*	+$67.53B
17	*S.Eastern-Africa*	+$62.60B
18	*N.E.South-America*	+$50.92B
19	*N.W.South-America*	+$48.67B
20	*Central-Africa*	+$48.47B
21	*N.South-America*	+$36.25B
22	*S.Central-America*	+$36.16B
23	*Madagascar*	+$35.74B
24	*N.Central-America*	+$28.04B
25	*S.Australia*	+$15.38B
26	*N.Australia*	+$9.29B
27	*Caribbean*	+$9.17B
28	*Equatorial.Pacific-Ocean*	+$8.30B
29	*New-Zealand*	+$6.18B
30	*Bay-of-Bengal*	+$3.76B
31	*N.W.North-America*	+$3.03B
32	*Equatorial.Indic-Ocean*	+$2.55B
33	*S.W.South-America*	+$1.73B
34	*N.Eastern-Africa*	+$1.16B
35	*S.Indic-Ocean*	+$0.93B
36	*C.Australia*	+$0.70B
37	*Greenland/Iceland*	+$0.63B
38	*Russian-Far-East*	+$0.62B
39	*N.E.North-America*	+$0.54B
40	*W.Southern-Africa*	+$0.42B
41	*N.Atlantic-Ocean*	+$0.42B
42	*S.South-America*	+$0.18B
43	*Equatorial.Atlantic-Ocean*	+$0.15B
44	*S.Atlantic-Ocean*	+$0.04B
45	*E.Europe*	+$0.03B
46	*Arabian-Sea*	+$0.01B
47	*Arctic-Ocean*	+$0.00B
48	*N.Pacific-Ocean*	+$0.00B
49	*S.Pacific-Ocean*	+$0.00B
50	*Southern-Ocean*	+$0.00B
51	*Russian-Arctic*	-$0.19B

TABLE A.13: Scenario of no additional adaptation - EAD 2100 – full rankings by region (values show change relative to 2015 in billion US$/year).

Rank #	*Country*	Million People/yr
1	*India*	7.523
2	*Vietnam*	5.217
3	*Bangladesh*	3.710
4	*Indonesia*	2.754
5	*Philippines*	2.279
6	*China*	2.188
7	*Nigeria*	2.146
8	*Myanmar*	1.709
9	*Japan*	0.982
10	*Egypt*	0.559

Rank #	*Country*	Billion $US/yr
1	*India*	46.259
2	*Japan*	38.620
3	*Vietnam*	31.985
4	*Indonesia*	29.166
5	*China*	27.379
6	*USA*	17.930
7	*Nigeria*	17.467
8	*Bangladesh*	14.211
9	*Philippines*	13.471
10	*China Hong Kong SAR*	9.731

TABLE A.14: Top 10 countries having the highest Expected Annual People Affected (EAPA) (left) (Millions of people affected/year) and Expected Annual Damage (EAD) (right) (billion $/year) for the present-day (2015).

Rank #	*Country*	RCP 4.5
1	*India*	+2.44
2	*Egypt*	+1.39
3	*Vietnam*	+1.35
4	*Bangladesh*	+0.71
5	*Indonesia*	+0.68
6	*China*	+0.49
7	*Nigeria*	+0.44
8	*Philippines*	+0.37
9	*Myanmar*	+0.27
10	*Japan*	+0.25

Rank #	*Country*	RCP 8.5
1	*India*	+2.88
2	*Egypt*	+1.57
3	*Vietnam*	+1.51
4	*Bangladesh*	+0.76
5	*Indonesia*	+0.74
6	*China*	+0.59
7	*Nigeria*	+0.49
8	*Philippines*	+0.40
9	*Myanmar*	+0.30
10	*Japan*	+0.29

TABLE A.15: Scenario of no socio-economic change - EAPA 2050 – top 10 rankings by country (change in M people affected/year, relative to 2015).

Rank #	*Country*	RCP 4.5
1	*India*	+4.77
2	*Vietnam*	+4.09
3	*Egypt*	+3.04
4	*Indonesia*	+1.88
5	*Bangladesh*	+1.82
6	*China*	+1.22
7	*Nigeria*	+0.98
8	*Philippines*	+0.85
9	*Myanmar*	+0.74
10	*Japan*	+0.55

Rank #	*Country*	RCP 8.5
1	*Vietnam*	+6.25
2	*India*	+6.23
3	*Egypt*	+4.01
4	*Indonesia*	+2.89
5	*Bangladesh*	+2.61
6	*China*	+1.74
7	*Nigeria*	+1.37
8	*Philippines*	+1.18
9	*Myanmar*	+1.10
10	*Japan*	+0.78

TABLE A.16: Scenario of no socio-economic change - EAPA 2100 – top 10 rankings by country (change in M people affected/year, relative to 2015).

Rank #	*Country*	RCP 4.5
1	*Egypt*	+$19.46B
2	*India*	+$16.55B
3	*USA*	+$10.34B
4	*Japan*	+$10.33B
5	*Vietnam*	+$8.98B
6	*Indonesia*	+$8.27B
7	*China*	+$7.60B
8	*Nigeria*	+$4.29B
9	*Spain*	+$4.02B
10	*Bangladesh*	+$2.77B

Rank #	*Country*	RCP 8.5
1	*Egypt*	+$22.05B
2	*India*	+$19.23B
3	*Japan*	+$12.07B
4	*USA*	+$11.00B
5	*Vietnam*	+$10.04B
6	*Indonesia*	+$9.10B
7	*China*	+$9.01B
8	*Spain*	+$6.22B
9	*Nigeria*	+$4.86B
10	*Bangladesh*	+$3.02B

Table A.17: Scenario of no socio-economic change - EAD 2050 – top 10 rankings by country (change in billion US$/year, relative to 2015).

Rank #	*Country*	RCP 4.5
1	*Egypt*	+$43.26B
2	*India*	+$34.82B
3	*Vietnam*	+$28.22B
4	*USA*	+$26.76B
5	*Japan*	+$25.10B
6	*Indonesia*	+$22.69B
7	*China*	+$20.20B
8	*Spain*	+$12.30B
9	*Nigeria*	+$10.55B
10	*Bangladesh*	+$7.67B

Rank #	*Country*	RCP 8.5
1	*Egypt*	+$53.45B
2	*India*	+$48.24B
3	*Vietnam*	+$44.52B
4	*USA*	+$37.53B
5	*Japan*	+$37.08B
6	*Indonesia*	+$35.85B
7	*China*	+$30.96B
8	*Nigeria*	+$15.32B
9	*Spain*	+$13.88B
10	*Netherlands*	+$11.67B

Table A.18: – Scenario of no socio-economic change - EAD 2100 – top 10 rankings by country (change in billion US$/year, relative to 2015).

Rank #	*Country*	SSP1
1	*India*	+2.10
2	*Nigeria*	+1.65
3	*Bangladesh*	+1.50
4	*Egypt*	+0.34
5	*Vietnam*	+0.33
6	*Mozambique*	+0.27
7	*Brazil*	+0.19
8	*USA*	+0.19
9	*Pakistan*	+0.16
10	*Yemen*	+0.13

Rank #	*Country*	SSP3
1	*India*	+4.49
2	*Bangladesh*	+3.24
3	*Nigeria*	+2.84
4	*Vietnam*	+1.51
5	*Egypt*	+0.81
6	*Indonesia*	+0.62
7	*Philippines*	+0.58
8	*Myanmar*	+0.50
9	*Mozambique*	+0.40
10	*Senegal*	+0.35

Rank #	*Country*	SSP5
1	*India*	+2.07
2	*Nigeria*	+1.62
3	*Bangladesh*	+1.31
4	*Egypt*	+0.32
5	*USA*	+0.27
6	*Mozambique*	+0.26
7	*Vietnam*	+0.23
8	*Brazil*	+0.19
9	*Pakistan*	+0.15
10	*Kuwait*	+0.14

TABLE A.19: Scenario of constant flood probability - EAPA 2050 – top 10 rankings by country (change in M people affected/year, relative to 2015).

Rank #	*Country*	SSP1
1	*Nigeria*	+2.61
2	*Mozambique*	+0.26
3	*USA*	+0.24
4	*Yemen*	+0.16
5	*United Republic of Tanzania*	+0.14
6	*Pakistan*	+0.13
7	*Ghana*	+0.12
8	*Australia*	+0.11
9	*Egypt*	+0.11
10	*Kuwait*	+0.10

Rank #	*Country*	SSP3
1	*India*	+8.05
2	*Nigeria*	+7.21
3	*Bangladesh*	+4.35
4	*Philippines*	+1.95
5	*Egypt*	+1.39
6	*Vietnam*	+1.24
7	*Senegal*	+0.81
8	*Mozambique*	+0.73
9	*Myanmar*	+0.57
10	*United Republic of Tanzania*	+0.44

Rank #	*Country*	SSP5
1	*Nigeria*	+2.54
2	*USA*	+0.51
3	*Mozambique*	+0.24
4	*Australia*	+0.24
5	*Yemen*	+0.15
6	*Canada*	+0.13
7	*Kuwait*	+0.13
8	*United Republic of Tanzania*	+0.12
9	*Pakistan*	+0.12
10	*Ghana*	+0.11

TABLE A.20: Scenario of constant flood probability - EAPA 2100 – top 10 rankings by country (change in M people affected/year, relative to 2015).

Rank #	*Country*	SSP1
1	*India*	+$247.04B
2	*Vietnam*	+$106.50B
3	*Bangladesh*	+$88.59B
4	*China*	+$83.20B
5	*Indonesia*	+$79.05B
6	*Nigeria*	+$54.56B
7	*Philippines*	+$30.76B
8	*Japan*	+$30.43B
9	*USA*	+$28.28B
10	*Egypt*	+$18.69B

Rank #	*Country*	SSP3
1	*India*	+$103.55B
2	*Vietnam*	+$60.51B
3	*Bangladesh*	+$39.90B
4	*China*	+$35.00B
5	*USA*	+$25.60B
6	*Indonesia*	+$23.75B
7	*Nigeria*	+$19.92B
8	*Kuwait*	+$12.17B
9	*Egypt*	+$11.68B
10	*Philippines*	+$11.56B

Rank #	*Country*	SSP5
1	*India*	+$322.88B
2	*Vietnam*	+$140.43B
3	*Bangladesh*	+$116.95B
4	*China*	+$110.44B
5	*Indonesia*	+$107.96B
6	*Nigeria*	+$75.32B
7	*Japan*	+$48.21B
8	*Philippines*	+$42.53B
9	*USA*	+$41.39B
10	*Egypt*	+$23.28B

TABLE A.21: Scenario of constant flood probability - EAD 2050 – top 10 rankings by country (change in billion US$/year, relative to 2015).

Rank #	*Country*	SSP1
1	*India*	+$652.32B
2	*Nigeria*	+$469.37B
3	*Bangladesh*	+$263.97B
4	*Vietnam*	+$223.54B
5	*Indonesia*	+$180.19B
6	*Philippines*	+$120.05B
7	*China*	+$71.84B
8	*Mozambique*	+$66.83B
9	*USA*	+$55.08B
10	*Japan*	+$54.20B

Rank #	*Country*	SSP3
1	*India*	+$238.47B
2	*Nigeria*	+$179.21B
3	*Vietnam*	+$150.63B
4	*Bangladesh*	+$123.21B
5	*Philippines*	+$72.93B
6	*Indonesia*	+$46.25B
7	*Egypt*	+$40.16B
8	*China*	+$33.22B
9	*Malaysia*	+$23.94B
10	*USA*	+$22.01B

Rank #	*Country*	SSP5
1	*India*	+$1,111.76B
2	*Nigeria*	+$786.05B
3	*Bangladesh*	+$422.97B
4	*Vietnam*	+$375.19B
5	*Indonesia*	+$310.94B
6	*Philippines*	+$204.75B
7	*Japan*	+$161.96B
8	*USA*	+$148.11B
9	*China*	+$132.32B
10	*Mozambique*	+$112.71B

TABLE A.22: Scenario of constant flood probability - EAD 2100 – top 10 rankings by country (change in billion US$/year, relative to 2015).

Rank #	*Country*	SSP1
1	*India*	+5.57
2	*Bangladesh*	+2.59
3	*Egypt*	+2.38
4	*Nigeria*	+2.36
5	*Vietnam*	+1.84
6	*Indonesia*	+0.71
7	*USA*	+0.55
8	*Mozambique*	+0.40
9	*Brazil*	+0.39
10	*Myanmar*	+0.35

Rank #	*Country*	SSP3
1	*India*	+8.77
2	*Bangladesh*	+4.78
3	*Nigeria*	+3.90
4	*Egypt*	+3.73
5	*Vietnam*	+3.55
6	*Indonesia*	+1.51
7	*Philippines*	+1.02
8	*Myanmar*	+0.88
9	*Mozambique*	+0.57
10	*Senegal*	+0.55

Rank #	*Country*	SSP5
1	*India*	+6.19
2	*Egypt*	+2.68
3	*Bangladesh*	+2.43
4	*Nigeria*	+2.43
5	*Vietnam*	+1.89
6	*Indonesia*	+0.74
7	*USA*	+0.69
8	*Mozambique*	+0.40
9	*Brazil*	+0.39
10	*Japan*	+0.39

TABLE A.23: Scenario of no additional adaptation - EAPA 2050 – top 10 rankings by country (change in M people affected/year, relative to 2015).

Rank #	*Country*	SSP1
1	*India*	+4.81
2	*Nigeria*	+4.72
3	*Egypt*	+4.07
4	*Bangladesh*	+1.41
5	*USA*	+1.18
6	*Vietnam*	+0.63
7	*Mozambique*	+0.51
8	*Spain*	+0.41
9	*Brazil*	+0.33
10	*Pakistan*	+0.32

Rank #	*Country*	SSP3
1	*India*	+19.60
2	*Nigeria*	+12.93
3	*Egypt*	+12.42
4	*Bangladesh*	+9.97
5	*Vietnam*	+8.53
6	*Philippines*	+3.96
7	*Indonesia*	+3.49
8	*Myanmar*	+2.04
9	*Senegal*	+1.72
10	*Mozambique*	+1.34

Rank #	*Country*	SSP5
1	*India*	+6.22
2	*Nigeria*	+5.38
3	*Egypt*	+4.93
4	*USA*	+2.37
5	*Bangladesh*	+1.81
6	*Vietnam*	+1.67
7	*Indonesia*	+0.82
8	*Japan*	+0.71
9	*Spain*	+0.67
10	*Mozambique*	+0.58

TABLE A.24: Scenario of no additional adaptation - EAPA 2100 – top 10 rankings by country (change in M people affected/year, relative to 2015).

Rank #	*Country*	SSP1
1	*India*	+$371.62B
2	*Vietnam*	+$147.23B
3	*China*	+$116.96B
4	*Bangladesh*	+$109.46B
5	*Indonesia*	+$108.76B
6	*Egypt*	+$106.04B
7	*Nigeria*	+$71.65B
8	*USA*	+$57.87B
9	*Japan*	+$50.92B
10	*Philippines*	+$39.51B

Rank #	*Country*	SSP3
1	*India*	+$166.28B
2	*Vietnam*	+$90.53B
3	*Egypt*	+$79.19B
4	*China*	+$57.32B
5	*USA*	+$53.56B
6	*Bangladesh*	+$51.49B
7	*Indonesia*	+$39.94B
8	*Nigeria*	+$29.97B
9	*Japan*	+$18.61B
10	*Philippines*	+$17.08B

Rank #	*Country*	SSP5
1	*India*	+$503.85B
2	*Vietnam*	+$196.61B
3	*China*	+$160.16B
4	*Egypt*	+$149.51B
5	*Indonesia*	+$149.00B
6	*Bangladesh*	+$146.05B
7	*Nigeria*	+$100.17B
8	*USA*	+$81.36B
9	*Japan*	+$77.68B
10	*Philippines*	+$54.69B

TABLE A.25: Scenario of no additional adaptation - EAD 2050 – top 10 rankings by region (change in billion US$/year, relative to 2015).

Rank #	*Country*	SSP1
1	*India*	+$1,268.65B
2	*Nigeria*	+$755.57B
3	*Egypt*	+$541.34B
4	*Vietnam*	+$442.06B
5	*Bangladesh*	+$424.42B
6	*Indonesia*	+$348.96B
7	*Philippines*	+$188.54B
8	*USA*	+$173.38B
9	*China*	+$150.84B
10	*Japan*	+$118.92B

Rank #	*Country*	SSP3
1	*India*	+$514.21B
2	*Egypt*	+$483.36B
3	*Vietnam*	+$376.56B
4	*Nigeria*	+$345.34B
5	*Bangladesh*	+$228.54B
6	*Indonesia*	+$139.04B
7	*Philippines*	+$137.04B
8	*USA*	+$108.32B
9	*China*	+$106.01B
10	*Malaysia*	+$62.23B

Rank #	*Country*	SSP5
1	*India*	+$2,453.15B
2	*Nigeria*	+$1,471.04B
3	*Egypt*	+$1,025.65B
4	*Vietnam*	+$904.60B
5	*Bangladesh*	+$803.75B
6	*Indonesia*	+$730.95B
7	*USA*	+$522.89B
8	*Philippines*	+$368.15B
9	*Japan*	+$362.01B
10	*China*	+$324.41B

TABLE A.26: Scenario of no additional adaptation - EAD 2100 – top 10 rankings by country (change in billion US$/year, relative to 2015).

Rank #	*Country*	RCP4.5-SSP1
1	*Vietnam*	8.6
2	*Myanmar*	5.9
3	*Guyana*	4.9
4	*Mauritania*	4.9
5	*Bangladesh*	4.7
6	*Kuwait*	3.5
7	*Egypt*	3.3
8	*Guinea-Bissau*	3.1
9	*Fiji*	2.9
10	*China Hong Kong SAR*	2.9
11	*China Macao Kong SAR*	2.8
12	*Senegal*	2.8
13	*Solomon Islands*	2.7
14	*Mozambique*	2.7
15	*Gabon*	2.6
16	*Singapore*	2.3
17	*Bahamas*	2.3
18	*Philippines*	2.3
19	*Tunisia*	2.0
20	*Suriname*	1.9
21	*Cyprus*	1.9
22	*Brunei Darussalam*	1.9
23	*Nigeria*	1.8
24	*Belgium*	1.7
25	*Indonesia*	1.5
26	*Taiwan*	1.5
27	*Bahrain*	1.5
28	*Puerto Rico*	1.4
29	*Japan*	1.4
30	*Guinea*	1.3
31	*Denmark*	1.3
32	*Papua New Guinea*	1.2
33	*Sierra Leone*	1.2
34	*India*	1.1
35	*Belize*	1.1
36	*Ireland*	1.1
37	*Malaysia*	1.1
38	*Gambia*	1.1
39	*Ghana*	1.0
40	*Thailand*	1.0
41	*Ecuador*	1.0
42	*Uruguay*	1.0
43	*Libya*	0.9
44	*Australia*	0.9
45	*Djibouti*	0.8
46	*Yemen*	0.8
47	*Panama*	0.7
48	*Comoros*	0.7
49	*Spain*	0.6
50	*Sweden*	0.6

Rank #	*Country*	RCP8.5-SSP3
1	*Vietnam*	9.8
2	*Mauritania*	7.9
3	*Myanmar*	6.2
4	*Bangladesh*	5.3
5	*Guyana*	5.0
6	*Egypt*	3.9
7	*Gabon*	3.7
8	*China Hong Kong SAR*	3.5
9	*Kuwait*	3.3
10	*Guinea-Bissau*	3.3
11	*Senegal*	3.1
12	*Solomon Islands*	2.7
13	*Fiji*	2.6
14	*Bahamas*	2.6
15	*Mozambique*	2.5
16	*Cyprus*	2.4
17	*Suriname*	2.3
18	*Philippines*	2.2
19	*Singapore*	2.0
20	*Nigeria*	1.8
21	*Tunisia*	1.7
22	*Belgium*	1.7
23	*Brunei Darussalam*	1.6
24	*Taiwan*	1.6
25	*Indonesia*	1.5
26	*Guinea*	1.5
27	*Belize*	1.5
28	*Denmark*	1.5
29	*Bahrain*	1.5
30	*Japan*	1.4
31	*Sierra Leone*	1.3
32	*Malaysia*	1.2
33	*Papua New Guinea*	1.2
34	*Ireland*	1.2
35	*Ecuador*	1.2
36	*Puerto Rico*	1.1
37	*India*	1.1
38	*Australia*	1.0
39	*Thailand*	1.0
40	*Libya*	1.0
41	*Gambia*	1.0
42	*Ghana*	1.0
43	*Spain*	0.9
44	*Uruguay*	0.9
45	*Togo*	0.9
46	*Tonga*	0.8
47	*Albania*	0.8
48	*Panama*	0.8
49	*Jamaica*	0.7
50	*Benin*	0.6

Rank #	*Country*	RCP8.5-SSP5
1	*Vietnam*	8.8
2	*Mauritania*	8.3
3	*Myanmar*	6.0
4	*Guyana*	5.4
5	*Bangladesh*	4.8
6	*Egypt*	3.9
7	*Kuwait*	3.7
8	*Guinea-Bissau*	3.2
9	*Fiji*	3.1
10	*China Hong Kong SAR*	2.9
11	*Senegal*	2.8
12	*China Macao Kong SAR*	2.8
13	*Solomon Islands*	2.8
14	*Mozambique*	2.7
15	*Gabon*	2.7
16	*Bahamas*	2.4
17	*Philippines*	2.3
18	*Singapore*	2.3
19	*Tunisia*	2.0
20	*Suriname*	2.0
21	*Cyprus*	1.9
22	*Brunei Darussalam*	1.9
23	*Nigeria*	1.8
24	*Belgium*	1.7
25	*Indonesia*	1.5
26	*Taiwan*	1.5
27	*Bahrain*	1.5
28	*Puerto Rico*	1.4
29	*Japan*	1.4
30	*Denmark*	1.4
31	*Guinea*	1.3
32	*Papua New Guinea*	1.2
33	*Sierra Leone*	1.2
34	*India*	1.2
35	*Gambia*	1.2
36	*Belize*	1.2
37	*Malaysia*	1.1
38	*Ireland*	1.1
39	*Ghana*	1.1
40	*Thailand*	1.0
41	*Ecuador*	1.0
42	*Uruguay*	1.0
43	*Libya*	0.9
44	*Australia*	0.9
45	*Djibouti*	0.8
46	*Albania*	0.8
47	*Spain*	0.8
48	*Yemen*	0.8
49	*Panama*	0.7
50	*Comoros*	0.7

TABLE A.27: Scenario of no additional adaptation - EAD 2050 – top 50 rankings by country (EAD as a percentage of GDP).

Rank #	*Country*	RCP4.5-SSP1
1	*Guyana*	11.7
2	*Vietnam*	11.6
3	*Mauritania*	9.5
4	*Myanmar*	7.5
5	*Egypt*	6.9
6	*Bangladesh*	5.7
7	*Fiji*	5.6
8	*Gabon*	4.3
9	*Kuwait*	4.2
10	*Guinea-Bissau*	4.2
11	*China Macao Kong SAR*	4.1
12	*Suriname*	3.6
13	*Senegal*	3.5
14	*Mozambique*	3.4
15	*China Hong Kong SAR*	3.2
16	*Solomon Islands*	3.0
17	*Bahamas*	3.0
18	*Philippines*	2.7
19	*Singapore*	2.6
20	*Tunisia*	2.4
21	*Brunei Darussalam*	2.3
22	*Sierra Leone*	2.2
23	*Gambia*	2.2
24	*Nigeria*	2.2
25	*Cyprus*	2.1
26	*Puerto Rico*	2.1
27	*Indonesia*	2.0
28	*Taiwan*	1.9
29	*Denmark*	1.9
30	*Japan*	1.9
31	*Belgium*	1.8
32	*Bahrain*	1.7
33	*Albania*	1.6
34	*Guinea*	1.6
35	*Papua New Guinea*	1.6
36	*Thailand*	1.6
37	*Belize*	1.5
38	*India*	1.5
39	*Spain*	1.5
40	*Malaysia*	1.4
41	*Uruguay*	1.4
42	*Ghana*	1.3
43	*Ireland*	1.3
44	*Ecuador*	1.3
45	*Libya*	1.2
46	*Australia*	1.0
47	*Yemen*	1.0
48	*Djibouti*	0.9
49	*Panama*	0.9
50	*Cambodia*	0.8

Rank #	*Country*	RCP8.5-SSP3
1	*Guyana*	16.6
2	*Vietnam*	16.3
3	*Mauritania*	10.4
4	*Myanmar*	9.2
5	*Egypt*	8.4
6	*Bangladesh*	7.6
7	*Gabon*	6.5
8	*Guinea-Bissau*	5.9
9	*China Macao Kong SAR*	5.5
10	*Fiji*	5.4
11	*Suriname*	4.7
12	*Senegal*	4.6
13	*Bahamas*	4.4
14	*Kuwait*	4.3
15	*China Hong Kong SAR*	3.8
16	*Gambia*	3.6
17	*Mozambique*	3.5
18	*Solomon Islands*	3.4
19	*Belgium*	3.2
20	*Philippines*	3.2
21	*Sierra Leone*	3.1
22	*Cyprus*	2.7
23	*Denmark*	2.7
24	*Indonesia*	2.5
25	*Nigeria*	2.5
26	*Singapore*	2.4
27	*Brunei Darussalam*	2.2
28	*Taiwan*	2.2
29	*Guinea*	2.2
30	*Tunisia*	2.2
31	*Malaysia*	2.2
32	*Puerto Rico*	2.1
33	*Belize*	2.1
34	*Japan*	2.0
35	*Bahrain*	2.0
36	*Thailand*	2.0
37	*Spain*	1.9
38	*Albania*	1.8
39	*Ecuador*	1.7
40	*Papua New Guinea*	1.7
41	*Uruguay*	1.7
42	*Netherlands*	1.7
43	*India*	1.5
44	*Ireland*	1.5
45	*Australia*	1.5
46	*Ghana*	1.3
47	*Libya*	1.3
48	*Tonga*	1.3
49	*Togo*	1.2
50	*Panama*	1.2

Rank #	*Country*	RCP8.5-SSP5
1	*Guyana*	17.7
2	*Vietnam*	14.3
3	*Mauritania*	11.0
4	*Myanmar*	8.6
5	*Egypt*	8.2
6	*Fiji*	7.0
7	*Bangladesh*	6.7
8	*China Macao Kong SAR*	6.4
9	*Guinea-Bissau*	5.6
10	*Gabon*	5.3
11	*Suriname*	4.9
12	*Kuwait*	4.7
13	*Gambia*	4.2
14	*Senegal*	4.1
15	*Mozambique*	4.0
16	*Bahamas*	3.8
17	*China Hong Kong SAR*	3.3
18	*Solomon Islands*	3.3
19	*Philippines*	3.1
20	*Belgium*	3.0
21	*Sierra Leone*	2.9
22	*Tunisia*	2.7
23	*Singapore*	2.6
24	*Puerto Rico*	2.6
25	*Nigeria*	2.5
26	*Indonesia*	2.5
27	*Brunei Darussalam*	2.5
28	*Denmark*	2.4
29	*Taiwan*	2.2
30	*Japan*	2.2
31	*Cyprus*	2.2
32	*Thailand*	2.0
33	*Bahrain*	1.9
34	*Belize*	1.9
35	*Guinea*	1.8
36	*Albania*	1.8
37	*Malaysia*	1.8
38	*Papua New Guinea*	1.8
39	*Uruguay*	1.8
40	*India*	1.7
41	*Netherlands*	1.6
42	*Ecuador*	1.5
43	*Spain*	1.5
44	*Ghana*	1.5
45	*Ireland*	1.4
46	*Libya*	1.3
47	*Australia*	1.2
48	*Benin*	1.1
49	*Panama*	1.1
50	*Cambodia*	1.1

TABLE A.28: Scenario of no additional adaptation - EAD 2100 – top 50 rankings by country (EAD as a percentage of GDP).